

The Loma Prieta, California, Earthquake of October 17, 1989—Building Structures

MEHMET ÇELEBI, *Editor*

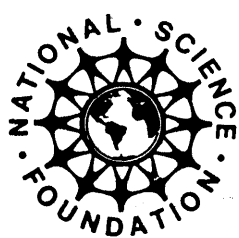
PERFORMANCE OF THE BUILT ENVIRONMENT

THOMAS L. HOLZER, *Coordinator*

U.S. GEOLOGICAL SURVEY PROFESSIONAL PAPER 1552-C

Prepared in cooperation with the National Science Foundation

<https://pubs.usgs.gov/pp/pp1552/pp1552c/pp1552c.pdf>
(checked 4 April 2021)



UNITED STATES GOVERNMENT PRINTING OFFICE, WASHINGTON : 1998

DEPARTMENT OF THE INTERIOR

BRUCE BABBITT, *Secretary*

U.S. GEOLOGICAL SURVEY

MARK SCHAFER, *Acting Director*

Any use of trade, product, or firm names in this publication
is for descriptive purposes only and does not imply endorsement
by the U.S. Government

Manuscript approved for publication ,
November 14, 1997

Library of Congress catalog-card No. 92-32287

For sale by the
U.S. Geological Survey
Information Services
Box 25286
Federal Center
Denver, CO 80225

CONTENTS

	Page
Introduction-----	C1
By Mehmet Çelebi	
Performance of building structures—A summary -----	5
By Mehmet Çelebi	
Measured response of two tilt-up buildings -----	77
By Sharon L. Wood and Neil M. Hawkins	
Seismic response of a six-story reinforced concrete building -----	91
By James C. Anderson and Vitelmo V. Bertero	
Seismic response of a 42-story building -----	113
By James C. Anderson and Vitelmo V. Bertero	
A summary of unreinforced masonry building damage patterns—Implications for improvements in loss-estimation methodologies -----	141
By Bret Lizundia, Weimin Dong, William T. Holmes, and Robert Reitherman	
Housing repair and reconstruction after the earthquake ---	161
By Mary C. Comerio	
Impact of the earthquake on habitability of housing units -----	169
By Jeanne B. Perkins and Ben Chuaqui	

THE LOMA PRIETA, CALIFORNIA, EARTHQUAKE OF OCTOBER 17, 1989: PERFORMANCE OF THE BUILT ENVIRONMENT

BUILDING STRUCTURES

INTRODUCTION

By Mehmet Çelebi,
U.S. Geological Survey

Several approaches are used to assess the performance of the built environment following an earthquake—preliminary damage surveys conducted by professionals, detailed studies of individual structures, and statistical analyses of groups of structures. Reports of damage that are issued by many organizations immediately following an earthquake play a key role in directing subsequent detailed investigations. Examples of these preliminary studies for the Loma Prieta earthquake are the readily available excellent reports cited below:

Astaneh, A., Bertero, V., Bolt, B., Mahin, S., Moehle, J., and Seed R., 1989, Preliminary report on the seismological and engineering aspects of the October 17, 1989 Santa Cruz (Loma Prieta) earthquake: University of California, Berkeley/Earthquake Engineering Research Center Report 89/14, October 1989, 51 p.

Benuska, L., ed., 1990, Earthquake spectra: Loma Prieta Earthquake Reconnaissance Report, May 1990, v. 6 (supp.), 448 p.

Housner, G.W., Chairman, and Thiel, C.C., ed., 1990, Competing against time: Report to the Governor of California from the Governor's Board of Inquiry on the 1989 Loma Prieta earthquake, 264 p.

Lew, H.S., ed., 1990, Performance of structures during the Loma Prieta earthquake of October 17, 1989: U.S. Dept. of Commerce, National Institute of Standards and Technology, National Institute of Standards and Technology Special Publication 778 (ICSSC TR11), 201 p.

Bay Area Regional Earthquake Preparedness Project (BAREPP) and Federal Emergency Management Agency (FEMA), 1990, Putting the pieces together—the Loma Prieta earthquake one year later, in Proceedings of a national conference, Oct. 15-18, 1990: 253 p.

Earthquake Engineering Research Institute, 1989, Loma Prieta earthquake of October 17, 1989—Preliminary reconnaissance report: Earthquake Engineering Research Institute Report 89-03, 51 p.

Plafker, G., and Galloway, J., eds., 1989, Lessons learned from the Loma Prieta, California, earthquake of Octo-

ber 17, 1989: U.S. Geological Survey Circular 1045, 48 p.

Detailed studies of individual structures and statistical analyses of groups of structures may be motivated by particularly good or bad performance during an earthquake (see table 1). Beyond this, practicing engineers typically perform stress analyses to assess the performance of a particular structure to vibrational levels experienced during an earthquake. The levels may be determined from recorded or estimated ground motions; actual levels usually differ from design levels. If a structure has seismic instrumentation to record response data, the estimated and recorded response and behavior of the structure can be compared. Following the Loma Prieta earthquake, the two reports listed below played an important role in providing information on recorded ground and structural response:

Maley, R., Acosta, A., Ellis, F., Etheredge, E., Foote, L., Johnson, D., Porcella, R., Salsman, M., and Switzer, J., 1989, U.S. Geological Survey strong-motion records from the Northern California (Loma Prieta) earthquake of October 17, 1989, U.S. Geological Survey Open-File Report 89-568, 85 p.

Shakal, A.F., Huang, M., Reichle, M., Ventura, C., Cao, T., Sherburne, R., Savage, R., Darragh, R., and Petersen, C., 1989, CSMIP strong-motion records from the Santa Cruz Mountains (Loma Prieta), California, earthquake of 17 October 1989: California Office of Strong Motion Studies Report 89-06, 196 p.

These reports are issued by two organizations that have established structural instrumentation programs: the California Strong Motion Instrumentation Program (CSMIP) of the California Division of Mines and Geology (CDMG) of the State of California and the National Strong Motion Program of the United States Geological Survey (USGS).

The paper in this volume by Çelebi provides an extensive summary of studies of recorded responses for instrumented structures in the San Francisco Bay area. Such studies constitute an integral part of earthquake-hazard-reduction programs leading to improved design/analyses procedures. In addition to the aim of studying recorded responses for buildings and other structures to improve

Table 1. Papers presented in this volume categorized as detailed investigations and statistical summaries

Author(s)	Title of paper
Detailed Investigations	
Çelebi	Performance of building structures—A summary
Wood	Measured response of two tilt-up buildings
Anderson and Bertero	Seismic response of a six-story reinforced concrete building
Anderson and Bertero	Seismic response of a 42-story building
Statistical Summaries	
Lizundia and others	A summary of unreinforced masonry building damage patterns—Implications for improvements in loss-estimation methodologies
Comerio	Housing repair and reconstruction after the earthquake
Perkins and Chuaqui	Impact of the earthquake on habitability of housing units

design/analyses procedures, a second motivation for studying the Loma Prieta earthquake response data from instrumented structures is that the probability of magnitude 7 or larger earthquakes occurring in the San Francisco Bay Area from major faults, including the San Andreas and Hayward faults, is considered to be approximately 67 percent or higher within a 30-year period (Working Group, 1990). Furthermore, for the tall buildings in San Francisco and vicinity, epicenters of these expected earthquakes may be closer than the distances to the Loma Prieta epicenter. These buildings may thus be subjected to motions larger and different from those recorded during the Loma Prieta earthquake. Therefore, studies of this type will help to better predict the performance of structures during future earthquakes. Furthermore, a considerable number of these tall buildings are on soft soil sites in San Francisco and vicinity, which provides an opportunity to assess their responses and design parameters under amplified motions. The paper summarizes numerous studies of recorded response data from instrumented structures that have been published to date. Also, the paper includes references to the low-amplitude (ambient) vibration testing of five buildings that also recorded the Loma Prieta earthquake.

The paper by Wood and Hawkins investigate the seismic behavior of two tilt-up buildings (a two-story building in Milpitas and a one-story building in Hollister), both built within the 10 years prior to the earthquake. Both buildings are within 50 km from the epicenter and recorded similar responses despite the fact that they were constructed by different methods. The authors report that the transverse accelerations at the center of the roof of each building were approximately three times that at the base of the buildings. The significance of this study is that design provisions of tilt-up buildings must be improved so that the flexibility of diaphragms is decreased. Similar studies and changes made in the building codes (for example, Uniform Building Code, 1991) are included in the paper by Çelebi.

Anderson and Bertero present studies of 6-story and 42-story buildings that had recorded response data. They developed three-dimensional, linear elastic models for both buildings and studied their responses. In the case of the 6-story building, under recorded Loma Prieta base motions the models confirm that limited inelastic behavior takes place, as was observed in the actual inspection of the building following the earthquake. They report that the 42-story building remained elastic during the earthquake. They attribute this to the fact that the designers of the building opted to use a site-specific design-response spectra range that was more conservative than the code minimum requirements.

Lizundia and others studied the performance of unstrengthened, unreinforced masonry (URM) bearing-wall buildings damaged during the earthquake from a data base of 4,800 such buildings. The results are compared with those from data bases of past earthquakes and correlated with intensity scales. They present a loss estimation methodology using the correlated results.

Perkins and Chuaqui studied the impact of the earthquake on 16,000 housing units in the San Francisco and Monterey areas that were assessed to be uninhabitable—defined as unable to be occupied due to structural problems. The data set was collected by telephone and in-person interviews with additional effort to quantify other characteristics of the units (such as the age and type of construction). Using models designed to provide estimates of a number of uninhabitable units, they produced such estimates for the San Francisco Bay area and Monterey areas for future earthquake scenarios. These estimates are important in directing efforts to retrofit vulnerable structures.

Comerio also studied housing losses that occurred as a result of the earthquake and consequent attempts to provide emergency, temporary, and housing recovery service in the San Francisco, Oakland, Santa Cruz, and Watsonville areas. She makes specific recommendations on how Federal, state and local governments can improve

recovery services. These recommendations are (1) postearthquake housing recovery requires planning, (2) existing recovery programs should be streamlined to expedite services, and (3) housing recovery programs will be most effective if they are administered at the local level.

REFERENCES CITED

- Uniform Building Code, 1991, International conference of building officials: Whittier, Calif., 1050 p. (and other editions).
- Working Group on California Earthquake Probabilities, 1990, Probabilities of large earthquakes in the San Francisco Bay Region, California: U.S. Geological Survey Circular 1053, 51 p.

**THE LOMA PRIETA, CALIFORNIA, EARTHQUAKE OF OCTOBER 17, 1989:
PERFORMANCE OF THE BUILT ENVIRONMENT**

BUILDING STRUCTURES

PERFORMANCE OF BUILDING STRUCTURES—A SUMMARY

By Mehmet Çelebi,
U.S. Geological Survey

CONTENTS

Abstract -----	Page
Introduction -----	C5
Methods of analyses -----	5
Response of reinforced concrete buildings -----	10
Pacific Park Plaza (Emeryville) -----	11
Six-story office building (San Bruno) -----	17
Response of steel structures -----	20
Transamerica Building (San Francisco) -----	20
Embarcadero Building (San Francisco) -----	28
Santa Clara County office building (San Jose) -----	45
Chevron Building (San Francisco) -----	52
Mixed construction -----	55
California State University [Hayward] Administration Building (Hayward) -----	55
Two-story office building (Oakland) -----	62
Tilt-up buildings and buildings with flexible diaphragms -----	63
Buildings with new technologies -----	67
Low-amplitude testing -----	67
Other studies -----	71
Pounding -----	71
Masonry buildings -----	71
Overturning forces -----	71
Code assessment and serviceability requirements -----	71
Soil-pile-structure interaction -----	72
Trends in behavior of regular buildings -----	72
Conclusions -----	72
References cited -----	74

ABSTRACT

The purpose of this paper is to summarize studies of the performance of building structures during the earthquake. The majority of studies summarized herein are of those buildings which were instrumented prior to the earthquake and whose responses were recorded during the earthquake. Planning for, acquiring, and studying the recorded responses of building structures is an important part of earthquake-hazard-reduction programs. Such studies help in forecasting performance during future events and therefore are essential for mitigation efforts. Furthermore, such studies facilitate confirmation and improvement of design and analyses methods.

There is as great a variation in the type of buildings studied as there is in their performance. In this summary,

the studies reflect, in varying detail, those issues related to the design and/or analyses methods. The dynamic characteristics of the buildings, if identified, have been included. The behavior of the buildings is discussed in terms of translational and torsional modal characteristics and actions such as soil-structure interaction (translational, rotational or rocking, and radiation damping), drift ratios, and resonance (or combination thereof) exhibited and identified from the recorded responses. Specific conclusions that are derived from the studies are also summarized.

Included in the paper are summaries of some specific studies of performance characteristics such as pounding based on observations made following the earthquake.

INTRODUCTION

Studies of recorded responses of instrumented structures constitute an integral part of earthquake-hazard-reduction programs leading to improved design/analyses procedures. The California Strong-Motion Instrumentation Program (CSMIP) of the California Division of Mines and Geology (CDMG) of the State of California and the National Strong Motion Program of the United States Geological Survey (USGS) have established structural instrumentation programs to measure structural responses to earthquakes. While these programs are prominent, other institutions and private owners have also instrumented structures throughout the continental United States, Alaska, Hawaii, and Puerto Rico.

During the earthquake the response of numerous buildings and other structures throughout the San Francisco Bay area, Santa Cruz, and vicinity were recorded. Summaries of strong-motion records retrieved by CDMG and USGS from different types of structures and ground stations are provided by Shakal and others (1989) and Maley and others (1989). A summary of records from instrumented buildings (only) are provided in table 1, which lists 5 buildings instrumented by USGS and 23 by CSMIP. Although there are records from buildings instrumented privately by their owners, they are not included in the table because the data from such structures are not generally available. Buildings instrumented by owners

Table 1.—Summary of instrumented buildings that recorded the earthquake

Epicentral distance(km)	Building description	Number of channels	Peak acceleration (g) (horizontal)	Organization
96	Pacific Park Plaza, 633 Christie Ave., Emeryville ; 30 stories, symmetrical, three-winged reinforced concrete (on bay mud)	24+3 FF FF=Free-Field	FF(0.26 g) Ground (0.22 g) Roof wing (0.39 g)	USGS
74	Hayward City Hall; 11-story, reinforced concrete framed structure (on consolidated alluvium)	12+6 FF	FF(0.10 g) Ground(0.07 g) 12th floor (0.13 g)	USGS
99	Great Western Bldg., 2168 Shattuck Ave., Berkeley; reinforced concrete core, truss structure at roof supports the suspended floors (on stiff soil)	18	Basement (0.11g) 13th floor (0.23 g)	USGS
96	Chevron Bldg., 575 Market St., San Francisco; 41-story, moment-resisting steel framed structure on precast piles	14	Basement (0.11 g) 25th floor (0.23 g)	USGS
97	Transamerica Bldg.; 48-story+204 ft tower steel framed on 9 ft basemat (on stiff soil)	22	Basement (0.11 g) 49th floor (0.31 g)	USGS
18	4-story concrete bldg., Watsonville (CSMIP No. 47459)	13	Ground (0.39 g) Roof (1.24 g)	CSMIP
21	3-story steel bldg., San Jose (57562)	10	Ground (0.28 g) Roof (0.67 g)	CSMIP
27	1-story gymnasium, West Valley College, Saratoga (58235)	11	Ground (0.33 g) Roof (0.87 g)	CSMIP
28	2-story historic commercial building, Gilroy (57476)	6	Ground (0.25 g) Roof (0.99 g)	CSMIP
48	1-story warehouse, Hollister (47391)	13	Ground (0.18 g) Roof (0.82 g)	CSMIP
33	10-story concrete residential bldg., San Jose (57356)	13	Ground (0.13 g) Roof (0.37 g)	CSMIP
33	10-story concrete commercial bldg., San Jose (57355)	13	Ground (0.11 g) Roof (0.38 g)	CSMIP
35	13-story, steel, Santa Clara County Office Bldg., San Jose (57357)	22	Ground (0.11 g) Roof (0.36 g)	CSMIP
50	2-story masonry office bldg., Palo Alto (58264)	7	Ground (0.21 g) Roof (0.55 g)	CSMIP
57	3-story concrete school office bldg., Redwood City (58263)	6	Ground (0.09 g) Roof 0.17 g)	CSMIP
65	2-story concrete office bldg., Belmont (58262)	7	Ground (0.11 g) Roof (0.20 g)	CSMIP
81	9-story concrete government office bldg., San Bruno (58394)	16	Ground (0.16 g) Roof (0.36 g)	CSMIP
81	6-story office bldg., San Bruno (58490)	13	Ground (0.14 g) Roof (0.46 g)	CSMIP
85	4-story steel hospital bldg, So. San Francisco (58261)	11	Ground (0.15 g) Roof (0.68 g)	CSMIP
95	6-story, concrete UCSF bldg., San Francisco (58479)	13	Ground (0.09 g) Roof (0.28 g)	CSMIP

Table 1.—Continued.

Epicentral distance(km)	Building description	Number of channels	Peak acceleration (g) (horizontal)	Organization
95	18-story, steel/concrete, commercial bldg., San Francisco (58480)	13	Ground (0.14 g) Roof (0.27 g)	CSMIP
96	47-story steel office bldg., San Francisco (58532)	18	Ground (0.20 g) Roof (0.48 g)	CSMIP
124	3-story steel/concrete office bldg., San Rafael (68341)	16	Ground (0.04 g) Roof (0.13 g)	CSMIP
171	14-story concrete residential bldg., Santa Rosa (68489)	16	Ground (0.06 g) Roof (0.21 g)	CSMIP
172	5-story concrete commercial bldg., Santa Rosa (68387)	16	Ground (0.06 g) Roof (13 g)	CSMIP
43	2-story, tilt-up, industrial bldg., Milpitas (57502)	13	Ground (0.14 g) Roof (0.58 g)	CSMIP
69	6-story concrete office bldg., Hayward (58462)	13	Ground (0.12 g) Roof (0.45 g)	CSMIP
70	13-story steel/concrete CSUH Admin. Bldg., Hayward (58354)	16	Ground (0.09 g) Roof (0.24 g)	CSMIP
70	4-story, concrete, CSUH Science Bldg., Hayward (58488)	16	Ground (0.05 g) Roof (0.18 g)	CSMIP
91	24-story, concrete, residential bldg., Oakland (58483)	16	Ground (0.18 g) Roof (0.38 g)	CSMIP
92	2-story masonry/steel office bldg., Oakland (58224)	10	Ground (0.26 g) Roof (0.69 g)	CSMIP
93	3-story concrete Piedmont Jr. High School., Piedmont (58334)	11	Ground (0.08 g) Roof (0.18 g)	CSMIP
97	2-story steel hospital bldg., Berkeley (58496)	12	Ground (0.12 g) Roof (0.30 g)	CSMIP
98	10-story concrete commercial bldg., Walnut Creek (58364)	16	Ground (0.10 g) Roof (0.25 g)	CSMIP
102	3-story concrete commercial bldg., Pleasant Hill (58348)	12	Ground (0.13 g) Roof (0.24 g)	CSMIP
105	8-story, masonry, residential bldg., Concord (58492)	13	Ground (0.06 g) Roof (0.24 g)	CSMIP
108	3-story, concrete, City Hall, Richmond (58503)	13	Ground (0.12 g) Roof (0.24 g)	CSMIP
112	3-story, steel, office bldg., Richmond (58506)	12	Ground (0.12 g) Roof (0.29 g)	CSMIP

according to the Uniform Building Code (UBC) recommendations also are not included in this table. Figure 1 shows the locations of some of the buildings discussed in this summary relative to the epicenter.

While the primary motivation in studying recorded responses of buildings and other structures is to improve design/analyses procedures, a second motivation for studying the Loma Prieta response data is that the probability of magnitude 7 or larger earthquakes occurring in the San Francisco Bay area from major faults, including the San Andreas and Hayward faults, is considered to be approximately 67 percent or higher within a 30-year period (Working Group, 1990). Furthermore, these earthquakes may originate at distances that are closer to major urban areas

than the 97-km distance of the Loma Prieta event from San Francisco and may generate motions larger than those recorded during Loma Prieta. Therefore, studies of this type will help to better predict the performance of structures during future earthquakes.

A third motivation for these studies is that in the San Francisco Bay area there are several tall buildings on soft soil sites having seismic instrumentation. Records obtained from these buildings are particularly important to evaluate the performance of such structures in response to amplified ground motions and possible soil-structure interaction effects. Figure 1 shows the location of some of the buildings that are covered in this paper and that were subjected to amplified motions during the earthquake at

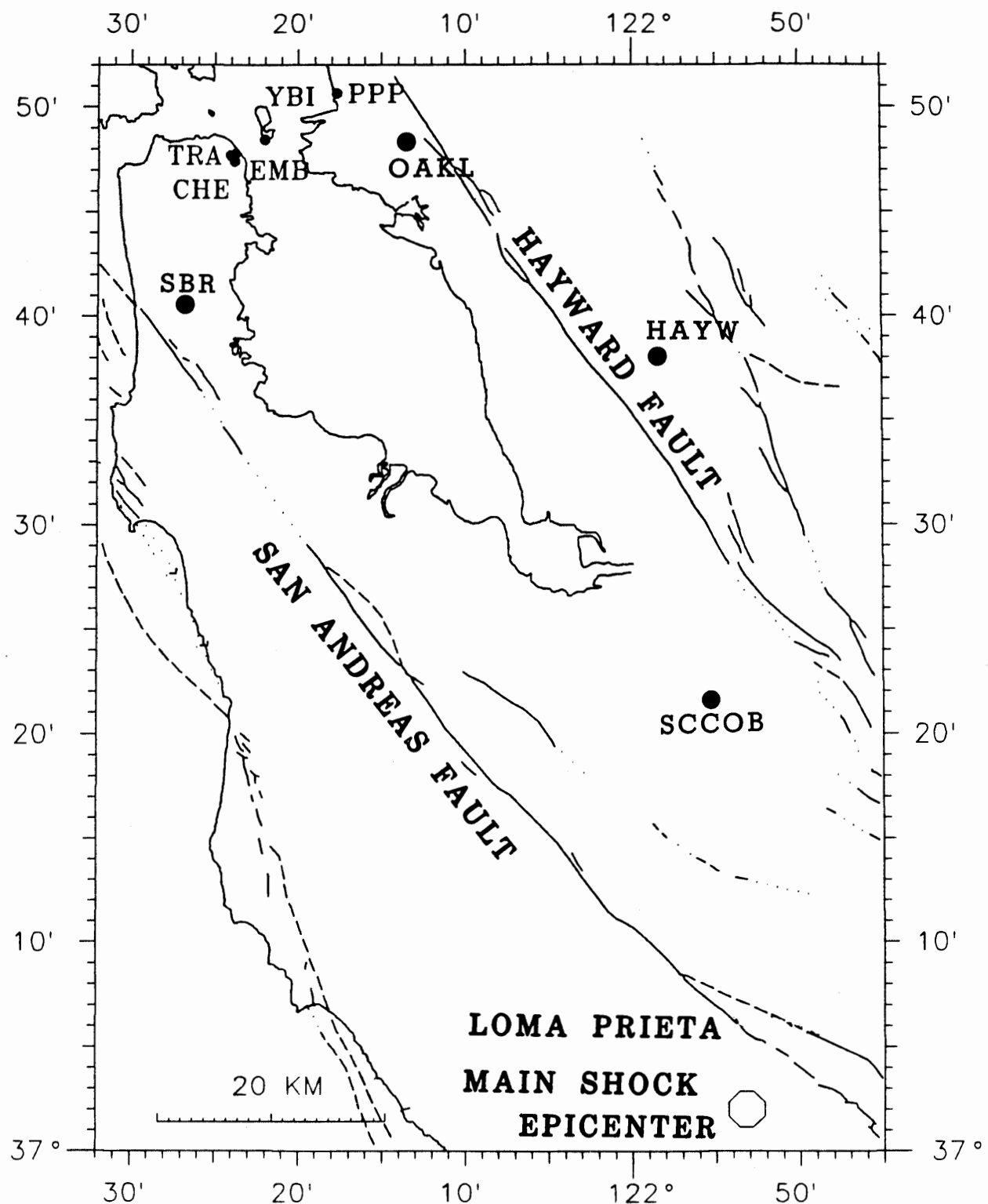


Figure 1.—Location of some instrumented buildings relative to epicenter. Pacific Park Plaza (PPP), Transamerica Building (TRA), Embarcadero Building (EMB), Chevron Building (CHE), two-story building in Oakland (OAKL), California State University (Hayward) (HAYW), Santa Clara County Office Building (SCCOB), Yerba Buena Island (YBI).

approximately 100 km from the epicenter. To demonstrate the degree of amplified motions at these sites during the earthquake, response spectra of ground motions recorded

at dedicated free-field stations in the vicinity or at the ground floor or basement of the four tall buildings are compared (fig. 2) to the spectrum from the station on

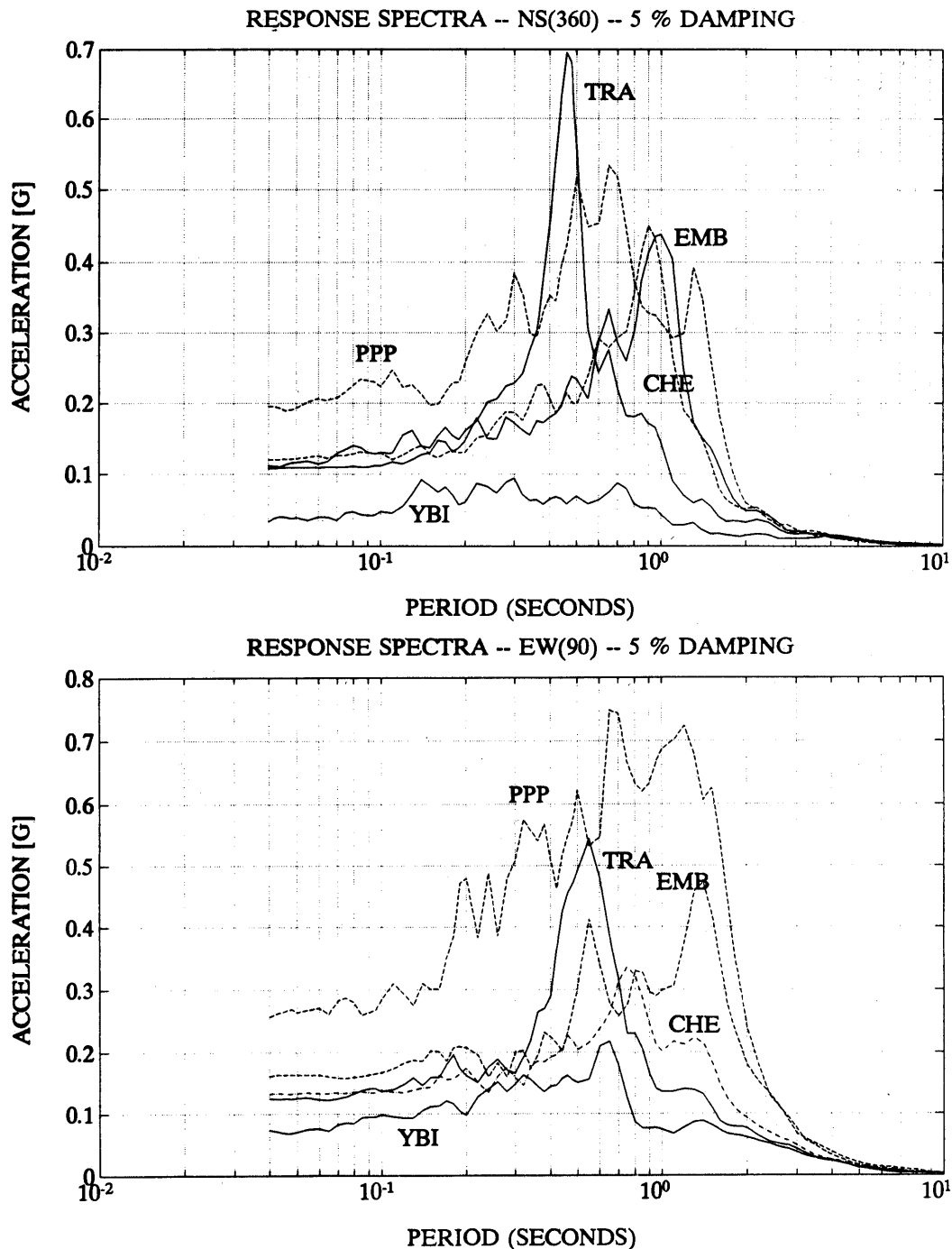


Figure 2.—Response spectra of free-field Emeryville site of Pacific Park Plaza (PPP), Transamerica Building (TRA), Embarcadero Building (EMB), and Chevron Building (CHE) compared to response spectrum of rock site Yerba Buena Island (YBI).

Yerba Buena Island, a rock site, also located at approximately 100 km from the epicenter. While the largest peak acceleration at Yerba Buena Island was 0.06 g, the amplified peak accelerations at the soft soil sites of some of these tall buildings varied between 0.12 and 0.26 g. The response spectra depict the degree of amplification of peak acceleration, represented by zero-period accelerations as well as the frequency (period)-dependent spectral acceleration. Particularly between the periods 0.1 and 2 seconds, which is of engineering interest, the spectral amplification ratio is as high as 5 or 6.

The purpose of this paper is to review and summarize studies of instrumented buildings that recorded the Loma Prieta earthquake. Since the earthquake, almost all of the recorded building response data has been made available by CSMIP and USGS, and a significant number of studies of the data set have been completed. Damage surveys or subsequent related studies of buildings are not within the scope of this paper. For further information of such studies, the readers are referred to the numerous reports published since the earthquake (see Benuska, 1990). Although every effort was made to include summaries of all the studies herein, it is likely that some were not in wide circulation and thus were not available.

Also of interest to the engineering and scientific community is the low-amplitude (ambient) vibration testing of five of the buildings in table 1 (Marshall and others, 1991, 1992; Çelebi and others, 1991, 1993; Çelebi, 1996). The results are summarized later in this paper.

METHODS OF ANALYSES

In studying the recorded responses of buildings and other structures, several methods have been used, including spectral techniques, system identification methods, and finite element modeling and analyses. The spectral analyses are based on Fourier amplitude spectra, autospectra S_x and S_y , cross-spectral amplitudes S_{xy} , and coherence functions (γ) and associated phase angles using the equation from Bendat and Piersol (1980):

$$\gamma^2_{xy}(f) = S_{xy}^2(f) / S_x(f)S_y(f). \quad (1)$$

The procedures used in system identification analyses estimate a model based on observed input-output data (Ljung, 1987). Simply stated, the input is the basement or

ground-floor motion and the output is the roof-level motion or one of the levels where the structural response is detectable. In most of the system identification analyses presented in this paper (for example, Çelebi, 1996), the ARX (acronym meaning AR for autoregressive and X for extra input) model based on the least-squares method for single input-single output (Ljung, 1987) coded in commercially available system identification software was used (The MathWorks, 1988).

The damping ratios are extracted by system identification analyses in accordance with the procedures outlined by Ghanem and Shinozuka (1995) and Shinozuka and Ghanem (1995). These procedures are based on the following equations:

$$\xi = \frac{\delta_j}{\sqrt{\lambda_j^2 + \delta_j^2}} \quad (2)$$

$$\omega_j = \frac{\sqrt{\lambda_j^2 + \delta_j^2}}{\Delta t} \quad (3)$$

where

$$\delta_j = -\ln|z_j|^2 \quad (4)$$

$$\lambda = \arg|z_j| \quad (5)$$

which are readily calculable from results of system identification routines. In this case, z_j is the j -th pole of $S(z)$ which represents the system of linear equations defining the model accepted to represent observations. The poles, z_j , are the positive imaginary part represented by the equation:

$$z_j = e^{(-\xi\omega_j + \omega_j)\sqrt{1-\xi^2}\Delta t} \quad (6)$$

The low-amplitude (ambient) vibration data was analyzed by conventional spectral analysis techniques. System identification techniques were not applied to the ambient vibration data because of the unknown system input characteristics. Furthermore, because of the higher noise-to-signal ratio, system identification techniques do not minimize the errors simply and solutions appear unreliable.

RESPONSE OF REINFORCED CONCRETE BUILDINGS

PACIFIC PARK PLAZA (EMERYVILLE)

The set of records from Pacific Park Plaza is possibly the most studied building response data during this earthquake. The building was constructed in 1983 and instrumented in 1985, is 30 stories, and is the tallest reinforced concrete building in northern California. A general view, a plan view, a three-dimensional schematic, and its instrumentation are shown in figure 3 (Çelebi, 1992, 1996). Twenty-one channels of synchronized uniaxial accelerometers are deployed throughout this structure, with an additional three channels of accelerometers located at the north free-field outside the building. All are connected to central recording systems. In addition, a triaxial strong-motion accelerograph is deployed at a free-field site on the south side of the building (SFF or EMV¹).

The building is an equally spaced three-winged, cast-in-place, ductile, moment-resistant reinforced concrete framed structure. The foundation is a 5-foot-thick concrete mat supported by 828 (14-inch-square) prestressed concrete friction piles, each 20-25 m in length, in a primarily soft-soil environment, with an average shear-wave velocity between 250 and 300 m/s and a depth of approximately 150 m to harder soil. The building had considerably amplified input motions but was not damaged during the earthquake. The east-west components of acceleration recorded at the roof and the ground floor of the structure and at the associated free-field station (SFF in fig. 3B), all at approximately 100 km from the epicenter, are shown in figure 4A. The motion at Yerba Buena Island (YBI), the closest rock site, had a peak acceleration of 0.06 g and is shown in figure 4 to indicate the level of amplified shaking at the free-field site and at the ground floor of the building. The corresponding response spectra are shown in figure 4B. For all three components of acceleration, the calculated response spectra of the south free-field site (SFF or EMV) of Pacific Park Plaza and Yerba Buena Island are compared in figure 4C (Çelebi, 1992). These response spectra show that the motions at EMV were amplified by as much as five times when compared with YBI. This is also inferred by the amplitude of the peak accelerations (0.26 g for EMV and 0.06 g for YBI). Furthermore, the differences in peak acceleration at the free-field station (0.26 g) and that at the ground floor of the building (0.21

g) (fig. 4A) suggest the possibility of significant soil-structure interaction.

The building has been studied in detail by Çelebi and Şafak (1992), Şafak and Çelebi (1992), Anderson and Bertero (1994), Anderson and others (1991), Bertero and others (1992), Kagawa and others (1993), Kagawa and Al-Khatib (1993), Aktan and others (1992), and Kambhatla and others (1992). The predominant response modes of the building and the associated frequencies (periods) [0.38 Hz (2.63 s), 0.95 Hz (1.05 s), and 1.95 Hz (0.51 s)] are identified by all these investigators using different methods, including spectral analyses, system identification techniques, and mathematical models. These three modes of the building are torsionally-translationally coupled (Çelebi, 1996). The frequencies are clearly identified in the cross-spectra (S_{xy}) of the orthogonal records obtained from the roof and ground floor (fig. 5A, B), the south free-field site (SFF) (fig. 5C), and the normalized cross-spectra of the orthogonal records (fig. 5D). A site



Figure 3.—A, Pacific Park Plaza. B, Plan layout and three-dimensional schematic of Pacific Park Plaza showing dimensions and strong-motion instrumentation (Çelebi, 1992, 1996).

¹In most studies, the site of the south free-field (SFF) is referred to as the Emeryville site (EMV). The data from this site is one of the most-used ground motion records from the Loma Prieta strong-motion data set.

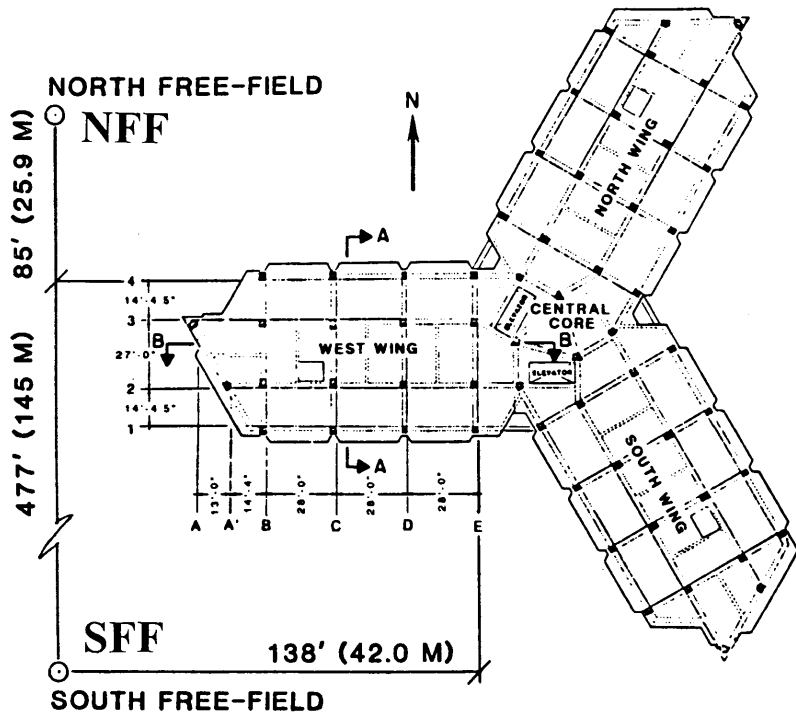
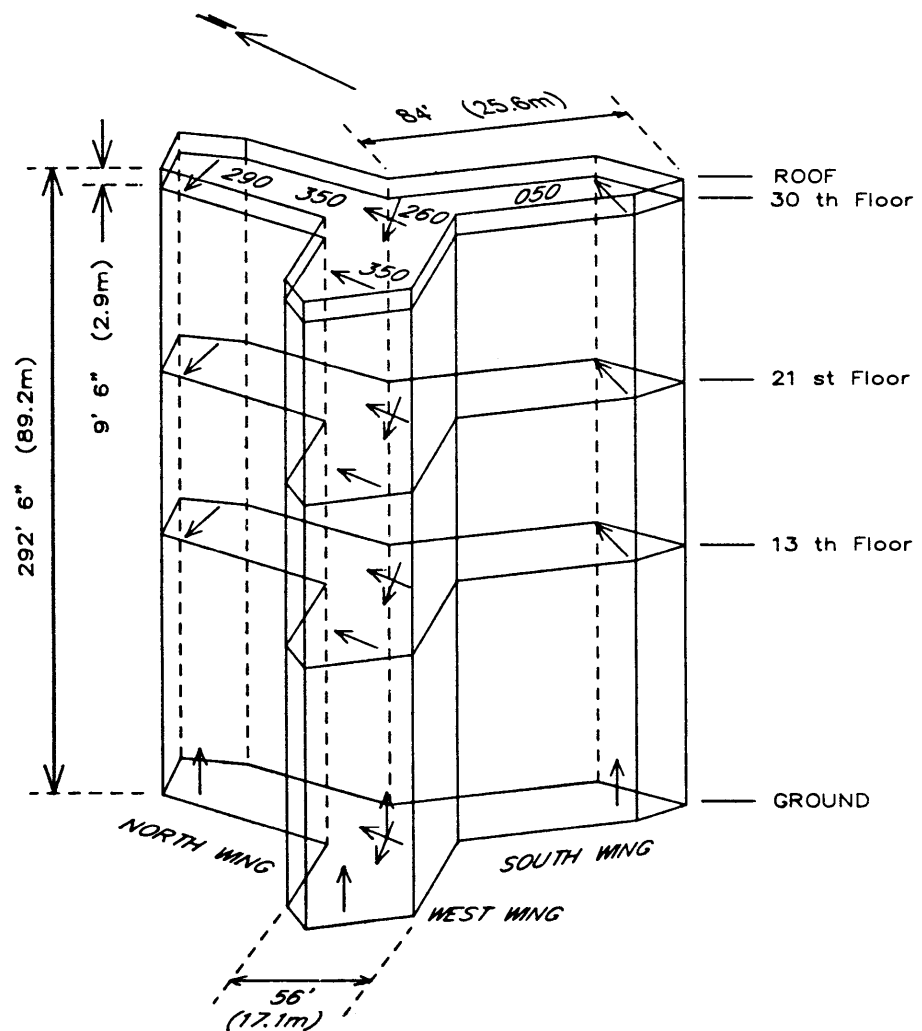
**B**

Figure 3.—Continued.

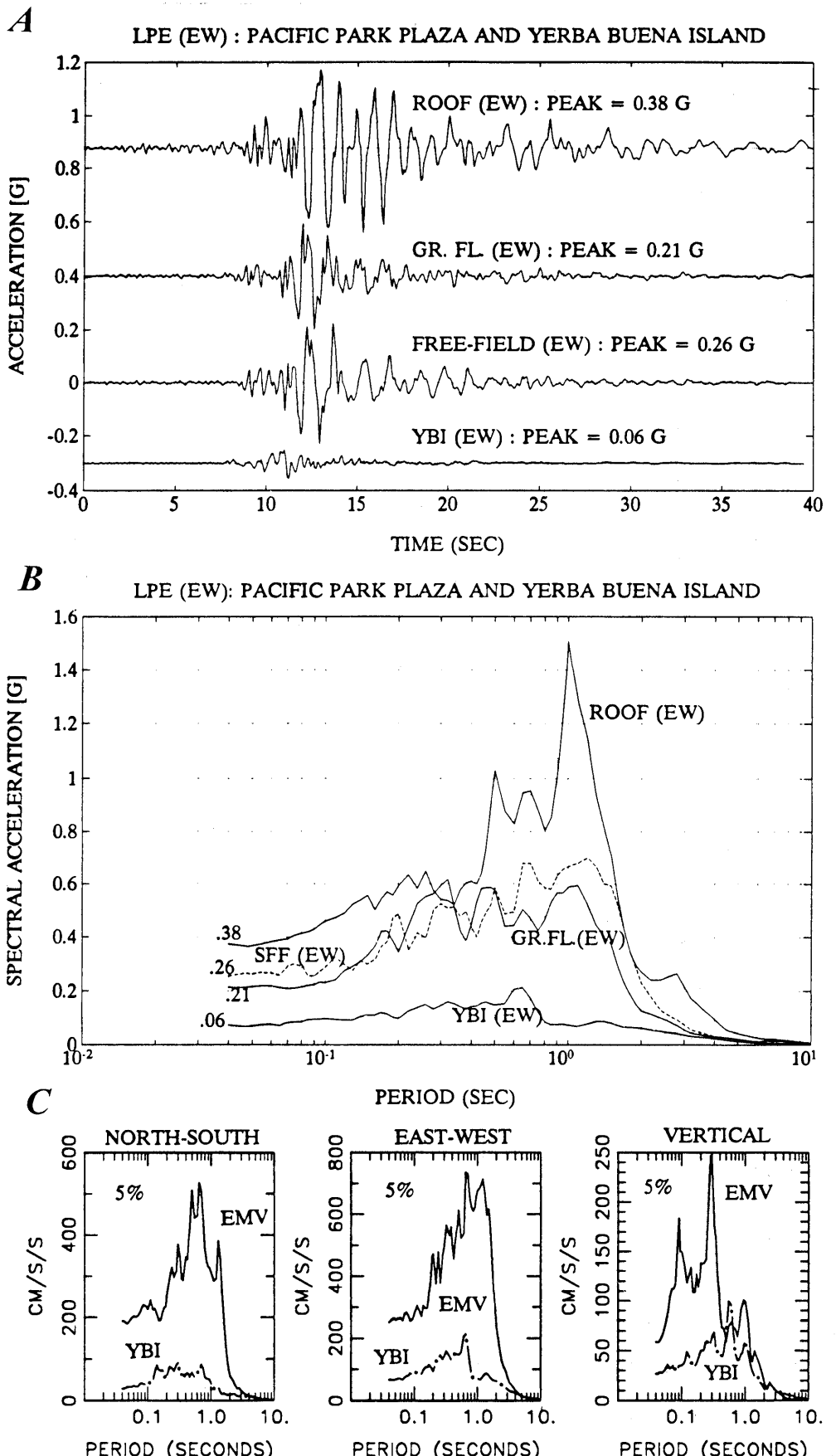


Figure 4.—*A*, Loma Prieta earthquake (LPE) east-west components of acceleration recorded at roof, ground floor, and south free-field (SFF) station of Pacific Park Plaza. Also shown is east-west component of acceleration at Yerba Buena Island (YBI). *B*, Response spectra of motions. *C*, response spectra of all three components of acceleration at south free-field (EMV) compared with YBI.

frequency at 0.7 Hz (1.43 s) is also identified. The peak at 0.7 Hz that appears in the cross-spectrum of the roof (fig. 5A) appears as the dominant peak in the cross-spectra of the ground floor and the south free-field (SFF) (figs. 5B, C). When the normalized cross-spectra are calculated for the ground floor and free-field, the site frequency at 0.7 Hz is distinguishable from the structural frequencies in the normalized cross-spectrum of the roof (fig. 5D). The

0.7-Hz site frequency is further confirmed by the transfer function (fig. 6) calculated by using Haskell's shear-wave propagation method (Haskell, 1953, 1960) and site characterization information by Gibbs and others (1994). The figure shows the transfer function and the variation of shear-wave velocities with depth. The depth to bedrock has been adopted from a map by Hensolt and Brabb (1990) as 150 m (~500 ft).

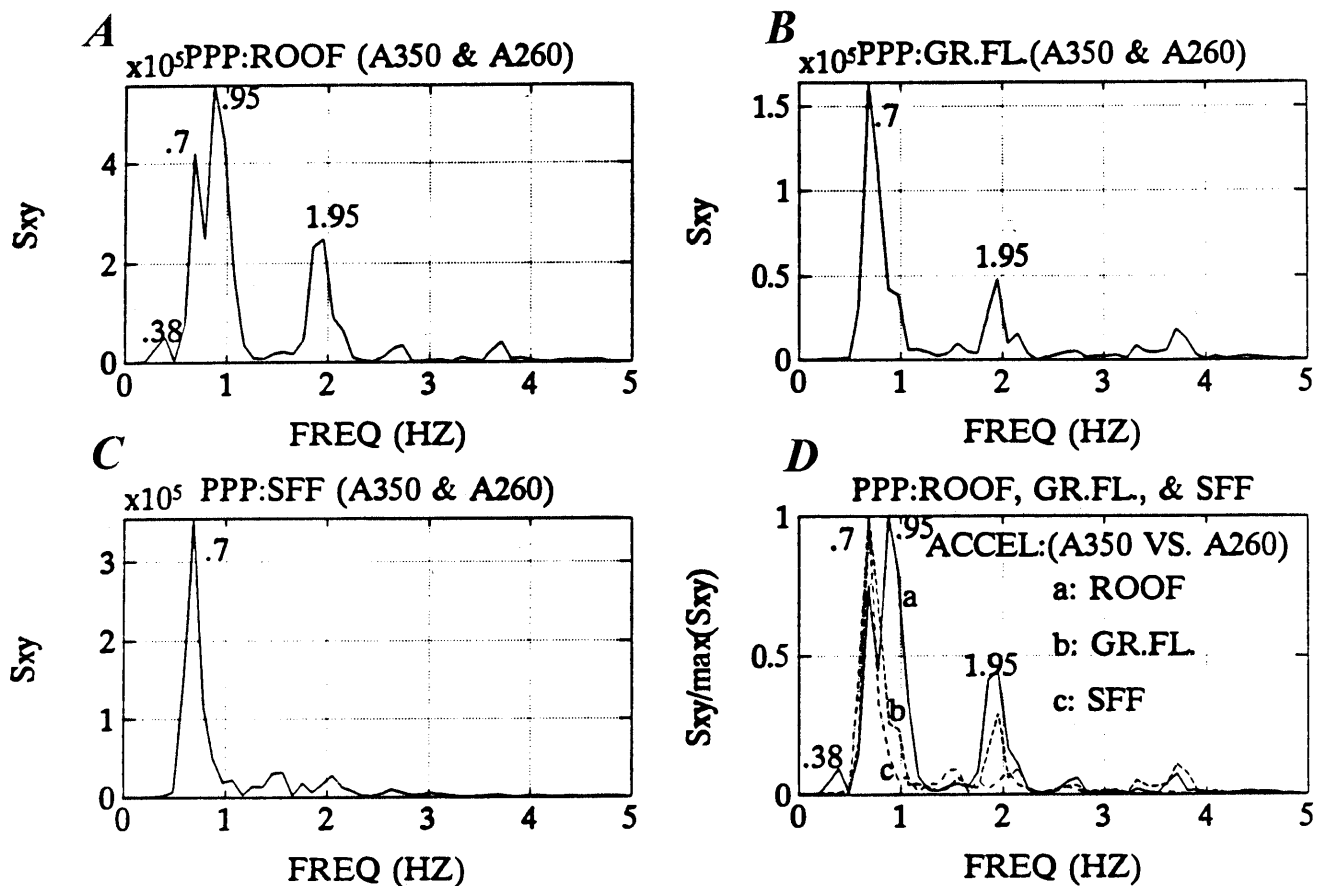


Figure 5.—Cross-spectra of accelerations at (A) roof, (B) ground floor, and (C) south free-field (SFF). Normalized cross spectra (D) show site frequency 0.7 Hz at ground floor and SFF but not at roof.

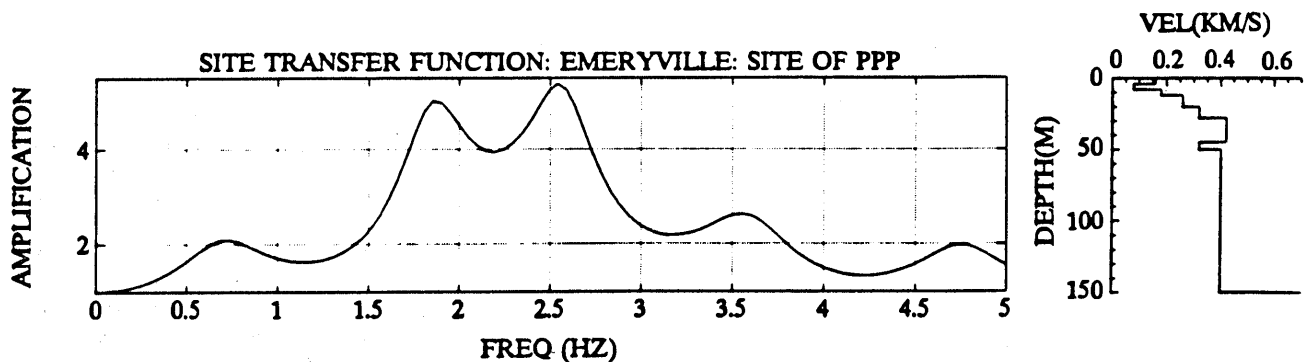


Figure 6.—Site transfer function of Pacific Park Plaza indicates first peak at 0.7 Hz.

Figure 7 shows the results of applying the system identification technique. The match between the observed and calculated response is excellent, as evidenced by comparison of the calculated and observed responses at the

top floor and by comparison of the amplitude spectra of these responses. The damping ratios extracted from the system identification analyses corresponding to the 0.38-Hz first-mode frequency are 11.6 percent (north-south)

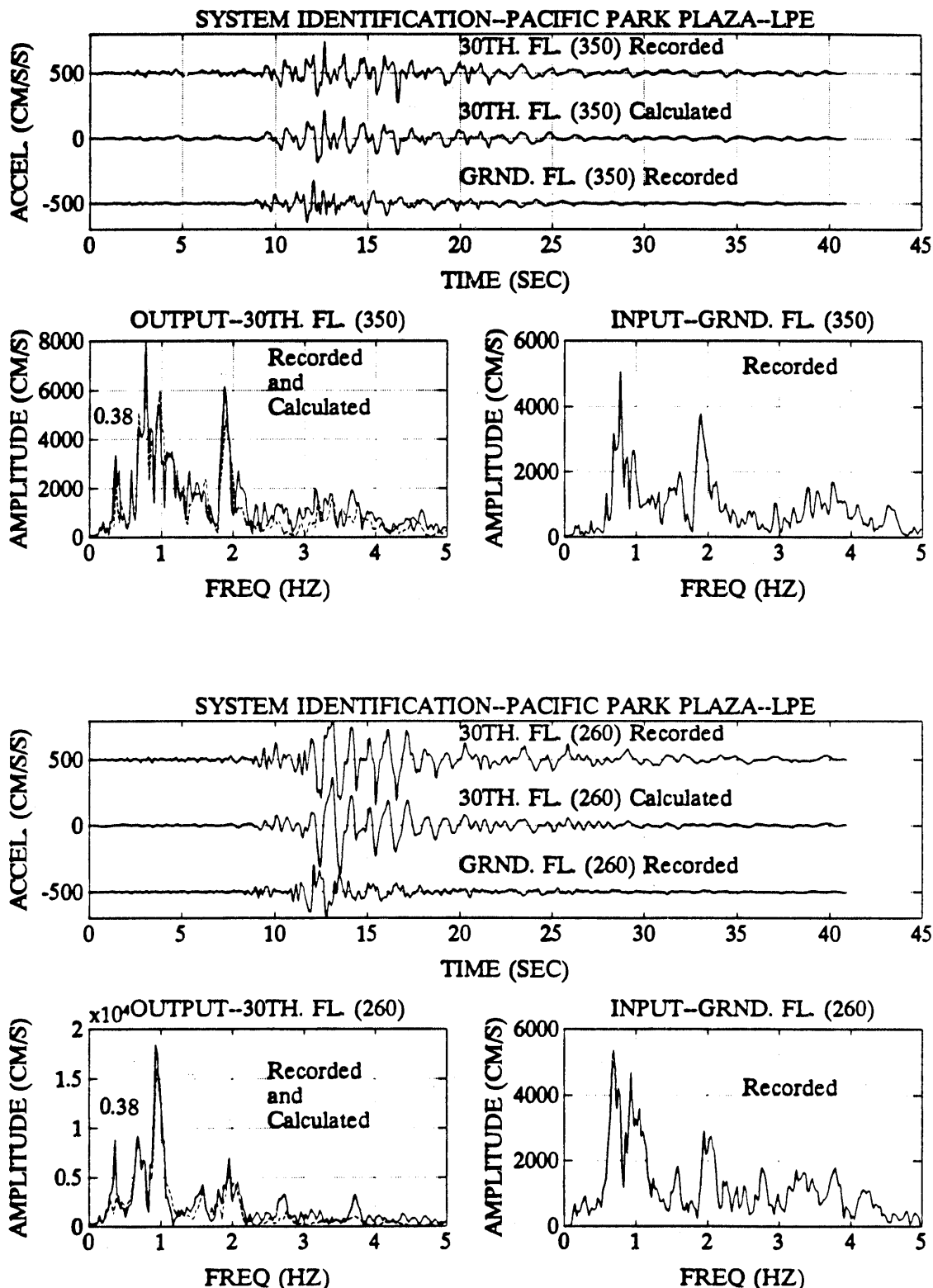


Figure 7.—System identification applied with accelerations recorded at roof and ground floor of Pacific Park Plaza.

Table 2.—*Summary of dynamic characteristics for Pacific Park Plaza*

[-- not available]

	Frequencies (Hz)			Damping (percent)		
	MODE			MODE		
	1	2	3	1	2	3
1990 AMBIENT TESTS (from Çelebi, Phan, and Marshall, 1993)						
N-S	0.48	---	---	0.6	---	---
E-W	0.48	---	---	3.4	---	---
1989 (LPE) STRONG-MOTION TESTS (from Çelebi, Phan, and Marshall, 1993)						
N-S	0.38	0.95	1.95	11.6	---	---
E-W	0.38	0.95	1.95	15.5	---	---
1985 FORCED VIBRATION TESTS (from Stephen and others, 1985)						
N-S	0.590	1.660	3.09	1.7	1.3	2.9
E-W	0.595	1.675	3.12	1.8	1.9	3.2
Torsion	0.565	1.700	3.16	1.5	1.32	1.7
1985 AMBIENT VIBRATION TESTS (from Stephen and others, 1985)						
N-S	0.586	1.685	3.149	2.6	1.8	0.8
E-W	0.586	1.685	3.125	2.6	1.2	0.4
Torsion	0.586	1.709	3.125	3.8	1.4	1.0
MODAL ANALYSES [rigid (R) and flexible (F) foundation] (from Stephen and others, 1985)						
N-S	R F	0.596 0.595	1.666 1.650	3.115 3.081		
E-W	R F	0.596 0.595	1.666 1.650	3.115 3.081		
Torsion	R F	0.565 0.562	1.711 1.686	3.275 3.220		

and 15.5 percent (east-west) (Çelebi, 1996). Such unusually high damping ratios attributed to a conventionally designed/constructed building require explanation. The building with its large mat foundation in a relatively soft geotechnical environment is capable of energy dissipation in the soil due to radiation (or foundation) or material damping. The subject of radiation damping for this building has been discussed in detail by Çelebi (1996).

The dynamic characteristics determined from Loma Prieta response records of Pacific Park Plaza as well as those determined from low-amplitude tests prior to (Stephen and others, 1985) and after the earthquake (Marshall and others, 1992; Çelebi and others, 1993) are summarized in table 2. These low-amplitude tests will be discussed later in this paper; however, it is important to note that there are significant differences in the dynamic characteristics of the building that were derived from the strong (Loma Prieta) shaking data and from the low-amplitude data. Also, it is noted in table 2 that although flexibility of the foundation was considered in the 1985 analyses, the structural frequency remained the same as the frequency determined with fixed base assumption. The differences in the frequencies for strong- and low-amplitude motions are attributed to soil-structure interaction (SSI), as studied from the records and mathematical modeling (Çelebi and Şafak, 1992; Şafak and Çelebi, 1992; Kagawa and others, 1993; Kagawa and Al-Khatib, 1993; Aktan and others, 1992; Kambhatla and others, 1992). A study of the building for dynamic-pile-group interaction by (Kagawa and Al-Khatib, 1993; Kagawa and others, 1993) indicates that there is significant interaction. The study shows that computed responses of the building using state-of-the-art techniques for dynamic-pile-group interaction compares well with the recorded responses.

Anderson and others (1991) and Anderson and Bertero (1994) compared the design criteria, code requirement, and the elastic and nonlinear dynamic response due to the earthquake. They also compared current U.S. and Japanese design procedures and requirements for this type of building and analyzed probable performance under more severe base motions. In order to achieve these objectives, linear elastic and nonlinear dynamic response analyses were conducted using both simplified and detailed analytical models. The results have been compared with Japanese design procedures. Contrary to others, the authors conclude that soil-structure interaction was insignificant for Pacific Park Plaza during the earthquake.

The response of the building was also found to be sensitive to the dominant orientation of the maximum energy of Loma Prieta ground motions. For this building, the orientation was similar to the rupture direction of the earthquake. A significant effect of the orientation of the ground motion for an unsymmetrical three-winged building such as Pacific Park Plaza was that it exhibited a disproportionate (as much as three times) response in one wing of the building compared to another, as shown in figure 8 (Çelebi, 1992). Therefore, the propagation direction of different waves (in most cases, surface waves) arriving at a building can be significant. As a general conclusion, because the energy of the ground motions can be azimuthally variable, structures with wings or unsymmetrical structures can be significantly affected by it.

SIX-STORY OFFICE BUILDING (SAN BRUNO)

A general view and the instrumentation scheme a six-story, reinforced concrete framed building in San Bruno (SBR) is shown in figure 9 (Çelebi, 1996). The building is rectangular in plan and has four moment-resistant frames in the exterior and one in the interior in the transverse direction (355°). Anderson and Bertero (this chapter) developed three-dimensional, linear elastic models of the building and studied its response under recorded base motions and code-prescribed lateral forces. They reported that under Loma Prieta motions the models confirmed limited inelastic behavior, as was observed in the building following the earthquake.

Phan and others (1994) also studied the building by using a mathematical model with a fixed base and with springs simulating soil-structure interaction effects. Their analyses showed that the frequency of the building determined from Loma Prieta response data (0.98 Hz, north-south, and 1.17, east-west) was approximately 69 percent of the frequency determined from ambient test data (1.41 Hz, north-south, and 1.72 Hz, east-west) (Marshall and others, 1991, 1992; Çelebi and others, 1991, 1993, Çelebi, 1996). Furthermore, the frequency determined from ambient vibration data matches the analysis results of the model with a fixed base. On the other hand, the Loma Prieta frequency matched the results of the model with soil-structure interaction springs. They concluded that soil-structure interaction plays a significant role in the response of this building.

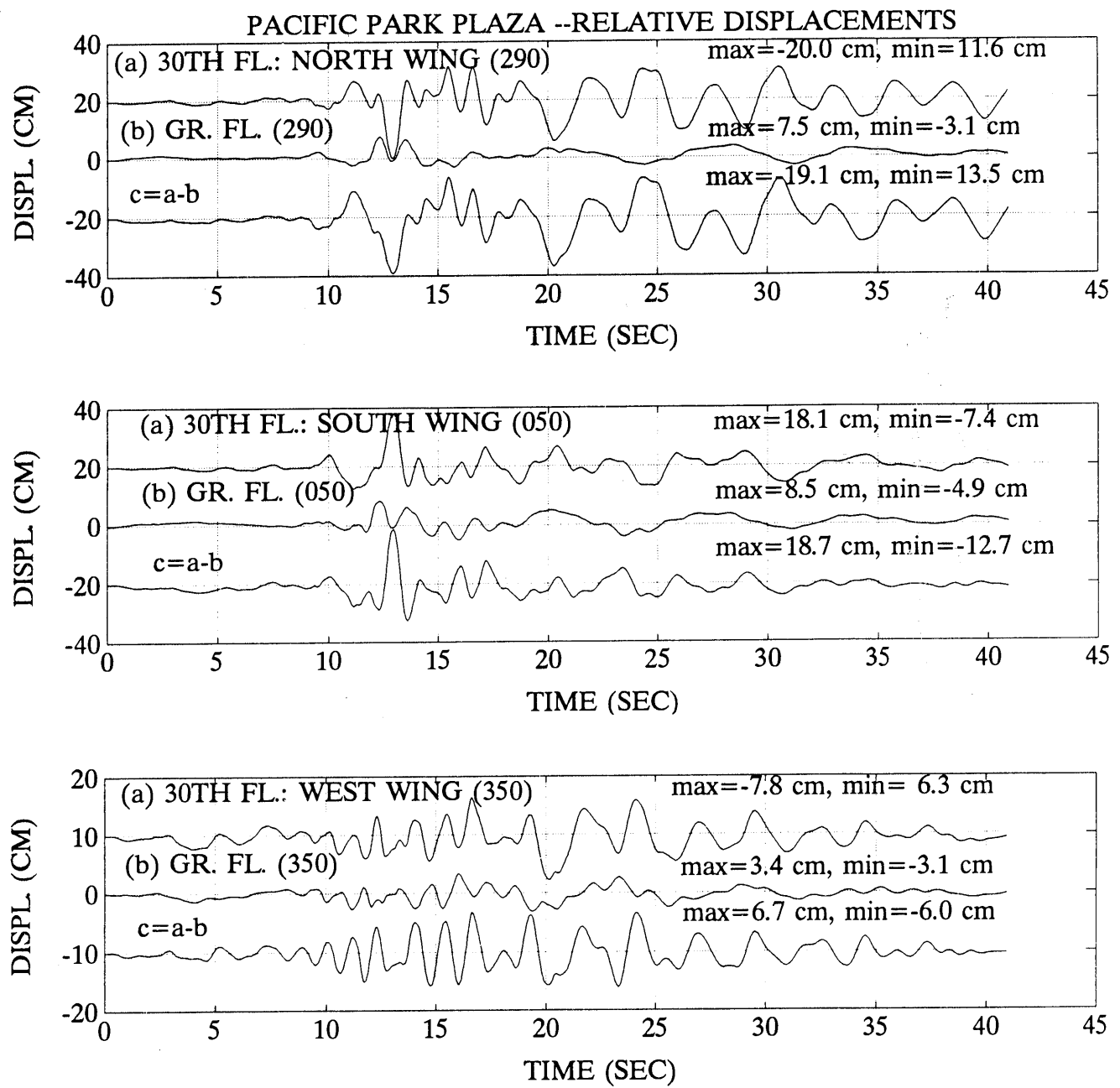


Figure 8.—Relative displacements at the wings of 30th floor of Pacific Park Plaza.

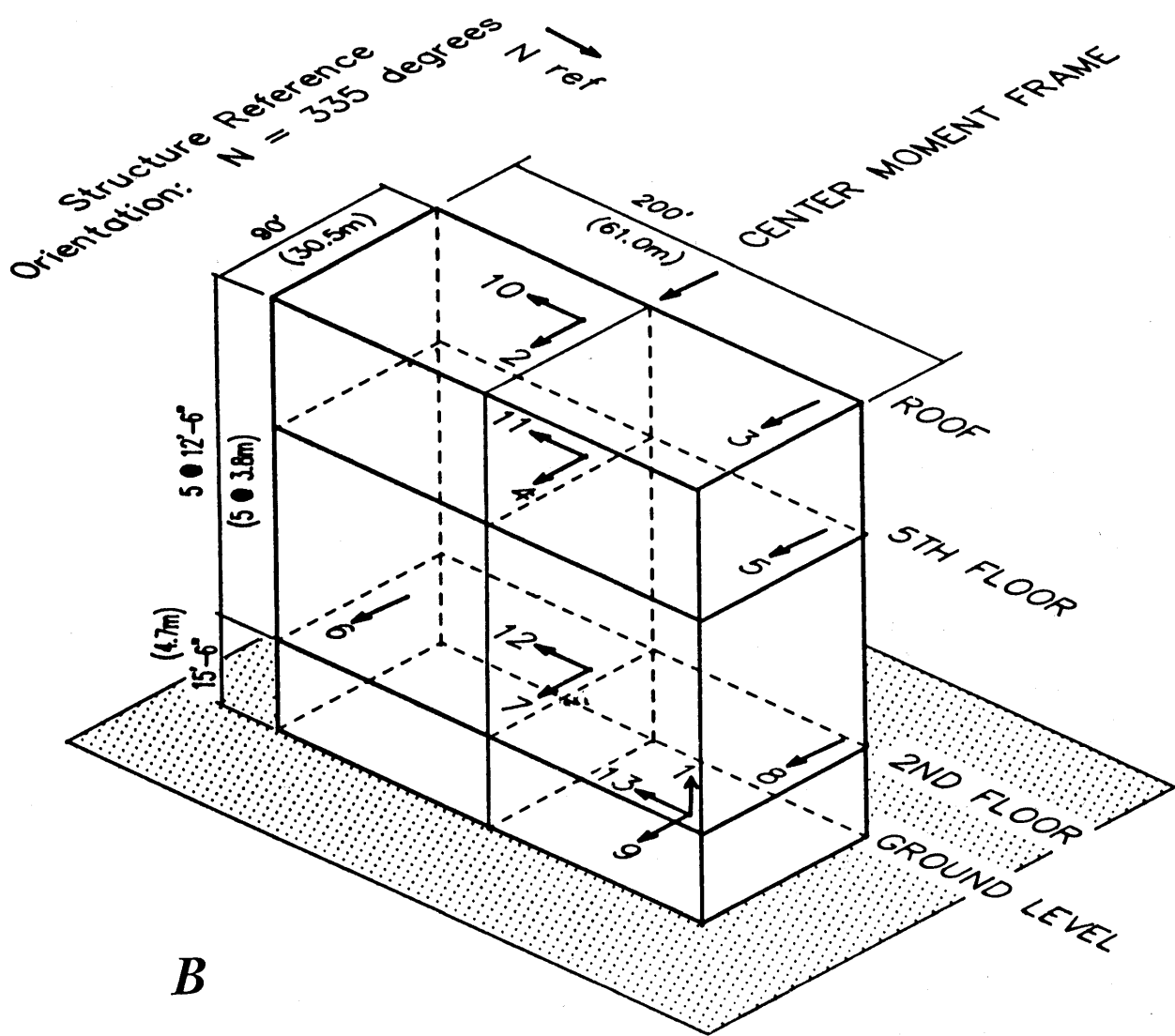
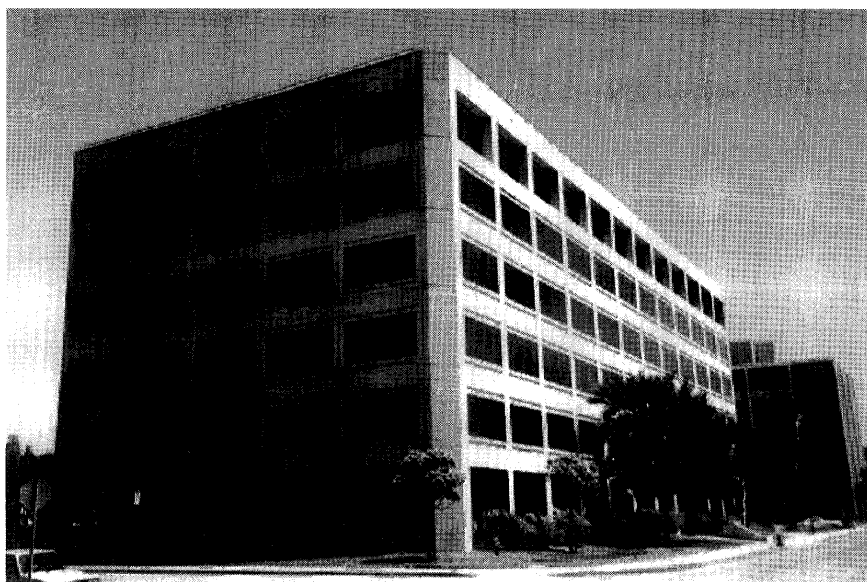


Figure 9.—A, Six-story commercial building in San Bruno. B, Three-dimensional schematic of San Bruno building.

RESPONSE OF STEEL STRUCTURES

TRANSAMERICA BUILDING (SAN FRANCISCO)

The response of one of the landmarks of San Francisco, the pyramidal Transamerica Building, 97 km from the epicenter of the earthquake, was recorded through an array of strong-motion instruments deployed by the USGS in 1985. The building was designed according to code requirements of that time; however, design evaluation was made using a site-specific design-response spectrum with seismic forces that were higher than the code requirements (R. Clough, personal commun., 1990). The building is 60 stories, 257.3 m (844 ft) high, and square in plan. At ground level, the plan dimensions are 53×53 m (174×174 ft). This plan starts reducing at the second floor to 44×44 m (145×145 ft) at the fifth floor and then follows an exterior wall slope of 1 to 11 upward. A perimeter truss system decorates and supports the building between the second and fifth floors. In addition to the exterior frame system, interior frames extend to the top of the structure, with some of them ending at the 17th and 45th floors. The exterior pre-cast concrete panels are attached structurally to the exterior frames. The basement (three levels below the ground level) consists of a very rigid shear wall box system. The foundation of the building consists of a 2.7-m (9 ft)-thick basemat without piles. The underlying soil media consists, in general, of clays and dense sands. Below the ground level to a depth of 8 m (25 ft), there is weak and compressible sand and rubble fill and recent bay deposits of sand and clay. Below 20 m (60 ft), the sands are partially cemented. The bedrock is between 48 and 60 m (145-185 ft) below the present street grade.

A general view, a three-dimensional schematic, overall dimensions, the instrumentation scheme, and recorded accelerations and displacements at some locations of the building are shown in figure 10. The instrumentation scheme was designed and implemented to study the response and associated dynamic characteristics of the building, including its translational, rocking, and torsional motions. There are a total of 22 channels.² Three triaxial strong-motion accelerographs with a total of nine channels are deployed synchronously with 13 uniaxial force-balance accelerometers, all connected to a central recorder with common-time recording capability. The three triaxial accelerographs are located on the 49th, 29th, and basement levels. At the 21st, 5th, and ground levels, three uniaxial accelerometers are deployed, two parallel

to one another at the nominal west and east ends (nominal north-south orientation—actually 351° clockwise from true north) and the third with a nominal east-west orientation (081° clockwise from true north). These orientations are coincident with the orientations of the horizontal channels of the three triaxial accelerographs at the 49th, 29th, and basement levels. The remaining four uniaxial accelerometers are deployed in the basement; one each is positioned vertically at three corners of the building, and one is positioned horizontally and parallel to the nominal north-south horizontal channel of the triaxial accelerograph in the basement. The senses of the orientations of the channels are also shown in figure 10. The perpendicular distance between the two parallel vertical sensors at the basement level is 58.98 m (193.5 ft). In summary, there are parallel pairs of horizontal accelerometers in each of the 21st, 5th, ground, and basement levels and another single accelerometer deployed orthogonally to the pair in the horizontal direction at the same levels.

The response of the Transamerica Building has been studied in detail by Çelebi and Şafak (1991) and Şafak and Çelebi (1991). The peak accelerations and displacements derived from the processed data are summarized in table 3. The fundamental frequency (period) is 0.28 Hz (3.6 s) in both the north-south and east-west directions, as extracted from the spectral analyses and system-identification techniques. Other frequencies are 0.5, 1.2, 1.5, and 1.8 Hz for the east-west direction and 1.0, 1.35, 2.0, and 2.6 Hz for the north-south direction. Figure 11 shows the results of the application of the system-identification technique for the Transamerica Building records at the 49th floor as output and at the basemat as input (Çelebi, 1996). The match between the observed and calculated response is excellent, as evidenced by comparison of the calculated and observed responses at the 49th floor and by comparison of the amplitude spectra of these responses. The critical viscous damping ratios extracted from the system-identification analyses corresponding to the 0.28 Hz first mode frequency are 4.9 percent (north-south) and 2.2 percent (east-west) (Çelebi, 1996).

The analyses of the records showed that there is no significant torsional motion, as evidenced by the differences in the parallel accelerations and displacements on each floor. These relative displacements or the relative accelerations, as nominal torsional motions (and their corresponding Fourier spectra, not shown here), are negligible compared to those of the translational components.

The possibility of rocking was investigated using both the vertical motions recorded at the basemat and the horizontal motions recorded at the ground level and the basemat. Shown in figure 12 are the coherency, phase angle, and cross-spectrum plots for both north-south (351°) and east-west (081°) directions of pairs of horizontal acceleration on the 21st floor and vertical acceleration of

²It is noted herein that channels 11 and 12 of the central recording system did not function properly. However, the remaining records are sufficient to perform analyses of the response of this important building.

the basemat. It is observed from these that the rocking motion occurs at 2.0 Hz (or 0.5 s) in the north-south (351°) direction and at 1.8 Hz (or 0.56 s) in the east-west (081°) direction, since at these frequencies the horizontal motion

at the 21st floor and the vertical motion in the basement are coherent and in phase. These frequencies are also observed in the Fourier amplitude spectra for the horizontal acceleration components (both directions) at the roof level,

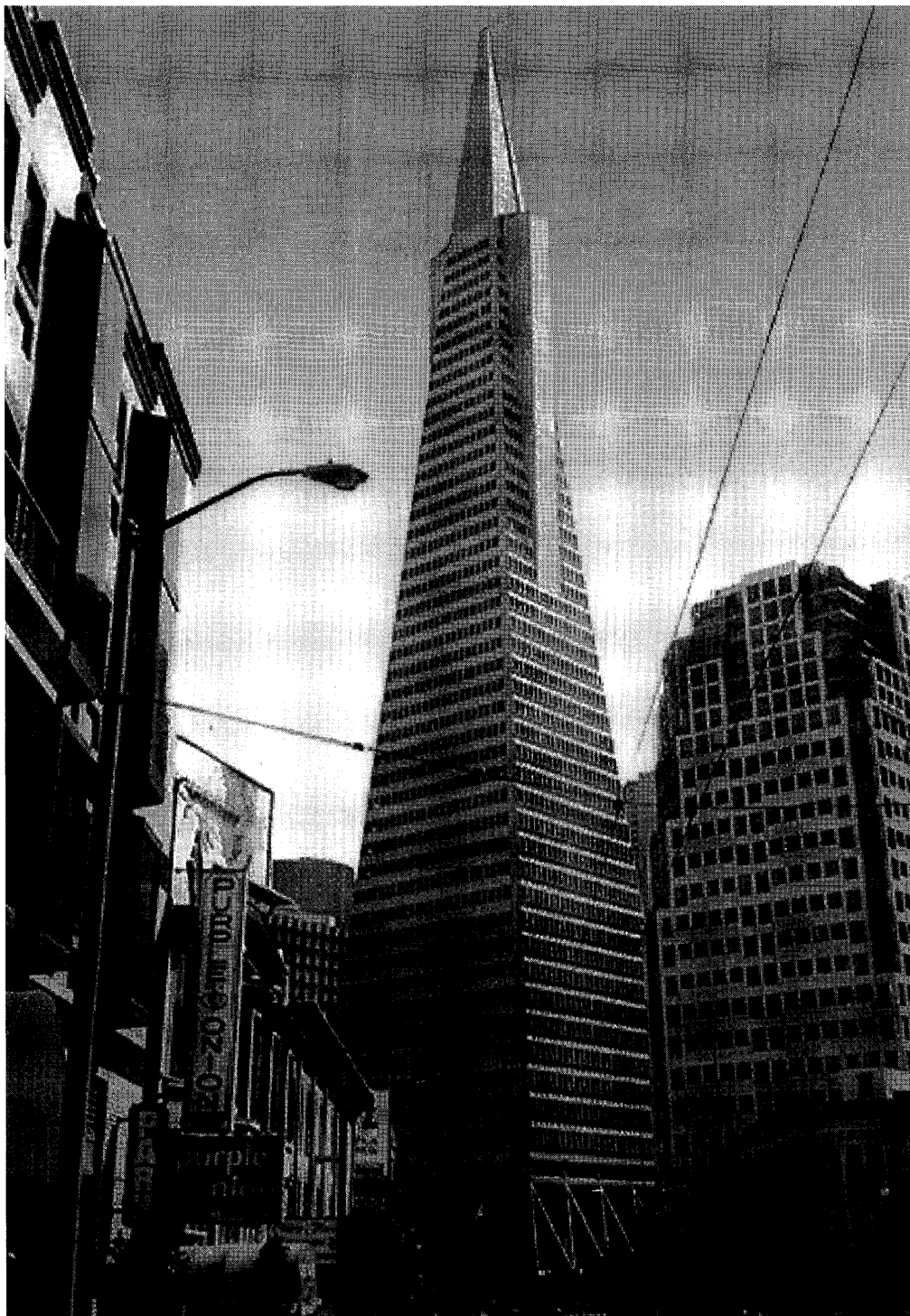


Figure 10.—A, Transamerica Building. B, Three-dimensional schematic of Transamerica Building and recorded accelerations and displacements (Çelebi, 1992, 1996).

as shown in figure 11. Figure 13 shows (A) the east-west component of acceleration at the 49th floor, (B) its amplitude spectrum, (C) the east-west displacement at the 49th floor, (D) the rocking contribution of acceleration at the 49th floor, (E) its amplitude spectrum clearly displaying the 2 Hz (0.5 s) rocking frequency (period), and (F) the rocking contribution of displacement at the 49th floor. It is noted that amplitudes of the rocking contribution (calculated by multiplying the rotation by the total distance between the basemat and the 49th floor) to the 49th floor displacement are very small.

The maximum vertical displacement due to rocking motion (the difference in the two vertical displacements at the two corners of the basemat) is 0.313 cm or 5.31×10^{-5} radians (0.003°) when divided by the distance between the two vertical sensors. The peak relative horizontal displacement between the ground level and the basement is

0.59 cm in the 081° (east-west) direction and 0.77 cm in the 351° (north-south) direction, which translates into 4.6×10^{-4} radians (or 0.026°) of rotation around the 351° axis and 6.0×10^{-4} radians (or 0.034°) around the 081° axis. All of these peaks occur at approximately 11 s into the record. These rotations are shown in figure 14. The rotation of the wall around the north-south axis is approximately tenfold that of the rotation of the basemat around the same axis.

The comparison of the rotations around the north-south (351°) axis shows that there is a very significant difference between the peak rotations calculated from the difference of the vertical displacements at the basemat and those calculated from the difference of east-west direction displacements at the ground floor and the basemat. This disparity could be due to (1) the bending of the basemat, (2) the shear deformation and bending of the shear walls

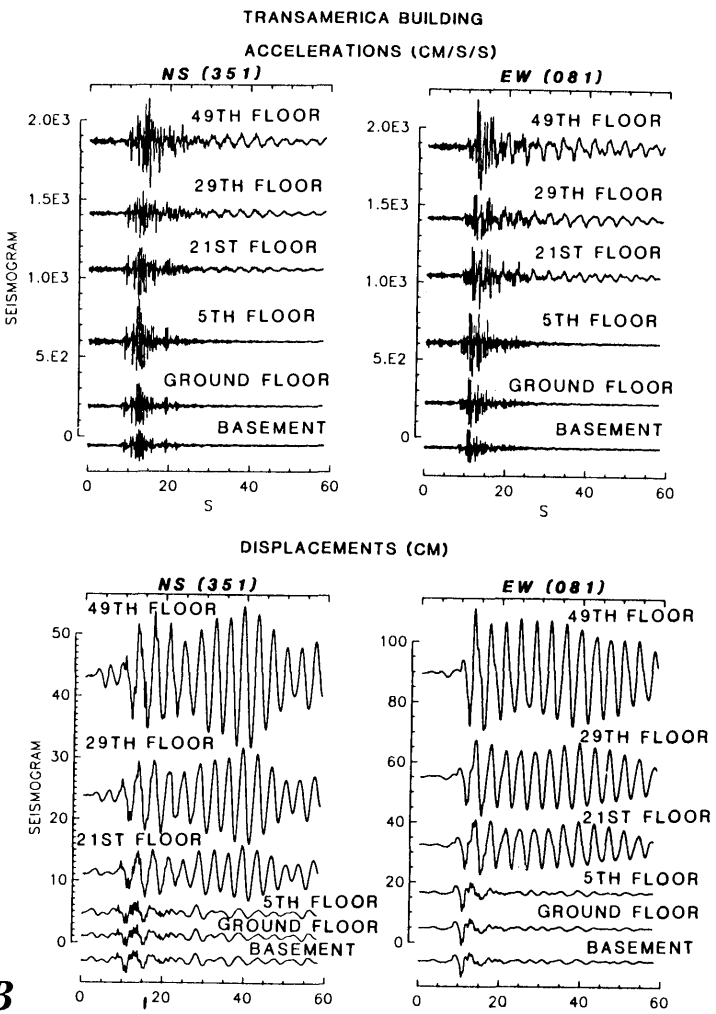
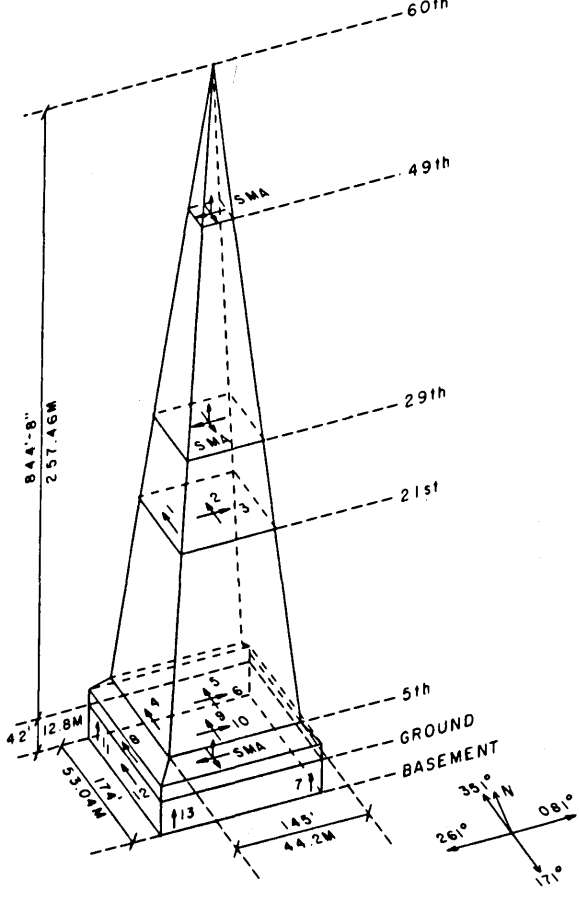


Figure 10.—Continued.

Table 3.—*Peak accelerations and displacements for Transamerica Building*

[--, only one channel in this direction; +++, not placed in this direction; SMA, triaxial strong-motion accelerograph; FBA, force-balance accelerometer; CH, channel]

Floor	Acceleration				Displacement			
	081°	351°	351°	Up	081°	351°	351°	Up
	(g)	(g)	(g)	(g)	(cm)	(cm)	(cm)	(cm)
49 (SMA)	0.28	0.29	---	0.13	18.6	11.3	---	1.22
29 (SMA)	0.14	0.16	---	0.11	12.9	7.7	---	0.92
Base (SMA)	0.10	0.10	---	0.05	5.2	1.9	---	1.10
21 (FBA)	0.19	0.13	0.14	+++	8.5	4.4	4.8	+++
5 (FBA)	0.19	0.26	0.26	+++	3.5	2.0	2.3	+++
Ground (FBA)	0.17	0.14	0.16	+++	3.3	2.0	2.0	+++
Base (CH13)(FBA)	+++	+++	+++	0.04	+++	+++	+++	1.0
Base (CH 7)(FBA)	+++	+++	+++	0.07	+++	+++	+++	0.9

and columns in the three levels below the ground level, and (3) perhaps, the effect of the smaller stiffness of the embedment in the horizontal direction as compared to the vertical direction. Another possibility is the presence of integration errors introduced during processing of the digitized data. The large ratio of the wall-to-basemat rotation may be important in assessing forces used in the design of basements. A detailed study of this issue was carried out by Soydemir and Çelebi (1992). In usual practice, the basements are designed for seismic forces similar to that of the ground floor. No difference in the

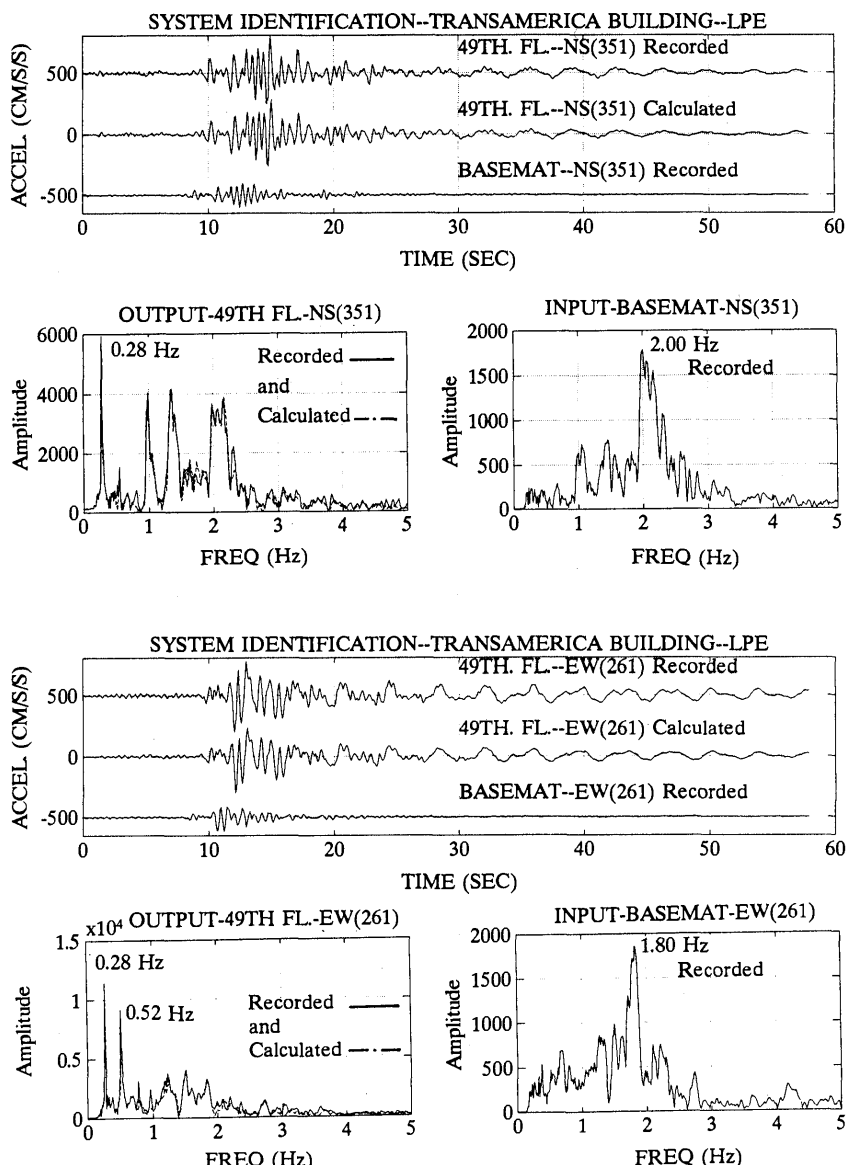


Figure 11.—System identification applied with accelerations recorded at 21st floor and basement of Transamerica Building.

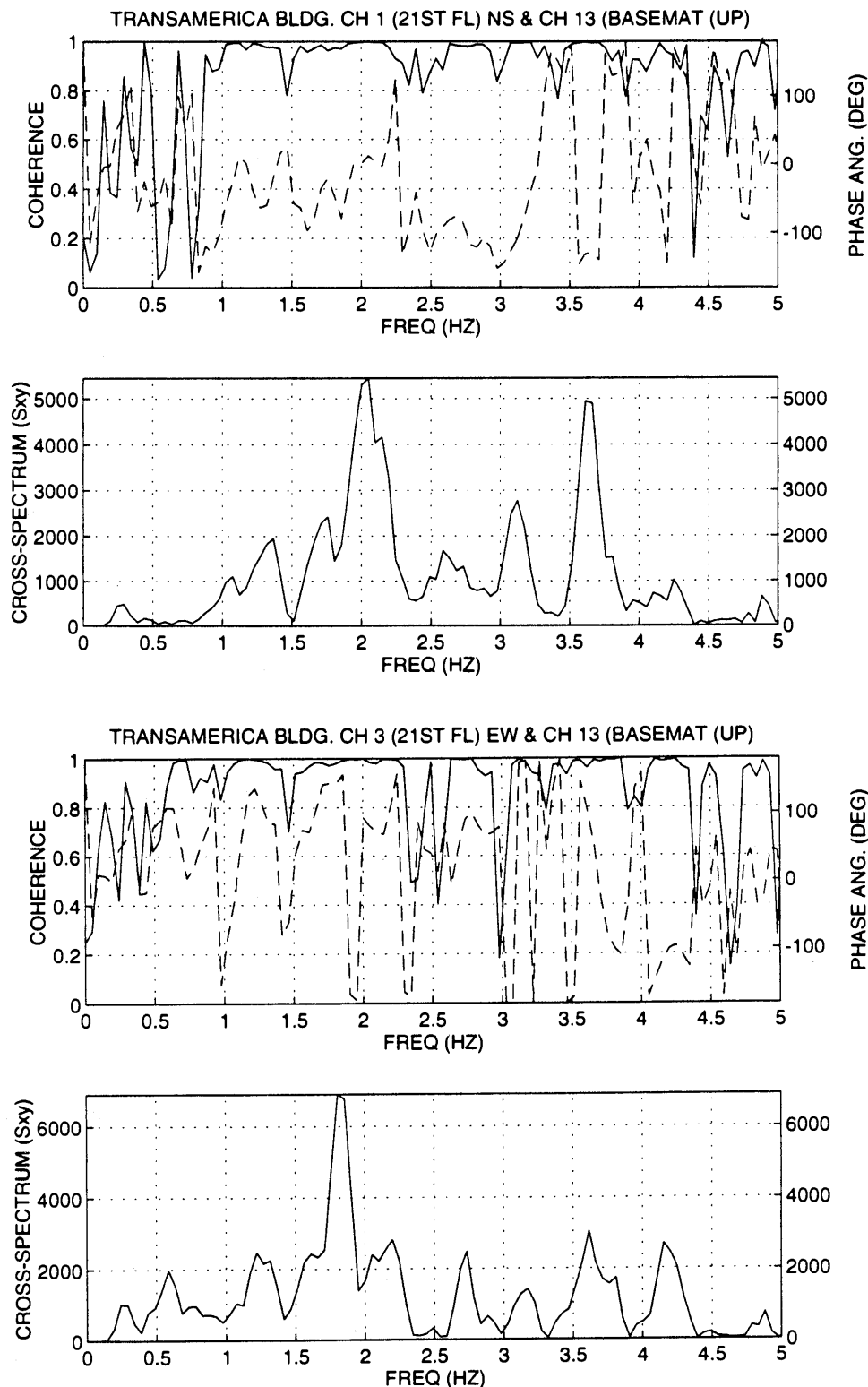


Figure 12.—Rocking investigated with cross-spectrum, coherency (solid line), and phase angle (dashed line) plots of horizontal motions at 21st floor and vertical motion at basemat of Transamerica Building.

seismic forces and/or accelerations are considered between the ground level and the embedded basement levels. However, the data set from the Transamerica Building shows that significant differences may occur between the motions at the ground floor and those at the basemat level of embedded basements and that the deformations of basemat and basement walls can also be significantly different. To compensate for this in design, a simplified approximate procedure has been developed by Soydemir and Çelebi (1992). A similar disparity in the deformation of the basemat and walls of the basements has been observed from the data of Embarcadero Building in San Francisco, discussed later in this paper.

Although very small in amplitude, the rocking motions significantly influenced the motions at the basement and the ground level. This is evidenced by the normalized response spectra (fig. 15) for the records from the three components of the triaxial accelerograph at the basement. Thus, this type of response may be pertinent to the incorporation of response spectra used in the design process of buildings. The design response spectra represents, in general, free-field motions assumed to be applicable at the foundation level of a structure; while it may include site effects, it should not include the effect of the vibration of the structure or soil-structure interaction. In this case, it was shown that the motions at the foundation (basemat) level are influenced by the soil-structure interaction effects.

Forced vibration tests and dynamic analyses were performed on the Transamerica Building in 1972-73 by Stephen and others (1974). Ambient vibration tests were performed by Kinematics (1979). The data from these investigations permit (1) the comparison of the actual earthquake response characteristics with those from small amplitude tests and (2) the assessment of the validity of various assumptions made in the dynamic analyses. The results of these small-amplitude tests and related analyses are summarized later in this paper. It is important to note that both the forced-vibration and ambient-vibration tests were performed when the construction of the building was just completed and the building was not yet occupied. Therefore, it did not contain nonstructural partitions and live load.

The dynamic analysis was performed with a mathematical model that considered only one-quarter of the building above the plaza (ground) level with appropriate boundary conditions. Translational and rotational responses were assumed to be uncoupled (Stephen and others, 1974). This assumption is valid for a symmetrical structure such as the Transamerica Building. Although the attachments of exterior panels were detailed with the intention to minimize their effect on the lateral stiffness of the building during small amplitudes of vibration, Stephen and others (1974) concluded that the panels contributed significantly to the lateral stiffness.

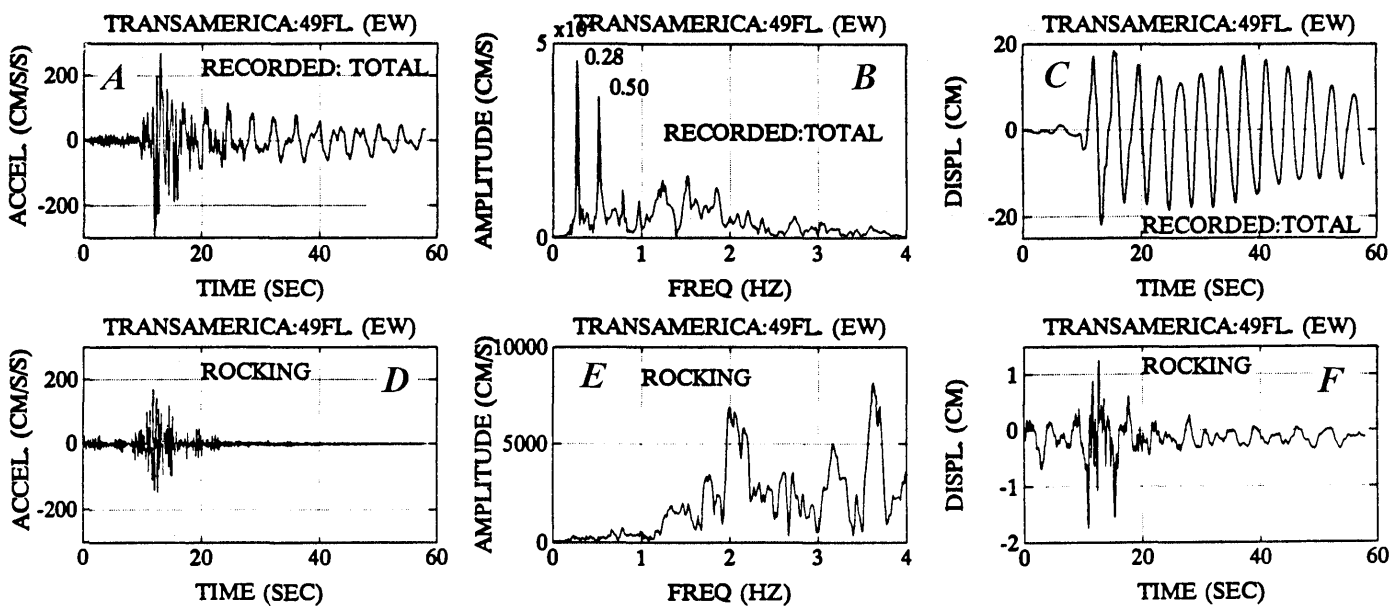


Figure 13.—*A*, East-west component of acceleration at 49th floor. *B*, Amplitude spectrum of east-west component at 49th floor. *C*, East-west displacement at 49th floor. *D*, Rocking contribution of acceleration at 49th floor. *E*, Amplitude spectrum of rocking contribution of acceleration at the 49th floor clearly displaying the 2 Hz (0.5 s) rocking frequency (period). *F*, Rocking contribution of displacement at 49th floor.

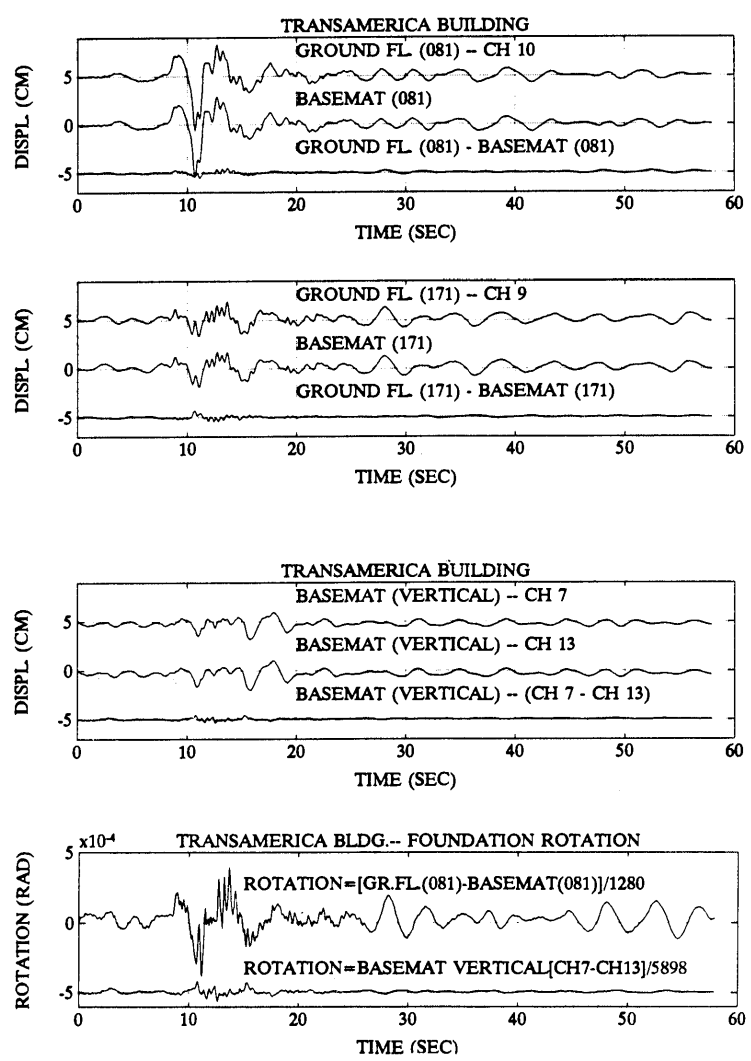
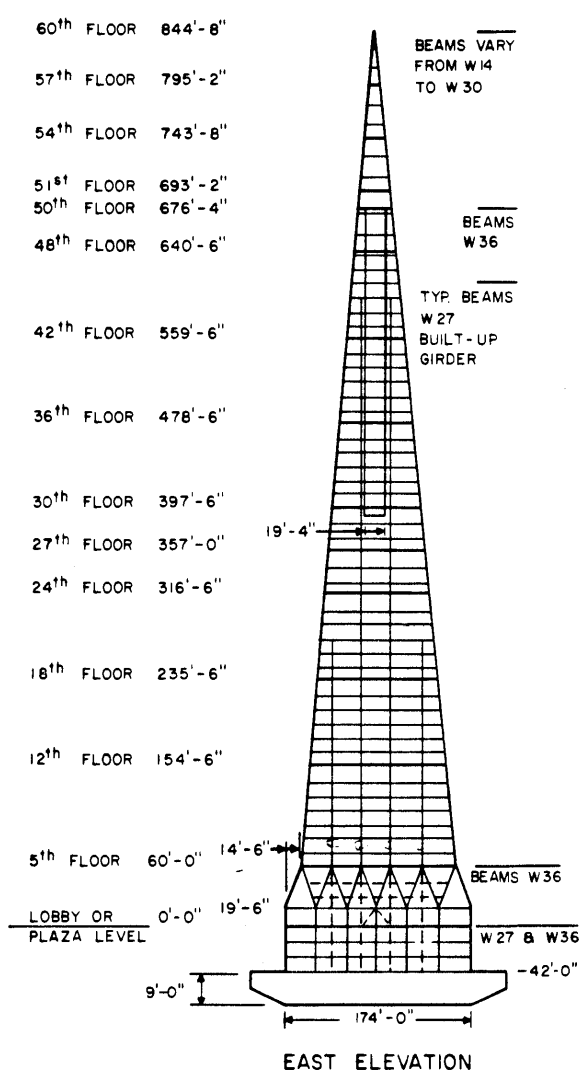


Figure 14.—Rotation of basemat and basement walls at Transamerica Building.

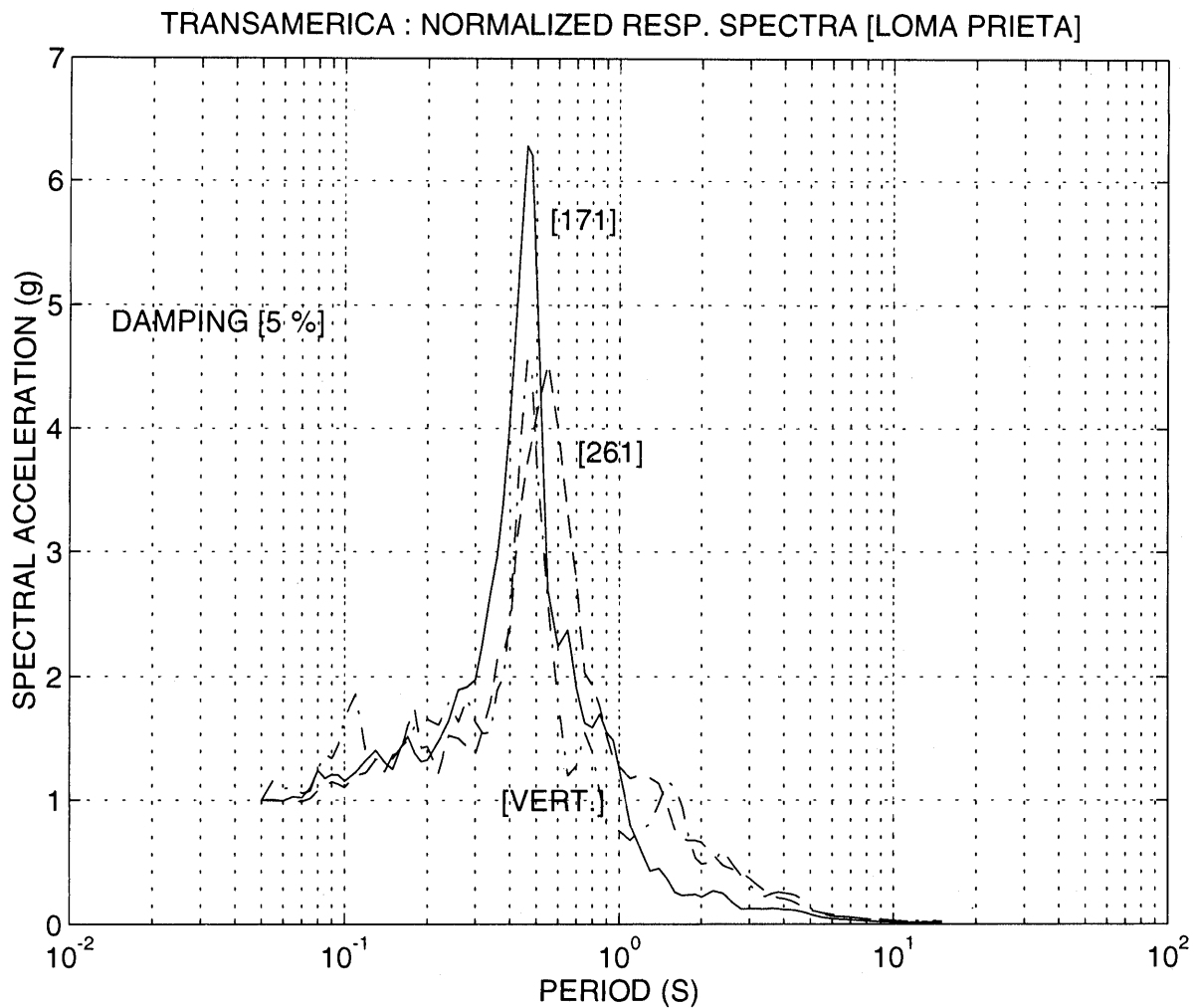


Figure 15.—Normalized response spectra for records from three components of the triaxial accelerograph at basement of Transamerica Building.

EMBARCADERO BUILDING (SAN FRANCISCO)

The 47-story Embarcadero Building (No. 4) is the first building in the United States constructed with eccentric bracing. The building, approximately 97 km from the epicenter of the earthquake, was constructed in 1979 in accordance with the UBC 1976 design provisions but using design response spectra relating to much higher seismic performance requirements.

The Embarcadero Building is 172 m (564 ft) high. The building actually consists of two structures; an above-grade 47-story building and an above-grade 3-story building. The below-grade 2-story shear walls and diaphragms are common to the two structures. The 47-story tower, referred to as the Embarcadero Building herein, is a moment-resisting steel-framed structure. Four center north-south frames are eccentrically braced (two up to the 41st floor and two up to the 29th floor). Plan dimensions decrease above the 39th and again above the 41st floors. Eccentric diagonal braces consist of double angles which are offset by approximately 1.5 m (4.5 ft) from the column-beam intersections. Recent codes (Uniform Building Code, 1991) term this type of structural framing as special moment-resisting frames. A general view of this building, the vertical sections showing the eccentric bracing and a typical plan view with significant dimensions, and a three-dimensional view of the building and instrumentation scheme are provided in figure 16 (Çelebi, 1993).

The Embarcadero Building is located in the Lower Market area of San Francisco, which is reclaimed fill area well known for its soft-soil characteristics that amplify ground motions originating at long distances. Due to these amplified motions, the Embarcadero Freeway, located within 100 m of the Embarcadero Building suffered extensive damage during the earthquake and was razed in 1991 (fig. 16A). The building was not damaged during the earthquake.

The building base is a 1.67-m (5 ft)-thick, reinforced concrete mat supported by approximately 50-67-m (150-200 ft)-long composite concrete and steel bearing piles. The underlying soil media consists of approximately 8.5 m of a top layer of silty fine sand fill with rubble (estimated shear wave velocity, V_s , 200 m/s, followed by 25 m of soft very dark greenish-gray Holocene silty clay (Bay mud, V_s 150 m/s), 9 m of sand (V_s , 250 m/s) and 21.5 m of very stiff to hard silty clay (old Bay mud, V_s 230 m/s). The rock at 64 m depth is sandstone with V_s of approximately 1,000 m/s (T. Fumal, personal commun., 1992). The transfer function, from rock to the surface, based on estimated shear-wave velocities of the layered media (provided by Fumal) and calculated by Haskell's formulations (Haskell, 1953, 1960; Silva, 1976) using software by C.S. Mueller (personal commun., 1992), is shown

in figure 17. From this, a site frequency (period) of 0.8 Hz (1.25 s) is inferred. Alternatively, using the well-known formula $T_s = 4H/V_s$, a depth (H) of 64 m, and an average shear-wave velocity (V_s) of 200 m/s, an approximate site frequency (period) of 0.77 Hz (1.3 s) is obtained (Çelebi, 1993). The match between the calculated site periods is very good. The significance of the site period is discussed later in this section.

The site characteristics of any area are deemed very important. To further assess the impact of soft-soil characteristics on a densely built-up urban environment, such as the Lower Market area of San Francisco, the USGS has installed downhole accelerograph arrays within 40 m of the Embarcadero Building (between the building and the razed Embarcadero Freeway).

For the design of the building, site-specific design response spectra based on two levels of performance of the building were used. The first level of performance requires elastic response without structural or nonstructural damage under a moderate earthquake ($M=7$) that is likely to occur during the economic life of the building. The second level of performance demands that the structure will not collapse under the most severe (major) earthquake ($M=8.3$) that could occur during the economic life of the building. Substantial structural and nonstructural damage (without collapse) is considered acceptable under such an event. Design response spectra based on United States Nuclear Commission Regulatory Guide 1.60 (United States Nuclear Regulatory Commission, 1973) of earthquake level I (anchored at zero period acceleration, 0.3 g and 3 percent damping) and earthquake level II (zero period acceleration, 0.5 g and 7 percent damping) are provided in figure 18, which also shows the 1976 Uniform Building Code spectrum for comparison (Çelebi, 1993).

The strong-motion instrumentation scheme implemented in 1985 by the California Strong Motion Instrumentation Program of the California Division of Mines and Geology at six different levels of the building is shown in figure 16C (Shakal and others, 1989). There are 6 digital seismic accelerographs (DSA-1) with a total of 18 channels of synchronous, uniaxial (FBA-11) and biaxial (FBA-21) force-balance accelerometers within the structure. One of the unidirectional accelerometers is in the adjacent building basement. The reference north-south orientation is 345° clockwise from true north (fig. 16C).

The processed 120 seconds of the recorded acceleration and the calculated displacements at different levels are shown in figures 19 and 20. This data has been band-pass filtered with ramps at 0.07-0.14 Hz and 23-25 Hz (Shakal and others, 1989). Peak accelerations and displacements are summarized in table 4. In figures 19 and 20 and in table 4, it is noted that the north-south peak responses (accelerations and displacements) at the 39th floor are

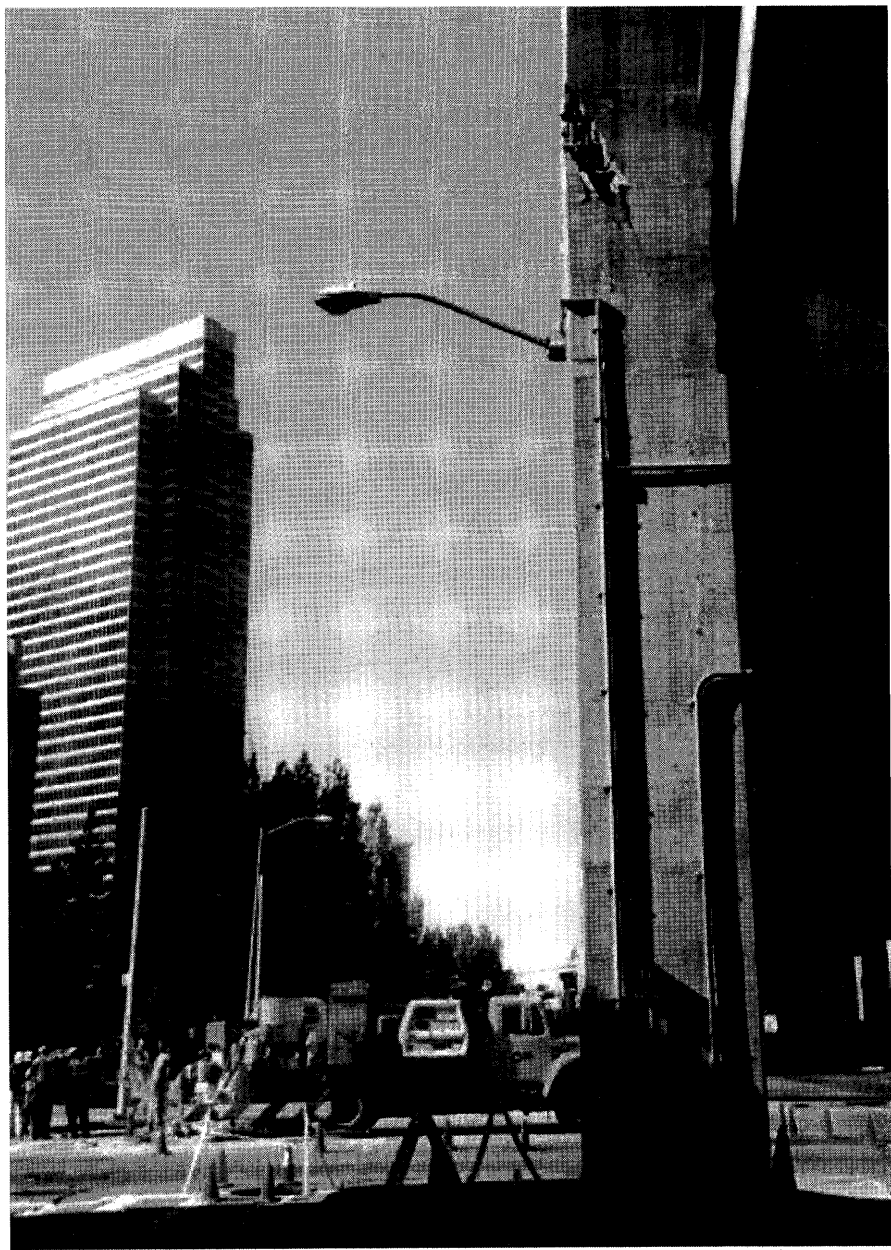


Figure 16.—*A*, Embarcadero Building. Also shown is one of the damaged columns of Embarcadero Freeway, razed in 1991. *B*, Typical plan view and vertical sections of Embarcadero Building. *C*, Three-dimensional view and instrumentation scheme of Embarcadero Building.

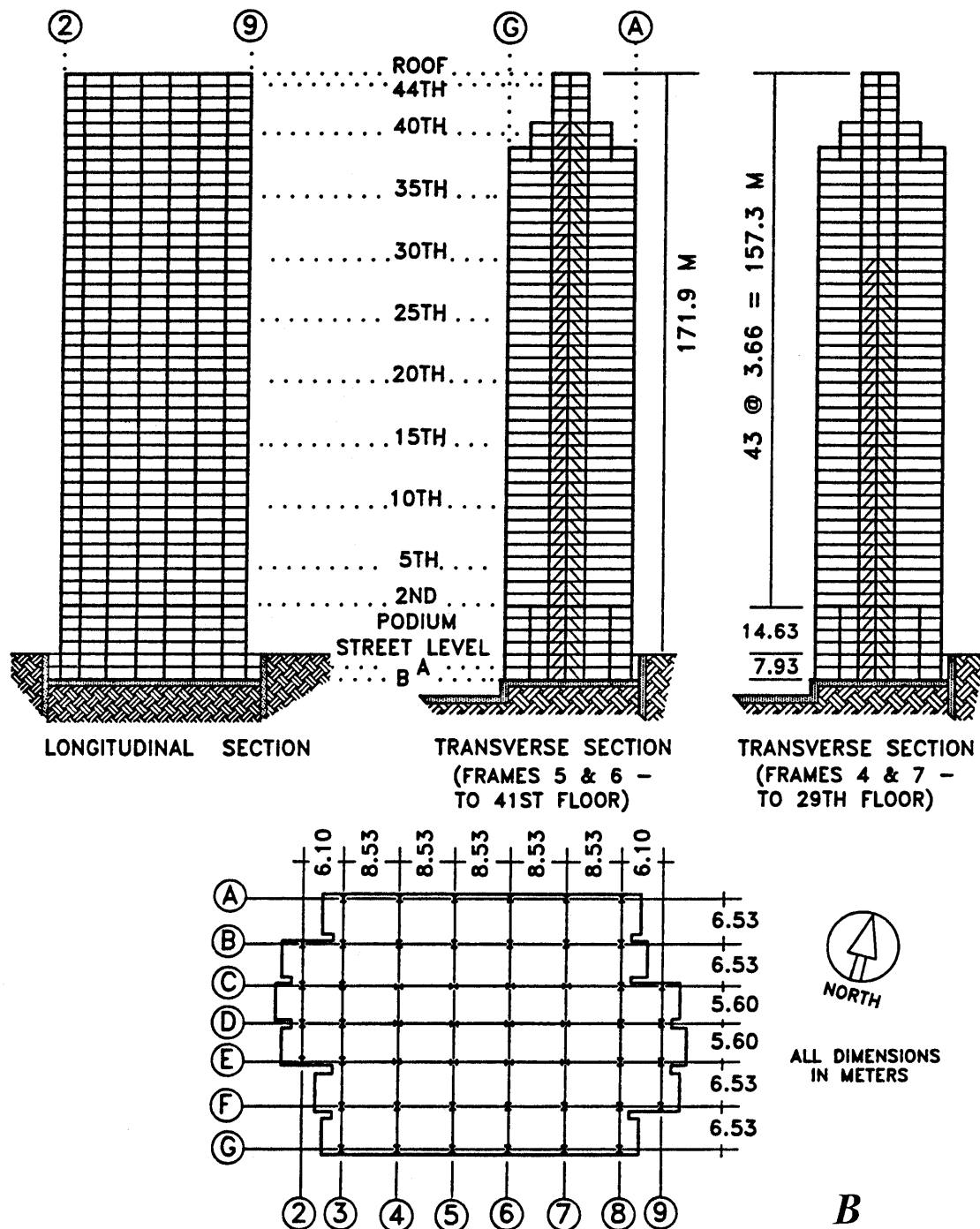


Figure 16.—Continued.

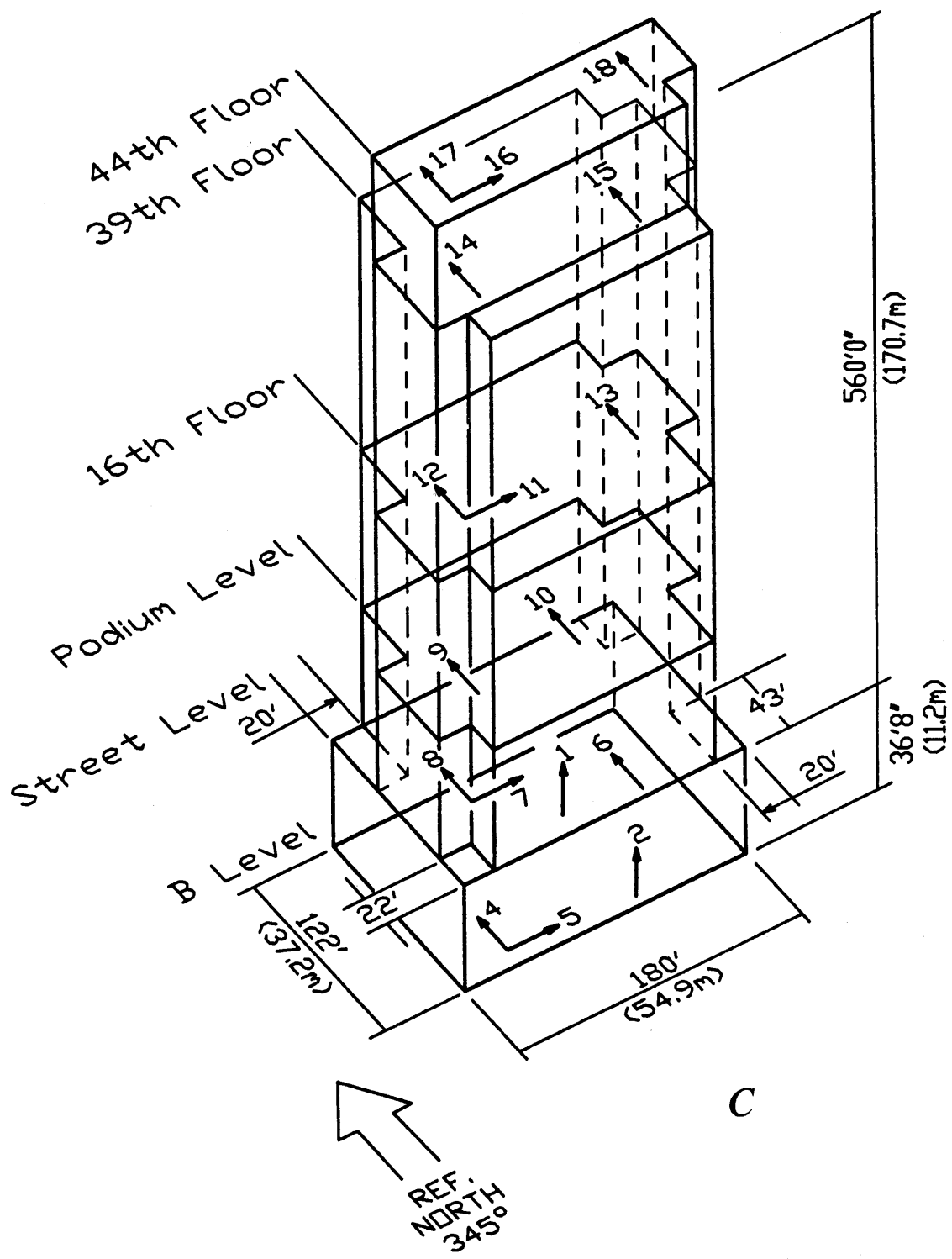


Figure 16.—Continued.

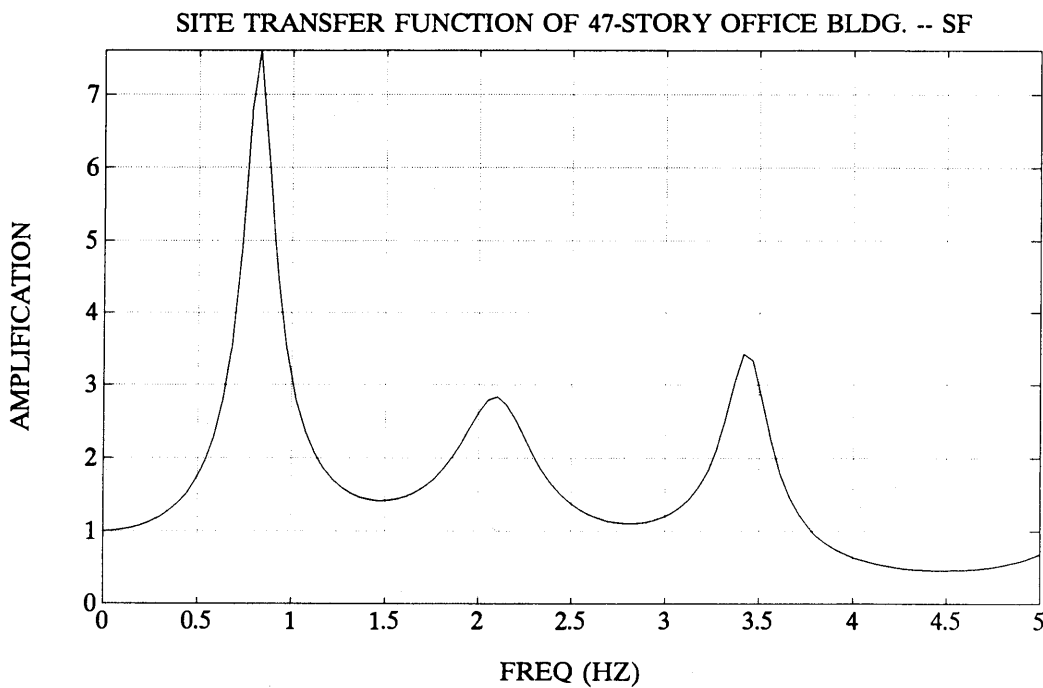


Figure 17.—Site transfer function of Embarcadero Building site.

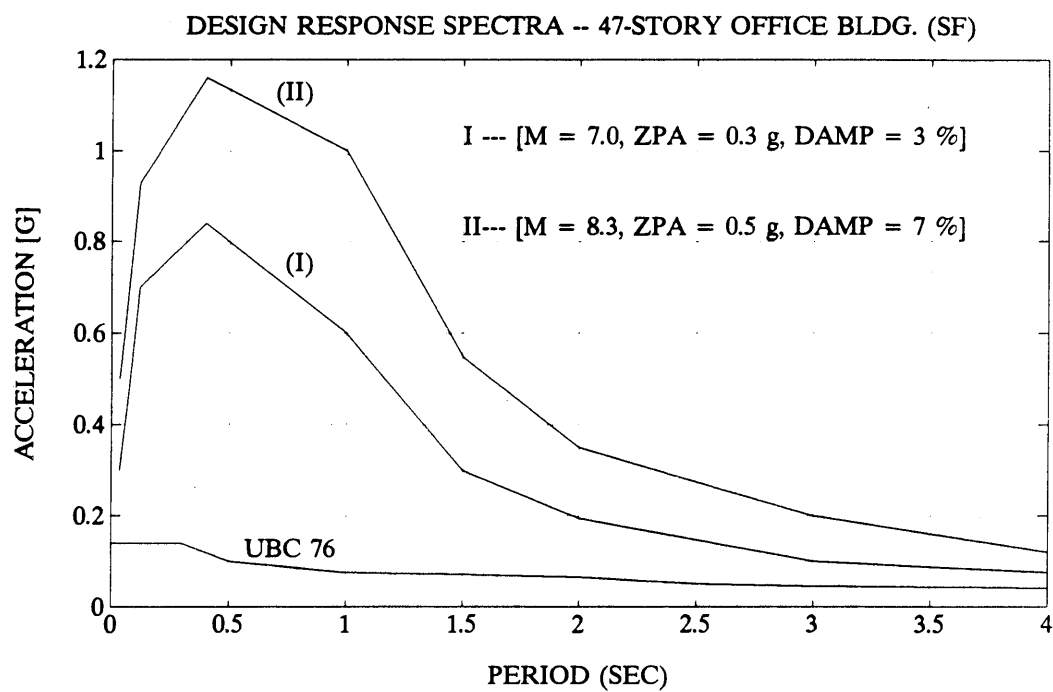


Figure 18.—Design response spectra of Embarcadero Building.

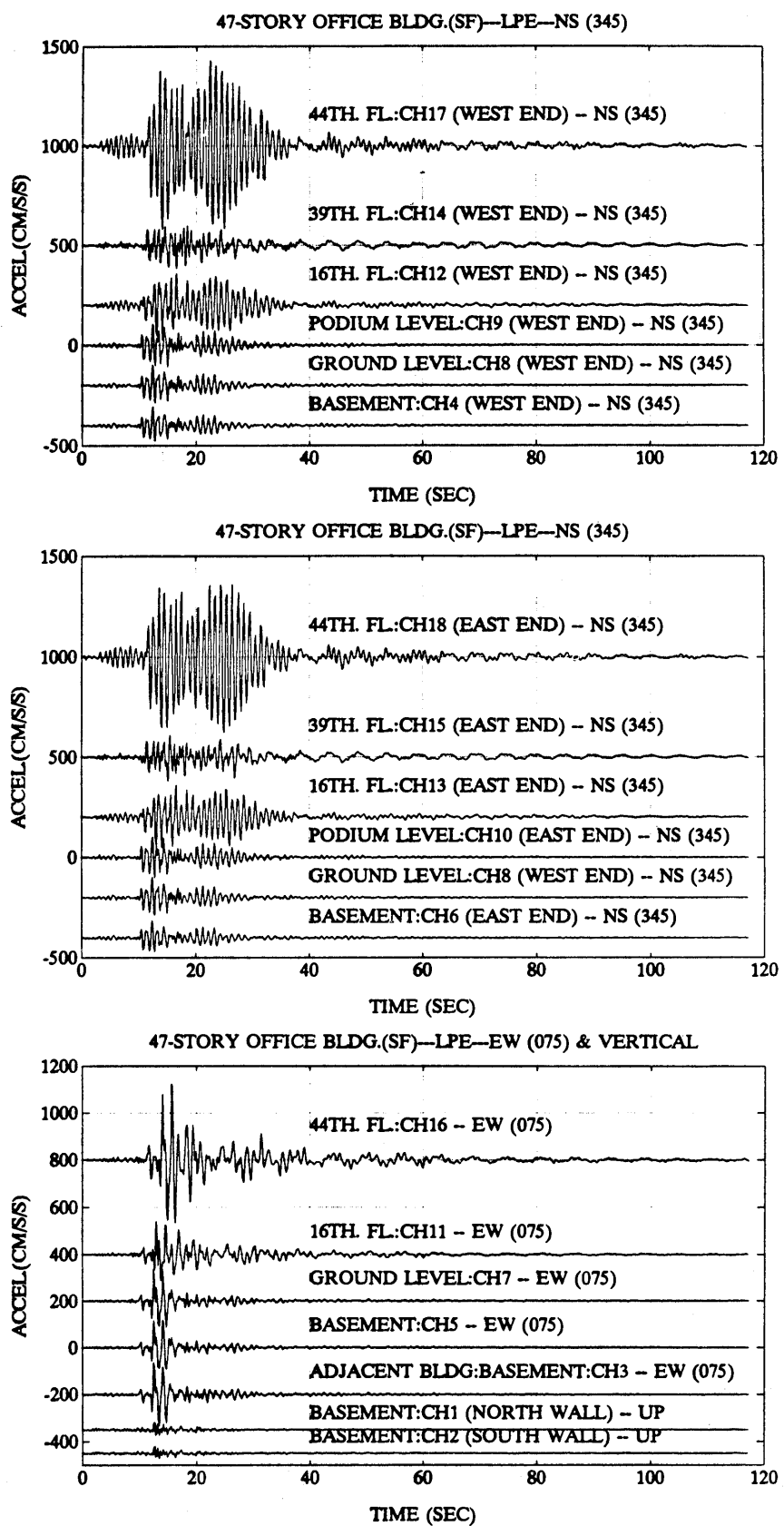


Figure 19.—Recorded accelerations. This data has been band-pass filtered with ramps at 0.07–0.14 Hz and 23–25 Hz (Shakal and others, 1989).

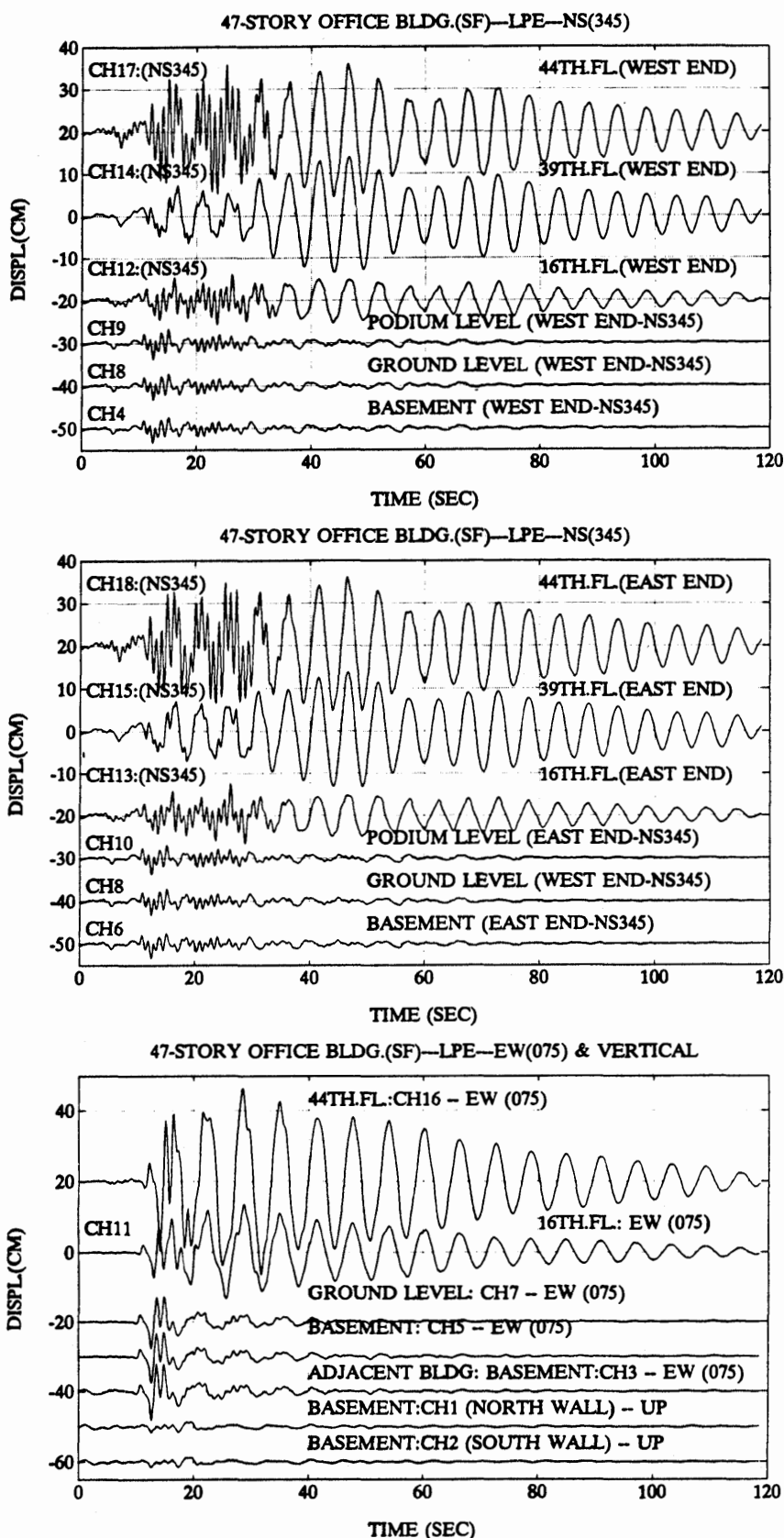


Figure 20.—Recorded displacements. This data has been band-pass filtered with ramps at 0.07–0.14 Hz and 23–25 Hz (Shakal and others, 1989).

Table 4.—*Peak accelerations and displacements for Embarcadero Building*

Level	Sensor	Direction	Acceleration (g)	Displacement (cm)
44	16	EW	0.38	27.2
44	17	NS	0.47	16.2
44	18	NS	0.43	16.4
39	14	NS	0.13	14.3
39	15	NS	0.12	14.1
16	11	EW	0.19	13.7
16	12	NS	0.19	6.3
16	13	NS	0.17	7.6
Podium	9	NS	0.15	3.9
Podium	10	NS	0.14	4.0
GR	7	EW	0.20	7.9
GR	8	NS	0.12	3.4
Basement B	4	NS	0.11	3.4
Basement B	5	EW	0.16	7.7
Basement B	6	NS	0.10	3.3
Basement B	1	UP	0.043	1.6
Basement B	2	UP	0.055	1.6
Basement C(*)	3	EW	0.17	8.4

* At C level below adjacent building.

less than the north-south peak responses at the 16th floor. This may be attributed to several reasons, including the discontinuity of stiffness at the 39th and 41st floors, as discussed later.

Figure 21 shows results of system-identification analysis, using 80 seconds of the recorded basement accelerations as input and the recorded 44th floor accelerations as output. Figure 22 shows the same, using displacements to obtain better identification at the lower frequencies. Both approaches exhibit excellent match between the calculated and observed outputs (Çelebi, 1993).

The modal acceleration contributions are extracted from the system identification analyses and compared to the total response at the 44th floor for the most significant four frequencies that contribute to the overall motions of the building (fig. 23, 0.19, 0.57, 0.98, and 1.33 Hz for the north-south direction; fig. 24, 0.16, 0.46, 0.77, and 1.06 Hz for the east-west direction). The figures also show the Fourier amplitude spectrum of each mode superimposed on that of the total response. The damping values, also determined from system identification procedures, are provided in these figures and summarized in table 5. It is noted that the four significant modal periods in each of the principal axes of the building follow the general rule of thumb approximation of T, T/3, T/5, and T/7. For all four modes in each of the two principal axes, modal damping percentages determined by system identification vary between 1.4 and 3.7 percent (table 5). As expected, the damping percentages of the north-south (braced) direction are lower than the east-west (unbraced) direction. The east-west modal damping percentages vary between 2.5 percent and 3.7 percent. The damping percentage of the east-west fundamental mode, when determined alternatively by the logarithmic decrement approach using the 44th floor displacements, yields 3.5 percent. The fundamental mode damping percentages are 2.5 percent and 3.7

percent for north-south and east-west, respectively (table 5). In summary, such low modal damping percentages explain why the response records are longer than the processed 120 seconds (figs. 19 and 20) (Çelebi, 1993).

The extracted modal displacements at the top three north-south instrumented floors are grouped and plotted in figure 25. A separate system identification analysis is performed for each of the additional input-output pairs (39th and ground floor, and 16th and ground floor). This is done primarily to investigate why the 39th level north-south motions are smaller than those of the 16th floor. It is noted in figure 25 that the third-mode contribution to the 39th floor motions is much smaller than at the 44th or the 16th floor. On the other hand, while the second-mode contribution is comparable in amplitude for the 44th, 39th, and 16th floors, it is in phase between the 44th and the 39th floor, 180° out of phase between the 39th and 16th floors. This anomaly of reduced motions at the 39th floor may be directly attributable to the discontinuity of the stiffness at the 40th floor, causing (1) the 39th floor to behave as the upper nodal point of the third mode, (2) a whipping effect of the top floors, and/or (3) a resonating appendage effect of the floors above the 39th floor, where the bracing is discontinued and the plan of the floors gets smaller (in stiffness and mass). Whatever combination occurs, the main reason is the change in stiffness (Çelebi, 1993; Astaneh and others, 1991; Chen and others, 1992).

The explanations provided above are also related to discussions on drift. For the north-south direction, figure 26 shows superimposed drift ratio time-history between the 44th and 39th floors and between the 44th floor and street level. Figure 26 shows superimposed drift ratios between the 16th floor and street level, between the 39th and 16th floors, and between the 44th floor and street level. When average drift ratios between the 44th floor and street level are considered, the peak is approximately 0.0014 or less (28 percent of 1976 Uniform Building Code allowable). Average drift ratio exceeds the 0.005 allowable only between the 44th and 39th floors (with a peak of 0.006). This may be attributed to either the discontinuity of the eccentric bracing above the 40th floor or the whipping effect at the top floor, which cannot be confirmed since there are no sensors at the two consecutive top floors. Similarly, for the east-west direction, the superimposed drift ratio time-histories between the 16th floor and street level, between the 44th floor and the 16th floor, and between the 44th floor and street level are provided in figure 26. Since, in the east-west direction, there are no sensors on the 39th floor or the two top consecutive floors, it is not possible to determine whether the code-allowable drift ratio of 0.005 was exceeded. However, there appears to be a mostly consistent average drift ratio with a peak of less than 0.002 in this direction. Maximum drift ratio is 0.0023 between the 44th and 16th floors. Therefore, drift ratios on the average were about 40 percent (or less) of

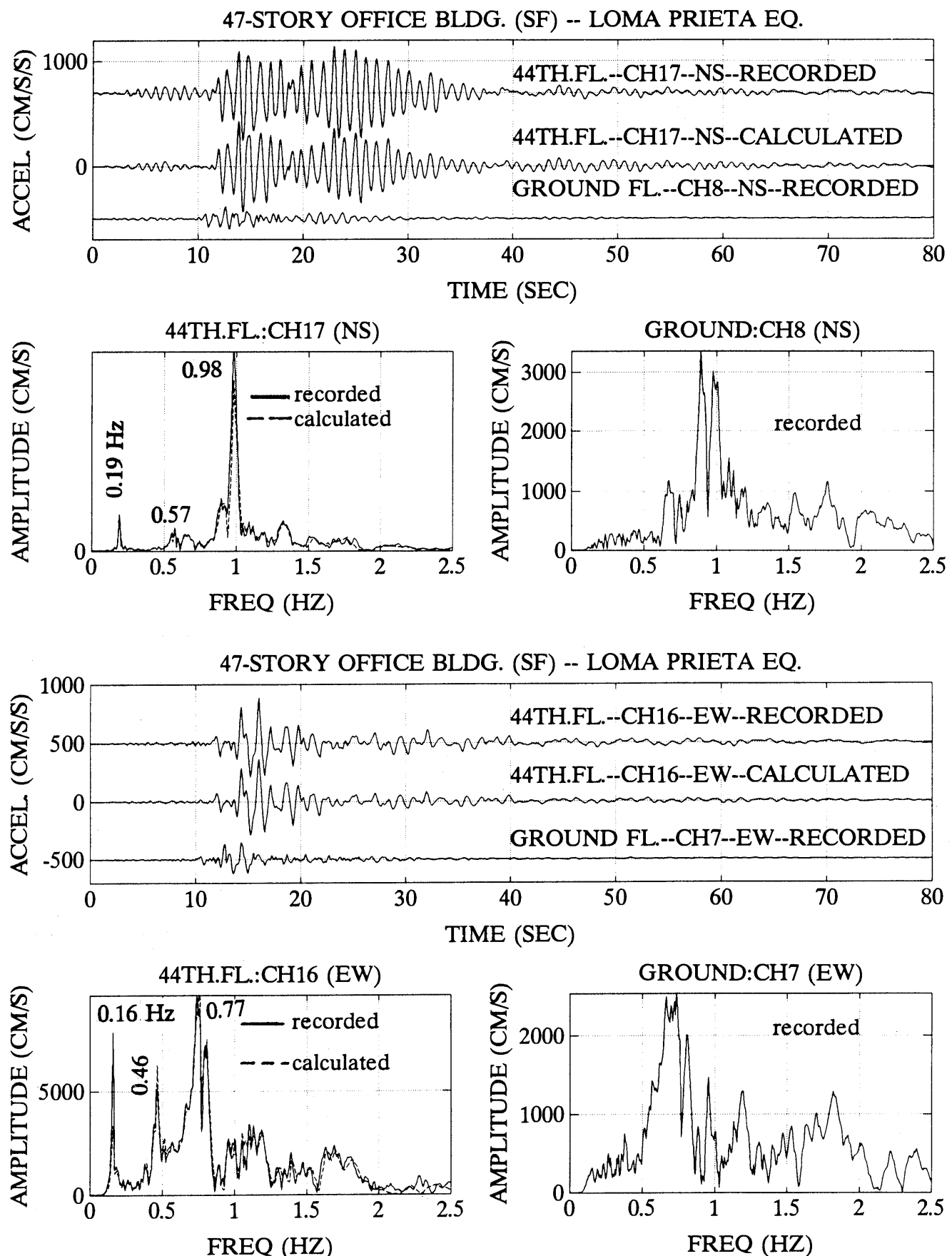


Figure 21.—System identification using ground-floor accelerations as input and 44th-floor accelerations as output for Embarcadero Building.

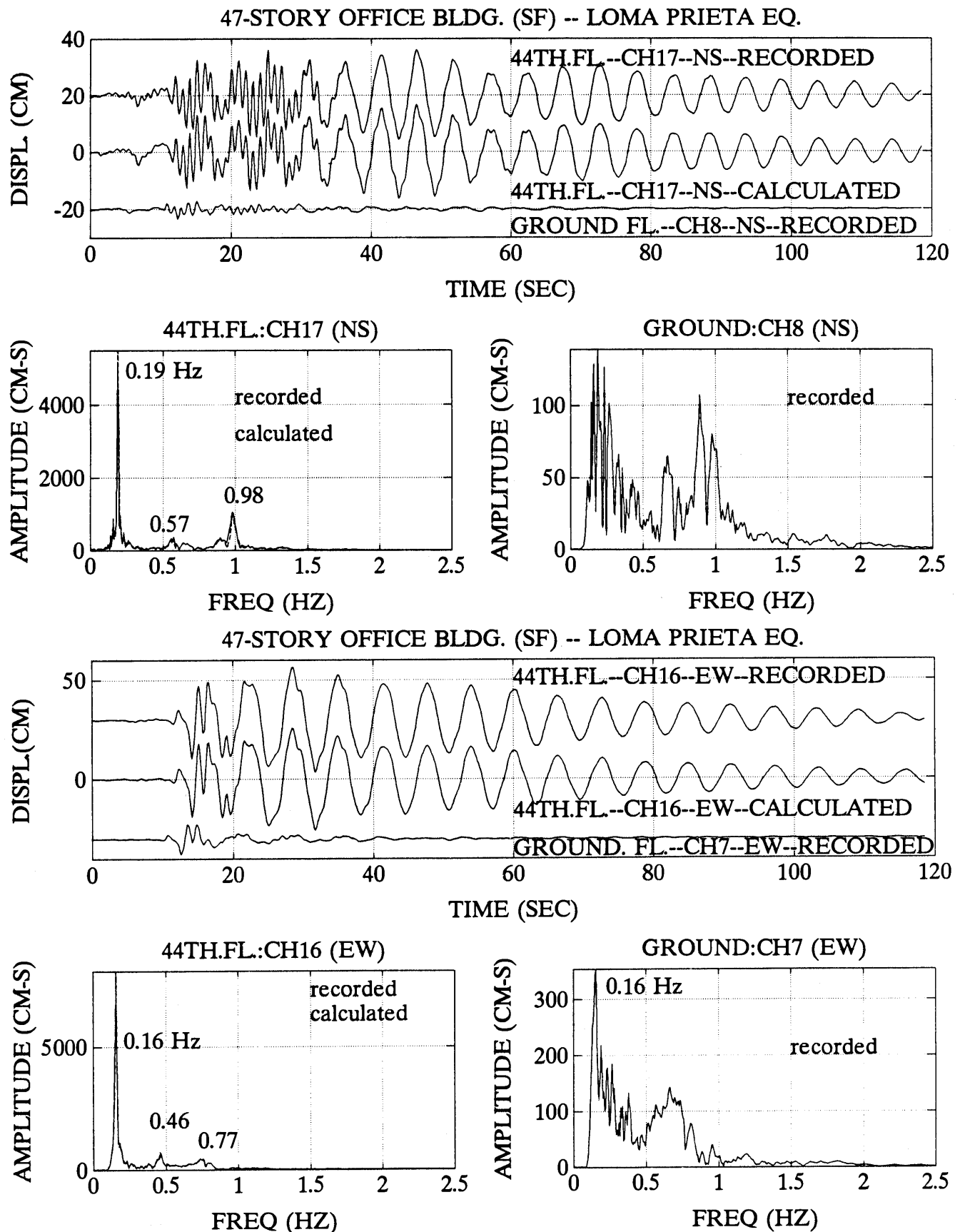


Figure 22.—System identification using ground-floor displacements as input and 44th-floor displacements as output for Embarcadero Building.

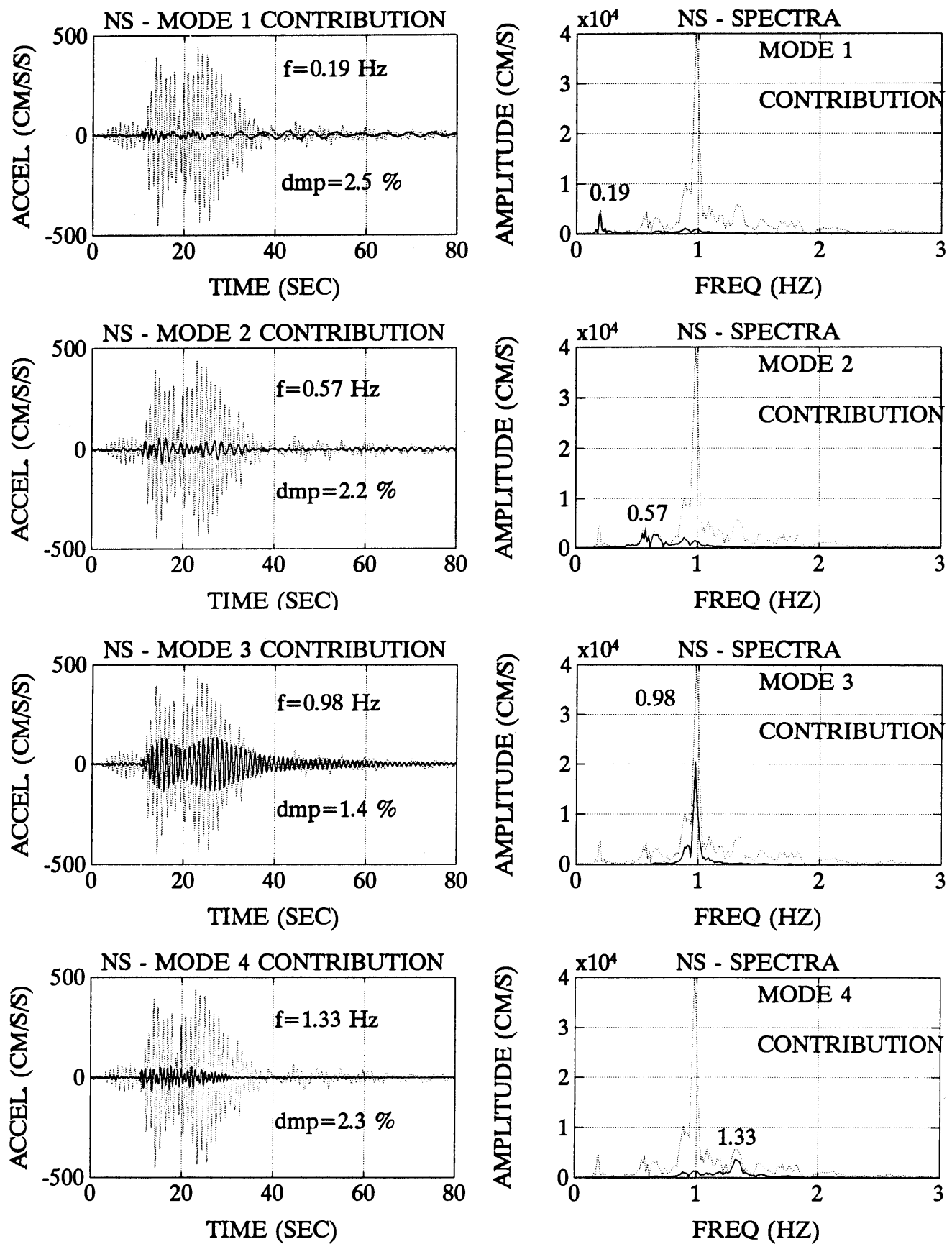


Figure 23.—Significant north-south modal accelerations (and their amplitude spectra) of the 44th-floor for Embarcadero Building extracted from system identification analysis and comparison with the total 44th-floor acceleration.

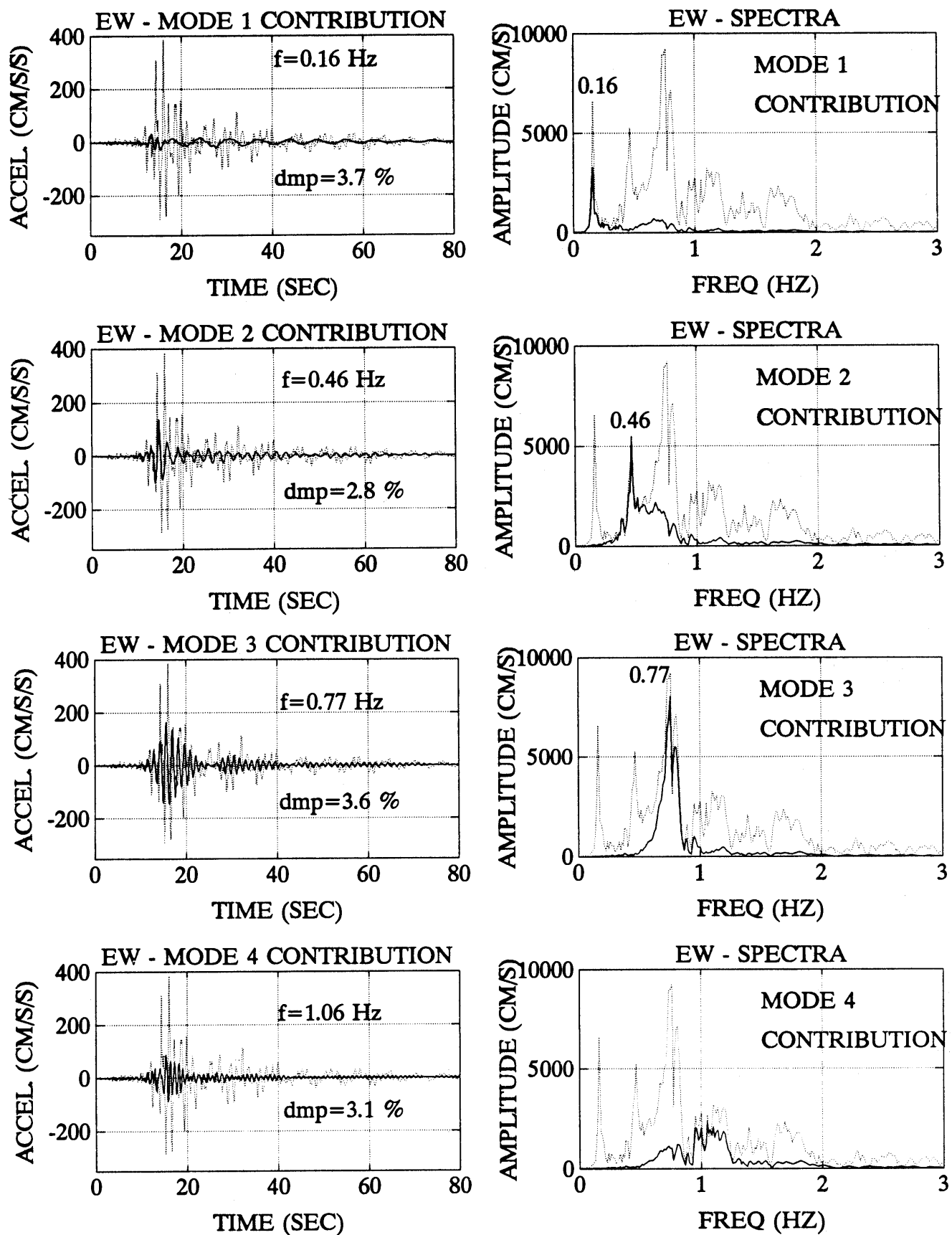


Figure 24.—Significant east-west modal accelerations (and their amplitude spectra) of the 44th-floor for Embarcadero Building extracted from system identification analysis and comparison with the total 44th-floor acceleration.

Table 5.—Identified dynamic characteristics for Embarcadero Building

MODE	NS			EW		
	f (Hz)	T (s)	ξ (pct.)	f (Hz)	T (s)	ξ (pct.)
1	0.19	5.26	2.5	0.16	6.25	3.7
2	0.57	1.75	2.2	0.46	2.17	2.8
3	0.98	1.02	1.4	0.77	1.30	3.6
4	1.33	0.75	2.3	1.06	0.94	3.1

code-allowable ratios during the earthquake. It is safe to predict that the allowable drift ratios could be exceeded for the design level II earthquake. This conclusion is from studies of Astaneh and others (1991), Chen and others (1992), and Çelebi (1993).

Torsional response and rocking of the building is insignificant (Astaneh and others, 1991; Chen and others, 1992; Çelebi, 1993).

The amplitude at approximately 0.75-0.8 Hz (1.25-1.33 s), noted in the Fourier amplitude spectra (figs. 21, 22), is attributed to belonging to the site because the amplitude at the roof does not increase significantly when compared to that at the ground floor. Furthermore, the site period, estimated to be around 1.25-1.40 s, falls within the range of modal periods of the building, and therefore the building may have been subjected to a double-resonance effect. It is noted that the site-specific response spectra (fig. 18) do not adequately reflect the resonating site period (fig. 17) (Çelebi, 1993).

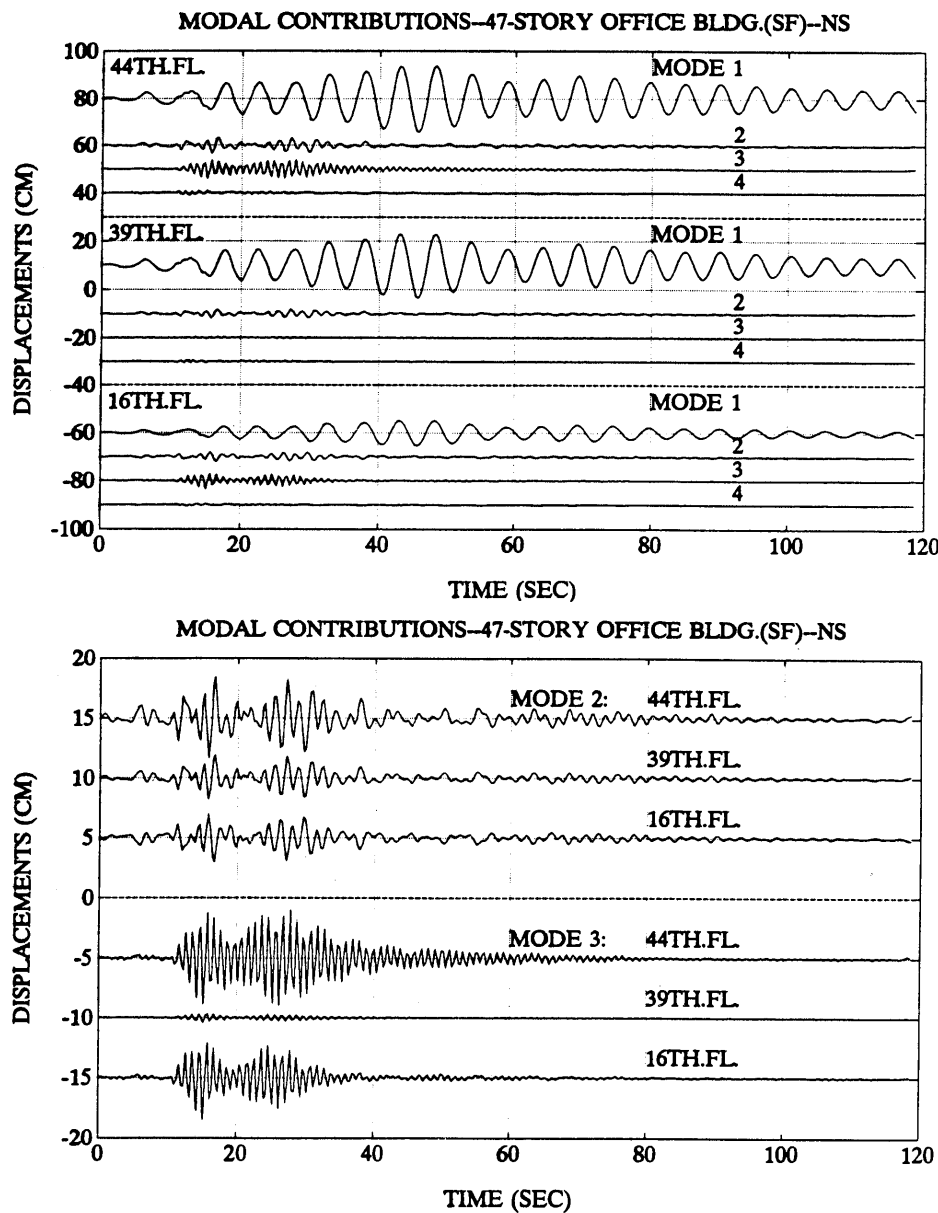


Figure 25.—Comparison of modal displacement contributions at the top three north-south instrumented floors for Embarcadero Building.

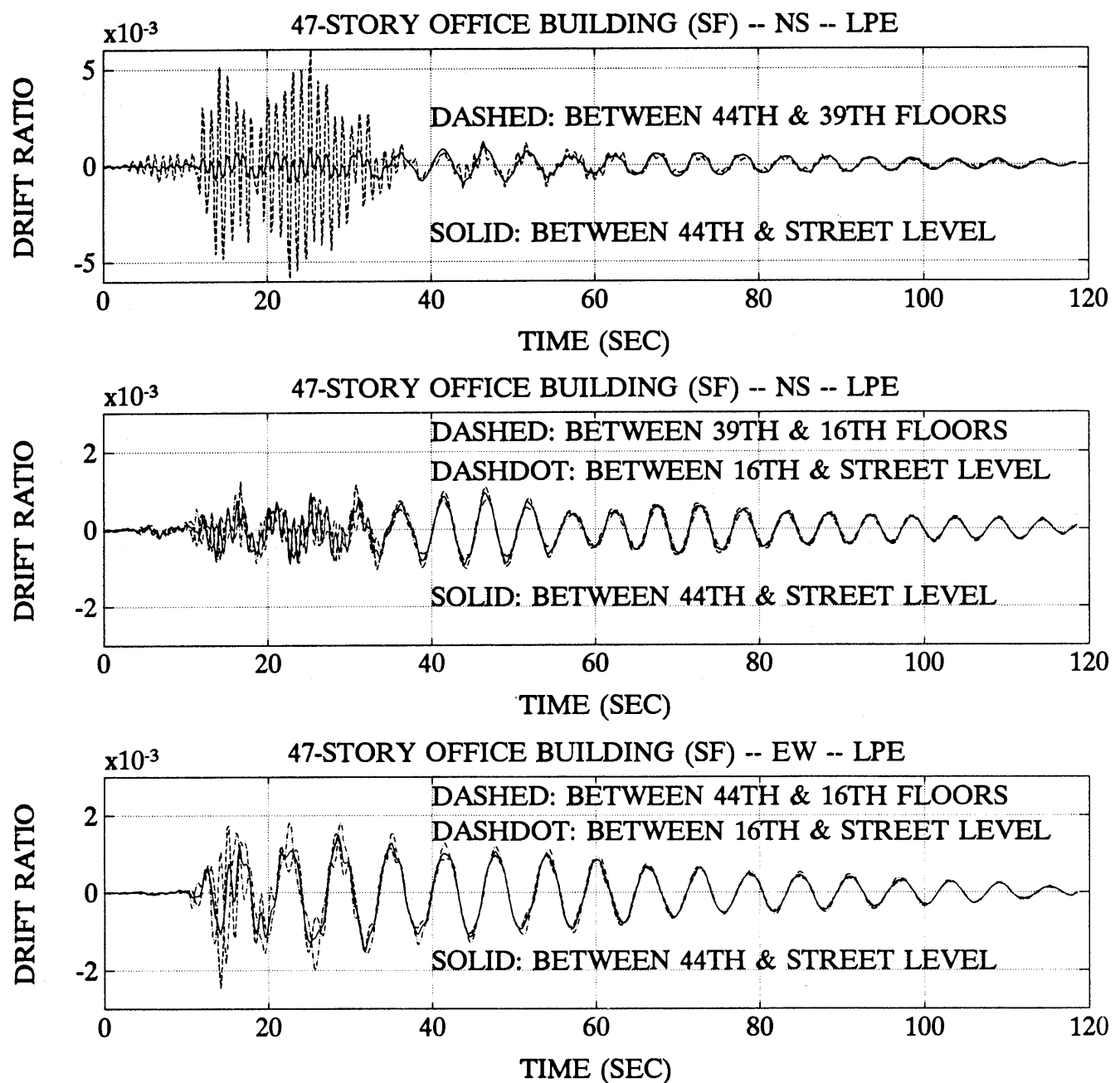


Figure 26.—Drift ratios for Embarcadero Building.

In figure 27, rotation time-histories (calculated from displacement time-histories) of the mat as well as the basement walls are shown. The significance of this plot is that (1) the mat rotation has a peak value of 0.000057 radians (0.0033°) while the peaks of the wall rotations are (north-south) 0.0004 radians (0.023°) and (east-west) 0.00048 radians (0.028°), and (2) the frequencies of these rotations are the same as those of significant translational frequencies in respective directions, thus confirming the presence of structural frequencies in the basement motions. The anomaly here is that the rotations of the walls are 7-8 times larger than the rotations of the mat. Although there may be some numerical errors related to data processing, these ratios are too high to ignore. Similar magnitude peak rotations were observed from the response data of the nearby Transamerica Building (Çelebi and Şafak, 1991; Soydemir and Çelebi, 1992).

In addition to detailed analyses presented above, Chajes and others (1992) used an approximate technique to conduct dynamic analysis of the Embarcadero Building. Their analysis utilizes a continuum methodology to create a reduced-order representation of the building. The accuracy of the approximate dynamic analysis is established by comparing the computed results to the actual response recorded during the earthquake.

Astaneh and others (1991) and Chen and others (1992) performed detailed dynamic elastic time-history and response spectrum analyses of the Embarcadero Building and compared the calculated responses with actual

recorded responses. They varied several parameters in the development of their mathematical models. The model buildings were then subjected to ground accelerations recorded at the basement level of the building during the earthquake. The set of analyses using the mathematical models produced floor displacement time-histories which were then compared with the recorded values. The results show that at Loma Prieta level ground motions, the design seems sufficient. They also performed nonlinear dynamic analyses using two-dimensional models of a typical frame, whereby the mathematical models were subjected to base excitations of (1) actual recorded motions during the earthquake, (2) motions represented by scaling-up of the peak accelerations of the earthquake record, and (3) motions of a hypothetical San Andreas M=8+ plus event to simulate a major earthquake. The trends in development of plastic hinges throughout the structures for these cases indicate that significant inelastic behavior occurs at the floors between the 36th and 42d levels and is attributed to the change in stiffness at those levels. The development of plastic hinges for cases 2 and 3 described above are exhibited in figures 28 and 29 (Astaneh and others, 1991; Chen and others, 1992; Bonowitz and Astaneh, 1994). These figures are important in that they indicate the behavior that may be expected from the Embarcadero Building during future earthquakes with large input motions (either due to larger magnitude earthquakes or earthquakes at closer distances to the building).

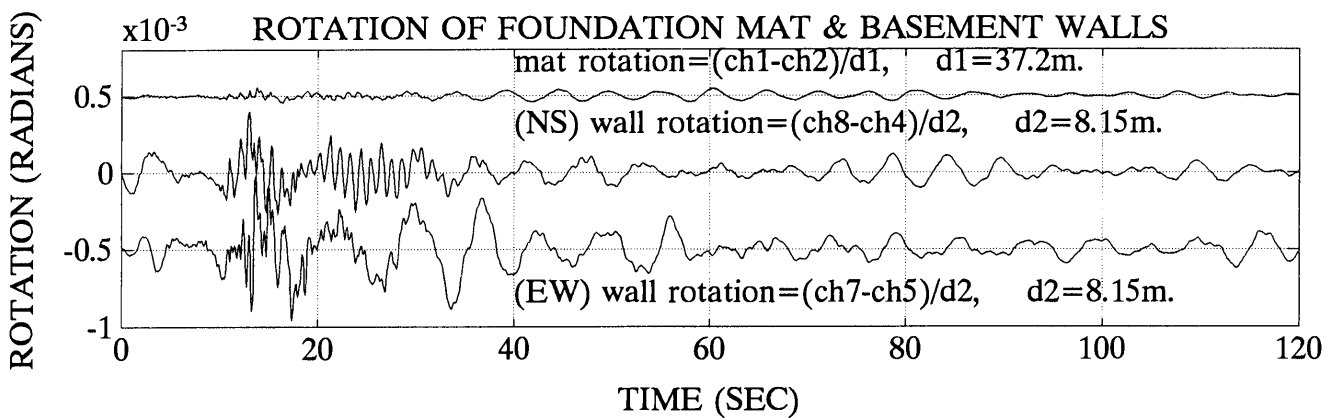


Figure 27.—Rotation of basemat compared to rotation of basement walls for Embarcadero Building.

**ENVELOPE OF PLASTIC HINGES – E-W FRAME
(2.75x LOMA PRIETA RECORD)**

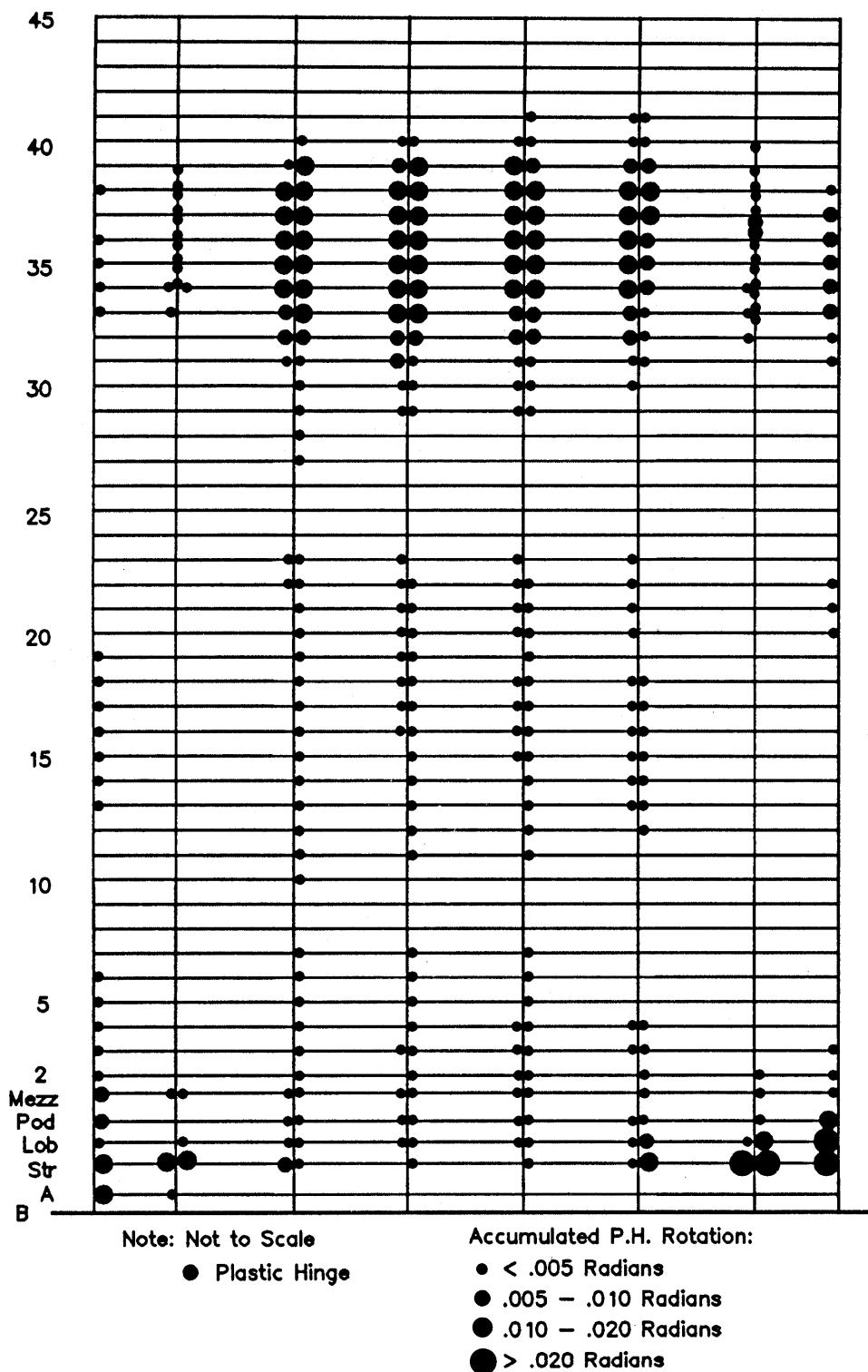


Figure 28.—Development of plastic hinges formed in the east-west frame modeled by Astaneh and others (1991) for 2.75 times the Loma Prieta earthquake motions (with permission of A. Astaneh).

**ENVELOPE OF PLASTIC HINGES – E-W FRAME
(SAN ANDREAS EVENT)**

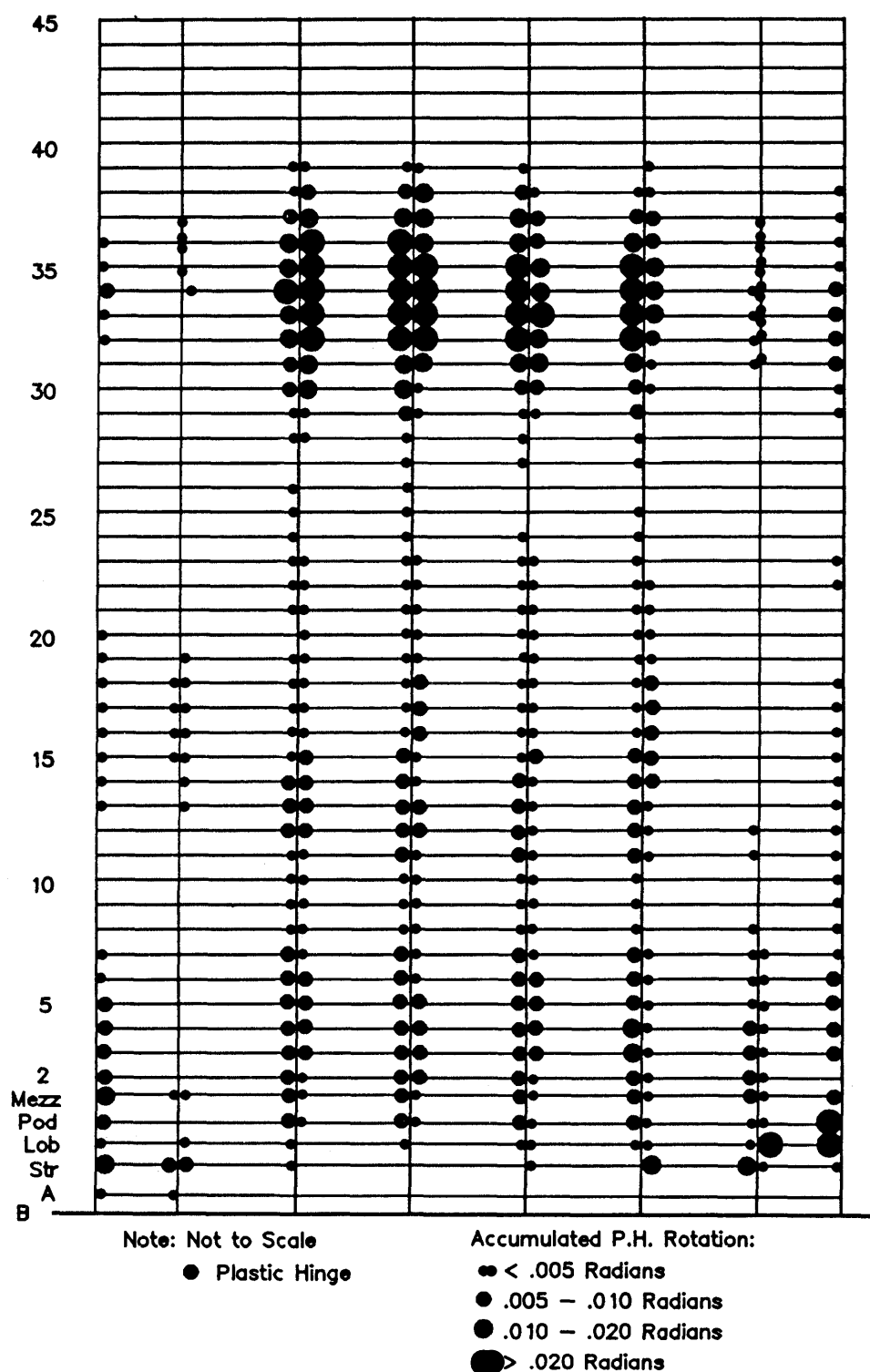


Figure 29.—Development of plastic hinges formed in the east-west frame modeled by Astaneh and others (1991) for a hypothetical M=8+ San Andreas event (with permission of A. Astaneh).

SANTA CLARA COUNTY OFFICE BUILDING (SAN JOSE)

One of the buildings that benefited from studies of its recorded responses during strong-motion events is the Santa Clara County Office Building in San Jose (fig. 30). A decision to retrofit was based on response data of the building recorded during the Loma Prieta earthquake and two previous but smaller earthquakes, the 24 April 1984 Morgan Hill ($M_s=6.1$) and the 31 March 1986 Mt. Lewis ($M_s=5.5$) (Huang and others, 1985; R. Darragh, personal commun., 1991). The set of data from these three earthquakes has been studied by Lin and Papageorgiou (1989), Boroschek and others (1990), Boroschek and Mahin (1991), and Çelebi (1994a). Although this building did not suffer structural damage during these earthquakes, it suffered extensive nonstructural and contents damage. Rihal (1994) studied the performance of nonstructural members of the building during these three earthquakes, when the occupants were uncomfortably and severely shaken during the prolonged and resonating vibration of the building. Consequently, in 1994, the building was retrofitted with viscous elastic dampers (Crosby and others, 1994).

A general view of the Santa Clara County Office Building is seen in figure 30A. The location of the building, the epicentral locations of the three earthquakes referred to above, and the instrumentation scheme are shown in figure 30B (Çelebi, 1994a). This 13-story, 56-m-tall, moment-resisting steel-framed building was built in 1975 according to the Uniform Building Code (1970). There are six column lines in each direction of the approximately 51×51m plan of the building.

Figure 31 shows acceleration responses at the roof recorded during the three earthquakes. The figure clearly indicates the long-duration and resonating responses of the structure and the beating effect observed in the responses. Figure 32 shows typical system identification analysis results (Çelebi, 1994a) for only Loma Prieta data. Peak accelerations at the roof and basement levels, the fundamental translational and torsional frequencies (and periods), and damping percentages extracted by system identification techniques (for all three earthquakes) are presented in table 6. The second and the third modes (at approximately 1.45 and 2.50 Hz) contribute very little to the overall response; therefore, the remainder of the discussion will be devoted to the fundamental modes only. The small differences between the periods determined from the three earthquake response data are noted. Since the structural characteristics of the building during the three earthquakes are very similar, only Loma Prieta is chosen to further characterize the structural response.

Figure 33A shows acceleration responses at the roof level, as well as the difference of parallel accelerations at the roof level (nominal torsional accelerations—actual tor-

sional accelerations can be calculated by dividing the nominal torsional accelerations by the distance between the two parallel sensors). Figure 33B shows the amplitude spectra of the unidirectional responses clearly peaking at the translational frequency (period) 0.45 Hz (2.22 s). Figure 33C shows amplitude spectra of the nominal torsional accelerations (calculated from parallel records in the north-south and east-west directions respectively) that peak at 0.57 Hz (1.69 s) and 0.45 Hz (2.22 s). Figures 33D and E show the coherence, phase angle, and normalized cross-spectra of the unidirectional response and confirm the translational frequency at 0.45 Hz. At this frequency, the motions are coherent and are in phase, clearly indicating that they are related. Figure 33F, on the other hand, confirms the torsional frequency at 0.57 Hz that were identified from the nominal torsional accelerations represented by the differential accelerations of two parallel sensors at a floor. There is unity coherence and the phase angle is zero at 0.57 Hz (Çelebi, 1994a). The proximity of the torsional frequency (period) at 0.57 Hz (1.69 s) to the translational frequency (period) at 0.45 Hz (2.2 s) causes the observed coupling and beating effect.

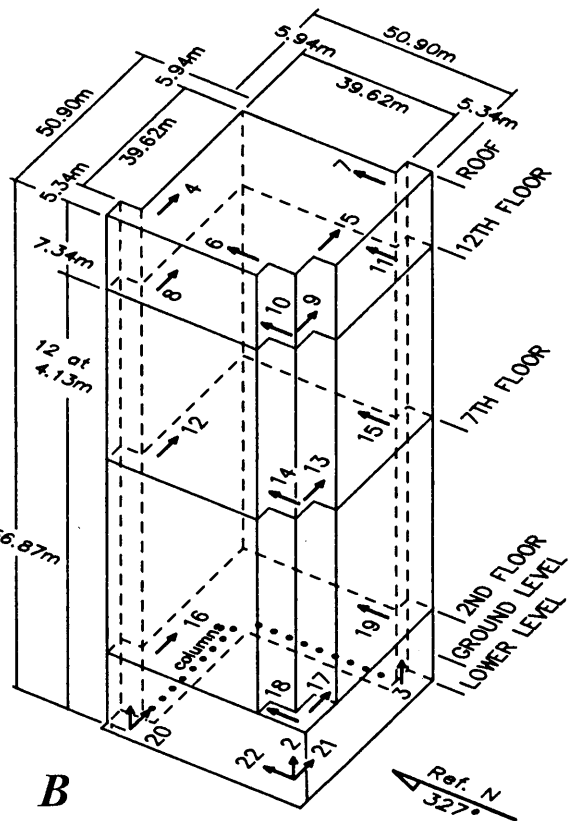
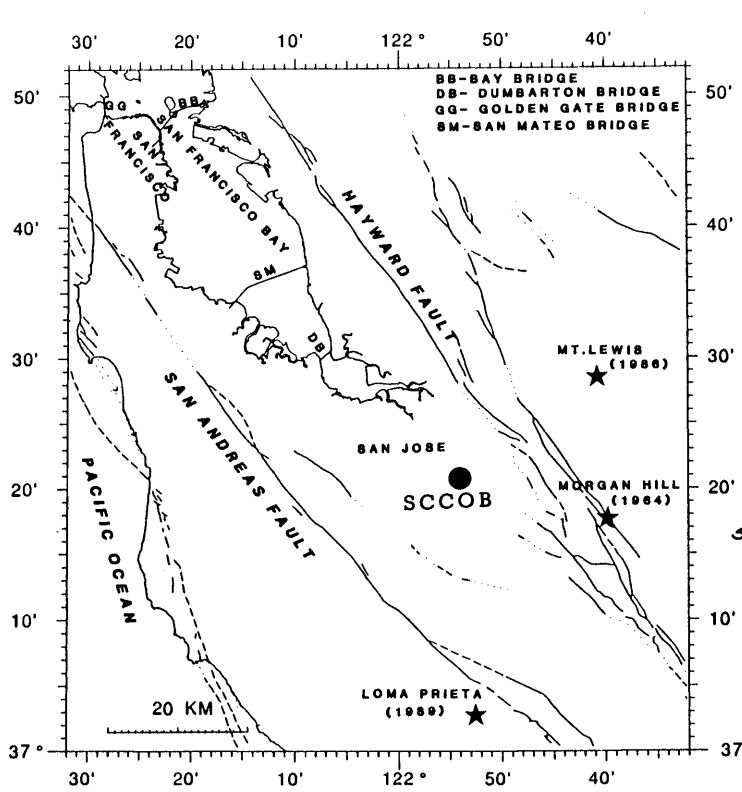
Lin and Papageorgiou (1989) studied the Santa Clara County Office Building response data from the Morgan Hill earthquake and concluded that strong beating-type phenomena occur in buildings with identifiable close-coupled torsional and translational modal characteristics, as in the case of the Santa Clara County Office Building. Boroschek and Mahin (1991) further elaborated on this issue. In their investigation of the behavior of this lightly damped, torsionally coupled structure, they developed three-dimensional linear and nonlinear numerical models and performed several elastic and inelastic computer analyses. As in the recorded data, Boroschek and Mahin found that the calculated responses of the building are characterized by (1) long duration, narrow-banded periodic motions with strong amplitude modulation, (2) large displacements and torsional motions, (3) large amplification of the input ground motions, and (4) slow decay of the building's dynamic responses. They concluded that the unusual response characteristics of the building are due to design parameters that produced a structural system with low equivalent viscous damping, resonance, and beating.

The close-coupling of the torsional and translational frequencies at low damping percentages (lightly damped system) clearly explains that the translational and torsional modes reinforce one another during vibration, with only small dissipation, and that beating occurs with a period of $T_b=2T_1T_2/(T_1-T_2)=2(2.22)(1.69)/(2.22-1.69)=14.2$ s (Boroschek and Mahin, 1991; Çelebi, 1994a).

The mat foundation of the building rests on alluvial site conditions. The depth to bedrock at the site is estimated to be between 270 m and 500 m. Figure 34 shows the site transfer function plots for two estimated depths to



A



B

Figure 30.—A, Santa Clara County Office Building (SCCOB). B, Location of Santa Clara County Office Building, its overall dimensions and epicenters of three nearby earthquakes.

bedrock and shear-wave velocities (V_s) assigned to each layer based on available geotechnical reports (Earth Sciences Associates, 1971). The figure indicates that the site is capable of generating resonating surface waves at low frequencies that are, as will be shown, close to the frequencies of the building. In a study of the Santa Clara Valley following Loma Prieta, Frankel and Vidale (1992) concluded that 2-5 second long-period motions in the basin can be generated during earthquakes.

Figure 35 shows the coherence, phase angle, and normalized cross-spectra for the roof and basement motions calculated only for the east-west direction, since at the basement the two parallel sensors are in this direction. The proximity of the site frequency at 0.33-0.38 Hz and the fundamental frequency at 0.45 Hz is the cause of the resonating (more or less steady-state surface wave) motions of the building. This is simply explained using the relationship for the amplification (A) of a damped system (in percent), with a frequency ratio (r) of ground to structure:

$$A = 1/\left[(1-r^2)^2 + (2\xi r)^2\right]^{1/2}.$$

For a lightly damped system with $r=0.33/0.45=0.73$ or $0.38/0.45=0.84$, significant amplification in the response can be expected (for example, $A \approx 1/(1-r^2) \approx 2.14-3.40$) (Çelebi, 1994a).

The average drift ratios calculated between the roof and the basement and between the 12th floor and 2nd floor reach 0.8 percent and exceed allowable code drift ratios (0.5 percent). The drift ratio between the roof and 12th floor is smaller than the average drift ratio or the code allowable.

In a recent study, Porter (1996) showed that the observed structural response of the building can be explained by the geometrical configuration between earthquake epicentral location and the orientation of the structure.

Rihal (1994) studied nonstructural damage in the building following the earthquake to correlate the recorded California Strong Motion Instrumentation Program response data with observed nonstructural component damage. A methodology is presented to assess the performance and behavior of nonstructural building components during earthquakes. One main objective of this case study was to investigate the relationship between seismic response parameters (for example, peak response acceleration levels, frequency content, and inter-story drift levels) and corresponding nonstructural component damage observed during the earthquake. Significant nonstructural component damage was observed to have occurred, particularly at the 7th and 11th floor levels. Comparison of the observed nonstructural damage and peak recorded accelerations at the 7th floor and at the 12th floor show the thresholds of response accelerations that produce nonstructural component damage. Rihal proposed a nonstructural component damage index expressed as a percentage of components damaged to characterize observed nonstructural component damage data.

In retrofitting the building, Crosby and others (1994) installed viscous elastic dampers in selective bays of the building. Figure 36A and B show the plan view and vertical sections. The bays of the framed structure where the dampers were installed are indicated in the figures. Figure 36C shows a typical viscous elastic damper (Crosby and others, 1994). Çelebi and Liu (1997) performed ambient tests of the building following the retrofit; preliminary results show that for low-amplitude excitation, the dampers produce small changes in the dynamic characteristics but are expected to alter the dynamic behavior significantly during strong shaking. Before the retrofit, Marshall and others (1991) and Çelebi (1996) observed significant differences in the dynamic characteristics of the building for strong- and low-amplitude shaking. This is discussed later in this paper.

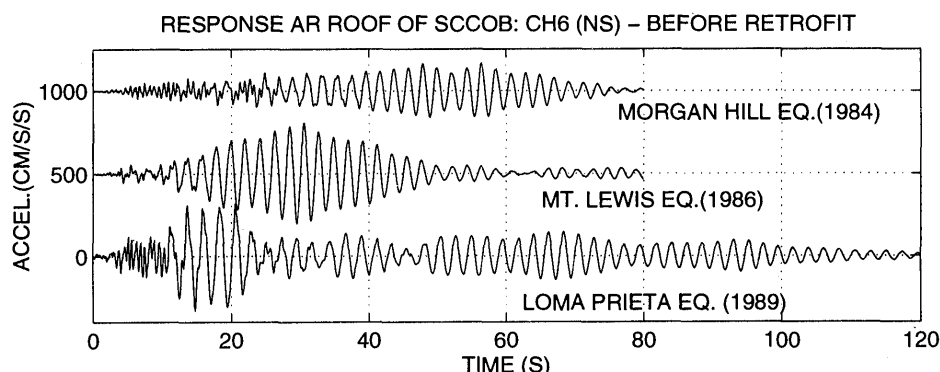


Figure 31.—Acceleration responses at the roof of Santa Clara County Office Building recorded during the Loma Prieta, Morgan Hill, and Mt. Lewis earthquakes.

In summary, there are three causes for the long-duration response of the Santa Clara County Office Building: (1) basin effect and site characteristics that contribute to resonating excitation, (2) the close-coupled translational-torsional mode that causes beating phenomena to occur, and (3) the inherent low-damping of the building. Under-

standing the cumulative structural and site characteristics that affect the response of the building is important in assessing earthquake hazards to other similar buildings (Celebi, 1994a). The results emphasize the need to better evaluate structural and site characteristics in developing earthquake resisting designs that avoid resonating effects.

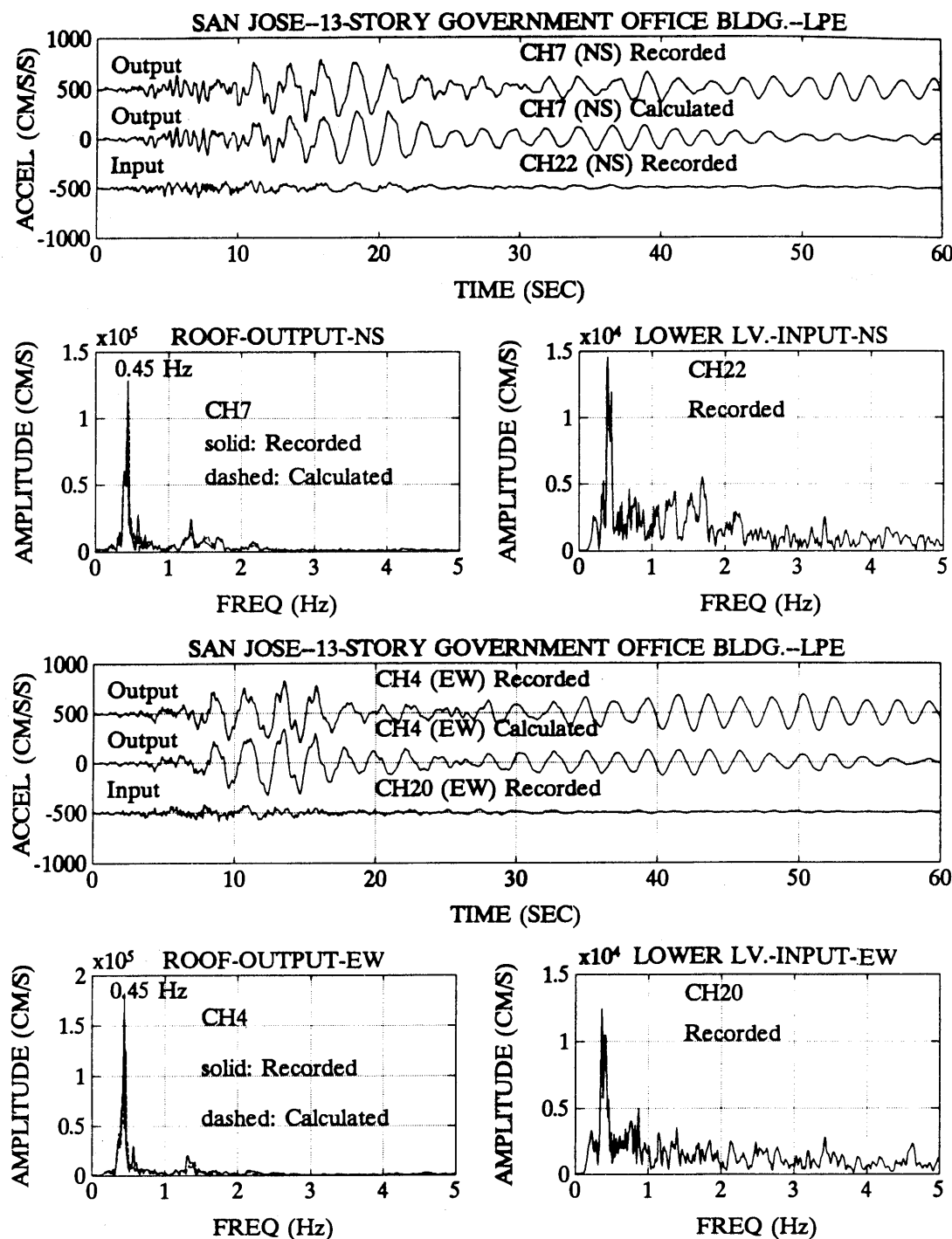


Figure 32.—Typical system identification analysis results of Santa Clara County Office Building for Loma Prieta data (Celebi, 1994).

Table 6.—Peak accelerations and dynamic characteristics for Santa Clara County Office Building

		Earthquake			
		Loma Prieta	Morgan Hill	Mt. Lewis	
Translational	Peak Acceleration (g)	Roof (NS)	0.34	0.17	0.32
		Roof (EW)	0.34	0.17	0.37
		Base (NS)	0.10	0.04	0.04
		Base (EW)	0.09	0.04	0.04
	Period [T (s)]	2.22	2.17	2.08	
	Frequency [f (Hz)]	0.45	0.46	0.40	
Torsional	Damping [ξ (pct.)]	2.70	1.95	2.12	
	Frequency [f (Hz)]	0.57	0.59	0.58	
	Damping [ξ (pct.)]	1.69	1.70	1.72	

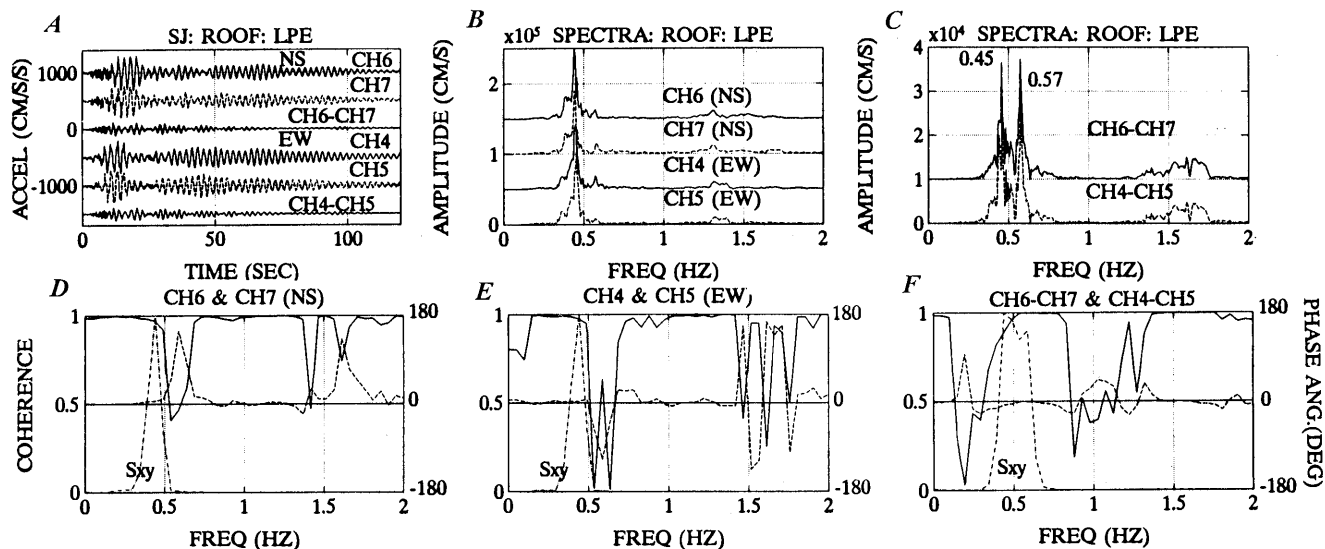


Figure 33.—A, Acceleration time histories of roof of Santa Clara County Office Building. B, C, Amplitude spectra. D, E, F, Coherence (solid line), phase angle (dashed line) plots with cross-spectra, S_{xy} , (dashed-dot line) superimposed to distinguish translational and torsional frequencies.

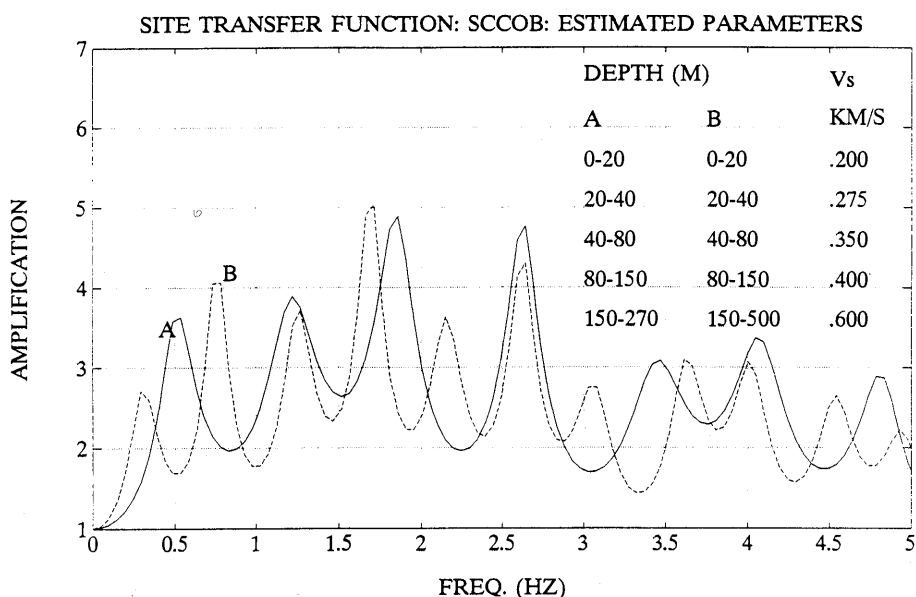


Figure 34.—Site transfer function for Santa Clara County Office Building.

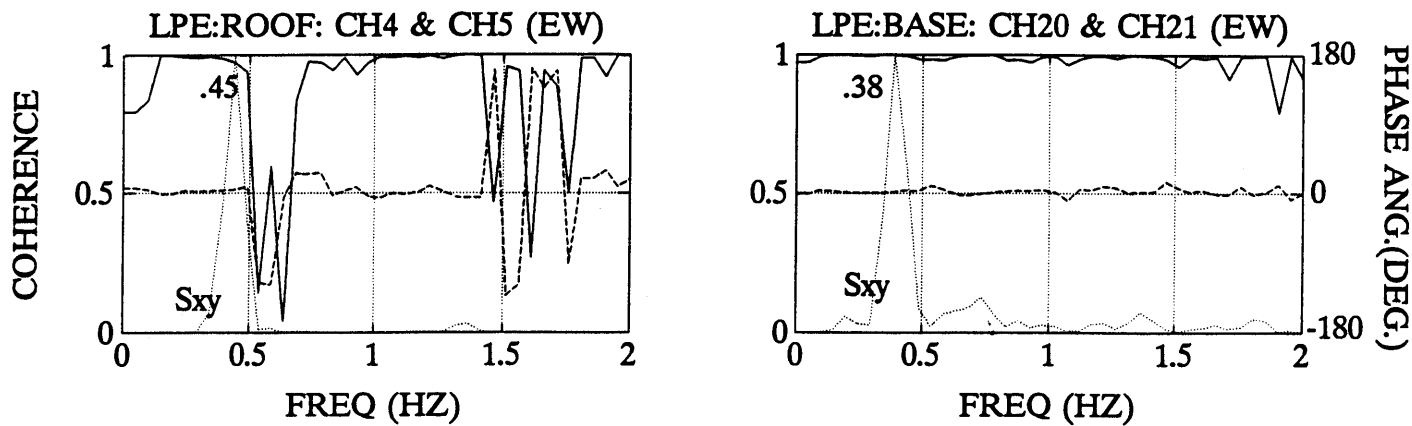


Figure 35.—Cross-spectra (dotted line), coherence (solid line), and phase angle (dashed line) plots for east-west motions at the roof and basement of Santa Clara County Office Building to distinguish structural and site frequencies.

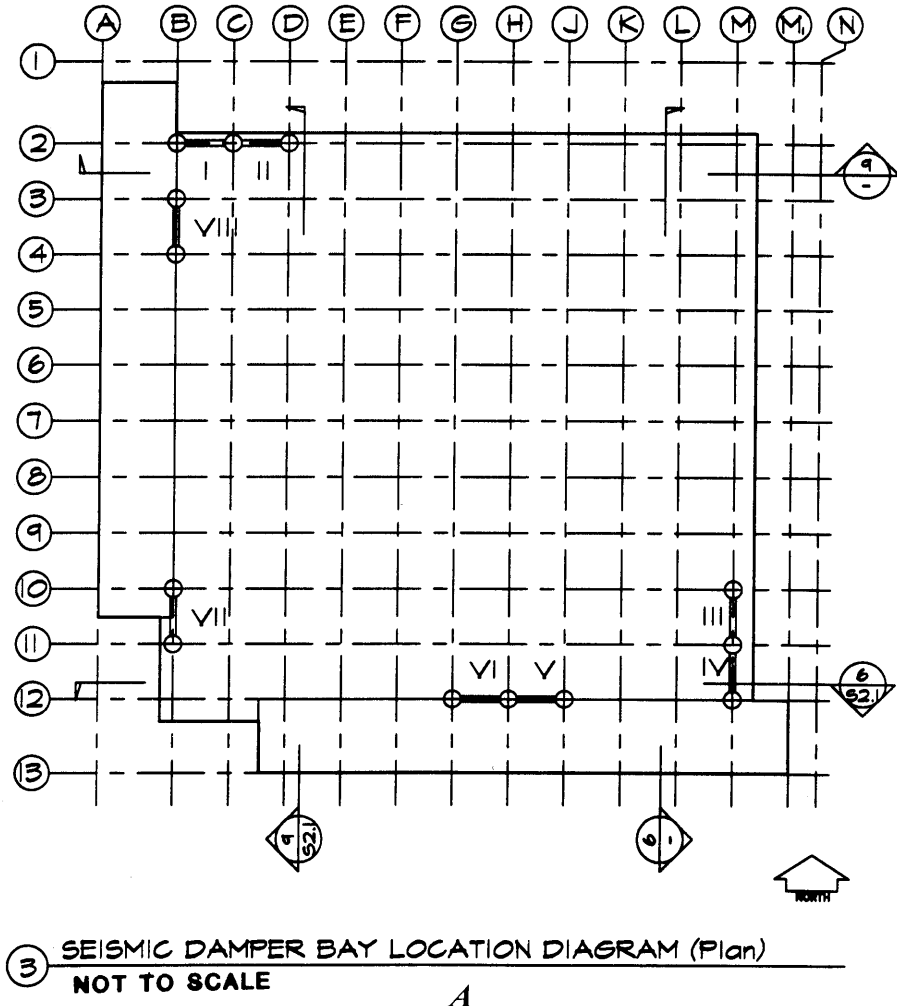
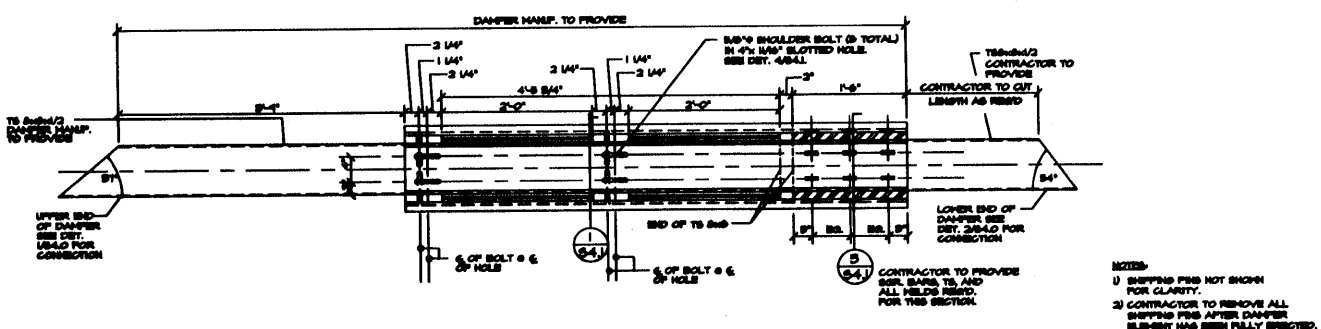
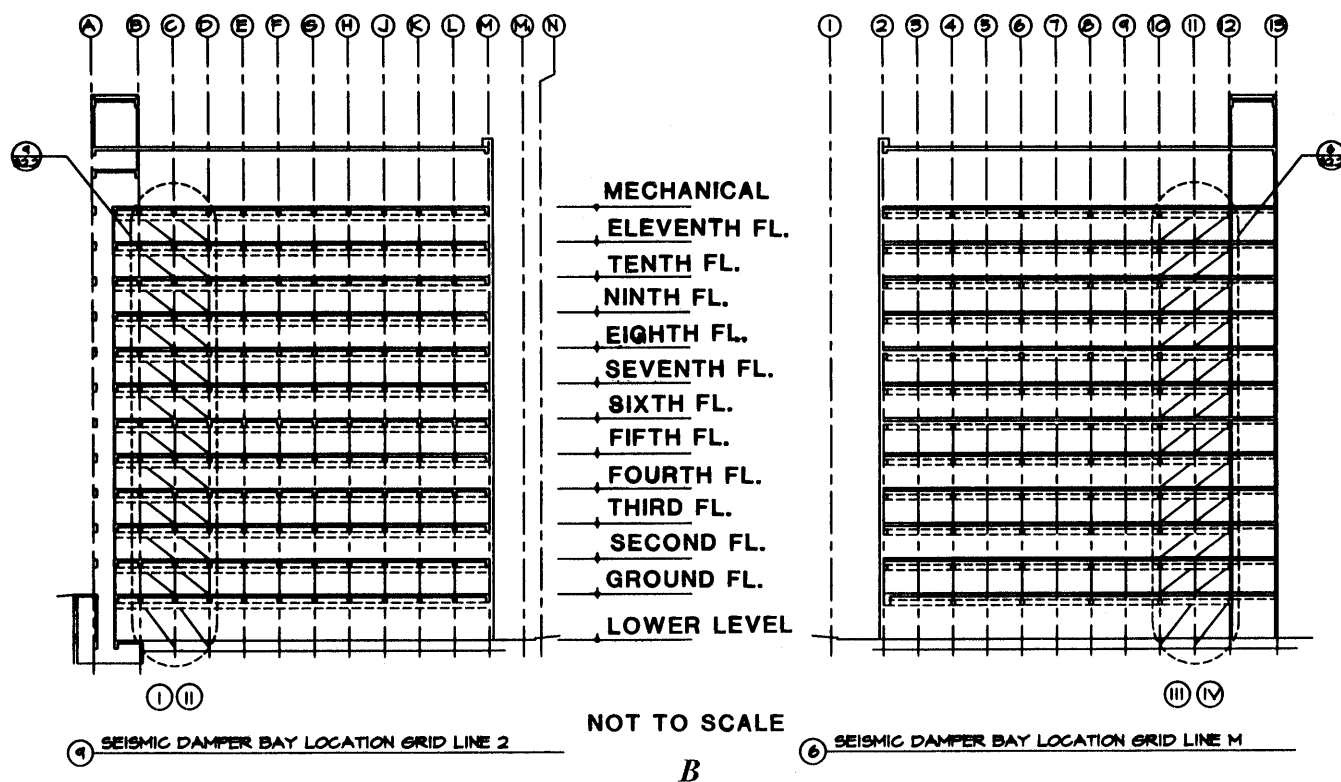
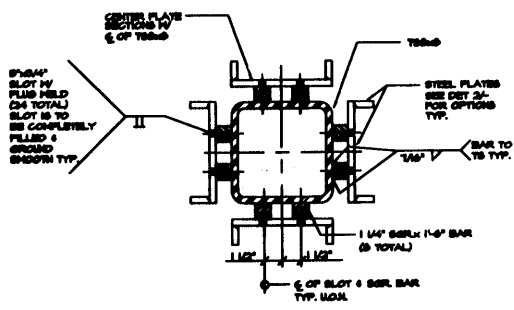


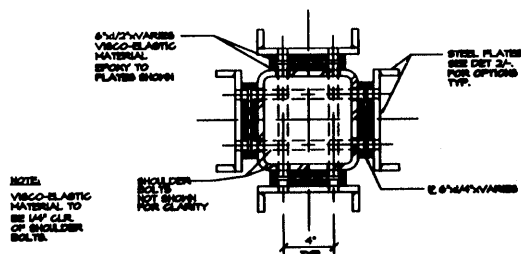
Figure 36.—A, Plan view of Santa Clara County Office Building. B, Vertical sections of building show bays where viscous elastic dampers have been installed for retrofitting the structural system to alter its dynamic behavior. C, Typical damper installed. (All figures courtesy of P. Crosby, The Crosby Group, Redwood City, Calif.)



7 DAMPER ELEMENT LENGTH A, TYPE I
SCALE 1:1000



8 SECTION • SQR. BARS
SCALE 1:100



9 SECTION • VISCO-ELASTIC MATERIAL
SCALE 1:100

Figure 36.—Continued.

CHEVRON BUILDING (SAN FRANCISCO)

The 42-story Chevron Building at 575 Market St. is a steel, moment-resisting framed, slender, rectangular in-plan building. It has two levels of basements and is built on 10-m-long precast pile clusters. A three-dimensional schematic of the building and its instrumentation scheme is shown in figure 37 (Çelebi, 1992). Recorded accelerations at different levels of the building and corresponding displacements are shown in figure 38. System identification analyses results are shown in figure 39.

Identified first-mode frequencies (periods) are 0.16 Hz (6.25 s) in the 225° direction and 0.21 Hz (4.76 s) in the 135° direction. Figure 40 shows coherency and phase-angle plots for (1) two parallel 225°-oriented motions (horizontal plane) at the roof, (2) two parallel 225° motions (in the vertical plane), and (3) two parallel 135° motions (also in the vertical plane) of the building. From these plots, we conclude that (1) torsion is insignificant since the motions in the horizontal plane at the roof are in

phase and coherent, (2) 0.55 Hz and 1.0 Hz in the 225° direction are the second and third modal frequencies since the phase angles are 180° and -180° out of phase, and (3) similarly for the 135° direction, 0.61 Hz and 1 Hz are the second and third modal frequencies. The recorded peak accelerations and extracted frequencies (periods) and damping percentages are summarized in table 7 (Çelebi, 1992).

Şafak (1993) studied the building in detail using a system identification method based on the discrete-time linear-filtering and the least-squares estimation techniques. He concluded that higher modes contribute significantly to the overall response and that soil-structure interaction occurs at 1.0 Hz. Anderson and Bertero (this chapter) studied the building also and concluded that the building remained elastic during the earthquake. They attributed this to the fact that the designers of the building opted to use site-specific design response spectra that was more conservative than the minimum code requirements.

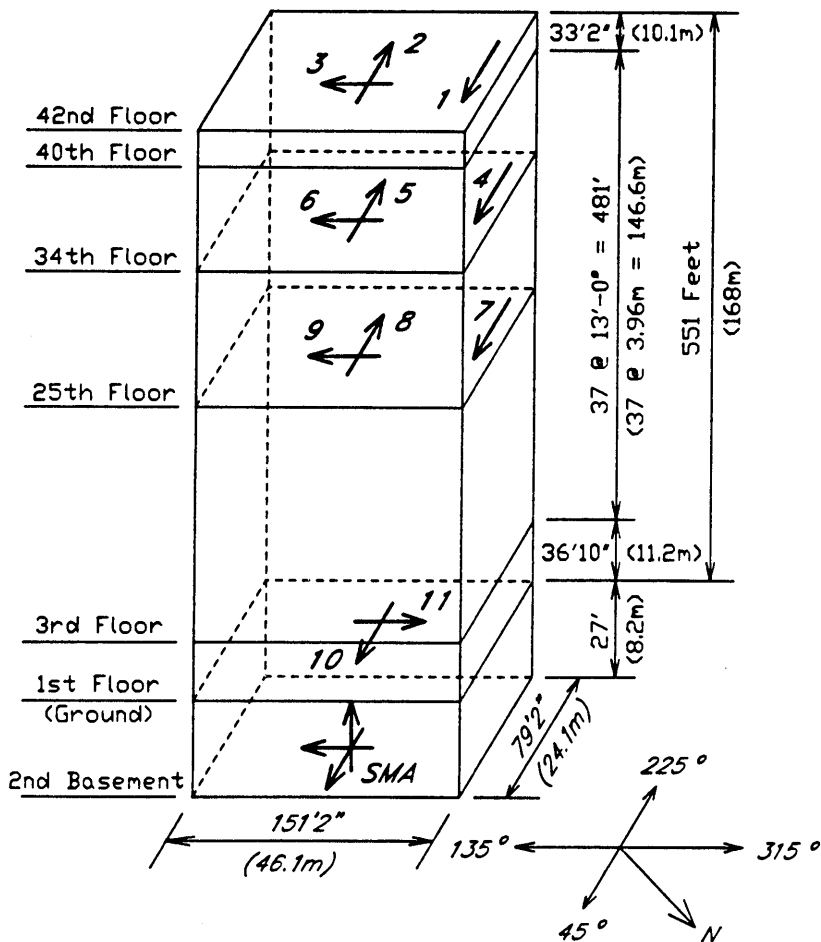


Figure 37.—General three-dimensional view and instrumentation scheme of Chevron Building, San Francisco.

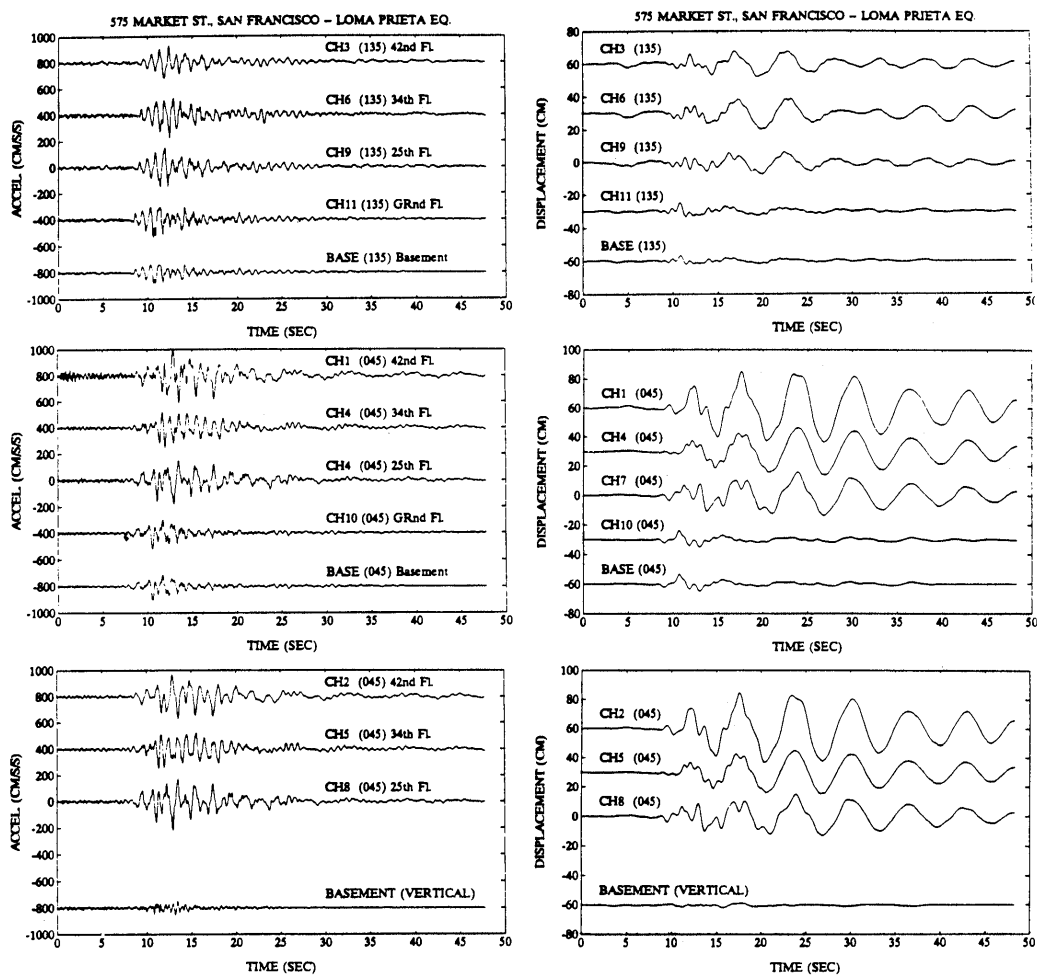


Figure 38.—Acceleration and displacement time-histories of Chevron Building.

Table 7.—Peak responses and dynamic characteristics of Chevron Building

A. Peak responses			
	Accel. (g)	Displ. (cm)	
Roof	0.31	18.6	
Basement	0.12	3.3	
B. Dynamic characteristics			
Mode	Direction	f (Hz)	T (s)
1	225	0.16	6.25
	135	0.21	4.76
2	225	0.55	1.82
	135	0.61	1.64
3	225	0.98	1.02
	135	1.00	9.2

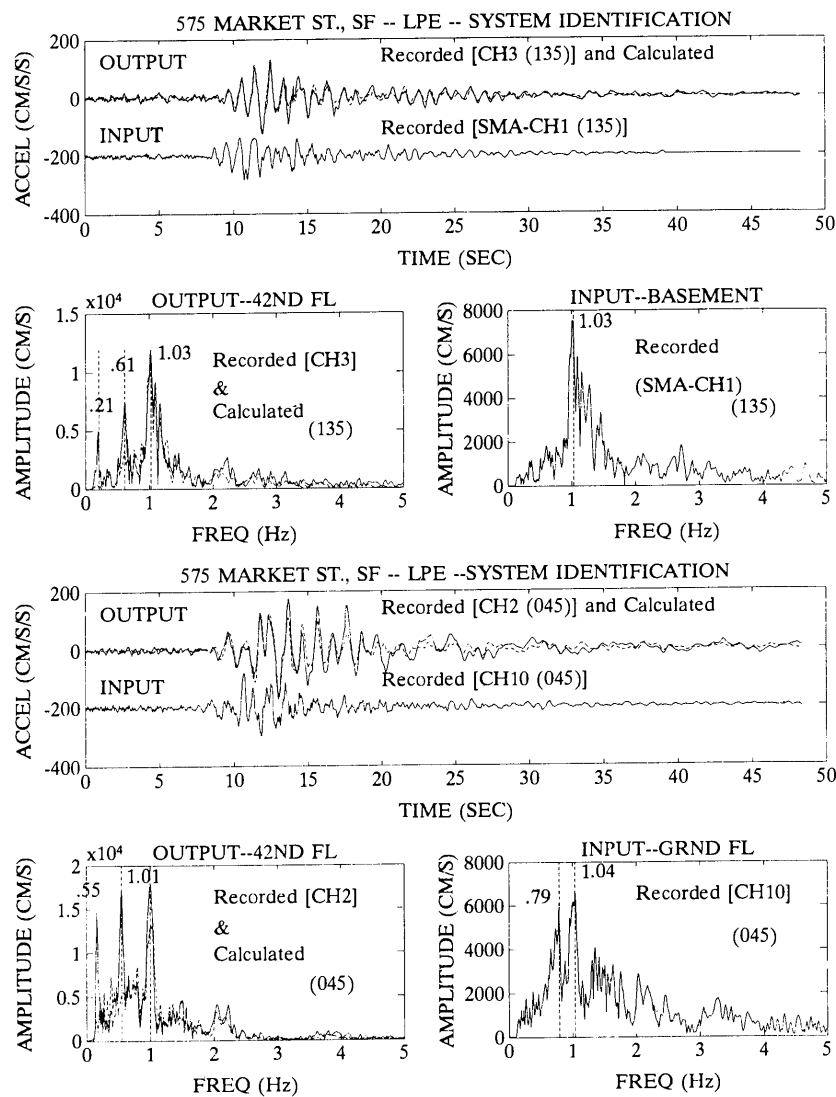


Figure 39.—System identification for Chevron Building.

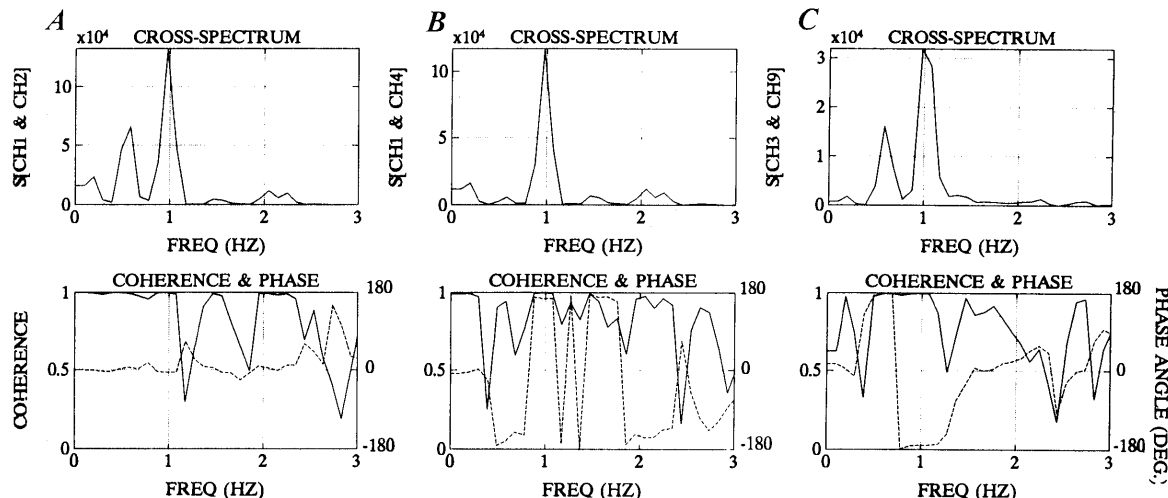


Figure 40.—Cross-spectrum, coherence, and phase angle plots for (A) parallel (225°) motions at 42d floor, (B) parallel (225°) motions at 42d and 34th floors, and (C) parallel (135°) motions at 42d and 34th floors.

MIXED CONSTRUCTION

CSUH ADMINISTRATION BUILDING (HAYWARD)

The 13-story California State University at Hayward (CSUH) Administration Building was constructed in 1971 in accordance with the Uniform Building Code (1967) design provisions. It is approximately 70 km from the Loma Prieta epicenter and is located within less than 5 km of the Hayward fault, also capable of generating large earthquakes. The general location of the building relative to the epicenter is shown in figure 1 (marked as HAYW). A general view of the building is shown in figure 41A. A three-dimensional view of the building and instrumentation scheme are shown in figure 41B. The availability of a free-field station on the university stadium grounds provides an opportunity to assess site and soil-structure interaction effects, if any. The building is 61.29 m high, with a structural system consisting of interior core moment steel frame and exterior perimeter concrete moment frame. The plan dimensions are 34.29×34.29 m. Up to the second floor, there are concrete shear walls around the elevator shafts. The building has a two-story extension bridge structure (enclosed on the second story) at its east side connecting it to an adjacent building (fig. 41B). The bridge structure is free to move on friction bearings at its junction with the adjacent structure. The building sits on bearing piles with a 45-cm-thick reinforced concrete mat on grade (Çelebi, 1994b).

Channels 2, 7, and 10 (parallel sensors in the north-south direction at the roof, 2d, and 1st floors, respectively) (fig. 41B) malfunctioned during the earthquake (Shakal and others, 1989); therefore, identification of torsional motions of the structure cannot readily be made.

The processed 40 seconds of the recorded acceleration and the displacements at different levels are shown in figure 42. The data from the building have been band-pass filtered with ramps at 0.2-0.4 Hz and 23-25 Hz (Shakal and others, 1989). The band-pass filter of the free-field data has a low-frequency ramp at 0.08-0.16 Hz. It is noted that the peak accelerations and displacements summarized in table 8 show significant differences, particularly in the displacement of the free-field versus the basement, due to the 0.08-0.16 Hz band-pass ramped filter of the free-field records. Also, longer periods are distinct in displacement plots of the free-field in figure 43. Such filtering errors and inconsistencies can provide misleading interpretations and can lead to wrong results in calculations using displacement (for example, drift).

In figure 44, calculated output of system identification analysis using 40 seconds of the basement accelerations

(recorded input) and roof accelerations (recorded output) of the building are shown. System identification calculations were also performed using the 5th floor accelerations as recorded output. The three significant frequencies (periods) and damping values also determined from system identification procedures are summarized in table 9. Figure 45 shows the structural frequencies in the spectral ratios calculated from amplitude spectra of roof and basement motions. It is noted that the three significant modal periods in each of the principal axes of the building follow the approximation of T , $T/3$, and $T/5$.

For all three modes in each of the two principal axes, modal damping percentages determined by system identification vary between 1.3 and 6.4 percent (table 9).



A

Figure 41.—A, California State University (Hayward) Administration Building. B, Three-dimensional schematic of building

The possibility of torsion was investigated by coherence function and phase angle plots as shown in figure 46. At 0.76 Hz, the two horizontal orthogonal motions at the roof are not coherent and are not in phase, which may imply that torsion is insignificant. However, this may be misleading if the two horizontal sensors are located at or close to the center of rigidity of the floor, in which case the torsional contributions would not show in the unidirectional motions. Thus, the importance of acquiring two parallel motions at a floor is emphasized.

Figures 46B and C show the peaks of the first three modes in the cross-spectrum of north-south and east-west motions at the roof and 5th floor, respectively, indicating that the coherence is unity for all modes and the phase angles are 0° at the fundamental frequency and 180° at the second and third modal frequencies.

Figures 47A and B show 5 percent damped response spectra of the north-south and east-west free-field and basement motions of the building. Figure 47C shows the basement north-south and east-west response spectra superimposed. It is clear from these spectra that both free-

field and basement have peaks in the range 0.25-0.3 s (3.3-4.0 Hz). Figure 47C shows roof and basement response spectra. Clearly, the first three modal frequencies (periods) can be identified directly from these spectra.

In the absence of a geotechnical report, available geotechnical and geological data of the strong-motion station site at the university stadium are used. It is assumed that the site conditions at the Administration Building are similar to those at the stadium. The top 3-4 m consists of sandy clay and clay (estimated V_s of 175 m/s) followed by 9-10 m of deeply weathered rhyolite (V_s of 315 m/s), followed by moderately weathered rhyolite (V_s of 825 m/s) (Fumal, 1991). The recommended average (to 30 meter depth) V_s is 525 m/s (Fumal, personal commun., 1991).

Due to absence of field measurements of site period, and considering only the top layer, a site period of approximately 0.1 seconds is estimated using $T_s = 4H/V_s$. This estimated period implies that this particular building would not be significantly influenced by the site effects. Furthermore, no site amplification is expected.

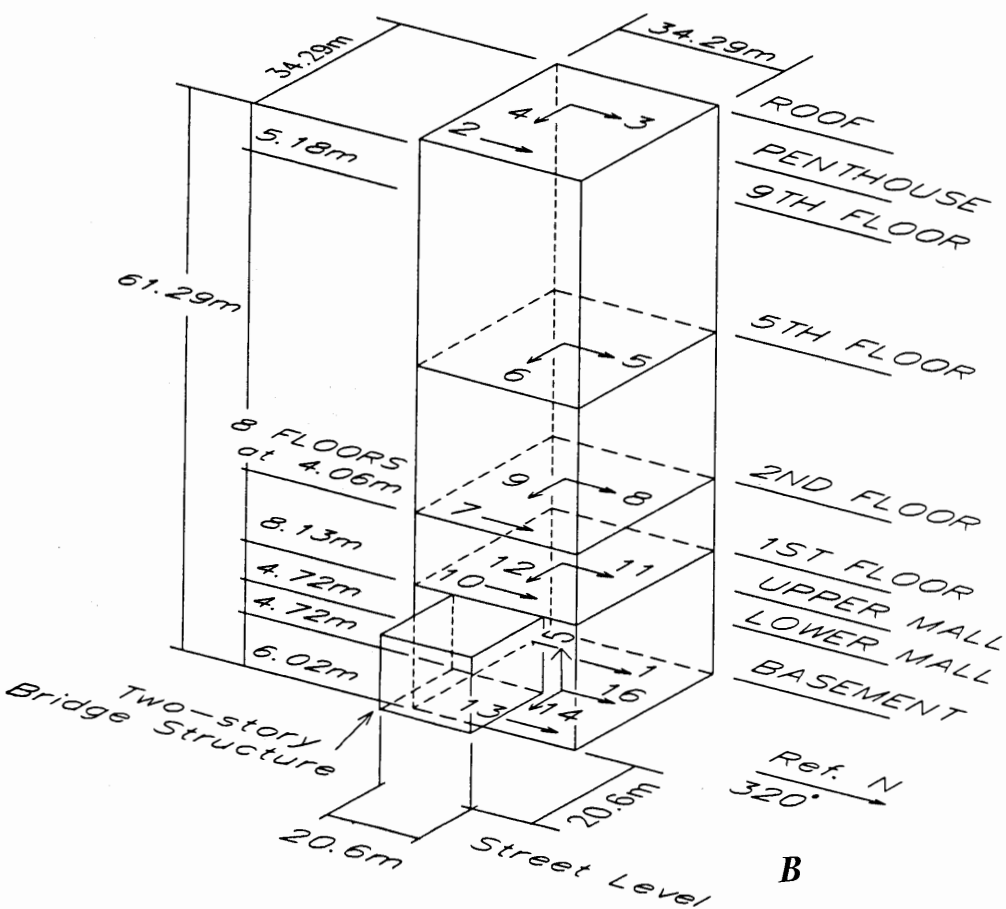


Figure 41.—Continued.

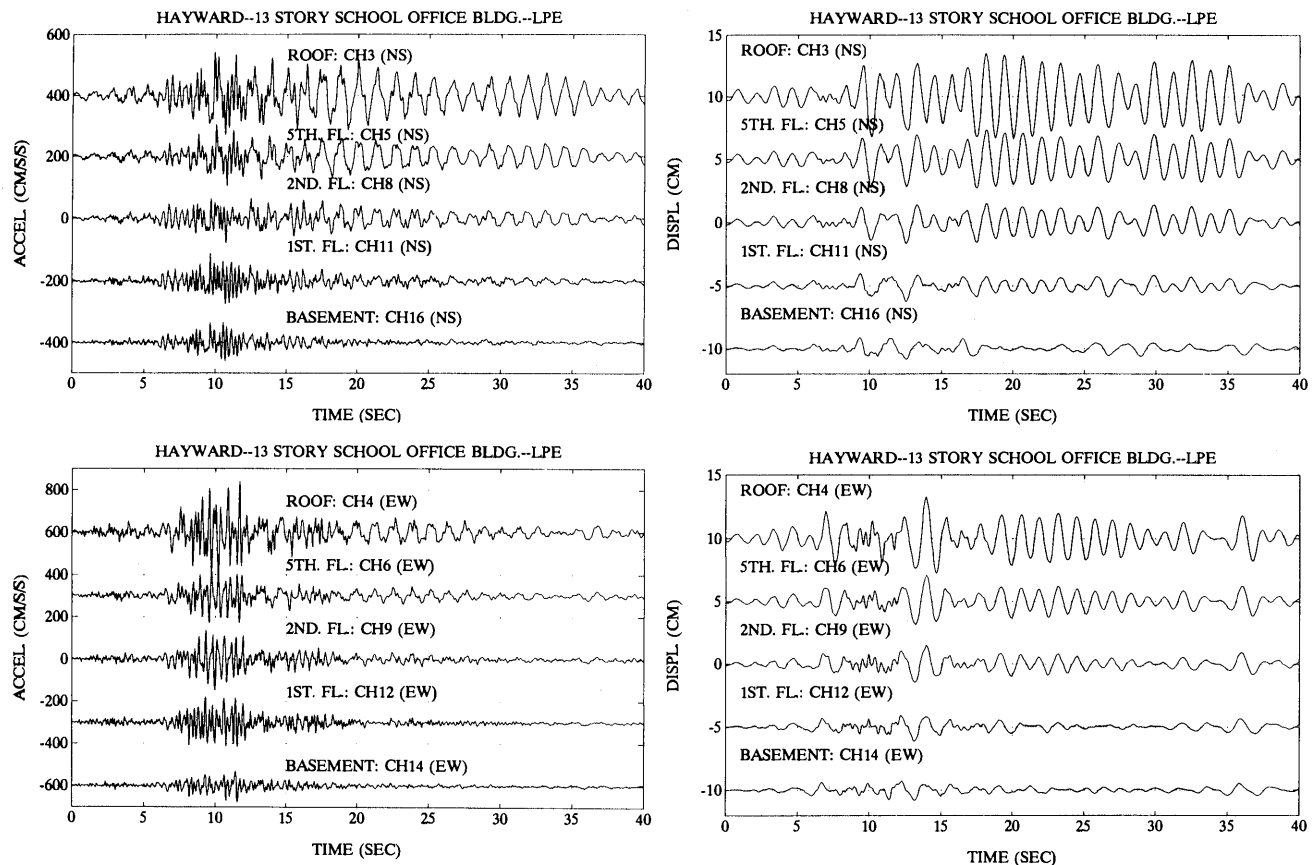


Figure 42.—Acceleration and displacement time-histories of California State University (Hayward) Administration Building.

Table 8.—*Accelerations and displacements at California State University (Hayward) Administration Building*

Location	Sensor	Direction	Accel. (g)	Displ. (cm)
Roof	3	NS(320°)	0.142	3.50
	4	EW(050°)	0.239	3.25
5th. floor.	5	NS	0.105	2.33
	6	EW	0.128	2.07
2d floor.	8	NS	0.078	1.69
	9	EW	0.146	1.50
1st floor.	11	NS	0.090	1.24
	12	EW	0.122	1.13
Basement	1	NS	0.069	0.90
	13	NS	0.065	0.89
	16	Ns	0.067	0.88
	14	EW	0.077	0.80
	15	UP	0.042	0.53
Free Field	FF1	EW (090°)	0.083	2.79
	FF2	UP	0.044	2.29
	FF3	NS(360°)	0.073	2.74

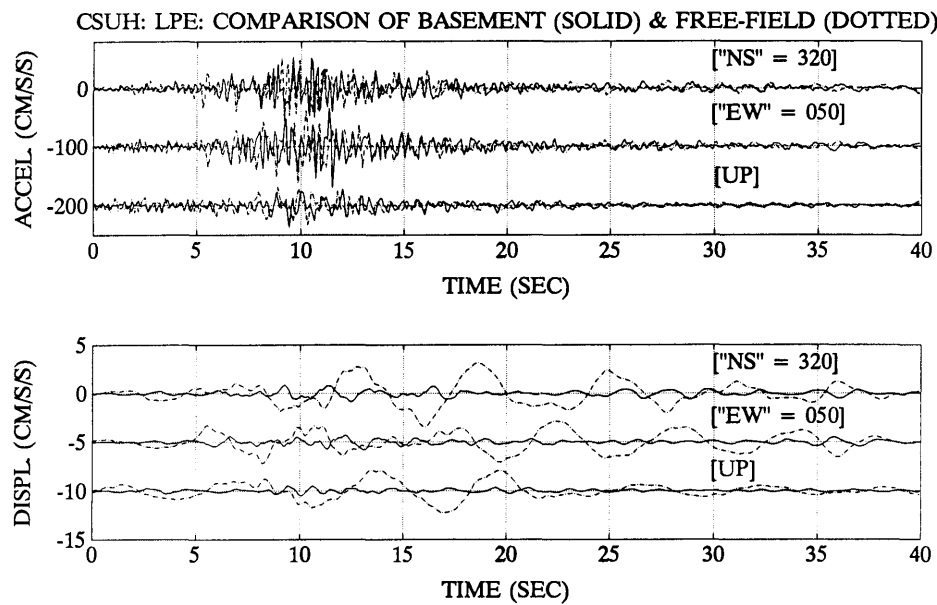


Figure 43.—Comparison of basement (solid line) and free-field (dash-dot lines) motions for California State University (Hayward) Administration Building.

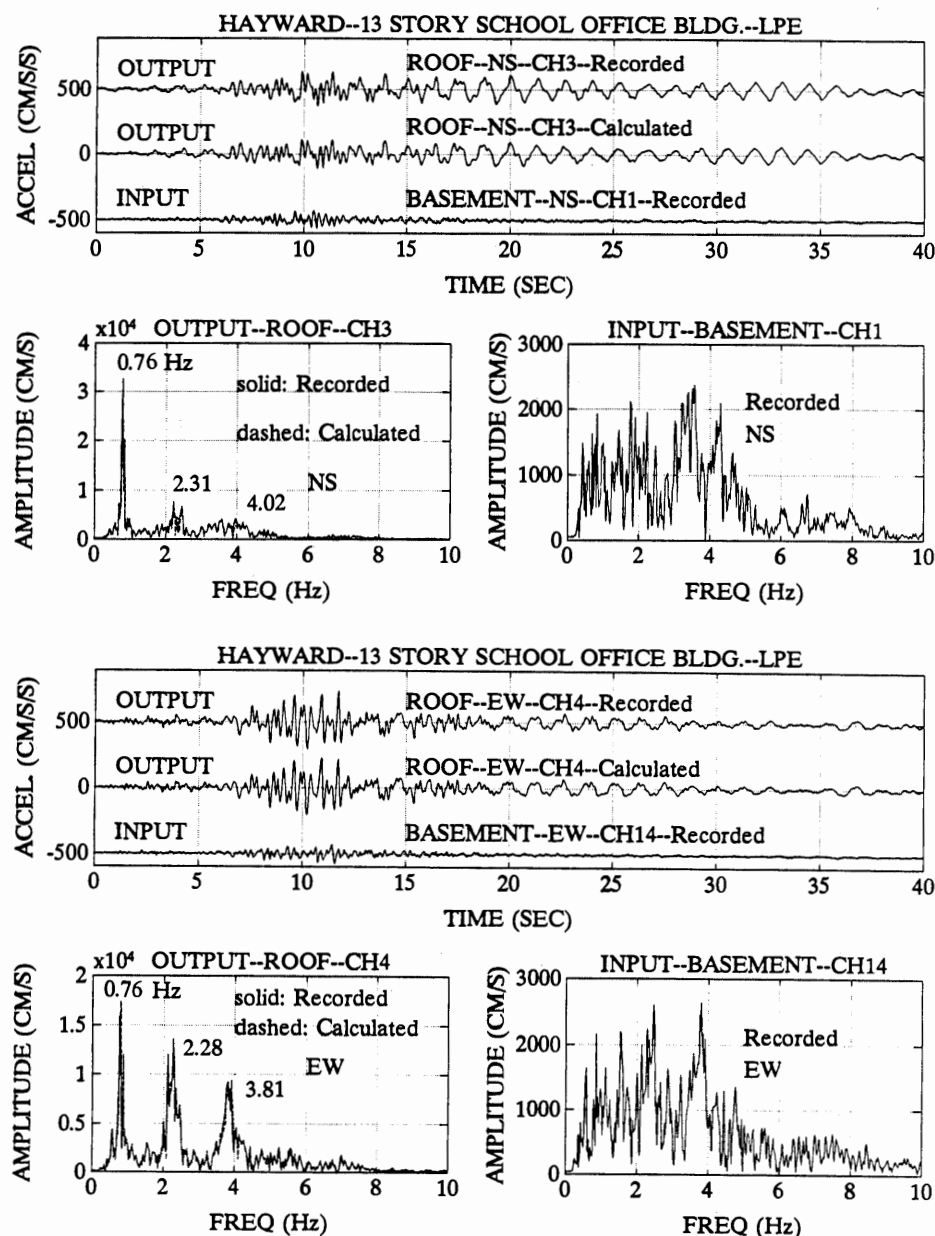


Figure 44.—System identification for California State University (Hayward) Administration Building.

Table 9.—*Identified dynamic characteristics for California State University (Hayward) Administration Building*

MODE	NS			EW		
	f (Hz)	T (s)	ξ (pct.)	f (Hz)	T (s)	ξ (pct.)
1	0.76	1.32	3.4	0.76	1.32	2.3
2	2.37	0.42	3.4	2.20	0.45	3.9
3	4.02	0.25	6.4	3.95	0.25	4.7

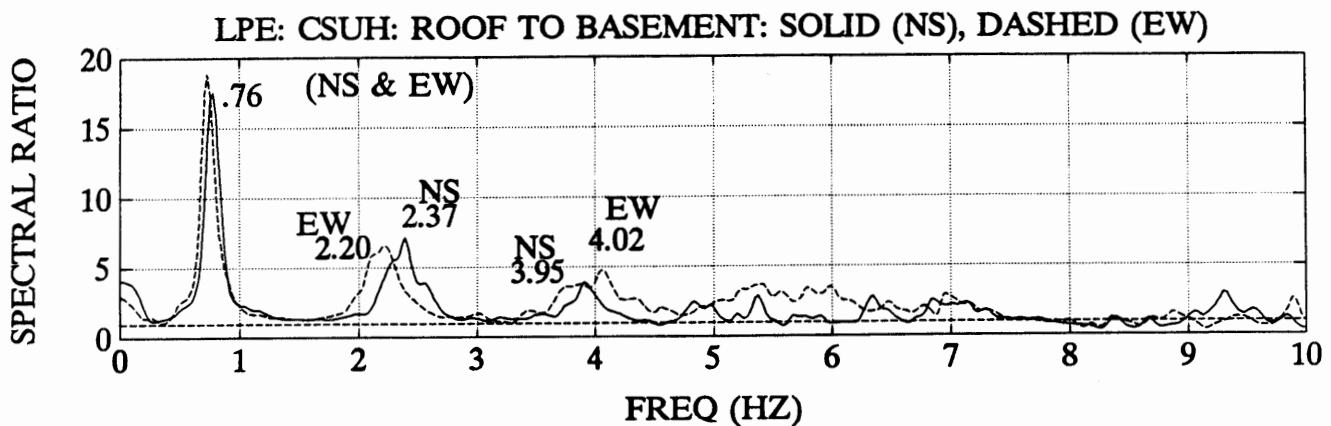


Figure 45.—Spectral ratios for California State University (Hayward) Administration Building.

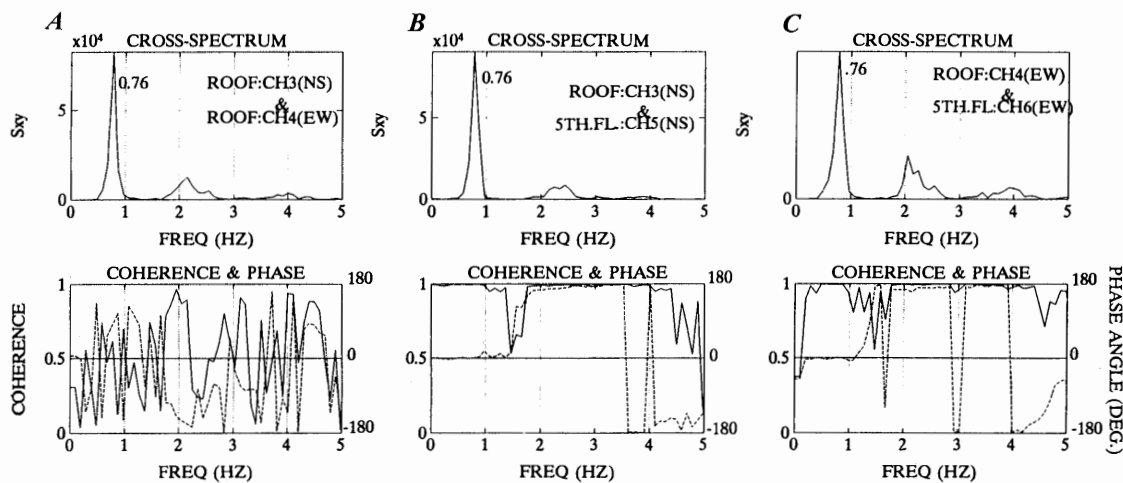


Figure 46.—Cross-spectrum, coherence, and phase-angle plots for California State University (Hayward) Administration Building.

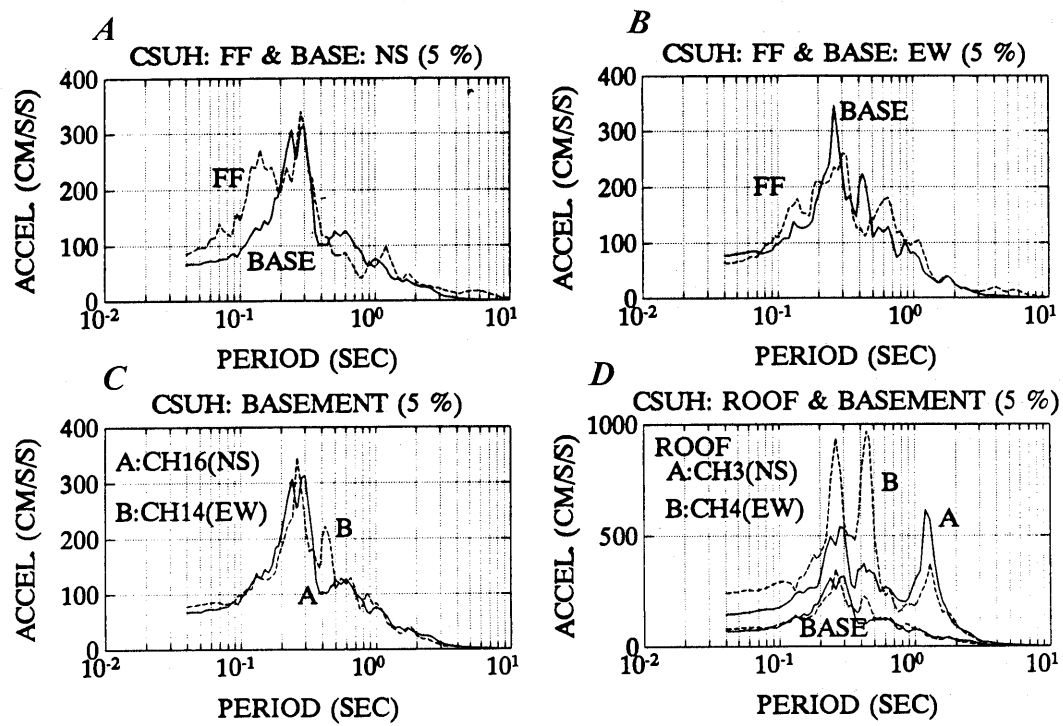


Figure 47.—Comparison of response spectra for California State University (Hayward) Administration Building. *A, B*, Free-field vs. basement. *C*, Orthogonal motions of basement. *D*, Roof and basement.

TWO-STORY OFFICE BUILDING (OAKLAND)

McClure (1991) analyzed the data from the two-story Oakland office building designed by him in 1964. The building was designed according to the 1961 Oakland City Building Code (same as 1961 Uniform Building Code). The building is essentially structural steel framed with reinforced concrete block masonry infill walls. A three-dimensional schematic of the building, its dimensions, and the instrumentation scheme is shown in figure 48 (Çelebi, unpub. data, 1997). As shown in figure 48, the building had a severe plan torsional irregularity. The building was subjected to large peak accelerations (ground 0.26 g, second-floor 0.54 g, and roof 0.69 g). Recorded accelerations and their peaks are shown in figure 49. The building suffered no damage. Its inherent stiffness provided by infill walls reduced the drift ratio. The three-dimensional computer model analyses by McClure (1991) showed that the building behaved elastically when subjected to Loma Prieta motions. The time-histories of the translational and torsional roof accelerations and corresponding amplitude spectra are shown in figure 50 (Çelebi, unpub. data, 1997). The amplitude spectra by themselves reveal frequencies at approximately 0.8, 1.7, and 1.95 Hz. To distinguish these frequencies, spectral

ratios are shown in figures 51A and B. It is noted that the spectral ratio in the north-south direction is approximately unity up to 2 Hz because the east wall of the building does not amplify the structural response (figure 51B). The building was subjected to severe torsional behavior that is close-coupled with the translational mode at approximately 1.67 and 2 Hz (0.67 and 0.5 s). These frequencies are identified in the spectral ratios of torsional accelerations of the roof (figs. 51C and D). The weak peak at approximately 0.7 Hz observed in the amplitude spectra is attributed to the site frequency (Çelebi, unpub. data, 1997). McClure (1991) stated that the ambient vibration tests of the building performed in 1965 by the USGS (then U.S. Coast and Geodetic Survey) indicated a period of 0.47 s for the building. Later, in 1966, forced vibration tests of the building by Bouwkamp and Blohm (1966) yielded a first-mode period of 0.416 s. The mathematical model McClure used to perform dynamic analyses of the building was based on matching the period of the building to one of those from the low-amplitude tests. However, McClure noted that the building periods were 0.5–0.6 s during Loma Prieta and attributed this to possible disengagement of the nonstructural elements that were not well connected to the structural frame (1991).

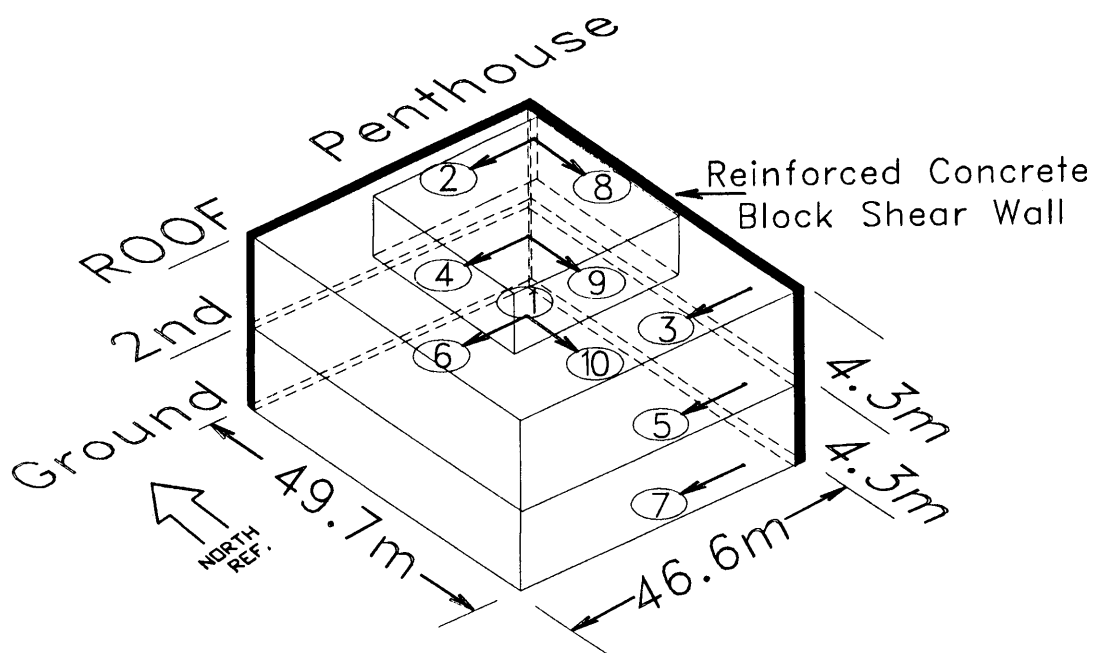


Figure 48.—Three-dimensional schematic of two-story building in Oakland.

TILT-UP BUILDINGS AND BUILDINGS WITH FLEXIBLE DIAPHRAGMS

Particularly used as industrial and storage facilities, tilt-up buildings commonly are designed with large aspect ratios and flexible long span plywood roof diaphragms. Bouwkamp and others (1991) studied some of the buildings with flexible diaphragms, including a warehouse in Hollister (which also has records from the 1984 Morgan Hill earthquake and the 1986 Hollister earthquake), West Valley College gymnasium in Saratoga (which has records

also from the 1984 Morgan Hill earthquake), and a two-story building in Milpitas (which also has records from the 1988 Alum Rock earthquake). The availability of data from several earthquakes for these tilt-up buildings allowed comparison of the frequencies and the loss of stiffness and the amplification of motions at the center of the roof diaphragm compared to its edges and the base. Bouwkamp and others (1991) reported that the stiffness of the Hollister building during Loma Prieta was approximately 50 percent of that calculated from the records of the 1984 Morgan Hill earthquake. The amplifications of motions at the walls were negligible, as they should be

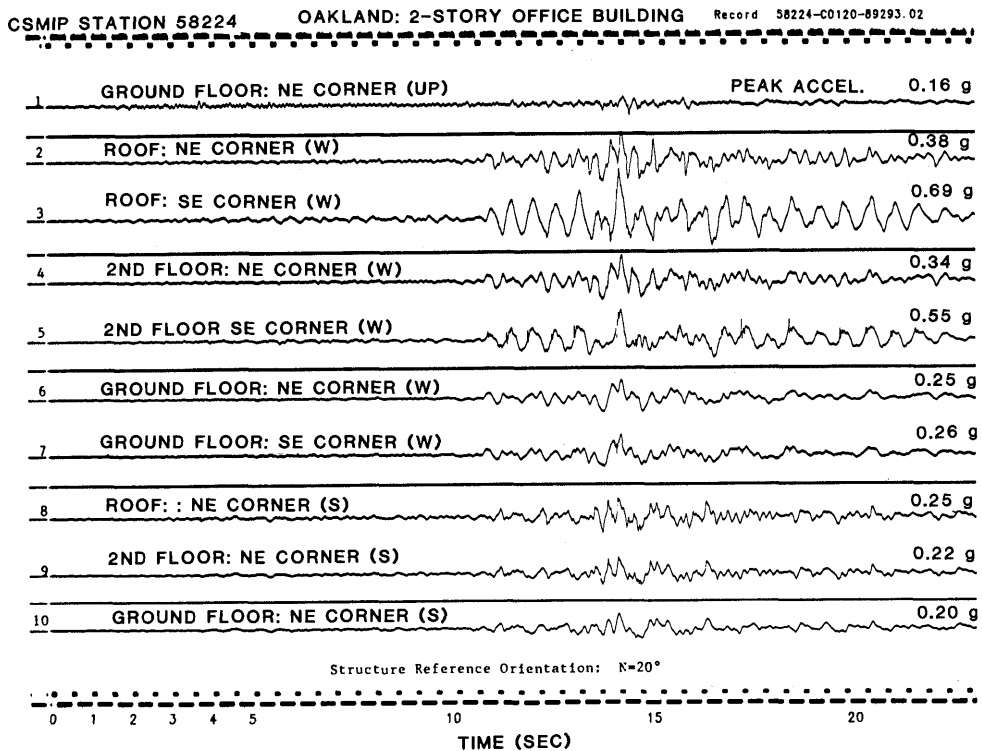


Figure 49.—Recorded responses of two-story building in Oakland.

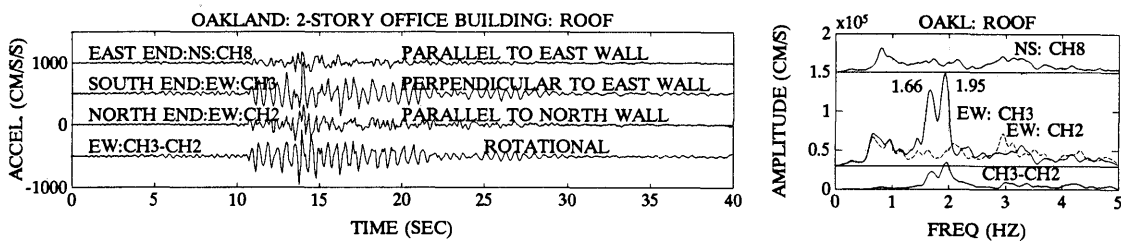


Figure 50.—Roof responses and amplitude spectra of two-story building in Oakland.

since the walls are extremely rigid in their planes. Furthermore, the code equations for estimating the diaphragm displacement did not match well with the recorded responses.

The West Valley College gymnasium was studied in detail by Çelebi and others (1989) using the 1984 Morgan Hill earthquake records. A general view and schematic of the gymnasium and its instrumentation scheme is shown in figure 52 (Çelebi and others, 1989). The Morgan Hill

earthquake records are compared to the Loma Prieta records in figure 53. In short, the records of the building are greatly influenced by the diaphragm frequency at approximately 4 Hz. Significant peak accelerations of the gymnasium are summarized in table 10 for the two earthquakes (Çelebi, 1990). As a result of these studies, the design requirements for the restraints at the edges of the roof diaphragm were increased in the 1991 Uniform Building Code by 50 percent.

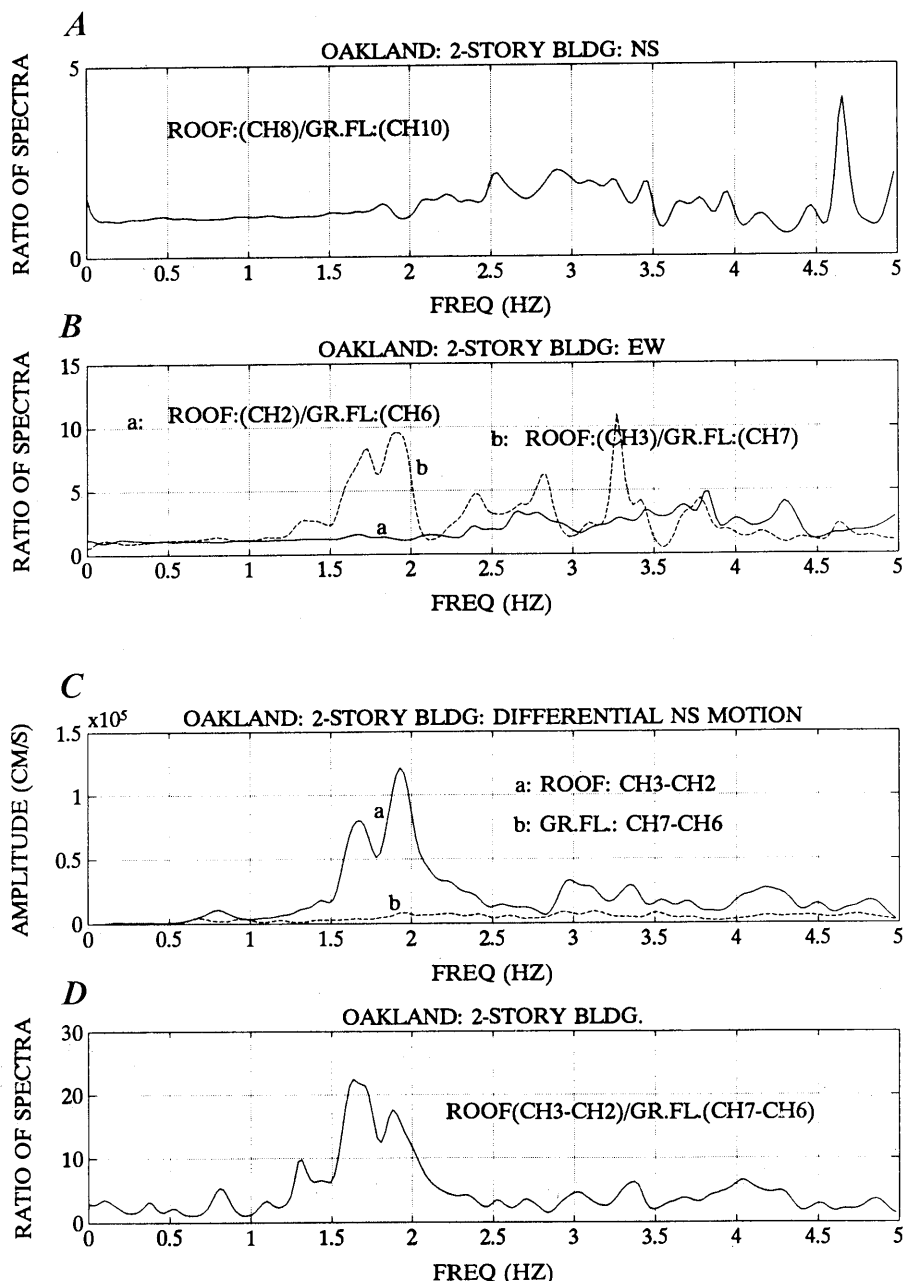
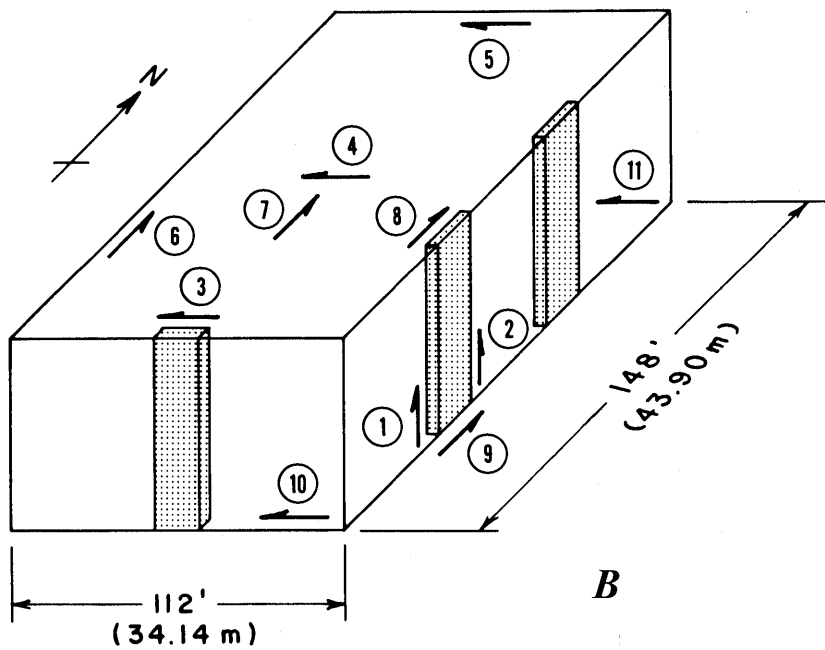


Figure 51.—Spectral ratios of amplitude spectra of two-story building in Oakland.



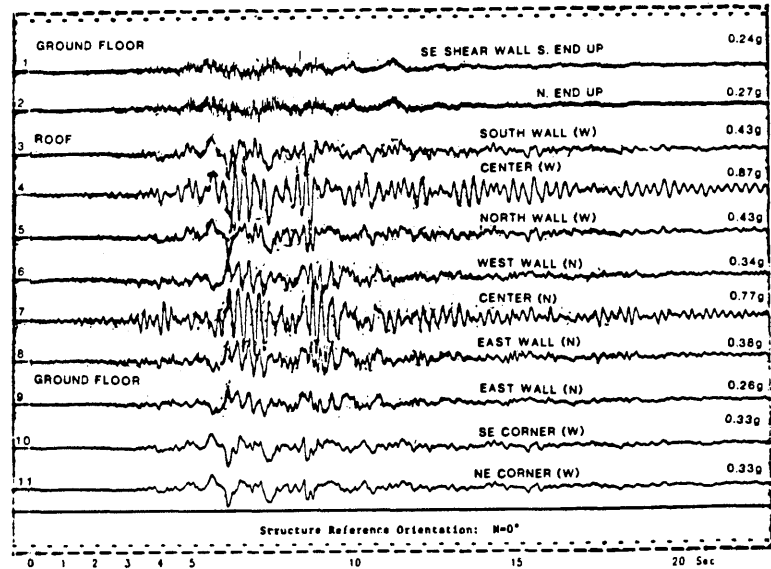
A



B

Figure 52.—A, West Valley College Gymnasium. B. Three-dimensional schematic of West Valley College Gymnasium.

WEST VALLEY COLLEGE (SARATOGA, CA.) GYMNASIUM
CDMG LOMA PRIETA RECORD (27 km from the epicenter)



CDMG MORGAN HILL RECORD (30 km from the epicenter)

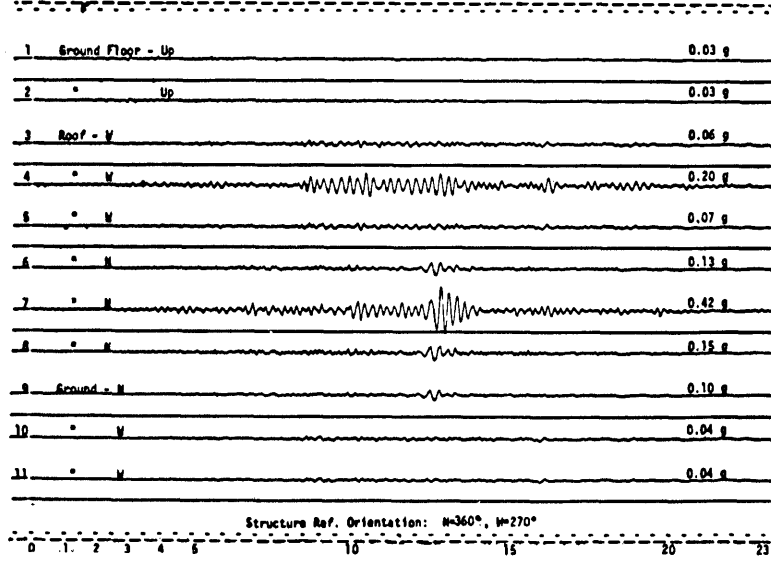


Figure 53.—Recorded responses of West Valley College Gymnasium for two earthquakes.

Table 10.—Peak acceleration responses for two earthquakes from West Valley College (Saratoga) Gymnasium

Location	Direction	Morgan Hill $M_w = 6.1$ April 24, 1984	Loma Prieta $M_w = 7.1$ October 17, 1989
		Accel (g)	Accel. (g)
Ground	NS	0.10	0.26
	EW	0.04	0.33
Roof edge	NS	0.14	0.36
	EW	0.065	0.43
Roof center	NS	0.42	0.77
	EW	0.20	0.87

Wood and Hawkins (this chapter) also investigated the trends in seismic behavior of two tilt-up buildings (the same two-story building in Milpitas and the same one-story building in Hollister). Both buildings were constructed by different methods, and both were relatively new buildings (constructed according to codes between 1979 and 1989). Both buildings are within 50 km of the Loma Prieta epicenter and both recorded similar responses. The authors report that the transverse accelerations at the center of the roof of both buildings were approximately three times that at the base of the buildings. This indicated that such buildings designed according to codes prior to Loma Prieta resulted in very flexible diaphragms. Therefore, the 1991 changes made in the Uniform Building Code are warranted.

The findings of Wood and Hawkins (this chapter) are similar to those of Tena-Colunga and Abrams (1992) and Abrams (1995), who studied the flexible diaphragm problem of a two-story, masonry office building located at Palo Alto, California. The latter investigations provide further insight into the role of floor or roof diaphragms in dynamic response of unreinforced masonry building systems and into deliberations on the impact of these responses to the design of masonry buildings.

BUILDINGS WITH NEW TECHNOLOGIES

At the time of the Loma Prieta earthquake, there were no buildings in the greater San Francisco Bay area that were constructed or retrofitted with base-isolation technology. Only an overpass bridge (Sierra Point in South San Francisco) had been retrofitted with base isolation (Kelly and others, 1991). However, since Loma Prieta, a number of base isolated buildings have been either recently constructed (for example, San Francisco Main Library Building) or retrofitted with this technology (for example, Court of Appeals Building in San Francisco, a four-story apartment building in the Marina District of San Francisco, and Oakland City Hall). Also, the Santa Clara County Office building in San Jose has been retro-

fitted with viscous elastic dampers (see section "Santa Clara County Office Building (San Jose)") (Crosby and others, 1994).

LOW-AMPLITUDE TESTING

The dynamic characteristics of five of the previously discussed buildings in the San Francisco Bay area that recorded the Loma Prieta earthquake were studied by recording their responses to low-amplitude ambient vibratory motions (Marshall and others, 1991, 1992; Çelebi and others, 1993; Çelebi, 1996). The five buildings studied are: (1) the Pacific Park Plaza Building, (2) the Transamerica Building, (3) the Santa Clara County Office Building, (4) an office building in San Bruno, and (5) the California State University (Hayward) Administration Building.

The primary reason for selecting these five buildings was that they recorded the earthquake and therefore low-amplitude tests provide an opportunity to compare their dynamic characteristics under strong- and low-amplitude motions. The Loma Prieta response of all these buildings has been investigated by several investigators, as summarized earlier in this paper.

The location of these five buildings relative to the Loma Prieta epicenter is shown in figure 1. The general dimensions and instrumentation schemes of each of the five buildings are provided previously in this paper. However, significant characteristics of these buildings (structural type, foundation type, and general dimensions), distance from the epicenter, number of channels of strong-motion sensors within the superstructure, and peak accelerations at ground level (or foundation level) and at roof level are summarized in table 11. The reference north building orientation in degrees clockwise from true north, provided in the table, is different than the adopted nominal north-south and east-west directions shown in the table. Results from dynamic analyses and low-amplitude tests performed on the Transamerica Building (Stephen and others, 1974; Kinematics, 1979) and Pacific Park Plaza Building (Stephen and others, 1985) prior to the earthquake and dynamic characteristics for the Santa Clara County Office Building extracted from response data of two earthquakes that occurred prior to the earthquake (R. Darragh, personal commun., 1991) are included in comparative studies by Marshall and others (1991, 1992), Çelebi and others (1993), and Çelebi (1994a).

The testing of each building was conducted from a recording room that contained the junction box of the cables of the force-balance accelerometers permanently deployed throughout the superstructure. These cables were hooked up to a digital (PC-based) data acquisition system (Marshall and others, 1991, 1992; Çelebi and others, 1993). This (1)

Table 11.—*Building characteristics and Loma Prieta peak accelerations*

[Data from Marshall and others (1992) and Çelebi (1996). The reference north building orientation in degrees clockwise from true north is different from adopted nominal north-south and east-west directions. Number of floors (N_A , above ground level; N_B , below ground level). Height of building=H. Distance to epicenter=D. Number of channels in instrumented building=n. Orientation of reference north (clockwise from true north)=N]

Building (instrumentation administrator, in parenthesis)	Comments	H (m)	N_A/N_B	D (m)	n	Loma Prieta Peak Accel. (g)		
						Nom. direc.	Gr. flr.	Roof
						NS	EW	UP
Pacific Park Plaza (USGS) N=350°	Reinforced concrete moment resisting frame (1.5-m-thick concrete mat on piles).	94	30/1	97	21	NS EW UP	0.17 0.21 0.06	0.24 0.38
Transamerica Bldg. (USGS) N=351°	Steel frame, 48th floor is the top occupied floor (2.75-m-thick concrete mat - no piles).	257	60/3	97	22	NS EW UP	0.11 0.12 0.07	0.29 0.31
Santa Clara County Office Building (CDMG) N=337°	Moment-resisting steel frame (Concrete mat - no piles)	57	12/1	35	22	NS EW UP	0.10 0.09 0.10	0.34 0.34
San Bruno Office Building (CDMG) N=335°	Reinforced concrete moment resisting frame (individual spread footing)	24	6/0	81	13	NS EW UP	0.14 0.11 0.12	0.25 0.32
California State University (Hayward) Administration Building (CDMG) N=320°	Steel moment-frame core; exterior reinforced concrete moment frame (0.45-m-thick slab on grade and bearing piles)	61	13/0	70	16	NS EW UP	0.07 0.09 0.05	0.15 0.24

facilitated easy access to various floors of the building without actually going to those floors or without having to provide temporary cables and sensors, (2) allowed ready access to record response data, (3) made it possible to compare directly the ambient and strong-motion response.

The damping ratios are extracted by system identification analyses of Loma Prieta data in accordance with the procedures outlined by Ghanem and Shinozuka (1995) and Shinozuka and Ghanem (1995) (see "Methods of Analyses" section). The low-amplitude (ambient) vibration data was analyzed by conventional spectral analysis techniques. System identification techniques were not applied to the ambient vibration data because of the unknown system input characteristics. Furthermore, because of the lower

signal-to-noise ratio, system identification techniques do not minimize the errors simply and solutions may be unreliable. The results of analyses of the strong-motion response data and the ambient vibration data are summarized in table 12. Also included for comparison are results of previous tests and analyses for the Pacific Park Plaza and Transamerica Buildings.

In each of the five buildings tested, the first-mode periods associated with the strong-motion records are longer than those associated with the ambient vibration records. The highest first-mode period ratio (Loma Prieta earthquake/ambient) is 1.47. Also, the percentages of critical damping for the first mode for the ambient data are significantly smaller than those from the strong-motion data.

Table 12.—*Dynamic characteristics of the five buildings discussed in report*

[Data from Marshall and others (1992) and Çelebi (1996). f, frequency (Hz); T, period (s); x, damping (percent)]

Building	Nominal direction	Pre-Loma Prieta test and analyses		Loma Prieta data		Post-Loma Prieta Ambient	
		f/(T)	ξ (pct.)	f/(T)	ξ (pct.)	f/(T)	ξ (pct.)
Pacific Park Plaza [PPP]	NS	0.59 (1.70)	2.6	0.38 (2.63)	11.6	0.48 (2.08)	0.6
	EW	0.59 (1.70)	2.6	0.38 (2.63)	15.5	0.48 (2.08)	3.4
Transamerica Building [TRA]	NS	0.34 (2.94)	0.9	0.28 (3.57)	4.9	0.34 (2.94)	0.8
	EW	0.34 (2.94)	1.4	0.28 (3.57)	2.2	0.32 (3.12)	1.4
Santa Clara County Office Building [SCCOB]	NS			0.45 (2.22)	2.7	0.52 (1.92)	-
	EW			0.45 (2.22)	2.7	0.52 (1.92)	-
San Bruno Office Building [SBR]	NS			1.17 (0.85)	7.2	1.72 (0.58)	2.2
	EW			0.98 (1.02)	4.1	1.41 (0.71)	2.3
California State University (Hayward) Administration Building [CSUH]	NS			0.76 (1.32)	3.4	0.92 (1.09)	0.6
	EW			0.76 (1.32)	2.3	0.86 (1.16)	0.6

These differences in periods and damping percentages may be caused by several factors, including (1) possible soil-structure and/or possible pile-foundation interaction, which is more pronounced during strong-motion events than during ambient excitations, (2) nonlinear behavior of the structure (such as microcracking of the concrete at the foundation or superstructure), (3) slip of steel connections, and (4) interaction of structural and nonstructural elements.

In the case of the Santa Clara County Office Building, the largest critical damping ratio assessed from the records is about 2.7 percent (tables 4, 12). Damping from the low-amplitude test data could not be determined due to its low signal/noise ratio. It is noted again that this building is now retrofitted with visco-elastic dampers to change its dynamic characteristics so that the global damping and the fundamental frequency both will increase. The resulting shift in the fundamental period and increase in damping is expected to eliminate excessive responses

and the beating effect (Crosby and others, 1994). Low-amplitude tests on the now retrofitted building recently performed by Çelebi and Liu (1997) preliminarily indicate that there is improvement in the dynamic characteristics.

For the Pacific Park Plaza, the post-Loma Prieta frequency (0.48 Hz) is lower than the pre-Loma Prieta frequency (0.59 Hz), but both are larger than the Loma Prieta frequency (0.38 Hz). For Transamerica Building, the frequencies from the pre- and post-LPE low-amplitude tests are in good agreement (0.34 vs. 0.34 and 0.32 Hz) and are larger than the Loma Prieta frequency (0.28 Hz) (Stephen and others, 1974; Kinematics, 1979; Stephen and others, 1985). The immediate conclusion drawn from table 12 is that the damping ratios and periods are consistently and significantly larger for the strong-shaking than for the low-amplitude vibrations.

In addition to these general conclusions, a specific characteristic for Pacific Park Plaza is noted: The damping

ratios extracted from the system identification analyses corresponding to the 0.38-Hz first mode frequency are 11.6 percent (north-south) and 15.5 percent (east-west). Such unusually high damping ratios for a conventionally designed/constructed building require explanation. The building with its large mat foundation in a relatively soft geotechnical environment is capable of energy dissipation in the soil due to radiation (or foundation) or material damping. Therefore, the 0.38-Hz frequency should be considered as the fundamental frequency that incorporates soil-structure interaction at the level of amplified shaking summarized in table 1. Analyses showed that rocking was insignificant.

Accepting 0.38 Hz (2.63 s) as the frequency (period) with soil-structure interaction and 0.48 Hz (2.08 s) or 0.57 Hz (1.75 s) as that without soil-structure interaction, then it is possible to make some quantification of the amount of foundation damping using equations developed by Veletsos (1977) and included in the Applied Technology Council's publication ATC 3-06 (Applied Technology Council, 1978). The area (A) of the foundation mat is approximately 1,600 m². The equivalent circular radius of the foundation is calculated as $r = (A/r)^{0.5} = 22.6$ m (this number is possibly too low considering that the Pacific Park Plaza is a three-winged building, and therefore the effective radius is possibly larger than the conversion provided above). The height of the building (h) is 89.2 m; the effective height (h_{eff}) as defined by the Applied Technology Council (1978) is $h_{\text{eff}} = 0.7h = 62.4$ m. For $h_{\text{eff}}/r = 62.4/22.6 = 2.8$, and for $T_{\text{ssi}}/T = 2.63/2.08 = 1.26$ or $2.63/1.75 = 1.50$, the foundation (including radiation and material) damping can be approximated at 5-6 percent from figure 54 (adopted from Applied Technology Coun-

cil, 1978). Inserting these into Veletsos' equation for effective damping (1977):

$$\xi_{\text{eff}} = \xi_{\text{str}} + \xi_{\text{ssi}} = \xi_{\text{str}} + \xi_0 / (T_{\text{ssi}} / T)^3.$$

The value of ξ_0 here is the structural damping without soil-structure interaction, normally accepted from empirically prepared tables to be between 3 and 7 percent. Therefore with T_{ssi}/T varying between 1.26 and 1.50, the structural damping is reduced to 29-50 percent of this accepted value. Thus, the estimated foundation damping of 5 to 6 percent is not unusual, given the fact that the ξ_{eff} determined from observed response data is 11-15 percent. More detailed discussions on foundation damping can be found in Veletsos (1977), Luco (1980), Roessel (1980), Dobry and Gazetas (1985), Todorovska (1992), and very recently in Wolf and Song (1996). It can therefore be categorically stated that radiation damping is beneficial in reducing responses of structures.

It should be stated that consideration of the effect of soil-structure interaction in estimation of damping for analysis and design purposes has not yet found its way into design offices, except for those involved with critical structures. In the past, during design/analysis processes of engineered structures, it was assumed that a structure's foundation is fixed to the underlying media. State-of-the-art knowledge and analytical approaches require, when warranted, the structure-foundation system to be represented by mathematical models that include the influence of the sub-foundation media. Identification of beneficial and adverse effects of soil-structure interaction is a necessity. Adverse effects of soil-structure interaction during

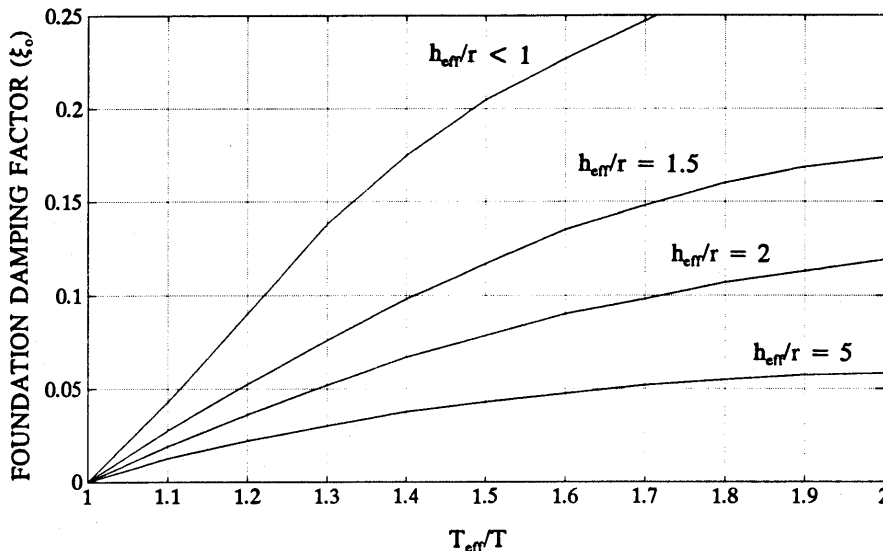


Figure 54.—Foundation damping in terms of ratio of periods and ratio of building height-to-equivalent radius of foundation (from Veletsos (1977) and Applied Technology Council (1978)).

the 1985 Michoacan (Mexico) earthquake was addressed by Tarquis and Roessel (1988), who showed that lengthened fundamental periods due to soil-structure interaction of mid-rise buildings (5-15 stories) in the Mexico City lakebed area placed them close to the resonating 2-s site period. This study points out that by neglecting the effect of soil-structure interaction, the dynamic characteristics, and specifically damping in structures can be underestimated if the values of damping assessed from low-amplitude testing are used in lieu of values supposedly for strong motions.

To repeat, current analyses and design procedures using estimated damping values may not be realistic due to (1) change in construction and design practices and (2) the fact that soil-structure interaction effects in most cases are ignored for buildings that are not considered to be critical facilities. However, results presented herein suggest that the critical damping percentages used for analyses and design of some buildings may not have been properly estimated (specifically, overestimated for the Santa Clara County Office Building and underestimated for the Pacific Park Plaza) and possibly not even considered for some buildings. Furthermore, changes in damping values and fundamental values commensurate with inferred strong-motion values should be considered to improve design and analyses results.

OTHER STUDIES

POUNDING OF STRUCTURES

Kasai and others (1991) surveyed the damage due to pounding in the San Francisco Bay area following the Loma Prieta earthquake. They determined that significant pounding of buildings occurred at sites ranging up to more than 90 km from the epicenter and discussed the implications of this finding in forecasting future possible catastrophic damage that may occur during earthquakes having epicenters closer to dense urban areas. They also present analytical research on pounding that includes development of dynamic analysis programs that incorporate pounding. Parametric studies were performed on building pounding response as well as appurtenance response. These analyses included a spectrum method to obtain peak pounding responses, actual case studies, and a spectrum method to determine required building separations to preclude pounding. Their analytical studies did not relate to any recorded pounding responses of buildings. This may be due to the fact that there is no specific instrumentation scheme implemented, by either California Strong Motion Instrumentation Program or U.S. Geological Survey, in adjacent buildings with possibility of pounding to record their responses during earthquakes.

MASONRY BUILDINGS

Hart and Jaw (1991) investigated the performance of a tall (approximately 87 ft) reinforced masonry building located in Santa Cruz, near the epicentral region. They observed that the building was not damaged, in spite of a probable maximum ground motion of 0.3-0.5 g.

OVERTURNING FORCES

Chen (1992) presented a newly developed time-delay method for earthquake analysis which incorporates the attribute of finite wave speed propagating upward into a structure. He showed verification of the method using data from the California Strong Motion Instrumentation Program applied to calculate the overturning moment of structures. He used one detailed three-dimensional model and nine simplified two-dimensional models for this purpose.

Gates and others (1994) investigated three high-rise shear wall buildings to evaluate overturning forces in the shear walls under three recent northern California earthquakes: 1984 Morgan Hill, 1986 Mt. Lewis, and 1989 Loma Prieta. The buildings are in the 9-10 story range, with three different shear wall configurations of (1) perimeter walls, (2) core walls, and (3) distributed walls. They employed two methods of data reduction and analysis to assess the significance of soil-structure interaction on building overturning forces: (1) simplified data analysis procedures using recorded motion, mode shapes, and building weights to assess dynamic performance and (2) three-dimensional linear elastic dynamic analyses using soil-structure models for the shear walls and foundation systems. They reported that the recorded responses show ample evidence of foundation/shear wall rocking under the moderate and strong shaking provided by the cited earthquakes. They also reported that the lengthening in the periods of the buildings take place due to both rocking and inelastic behavior. The analytical results are compared with code procedures for predicting the periods of the structures as well as the distribution of overturning forces. They showed that careful modeling of buildings refined by system identification techniques using actual recorded responses provides useful steps in the evaluation of buildings.

CODE ASSESSMENT AND SERVICEABILITY REQUIREMENTS

Fenves (1990) evaluated the lateral force procedures for buildings with irregular plans or vertical irregularities. He used recorded strong-motion response data from two instrumented buildings to determine vibration properties

and distribution of lateral forces. One of the two buildings is a four-story hospital with records from both Morgan Hill earthquake (1984) and Loma Prieta and the other with only Loma Prieta records. Fenves reported that due to the irregular configuration of the buildings, the distribution of lateral forces changes substantially with changes in the amplitude of earthquake response.

Uang and Maarouf (1991), Werner and others (1992), and Beck and others (1992) investigated the Uniform Building Code and serviceability requirements from building response data. They all investigated several buildings and compared their analyses with observed performance of each building during the Loma Prieta earthquake and other earthquakes for which data are available.

SOIL-PILE-STRUCTURE INTERACTION

Gould and Ahn (1991) studied one of the six-story wings of the Clarion Hotel near San Francisco International Airport. The reinforced concrete shear-wall and framed building rests on pile foundation penetrating into stiff, clayey soils underlying the soft Bay mud. With the premise that, in general, lengthening of the building period results in lower inertial forces, they studied the building with mathematical models that includes soil-pile-structure interaction. They used ground motion recorded at the San Francisco International Airport as surrogate input base motion to the subject building model. To differentiate the effect of the soil-pile-structure interaction, they performed fixed-base analyses of the structure. Their analyses show that the base shear and the base overturning moment are significantly reduced with lengthening of the building period from 0.35 s (fixed-base) to as much as 1.33 s due to soil-pile-structure interaction.

TRENDS IN BEHAVIOR OF REGULAR BUILDINGS

Li and Mau (1997) recently completed a study of 21 regular (typical, symmetric) buildings which have recorded response records. Of these, 11 buildings are from the San Francisco Bay area with records from the Loma Prieta earthquake and 9 are from the Los Angeles area with records from the 1987 Whittier earthquake. With this data base, they performed extensive analyses using system identification techniques as a tool. They arrived at the following conclusions:

1. Estimates of building periods by code formulas is less reliable for shear wall buildings than for framed buildings.
2. Estimates of building frequencies by code formulas for longitudinal and transverse direction is variable and is dependent on the structural framing and presence and distribution of shear walls.

3. The data base indicates that there is great variation of the damping ratios. The variation is larger for concrete buildings (2-14 percent) than for steel buildings (1-6 percent).

4. For reinforced concrete and steel framed buildings, the maximum story drift occurs at a middle or lower story, but for shear wall buildings the maximum story drift occurs at a middle or higher story.

5. Rocking occurs in some buildings as a result of translational vibration. For stiffer buildings, rocking can occur as a distinguishable mode of vibration.

6. Large variations in building frequency can be detected within the time-history of a response record of a building. This may or may not be a symptom of damage but can be used as an indicator of possible damage.

7. There is strong correlation between change of frequency and variation of drift.

CONCLUSIONS

This paper summarizes studies of performances of buildings during the Loma-Prieta earthquake. The studies referred to herein are mostly on the recorded responses of instrumented buildings. The conclusions derived from these studies are as follows:

1. Instrumentation of structures as part of hazard reduction programs is very beneficial, as studies of this type will help to better predict the performance of structures in future earthquakes.

a. Studies of recorded responses of buildings help researchers and practicing professionals to better understand the cumulative structural and site characteristics that affect the response of buildings and other structures. Such studies impact mitigation efforts.

b. In turn, the behavior that may be expected from buildings during future earthquakes with large input motions (either due to larger magnitude earthquakes or earthquakes at closer distances to the building) can be forecast. This is particularly true for the San Francisco Bay area where—

i. The probability of magnitude 7 or larger earthquakes occurring on major faults, including the San Andreas and Hayward faults, is considered to be approximately 67 percent or higher within a 30-year period (Working Group, 1990).

ii. There is a large inventory of buildings within 0-10 km of the two major faults capable of generating $M>7$ earthquakes. This is particularly important because, very recently, the Structural Engineers Association of California (SEAOC) issued the 1996 edition of the "Recommended Lateral Force Requirements and Commentary," which has provisions for increasing the design base shear by 0-100 percent depending on the 0-10-km distance of a building from a fault. This implies

that the forecasting of performance of buildings within 0-10 km of major faults must be done more informatively. This requisite information can be achieved only through acquiring and studying response data from buildings during earthquakes.

iii. Furthermore, some of the building response data are from tall buildings that are on soft soils. The motions at the soft-soil sites of some of the important tall buildings (for example, Pacific Park Plaza, Transamerica Building, Embarcadero Building, and Chevron Building) are amplified by 3-5 times within the periods of engineering interest when compared with the motions of Yerba Buena Island, a rock site approximately the same distance away from the epicenter of the earthquake.

2. There is an acute need to better evaluate structural and site characteristics in developing earthquake resisting designs of building structures. Studies in this paper show, as in the case of Santa Clara County Office Building, that designs of buildings with low structural damping, resonance, and beating effects caused by closely coupled translational and torsional modes must be avoided. Also, as expected in most tall buildings, higher modes are excited. As in the case of Embarcadero Building, higher modes play an important role in the response of building structures and therefore must be carefully evaluated to assess their future performances.

3. Drift ratios calculated from observed data in certain cases exceed code drift limitations for part or all of the structural systems. Assessing the drift exposure of structural systems are ever more important since the design/analyses of buildings are recently being shifted toward a performance-based design procedure.

4. Soil-structure interaction is one of the least understood actions that affects structural behavior. There may be beneficial or detrimental effects of this interaction to the overall behavior of structures. It stands to be prominent in the behavior of several buildings (for example, Pacific Park Plaza, Santa Clara County Office Building, Transamerica Building, and others) as assessed from studies of the recorded responses of buildings during the Loma Prieta earthquake. Therefore, two specific issues are that (1) identification of beneficial and adverse effects of soil-structure interaction is a necessity and (2) design offices must be informed and trained in consideration of the effect of soil-structure interaction in estimation of fundamental period and damping of a building, as this is not yet the case. Specifically, the damping percentages are overestimated for the Santa Clara County Office Building and underestimated for the Pacific Park Plaza, and possibly not even considered for some buildings.

5. Development of design response spectra deserves more intensive consideration by geotechnical engineers since site effects play an important role in the response of building structures. There are significant discrepancies in the compari-

son of the response spectra derived from recorded motions with the actual design response spectra. Amplified motions due to soft soil conditions, site-specific resonating, and frequency content must be kept in mind in the development of design response spectra (for example, the Embarcadero Building).

6. The propagation direction of surface waves arriving at buildings affect particularly unsymmetrical buildings or buildings with wings (for example, Pacific Park Plaza and Santa Clara County Office Building).

7. The basemat rotation of tall buildings with basements calculated by the displacements in the corners of the basemat is considerably smaller than the rotation of the basement walls calculated by the displacements derived from the horizontal sensors at the street level and basemat. This is observed for both the Transamerica Building and Embarcadero Building. The implication is that the current practice which assumes that the inertial forces at ground level and basemat level to be the same is not correct.

8. Low-amplitude tests have been conducted on five buildings that recorded the Loma Prieta earthquake. Results indicate, as expected, that the first-mode periods extracted from strong-motion response records are longer than those associated with the ambient vibration records. Similarly, the percentages of critical damping for the first mode for the ambient data are significantly smaller than those from the strong-motion data. These differences may be caused by several factors including (1) possible soil-structure interaction which is more pronounced during strong-motion events than during ambient excitations, (and similarly, in buildings with pile foundations, possible pile-foundation interaction which may not occur during ambient excitation), (2) nonlinear behavior of the structure (such as microcracking of the concrete at the foundation or superstructure), (3) slip of steel connections, and (4) interaction of structural and nonstructural elements. Changes in damping values and fundamental period values commensurate with inferred strong-motion values should be considered to improve design and analyses results.

9. In processing of data of recorded responses for buildings, use of different filters for basement versus free-field causes gross differences in displacements (as in the case of California State University, Hayward). A common rational filtering for basement and associated free-field motions is recommended.

10. Specific instrumentation schemes of some of the already instrumented buildings and of those buildings yet to be instrumented must be improved and/or implemented so that the response characteristics expected of that building can be captured (for example, soil-structure interaction, pounding, and variation of drift due to abrupt changes in stiffness). When applicable, specific buildings should be specially instrumented extensively to better capture their behavior in response to actions such as pounding and soil-structure interaction.

REFERENCES CITED

- Abrams, D.P., 1995, The importance of the diaphragm on seismic response of buildings, in Proceedings of Structures Congress XIII, Restructuring—America and beyond: American Society of Civil Engineers, New York, v. 2, p. 1813-1816.
- Aktan, H., Kagawa, T., Kambhatla, A., and Çelebi, M., 1992, Measured and analytical response of a pile supported building, in Proceedings, Tenth World Conference on Earthquake Engineering: A.A. Balkema, Rotterdam, v. 3, p. 1791-1796.
- Anderson, J.C., Miranda, E., and Bertero, V.V., and Kajima Project Research Team, 1991, Evaluation of the seismic performance of a thirty-story RC building: University of California, Berkeley, Earthquake Engineering Research Center, Report: UCB/EERC-91/16, 254 p.
- Anderson, J.C., and Bertero, V.V., 1994, Lessons learned from an instrumented high rise building, in Proceedings, Fifth U.S. National Conference on Earthquake Engineering: Earthquake Engineering Research Institute, Oakland, Calif., v. II, p. 651-660.
- Applied Technology Council, 1978, Tentative provisions for the development of seismic regulations for buildings: ATC3-06, 505 p.
- Astaneh, A., Bonowitz, D., and Chen, C., 1991, Evaluating design provisions and actual performance of a modern high-rise steel structure, in Seminar on Seismological and Engineering Implications of Recent Strong-Motion Data: California Department of Conservation, Division of Mines and Geology, p. 5-1-5-10.
- Beck, J.L., Werner, S.D., and Nisar, A., 1992, Analysis of building records from 1989 Loma Prieta, 1984 Morgan Hill and 1986 Mt Lewis earthquakes, in Structures Congress '92 compact papers: American Society of Civil Engineers, New York, p. 420-423.
- Bendat, J.S., and Piersol, A.G., 1980, Engineering applications of correlation and spectral analysis: John Wiley and Sons, 302 p.
- Benuska, L., ed., 1990, Earthquake spectra: Loma Prieta Earthquake Reconnaissance Report v. 6 (supp.), 448 p.
- Bertero, V.V., Miranda, E., and Anderson, J.C., 1992, Evaluation of seismic response of two RC buildings, in Structures Congress '92 compact papers: American Society of Civil Engineers, New York, p. 408-411.
- Bonowitz, D., and Astaneh, A., 1994, Comparing elastic models with recorded motion from the Loma Prieta earthquake: implications for the design of tall steel structures, in Proceedings, Third Conference on Tall Buildings in Seismic Regions: Los Angeles Tall Buildings Structural Design Council, Los Angeles, 10 p.
- Boroschek, R.L., and Mahin, S.A., 1991, Investigation of the seismic response of a lightly-damped torsionally-coupled building: University of California, Berkeley, Earthquake Engineering Research Center Report UCB/EERC-91/18, 291 p.
- Boroschek, R.L., Mahin, S.A., and Zeris, C.A., 1990, Seismic response and analytical modeling of three instrumented buildings, in Proceedings, 4th U.S. National Conference on Earthquake Engineering, Palm Springs, Calif., May 20-24: Earthquake Engineering Research Institute, Oakland, Calif., v. 2, p. 219-228.
- Bouwkamp, J.B., and Blohm, J.K., 1966, Dynamic response of a two-story steel frame structure: Bulletin of the Seismological Society of America, v. 56, no. 6, p. 1289-1303.
- Bouwkamp, J.B., Hamburger, R.O., and Gillengerten, J.D., 1991, Degradation of plywood roof diaphragms under multiple earthquake loading, in Seminar on Seismological and Engineering Implications of Recent Strong-Motion Data: California Division of Mines and Geology, Office of Strong Motion Studies, p. 6-1-6-10.
- Çelebi, M., 1990, Earthquake spectra: Loma Prieta Earthquake Reconnaissance Report, v.6 (supp.), p. 25-80.
- , 1992, Highlights of Loma Prieta responses for four tall buildings, in Proceedings, of the Tenth World Conference on Earthquake Engineering: A.A. Balkema, Rotterdam, v. 7, p. 4039-4044.
- , 1993, Seismic response of eccentrically braced tall building: Journal of Structural Engineering, v. 119, no. 4, p. 1188-1205.
- , 1994a, Response study of a flexible building using three earthquake records, in Proceedings, Structures Congress XII, Atlanta, Ga, April 24-28: American Society of Civil Engineers, New York, v. 2, p. 1220-1225.
- , 1994b, Response study of a 13-story building, in Fifth U.S. National Conference on Earthquake Engineering, July 10-14, Chicago, Ill.: Earthquake Engineering Research Institute, Oakland, Calif., v. 1, p. 87-96
- , 1996, Comparison of damping in buildings under low-amplitude and strong Motions: Journal of Wind Engineering and Industrial Aerodynamics, v. 59, p. 309-323.
- Çelebi, M., Bongiovanni, G., Şafak, E., and Brady, G., 1989, Seismic response of a large-span roof diaphragm: Earthquake Spectra, v. 5, no. 2, p. 337-350.
- Çelebi, M., Phan, L.T., and Marshall, R.D., 1991, Comparison of responses of a select number of buildings to the 10/17/1989 Loma Prieta (California) earthquake and low-level amplitude test results, in Proceedings of the 23rd Joint Meeting of the U.S.-Japan Cooperative Program in Natural Resources Panel on Wind and Seismic Effects: National Institute of Standards and Technology, U.S. Department of Commerce, NIST SP 820, p. 475-499.
- Çelebi, M., Phan, L.T., and Marshall, R.D., 1993, Dynamic characteristics of five buildings during strong and low-amplitude motions: International Journal of the Structural Design of Tall Buildings, v. 2, p. 1-15.
- Çelebi, M., and Şafak, E., 1991, Seismic response of Transamerica Building—I, Data and preliminary analysis: Journal of Structural Engineering, v. 117, no. 8, p. 2389-2404.
- Çelebi, M., and Şafak, E., 1992, Seismic response of Pacific Park Plaza—I, Data and preliminary analysis: Journal of Structural Engineering, v. 118, no. 6, p. 1547-1565.
- Çelebi, M., and Liu, H. P., 1997, Before and after retrofit—Response of a building during ambient and strong motions, paper submitted, Eighth U. S. National Conference on Wind Engineering, The John Hopkins University, June 5-7, 10 p.
- Chajes, M.J., Yang, C.Y., and Zhang, L., 1992, Simplified seismic analysis of a 47-story building, in Structures Congress '92 compact papers: American Society of Civil Engineers, New York, p. 448-451.
- Chen, C.-C., Bonowitz, D., and Astaneh-Asl, A., 1992, Studies of a 49-story instrumented steel structure shaken during the Loma Prieta earthquake: Earthquake Engineering Research Center, University of California, Berkeley, Report UBC/EERC-92/01, 136 p.
- Chen, M.-C., 1992, Verification of a method for estimating overturning moment of tall buildings, in Proceedings, Seminar on Seismological and Engineering Implications of Recent Strong-Motion Data: California Division of Mines and Geology, Strong Motion Instrumentation Program, p. 8-1—8-10.
- Crosby, P., Kelly, J., and Singh, J.P., 1994, Utilizing visco-elastic dampers in the seismic retrofit of a thirteen story steel framed building, in Structures Congress XII, Atlanta, Ga., v. 2: American Society of Civil Engineers, p. 1286-1291.
- Dobry, R., and Gazetas, G., 1985, Dynamic stiffness and damping of foundations by simple methods, in Proceedings, Symposium on Vibrational Problems in Geotechnical Engineering, Detroit, Michigan, October: American Society of Civil Engineers, p. 75-107.
- Earth Sciences Associates, 1971, Soil and foundation investigation for the proposed Santa Clara County Civic Center: Earth Sciences Associates, Palo Alto, Calif.
- Fenves, G. L., 1990, Evaluation of lateral force procedures for buildings, in Seminar on Seismological and Engineering Implications of Recent Strong-Motion Data: California Division of Mines and Geology, Strong Motion Instrumentation Program, p. 6-1-6-10.
- Frankel, A., and Vidale, J., 1992, A three-dimensional simulation of

- seismic waves in the Santa Clara Valley, California from a Loma Prieta aftershock: *Bulletin of the Seismological Society of America*, v. 82, no. 5, p. 2045-2074.
- Fumal, T., 1991, A compilation of the geology and measured and estimated shear-wave velocity profiles at strong-motion stations that recorded the Loma Prieta, California earthquake: U.S. Geological Survey Open-File Report 91-311, 163 p.
- Gates, W.E., Hart, G.C., Gupta, S., and Srinivasan, M., 1994, Evaluation of overturning forces on shear wall buildings, in *Seminar on Seismological and Engineering Implications of Recent Strong-Motion Data: California Division of Mines and Geology, Strong Motion Instrumentation Program*, p. 105- 120.
- Ghanem, R., and Shinotzuka, M., 1995, Structural system identification; I, Theory: *Journal of Engineering Mechanics*, v. 121, no. 2, p. 255-264.
- Gibbs, J. F., Fumal, T. E., and Powers, T. J., 1994, Seismic velocities and geologic logs from borehole measurements at seven strong-motion stations that recorded the 1989 Loma Prieta, California, earthquake: U.S. Geological Survey Open-File Report 94-222, 104 pages.
- Gould, P.L., and Ahn, K., 1991, Performance of a pile-supported structure under strong ground motion, in *Proceedings, Seventh International Conference on Computer Methods and Advances in Geomechanics*, Cairns, 6-10 May: A.A. Balkema, Rotterdam, p. 133-138.
- Hart, G.C., and Jaw, J.-W., 1991, Seismic response of a tall masonry building, in *Proceedings, Second Conference on Tall Buildings in Seismic Regions*, Report: Council on Tall Buildings and Urban Habitat, Lehigh University, Bethlehem, Pennsylvania, Council Report 903.409, p. 145-154.
- Haskell, N.A., 1953, The dispersion of surface waves on multilayered media: *Bulletin of the Seismological Society of America*, v. 43, no. 1, p. 17-34.
- , 1960, Crustal reflection of plane SH waves: *Journal of Geophysical Research*, v. 65, no. 12, p. 4147- 4150.
- Hensolt, W.H., and Brabb, E.E., 1990, Maps showing elevation of bedrock and implications for design of engineered structures to withstand earthquake shaking in San Mateo County, California, U.S. Geological Survey Open-File Report 90-496.
- Huang, M.J., and others, 1985, Processed data from the strong-motion records of the Morgan Hill earthquake of 24 April 1984; Part II, Structural-response records : California Department of Conservation, Division of Mines and Geology, Office of Strong Motion Studies, Report OSMS 85-05, 320 p.
- Kagawa, T., Aktan, H., and Çelebi, M., 1993, Evaluation of soil and structure model using measured building response during the Loma Prieta earthquake: Department of Civil and Environmental Engineering, Wayne State University, Detroit, Michigan, 169 p.
- Kagawa, T., and Al-Khatib, M.A., 1993, Earthquake response of 30-story building during the Loma Prieta earthquake, in *Third International Conference on Case Histories in Geotechnical Engineering*, June 1-4, v. I, University of Missouri-Rolla, p. 547-553.
- Kambhatla, A., Aktan, H.M., Kagawa, T., and Çelebi, M., 1992, Verification of simple soil-pile foundation-structure models, in *Structures Congress '92: American Society of Civil Engineers*, New York, p. 721- 724.
- Kasai, K., and others, 1991, A study on earthquake pounding between adjacent structures, in *Earthquake Engineering, Sixth Canadian Conference*: University of Toronto Press, p. 93-100.
- Kelly, J.M., Aiken, I.D., and Clark, P.W., 1991, Response of base-isolated structures in recent Californian earthquakes, in *Seminar on Seismological and Engineering Implications of Recent Strong-Motion Data*, Preprints: California Division of Mines and Geology, Strong Motion Instrumentation Program, p. 12-1—12-10.
- Kinemetrics, Inc, 1979, Application Note No 5—Transamerica Building ambient vibration survey: 3 p.
- Li, Y., and Mau, S.T., 1997, Learning from recorded earthquake motions of buildings: *Journal of Structural Engineering*, v. 123, no. 1, p. 62-69.
- Lin, B.C., and Papageorgiou, A.S., 1989, Demonstration of torsional coupling caused by closely spaced periods—1984 Morgan Hill earthquake response of the Santa Clara County Building: *Earthquake Spectra*, v. 5, no. 3, p. 539-556.
- Ljung, L., 1987, System identification—Theory for the User: Prentice-Hall, 519 p.
- Luco, E., 1980, Soil-structure interaction and identification of structural models, in *Second Specialty Conference on Civil Engineering and Nuclear Power*, October, v. 2, Knoxville, Tennessee, American Society of Civil Engineers, New York, p. 10/1/1-10/1/31.
- Maley, R., Acosta, A., Ellis, F., Etheredge, E., Foote, L., Johnson, D., Porcella, R., Salsman, M., and Switzer, J., 1989, U.S. Geological Survey strong-motion records from the northern California (Loma Prieta) earthquake of October 17, 1989: U.S. Geological Survey Open-File Report 89-568, 85 p.
- Marshall, R.D., Phan, L.T., and Çelebi, M., 1991, Measurement of structural response characteristics of full-scale buildings: selection of structures: National Institute of Standards and Technology, U.S. Department of Commerce, NISTIR Report 4511, Gaithersburg, Maryland, 16 p. (Also published as U.S. Geological Survey Open-File Report 90-667.)
- , 1992, Measurement of structural response characteristics of full-scale buildings—Comparison of results from strong-motion and ambient vibration records: National Institute of Standards and Technology, U.S. Department of Commerce, NISTIR Report 4884, 74 p.
- McClure, F.E., 1991, Analysis of a two story Oakland office building during the Loma Prieta earthquake, in *Seminar on Seismological and Engineering Implications of Recent Strong-Motion Data*, Preprints: California Division of Mines and Geology, Strong Motion Instrumentation Program, p. 13-1-13-11.
- Phan, L.T., Hendrikson, E.M., Marshall, R.D., and Çelebi, M., 1994, Analytical modeling for soil-structure interaction of a 6-story commercial office building, in *Fifth U.S. National Conference on Earthquake Engineering*, July 10-14, Chicago, Ill., p. 199-207.
- Porter, L.D., 1996, The influence of earthquake azimuth on structural response due to strong ground shaking, in *Eleventh World Conference on Earthquake Engineering*, Acapulco, Mexico (June), (No. 1623): Elsevier Science Ltd. (CD-ROM).
- Rihal, S.S., 1994, Correlation between recorded building data and non-structural damage during the 1989 Loma Prieta earthquake: California Division of Mines and Geology, Office of Strong Motion Studies, Data Utilization Report CSMIP/94-04, 65 p.
- Roessel, J.M., 1980, The use of simple models in soil-structure interaction, in *Proceedings, Second Specialty Conference on Civil Engineering and Nuclear Power*, October, v. 2, Knoxville, Tennessee, American Society of Civil Engineers, New York, p. 10/3/1-10/3/25.
- Şafak, E., 1993, Response of a 42-story steel-frame building to the $M_s = 7.1$ Loma Prieta earthquake: *Journal of Engineering Structures*, v. 15, no. 6, p. 403-421.
- Şafak, E., and Çelebi, M., 1991, Seismic response of Transamerica Building; II, System identification and preliminary analysis: *Journal of Structural Engineering*, v. 117, no. 8, p. 2405-2425.
- Şafak, E., and Çelebi, M., 1992, Recorded seismic response of Pacific Park Plaza; - II, System identification: *Journal of Structural Engineering*, v. 18, no. 6, p. 1566-1589.
- Shakal, A.F., Huang, M., Reichle, M., Ventura, C., Cao, T., Sherburne, R., Savage, R., Darragh, R., and Petersen, C., 1989, CSMIP strong-motion records from the Santa Cruz Mountains (Loma Prieta), California, earthquake of 17 October 1989: California Division of Mines and Geology, Office of Strong Motion Studies, Report: OSMS 89-06, 196 p.
- Shinozuka, M., and Ghanem, R., 1995, Structural system identification; I, Experimental verification: *Journal of Engineering Mechanics*, v.

- 121, no. 2, p. 265-273
- Silva, W., 1976, Body waves in a layered anelastic solid: *Bulletin of the Seismological Society of America*, v. 66, no. 5, p.1539-1554.
- Soydemir, Ç., and Çelebi, M., 1992, Seismic design of buildings with multi-level basements, *in* Proceedings, Tenth World Conference on Earthquake Engineering, Madrid, Spain: A.A. Balkema, Rotterdam, v. 3, p. 1731-1734.
- Stephen, R.M., Hollings, J.P., and Bouwkamp, J.G., 1974, Dynamic behavior of a multi-story pyramid shaped building: University of California, Berkeley, Earthquake Engineering Research Center, Report UCB/EERC 73-17, 94 p.
- Stephen, R.M., Wilson, E.L., and Stander, N., 1985, Dynamic properties of a thirty-story condominium tower building: University of California, Berkeley, Earthquake Engineering Research Center, Report UCB/EERC 85-03, 100 p.
- Tarquis, F., and Roessel, J.M., 1988, Structural response and design spectra for the 1985 Mexico City earthquake: University of Texas, Austin, Texas, Report No GD89-1, 208 p.
- Tena-Colunga, A., and Abrams, D.P., 1992, Response of an instrumented masonry shear wall building with flexible diaphragms during the Loma Prieta earthquake: University of Illinois, Urbana-Champaign, Department of Civil Engineering, Report UILU-ENG-92-2025, Structural Research Series 577, 114 p.
- The MathWorks, Inc., 1988 and 1995 editions, User's guide: System identification toolbox for use with Matlab: The MathWorks, Inc., South Natick, Mass., 200 p.
- Todorovska, M. I., 1992, Radiation damping during in-plane building-soil interaction, *in* Proceedings, Tenth World Conference on Earthquake Engineering: A.A. Balkema, Rotterdam, v. 3, p. 1549-1554.
- Uang, C.-M., and Maarouf, A., 1991, An investigation of UBC serviceability requirements from building responses recorded during the 1989 Loma Prieta earthquake: Northeastern University, Boston, Department of Civil Engineering, Report CE-91-06, 138 p.
- Uniform Building Code, 1976, 1979, 1982, 1985, 1988, 1991, 1994 editions: International Conference of Building Officials, Whittier, Calif.
- United States Nuclear Regulatory Commission, 1973, Design response spectra for design of nuclear power plants: Regulatory Guide 1.60.
- Veletsos, A.S., 1977, Dynamics of structure-foundation systems, *in* Hall, W.J., ed., *Structural and Geotechnical Mechanics*: Prentice-Hall, Inc., Englewood Cliffs, New Jersey, p. 333-361.
- Werner, S.D., Nisar, A., and Beck, J.L., 1992, Assessment of UBC seismic design provisions using recorded building motions from Morgan Hill, Mount Lewis, and Loma Prieta earthquakes, *in* Proceedings of the Tenth World Conference on Earthquake Engineering: A.A. Balkema, Rotterdam, p. 5723-5728.
- Working Group on California Earthquake Probabilities, 1990, Probabilities of large earthquakes in the San Francisco Bay Region, California: U.S. Geological Survey Circular 1053, 51 p.
- Wolf, J.P., and Song, C., 1996, To radiate or not to radiate: *Earthquake Engineering and Structural Dynamics*, v. 25, p. 1421-1432.

**THE LOMA PRIETA, CALIFORNIA, EARTHQUAKE OF OCTOBER 17, 1989:
PERFORMANCE OF THE BUILT ENVIRONMENT**

BUILDING STRUCTURES

MEASURED RESPONSE OF TWO TILT-UP BUILDINGS

By Sharon L. Wood, University of Texas; and
Neil M. Hawkins, University of Illinois

CONTENTS

Abstract -----	Page
Introduction -----	C77
Hollister warehouse -----	77
Milpitas industrial building -----	78
Measured acceleration response -----	78
Measured displacement response -----	83
Summary -----	86
Acknowledgment -----	88
References -----	89
	90

ABSTRACT

Acceleration response histories were recorded in two tilt-up buildings during the earthquake. The acceleration and displacement data are used to identify trends in the seismic behavior of tilt-up construction. Both buildings were less than 10 years old at the time of the earthquake, yet they represent significantly different construction practices. The one-story warehouse in Hollister is representative of traditional construction with a plywood roof diaphragm and cast-in-place pilasters. The two-story industrial building in Milpitas has window openings in every panel, includes a metal-deck floor diaphragm and a wood roof, and represents modern trends in tilt-up construction.

Structural damage was not observed in either building following the Loma Prieta earthquake. The general nature of the measured dynamic response is similar. Transverse accelerations measured at the center of the roof diaphragm were approximately three times larger than the corresponding ground accelerations. In-plane accelerations were transmitted up the wall panels with essentially no amplification.

INTRODUCTION

Tilt-up construction is used throughout the U.S. for low-rise commercial and industrial buildings. Construction costs are low due to the efficient system of casting wall

panels in a horizontal position on site and then lifting the panels into their final vertical position. Although economical to build, tilt-up construction is vulnerable to seismic damage. Following the collapse of a number of tilt-up buildings during the 1971 San Fernando earthquake, building code provisions were modified to strengthen critical connections between the wall panels and the roof diaphragm.

Tilt-up buildings typically include a number of different construction materials. The reinforced concrete wall panels are often combined with wood or metal-deck roof diaphragms to form a boxlike system. Design procedures for tilt-up construction tend to focus on proportioning the individual components, such as the thickness of the wall panels or the nailing patterns in the plywood roof diaphragm. Response histories recorded in two tilt-up buildings during the Loma Prieta earthquake provide a rare opportunity to study the seismic response of complete tilt-up systems (Shakal and others, 1989).

Both buildings were located within 50 km of the epicenter. Peak horizontal ground accelerations were approximately 0.36 g at the base of a one-story warehouse in Hollister and 0.14 g at the base of a two-story industrial building in Milpitas. Ground motions recorded at the two sites are shown in figure 1. The duration of the strong ground motion was between 5 and 10 seconds at both locations. Linear response spectra indicate that spectral accelerations and displacements in Hollister were higher than those in Milpitas (fig. 2).

The general nature of the measured dynamic response of the two tilt-up buildings is described in this paper. The two buildings represent extremes in styles of tilt-up construction. The building in Hollister represents a traditional tilt-up structural system. The one-story structure is a warehouse and little attention was paid to architectural features during design. In contrast, the building in Milpitas represents a recent trend of using tilt-up construction for multistory buildings. The tilt-up wall panels in the completed structure are more representative of frames than walls, due to frequent openings for windows.

Structural damage was not reported in either structure following the Loma Prieta earthquake.

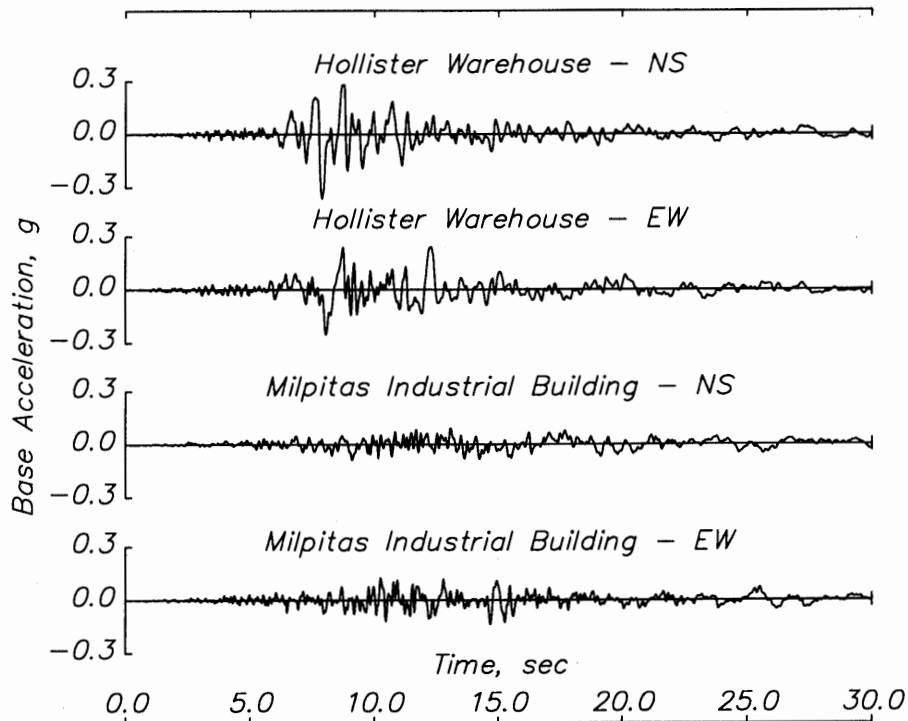


Figure 1.—Horizontal ground accelerations recorded in Hollister and Milpitas.

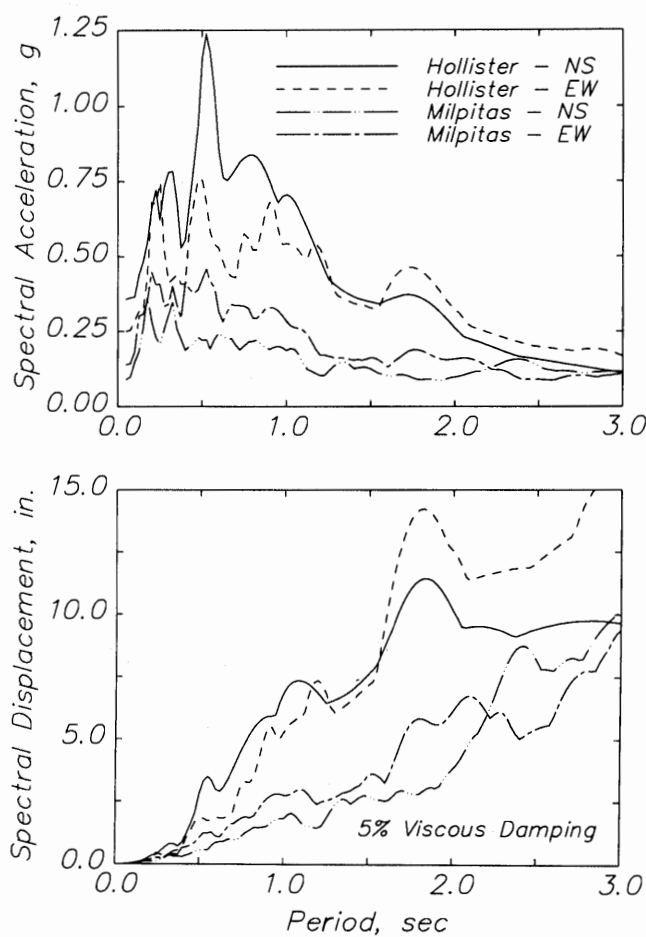


Figure 2.—Linear response spectra recorded in Hollister and Milpitas.

HOLLISTER WAREHOUSE

The warehouse in Hollister was built in 1979; however, the structural details are more representative of construction in the early 1970's. The building is 300 by 100 ft in plan (fig. 3). Concrete wall panels 6 in. thick are connected by cast-in-place pilasters which form continuous connections between adjacent wall panels. Cambered glulam beams run in both directions of the building and are supported on a single line of pipe columns. Purlins 14 in. deep are spaced at 8 ft on center in the roof and overlain with one-half in. structural plywood. The building was designed with nine openings: four overhead doors for fork-lift access and five personnel doors.

Typical reinforcement details are shown in figure 4. The panel reinforcement comprised a single layer of #4 bars spaced at 12 in. on center in each direction. Two #5 bars were added around panel openings. Chord reinforcement for the diaphragm was located in the wall panels. The reinforcing bars extended beyond the panel boundaries and were welded to chord reinforcement from adjacent panels. The chord reinforcement and horizontal panel reinforcement were then encased in the pilasters.

MILPITAS INDUSTRIAL BUILDING

The two-story industrial building in Milpitas was constructed in 1984. The building is 168 by 120 ft in plan (fig. 5), with the first story used as a warehouse and the second for offices. Nearly every wall panel has window

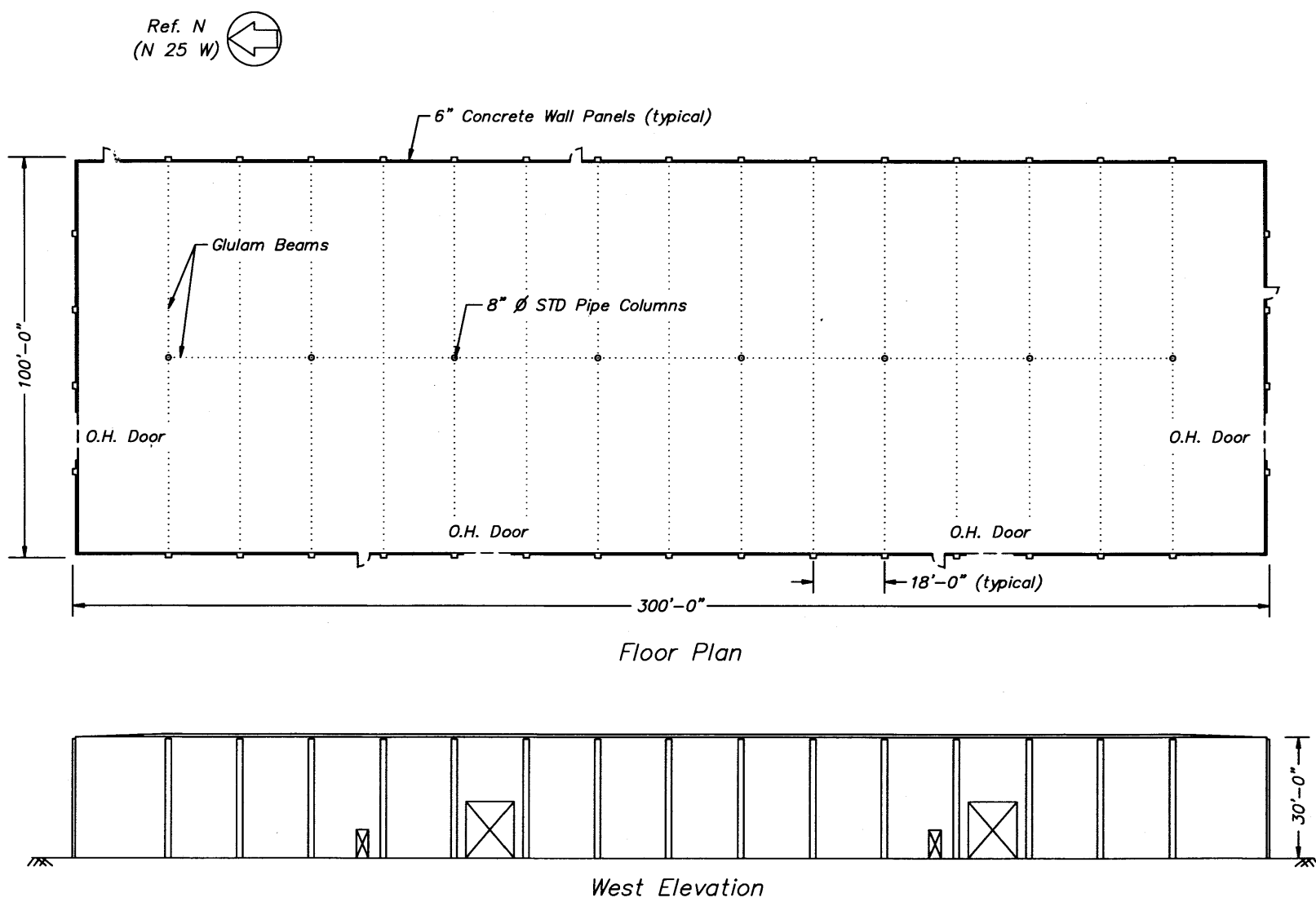
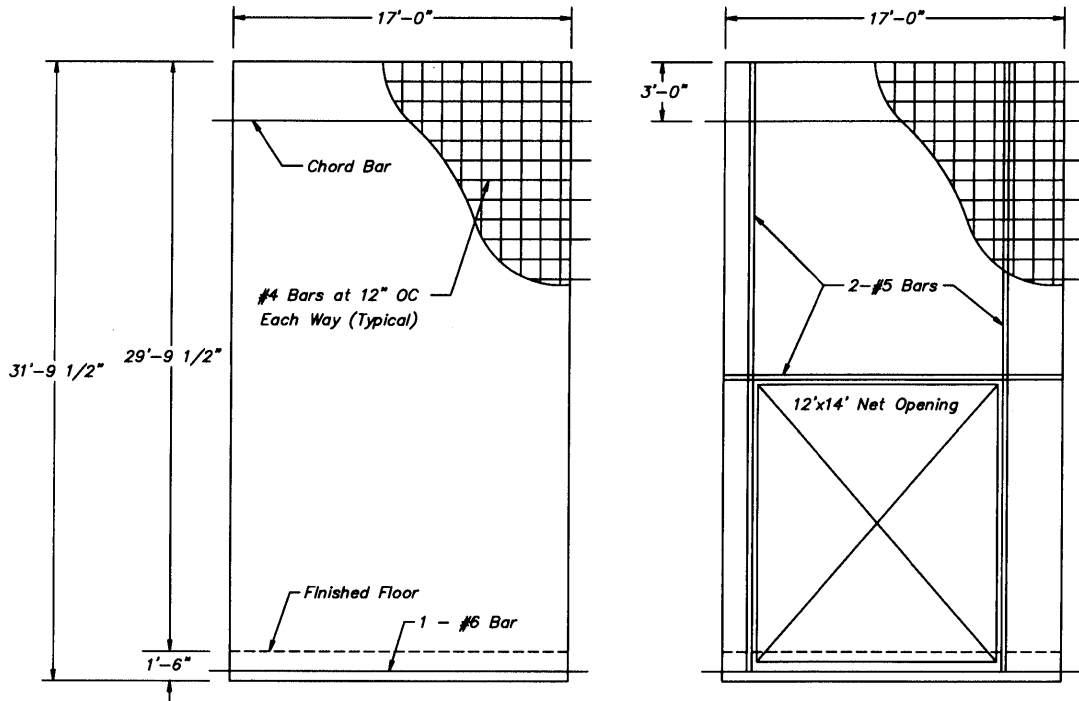


Figure 3.—Structural configuration of Hollister warehouse.

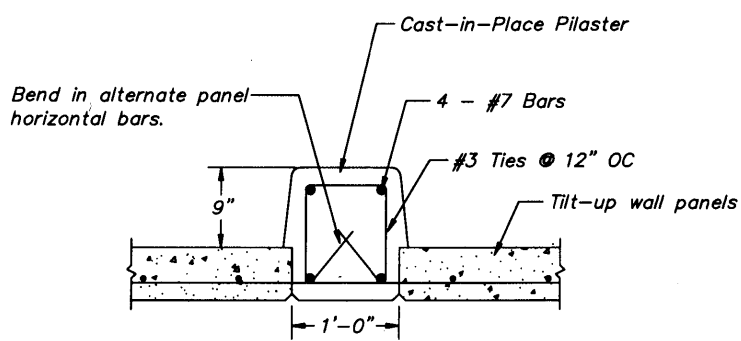
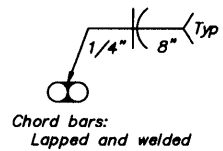
openings in both the first and second stories. Each wall panel varies in thickness between 8 and 16 in. for architectural reasons.

Eighteen structural tube columns carry the vertical loads from the floor and roof into the foundation. Open-web steel girders span in the longitudinal direction of the build-



TYPICAL PANEL DETAILS

CHORD BAR SCHEDULE	
PANEL LOCATION	BAR SIZE
Transverse Wall Panels	1 - #5 Bar
End Longitudinal Wall Panels (8 total)	1 - #9 Bar
Middle Longitudinal Wall Panels (24 total)	2 - #9 Bars



TYPICAL PANEL-TO-PANEL CONNECTION

Figure 4.—Typical structural details in Hollister warehouse.

ing at the second floor level. Open-web steel joists spaced at 8 ft on center run in the transverse direction between adjacent girders and support a composite metal deck and

$2\frac{1}{2}$ -in.-thick concrete slab. The pitched roof is supported by glulam beams running in the transverse direction. Purlins 16 in. deep are spaced at 8 ft on center in the longitudi-

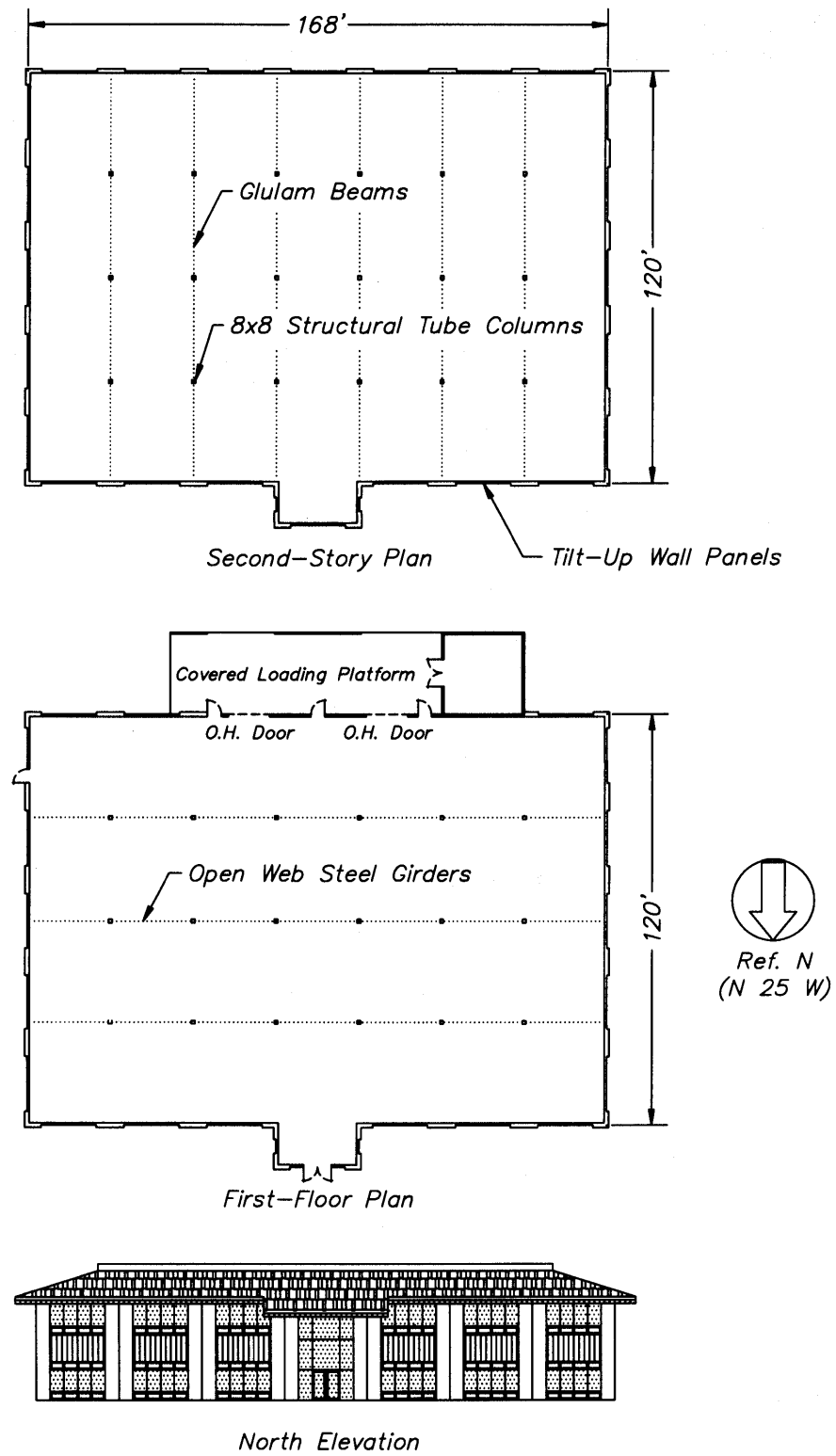
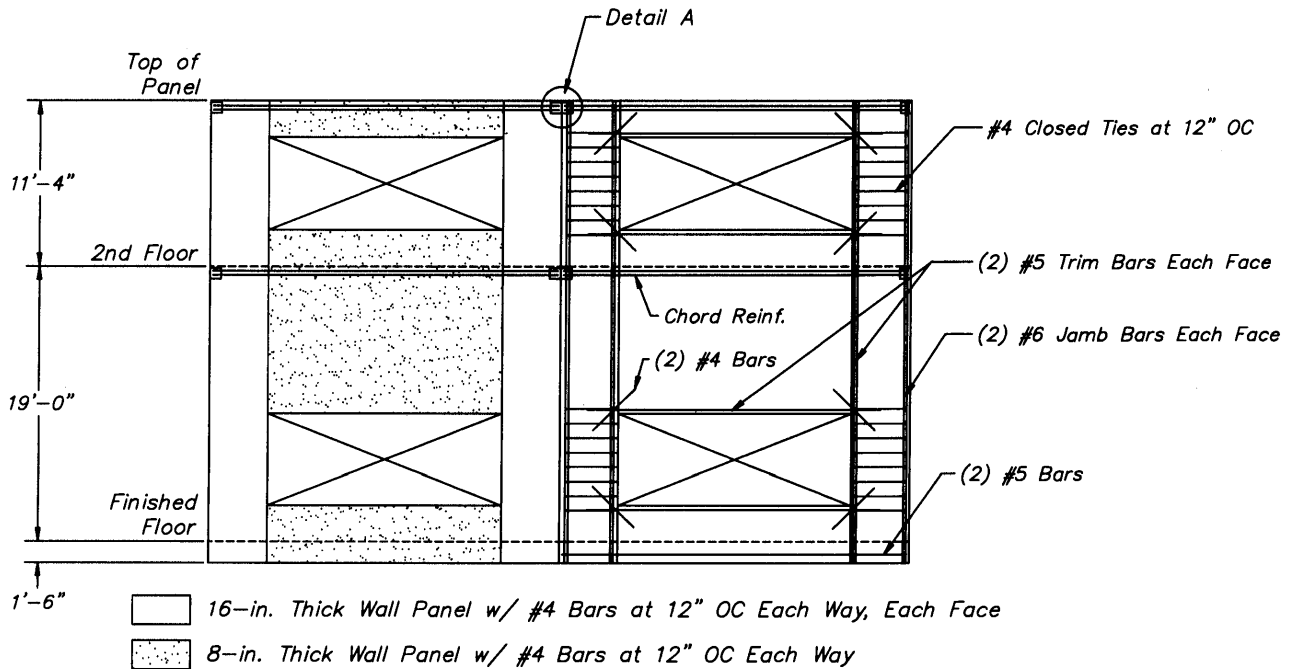


Figure 5.—Structural configuration of Milpitas industrial building.

dinal direction and are overlain with one-half-in. structural plywood.

Typical reinforcement details are shown in figure 6. The panel reinforcement may be divided into six categories: distributed vertical and horizontal panel reinforcement, vertical jamb bars along the panel edges, vertical and horizontal trim bars around the openings, diagonal reinforcement around the openings, closed ties in the wall

boundary elements near the openings, and chord reinforcement. A pocket was left around the chord reinforcement near the panel boundary at the second-story and roof levels to provide access to the chord reinforcement. Chord reinforcement from adjacent panels was welded to steel angles to create a lapped connection. Adjacent wall panels were connected only at the second-floor and roof levels.



TYPICAL PANEL DETAILS

CHORD REINFORCEMENT SCHEDULE

PANEL LOCATION	SECOND FLOOR	ROOF
Transverse Wall Panels	(3) #9	(2) #8
Longitudinal Wall Panels	(2) #8	(2) #6

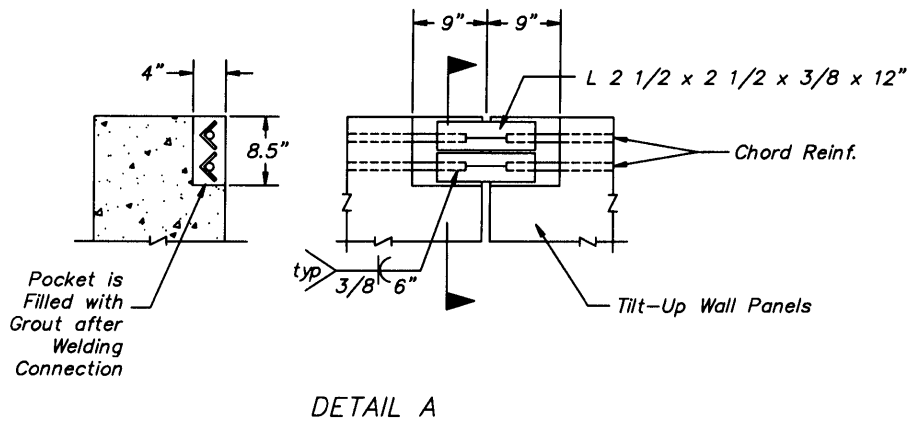


Figure 6.—Typical structural details in Milpitas industrial building.

MEASURED ACCELERATION RESPONSE

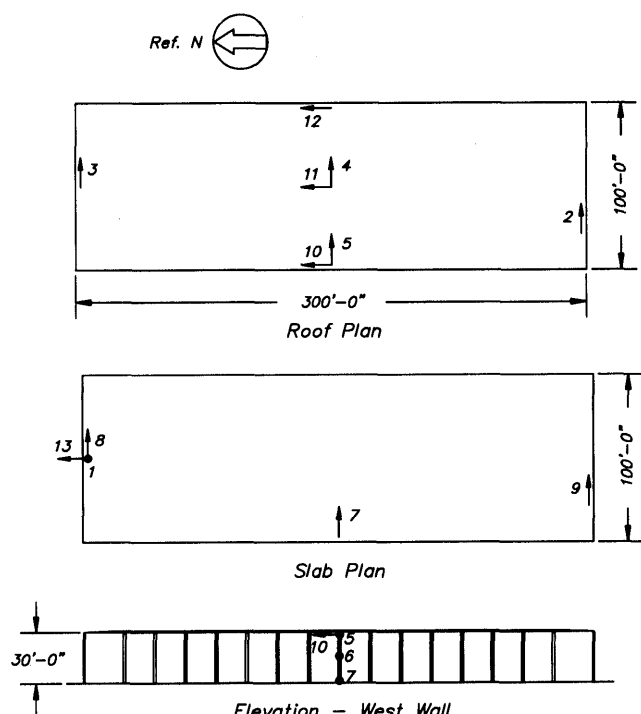
Records from 13 strong-motion instruments were obtained from each building during the earthquake (California Strong Motion Instrumentation Program, 1991). In the Hollister warehouse, five instruments recorded the ground motion, seven monitored motion at the roof, and one measured the out-of-plane response of a longitudinal wall panel at mid-height (fig. 7). In the Milpitas building, five instruments recorded the ground motion, four measured the response at the roof, and four measured the response of the second floor (fig. 8). Instrument locations are summarized in tables 1 and 2 for the Hollister and Milpitas buildings, respectively.

Measured acceleration histories from the Hollister warehouse are shown in figure 9. Response in the transverse (east-west) direction is shown at the base of the structure (channel 7), at the top of the transverse walls (channel 3), at mid-height of the center longitudinal wall panel (channel 6), and at the center of the roof (channel 4). In the longitudinal (north-south) direction, response histories are shown at the base of the structure (channel 13), the top of the longitudinal walls (channel 12), and the center of the

roof (channel 11). Acceleration maxima are presented in table 1.

Predominant frequencies were identified for each acceleration history from Fourier amplitude spectra (Carter and others, 1993) and are also reported in table 1.

The data indicate a significant amplification of the transverse accelerations at the center of the roof for the Hollister warehouse (fig. 10). The peak roof accelerations were approximately three times the ground peak accelerations at the center of the diaphragm. In contrast, the in-plane accelerations measured at the top of the transverse wall panels were essentially the same as the ground motions.



*Sensors 4 and 11 are mounted on glulam beams.
Sensor 13 is mounted on the floor slab.
All other sensors are mounted on the wall panels.*

Figure 7.—Location of strong motion instruments in Hollister warehouse.

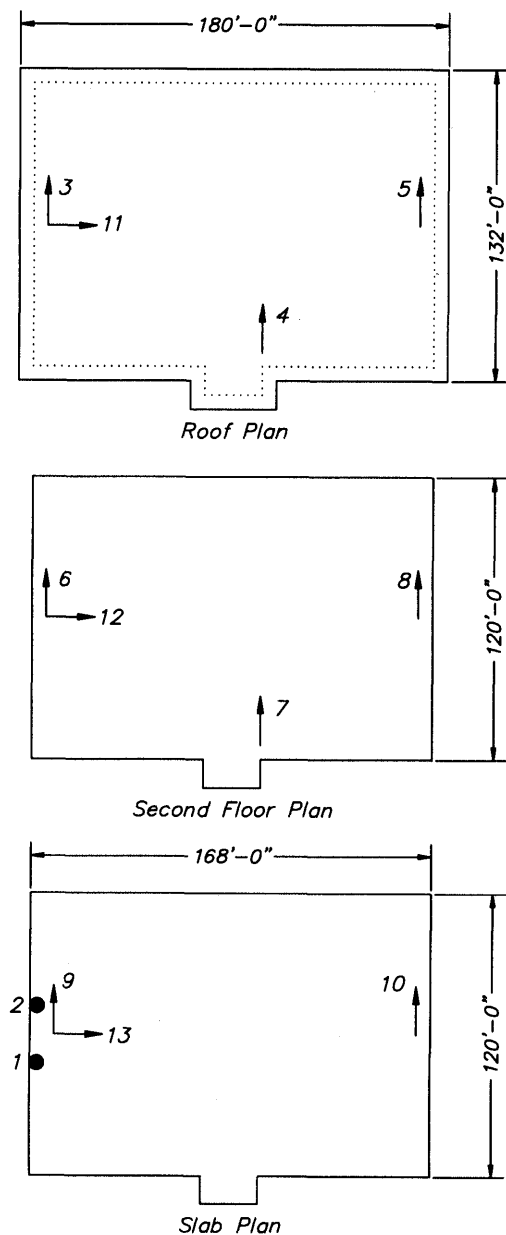


Figure 8.—Location of strong motion instruments in Milpitas industrial building.

Table 1.—Summary of strong motion data from Hollister warehouse

[—, Relative displacement data were calculated by subtracting the appropriate ground displacement from the structural displacement. Therefore, relative displacement were not calculated for channels recording ground motion.]

Channel number	Location	Elevation	Direction	Maximum acceleration (g)	Predominant frequency (Hz)	Maximum relative displacement (in.)	Reference channel
1	Center North Wall	Ground	Vertical	0.18	0.3	—	—
2	1/4 Point South Wall	Roof	EW	0.27	0.6	0.36	9
3	Center North Wall	Roof	EW	0.26	0.6	0.30	8
4	Center	Roof	EW	0.82	1.1	4.30	7
5	Center West Wall	Roof	EW	0.72	1.1	4.20	7
6	Center West Wall	Midpanel	EW	0.55	1.1	2.60	7
7	Center West Wall	Ground	EW	0.25	0.6	—	—
8	Center North Wall	Ground	EW	0.25	0.6	—	—
9	1/4 Point South Wall	Ground	EW	0.24	0.6	—	—
10	Center West Wall	Roof	NS	0.39	1.9	0.24	13
11	Center	Roof	NS	0.45	1.9	0.43	13
12	Center East Wall	Roof	NS	0.35	1.9	0.24	13
13	Center North Wall	Ground	NS	0.36	1.9	—	—

Table 2.—Summary of strong motion data from Milpitas industrial building

[—, Relative displacement data were calculated by subtracting the appropriate ground displacement from the structural displacement. Therefore, relative displacement were not calculated for channels recording ground motion.]

Channel number	Location	Elevation	Direction	Maximum acceleration (g)	Predominant frequency (Hz)	Maximum relative displacement (in.)	Reference channel
1	North End of East Wall	Ground	Vertical	0.08	0.4	—	—
2	South End of East Wall	Ground	Vertical	0.08	0.4	—	—
3	Center of East Wall	Roof	NS	0.11	0.2	0.03	9
4	Center of North Wall	Roof	NS	0.33	3.7	0.18	9
5	Center of West Wall	Roof	NS	0.14	0.2	0.04	10
6	Center of East Wall	2nd Floor	NS	0.11	0.2	0.02	9
7	Center of North Wall	2nd Floor	NS	0.17	0.2	0.08	9
8	Center of West Wall	2nd Floor	NS	0.13	0.2	0.04	10
9	Center of East Wall	Ground	NS	0.09	0.2	—	—
10	Center of West Wall	Ground	NS	0.10	0.2	—	—
11	Center of East Wall	Roof	EW	0.59	4.5	0.26	13
12	Center of East Wall	2nd Floor	EW	0.26	4.5	0.07	13
13	Center of East Wall	Ground	EW	0.14	0.4	—	—

Transverse accelerations measured at mid-height of the longitudinal wall were amplified with respect to the base, but did not exceed the amplitude of the roof accelerations.

Significant differences in the frequency content of the transverse accelerations were also observed between the ends and the center of the Hollister roof diaphragm. The predominant frequency of the transverse accelerations measured at the top of the north and south walls was 0.6

Hz, the same as that of the ground motion. However, the predominant frequency of the transverse accelerations measured at the center of the diaphragm and at the center of the west wall was 1.1 Hz.

Similar amplification was not observed in the longitudinal direction of the Hollister warehouse. The peak longitudinal acceleration response at the center of the roof was approximately 1.25 times the peak ground accelera-

tion, while the longitudinal acceleration histories measured at the top of the longitudinal walls were essentially the same as the ground accelerations. The predominant frequency of the longitudinal acceleration response at all three locations on the roof was the same as that of the ground motion.

Measured acceleration histories in the Milpitas industrial building are shown in figure 11. Response in the trans-

verse (north-south) direction is characterized by the ground motion (channel 9), the in-plane response of the transverse walls at the second-floor and roof levels (channels 6 and 3), and the out-of-plane response of the longitudinal walls at the second-floor and roof levels (channels 7 and 4). In the longitudinal (east-west) direction, measured response at the ground (channel 13) is shown along with the out-of-plane response at the second-floor and roof eleva-

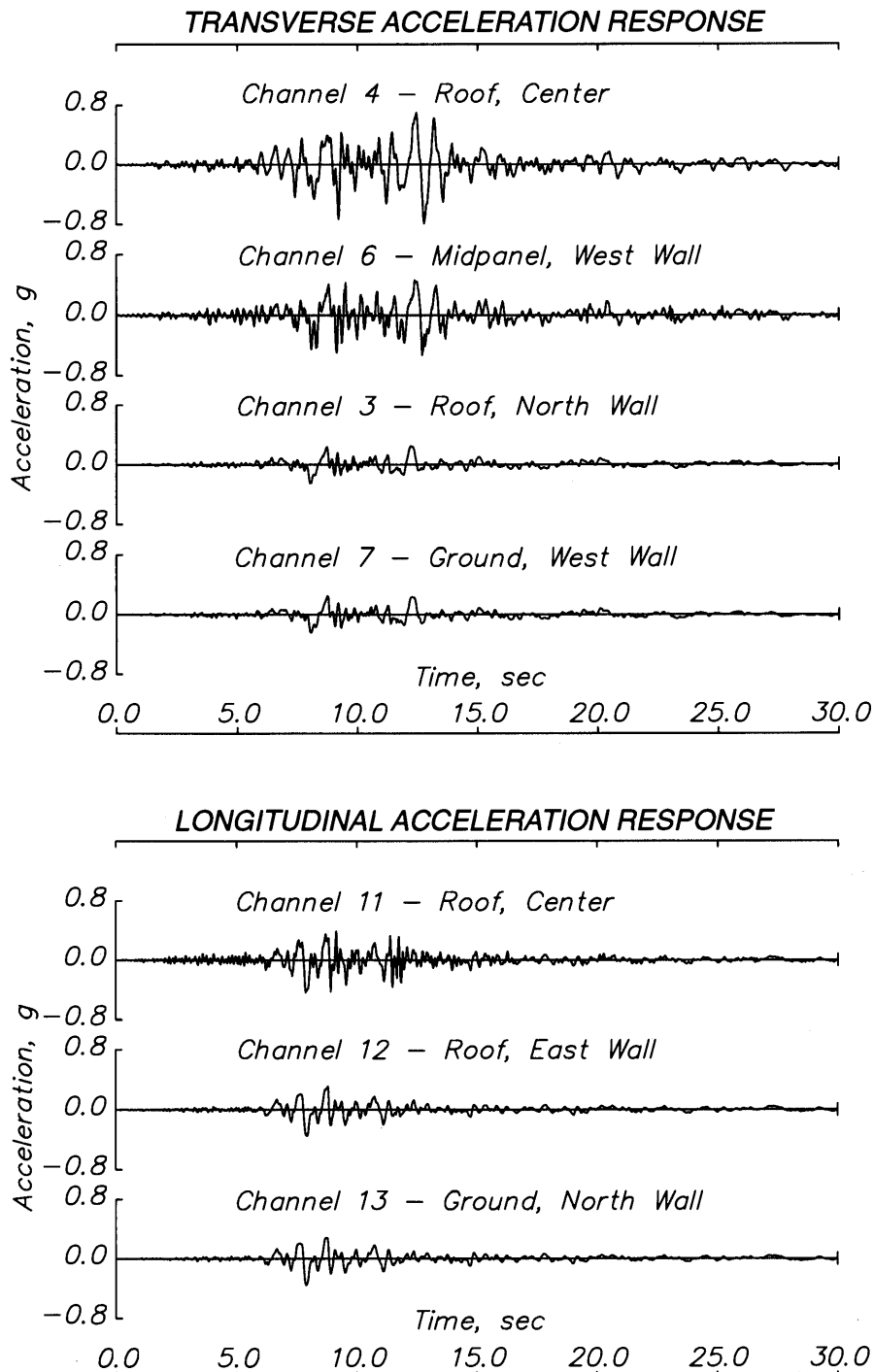


Figure 9.—Measured acceleration records in Hollister warehouse.

tions (channels 12 and 13). Peak accelerations and predominant frequencies are presented in table 2 for all channels.

In contrast to the Hollister warehouse, the measured data indicate significant amplification of both the longitudinal and transverse accelerations at the roof of the Milpitas industrial building (fig. 12). Amplification factors for peak roof response relative to the base exceeded four in the longitudinal direction and three in the transverse direction. Amplification factors for peak response at the second floor were approximately one-half those at the roof. Similar to the Hollister warehouse, the in-plane acceleration response of the wall panels was not amplified with height above the base.

The predominant frequency of the ground motion was 0.2 Hz in the transverse direction and 0.4 Hz in the longitudinal direction. Predominant frequencies identified from the in-plane wall response were the same as those identified from the ground motion. Predominant frequencies identified from the out-of-plane wall response were 3.7

Hz in the transverse direction and 4.5 Hz in the longitudinal direction.

The measured acceleration response of both the Hollister warehouse and the Milpitas industrial building highlight important differences between the in-plane and out-of-plane response of tilt-up wall panels. Little, if any, amplification of in-plane accelerations was observed with height above the base. The predominant frequency of the in-plane acceleration response measured at the top of the panels was the same as the predominant frequency measured at the base. Therefore, tilt-up wall panels may be considered to behave as rigid bodies when excited in plane. In contrast, the out-of-plane accelerations measured at the top of the wall panels exhibited significant amplification relative to the base, and the predominant frequencies of the out-of-plane response differed from the predominant frequencies at the base. The out-of-plane response at the top of the wall panels and the acceleration response at the center of the roof indicate the inherent flexibility of floor and roof diaphragms commonly used in tilt-up construction.

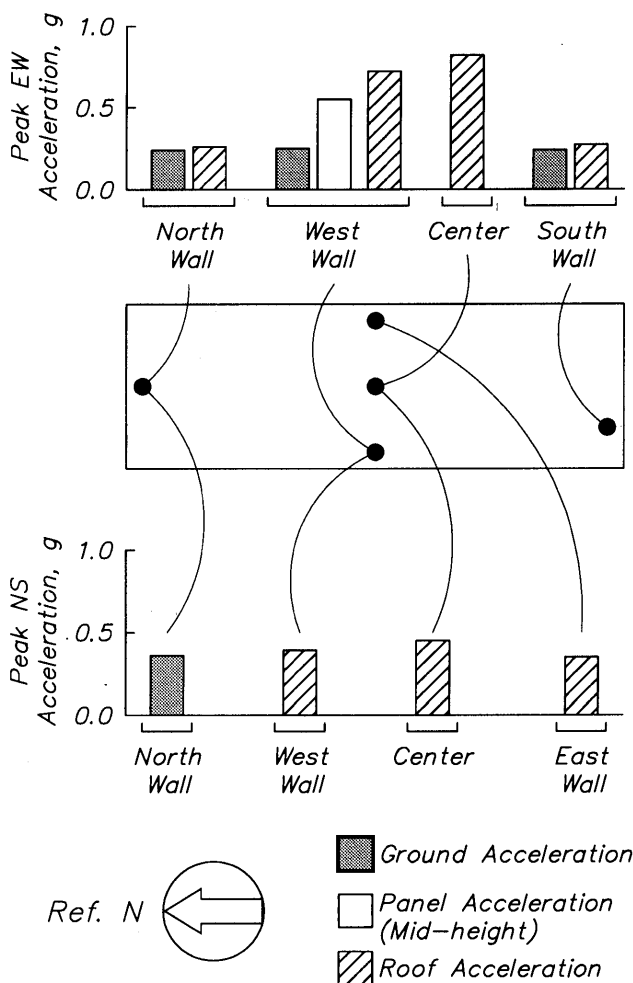


Figure 10.—Measured peak accelerations in Hollister warehouse.

MEASURED DISPLACEMENT RESPONSE

The digitized data provided by the California Department of Conservation included displacement histories that were obtained by integrating and filtering the corrected acceleration response (California Strong Motion Instrumentation Program, 1991). Recorded displacement data at the base of the two buildings and at the centers of the roofs are shown in figure 13. The peak ground displacement at both sites was approximately 10 in. With the exception of the transverse response of the Hollister warehouse, the absolute displacement response at the centers of the roofs of both buildings was approximately the same as the ground displacements. Amplification of the transverse displacements at the center of the roof in the Hollister warehouse may be observed.

An estimate of the displacements sustained by the buildings was made by subtracting the ground displacement from the structural displacement. The resulting relative displacement histories were then filtered to remove noise attributable to the ground motion (Carter and others, 1993). Due to the nature of the integration process used to obtain displacements from accelerations and the subsequent data manipulation, the relative displacement response histories should be considered to be approximate. Peak relative displacements are also presented in tables 1 and 2 for the Hollister and Milpitas buildings, respectively.

Relative displacement histories for the Hollister warehouse are shown in figure 14. Peak relative transverse displacements at the center of the roof exceeded 4 in., or

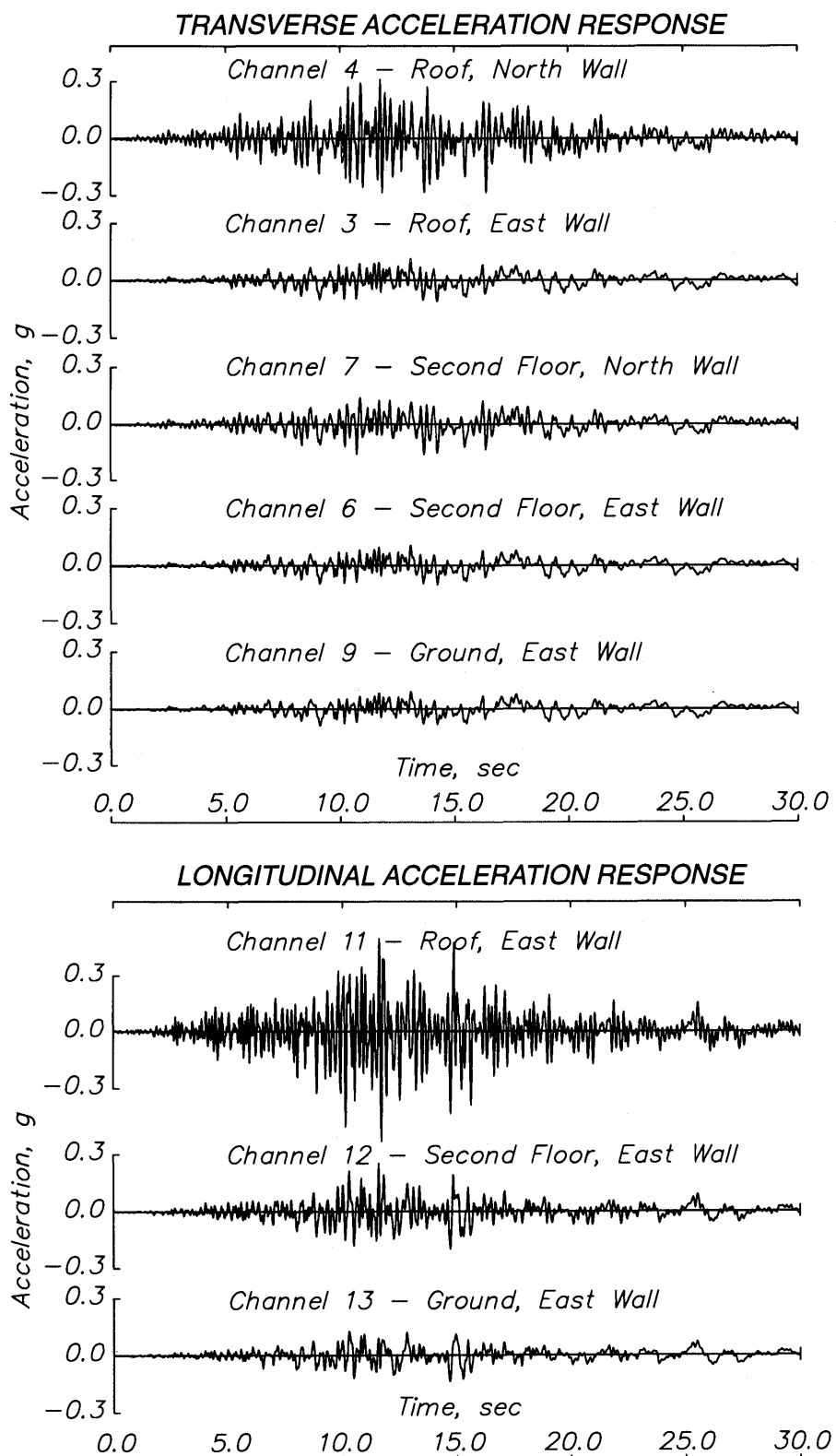


Figure 11.—Measured acceleration records in Milpitas industrial building.

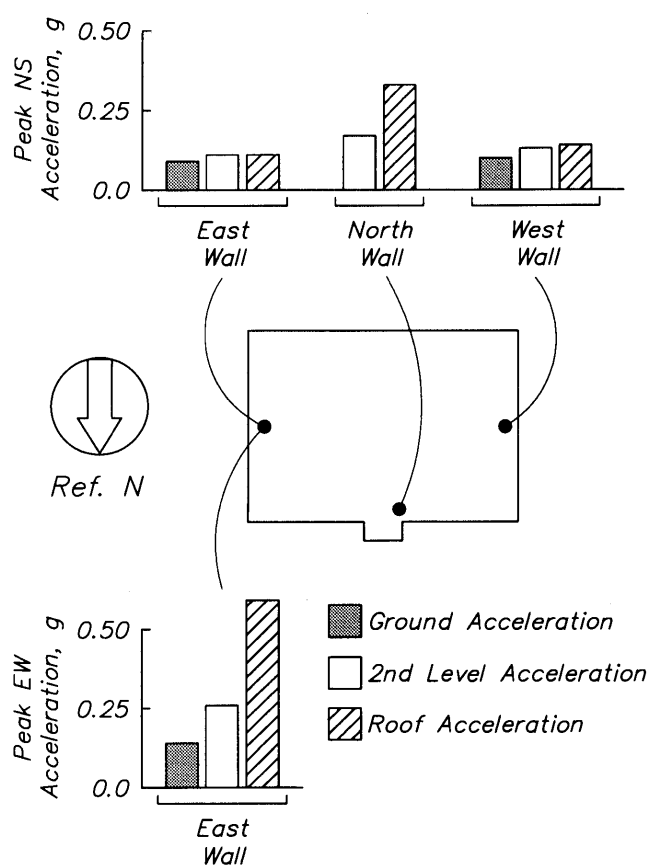


Figure 12.—Measured peak accelerations in Milpitas industrial building.

1 percent of the height of the building. The displacement response in the longitudinal direction and in the transverse direction at the top of the transverse walls was negligible. Elastic deformations within the plane of the diaphragm must occur to accommodate these displacements without structural damage.

Relative displacement histories for the Milpitas building are shown in figure 15. The amplitude of the peak response did not exceed one-fourth in., which is the same order of magnitude as the expected error in converting from accelerations to displacements (Shakal and Ragsdale, 1984). Therefore, the signal to noise ratio was considered to be too small to have confidence in these relative displacement data.

SUMMARY

The measured response of two tilt-up buildings located within 50 km of the epicenter of the earthquake were presented. Although the structural systems used in these buildings differ significantly, their dynamic response was similar.

Transverse accelerations were amplified by a factor of approximately three between the base and the center of the roof in both buildings. Peak transverse accelerations measured at mid-height of the longitudinal wall panels in the Hollister warehouse and at the second-floor level of the longitudinal wall panels in the Milpitas building were

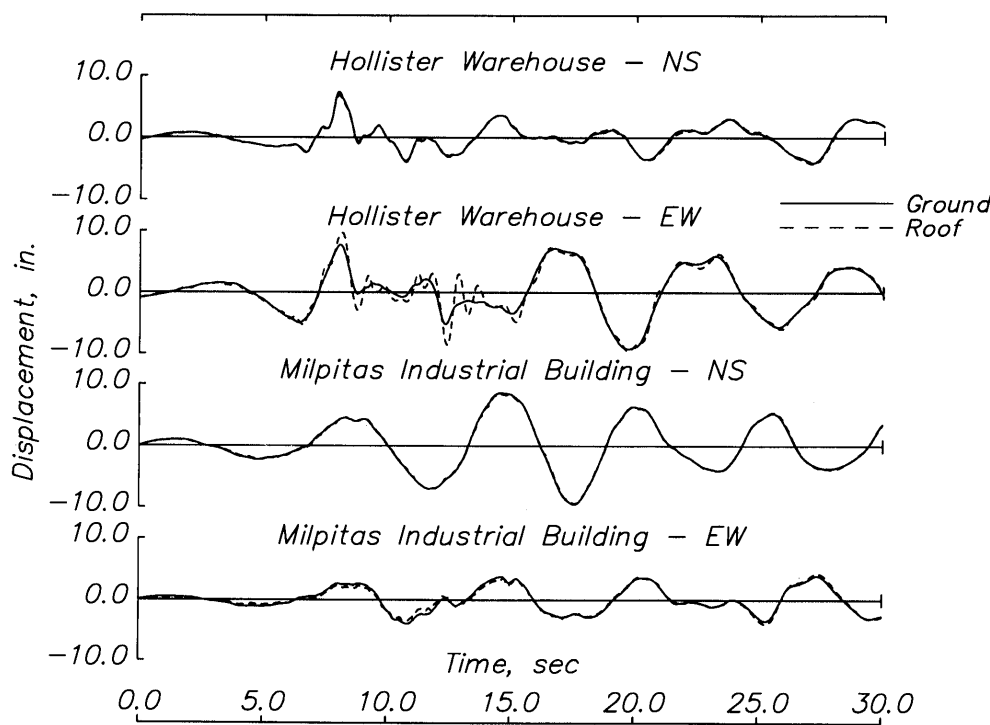


Figure 13.—Absolute displacement response of ground and roof.

greater than one-half the peak transverse accelerations measured at the center of the roof.

In the longitudinal direction, the peak roof accelerations in the Hollister warehouse were approximately 1.3 times the peak ground accelerations, while the peak roof accelerations in the Milpitas building exceeded the peak ground accelerations by a factor of 4.

Essentially no amplification of in-plane accelerations over the height of the wall panels was observed. The magnitude and frequency content of the in-plane acceleration histories measured at the roof of the buildings were essentially the same as the ground motion.

Displacement of the roof relative to the ground was more pronounced in the transverse, than the longitudinal direction. Maximum transverse displacements at the roof of the Hollister building exceeded 1 percent of the height of the building.

ACKNOWLEDGMENT

The work described in this paper was funded by the National Science Foundation under Grant No. BCS-9120281 at the University of Illinois. The California Department of Conservation, Strong Motion Instrumentation

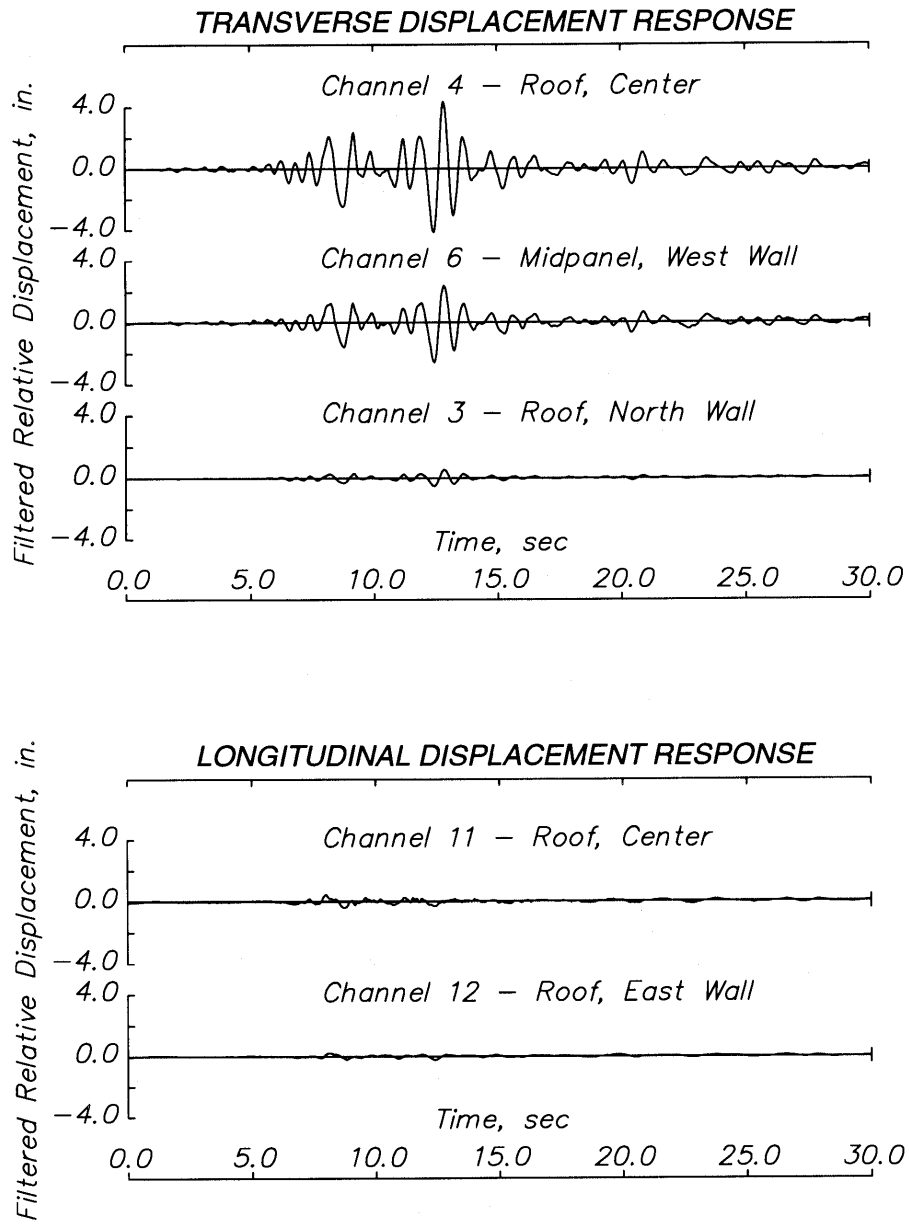


Figure 14.—Relative displacement response of Hollister warehouse.

Program is thanked for providing acceleration records and structural drawings.

REFERENCES

- California Strong Motion Instrumentation Program, 1991, Processed strong-motion data from the Loma Prieta earthquake of 17 October 1989—Building records: California Department of Conservation, Division of Mines and Geology, Office of Strong Motion Studies, Report No. OSMS 91-07, 196 p.
- Shakal, A., Huang, M., Reichle, M., Ventura, C., Cao, T., Sherburne, R., Savage, M., Darragh, R., and Peterson, C., 1989, CSMIP strong-motion records from the Santa Cruz Mountains (Loma Prieta), California earthquake of 17 October 1989: California Department of Conservation, Division of Mines and Geology, Office of Strong Motion Studies, Report No. OSMS 89-06.
- Shakal, A.F., and Ragsdale, J.T., 1984, Acceleration, velocity and displacement noise analysis for the CSMIP accelerogram digitization system, in Proceedings, Eighth World Conference on Earthquake Engineering, V. II, San Francisco: Earthquake Engineering Research Institute, p. 111-118.
- Carter, J.W., Hawkins, N.M., and Wood, S.L., 1993, Seismic response of tilt-up construction: University of Illinois, Urbana, Structural Research Series No. 581, 224 p.

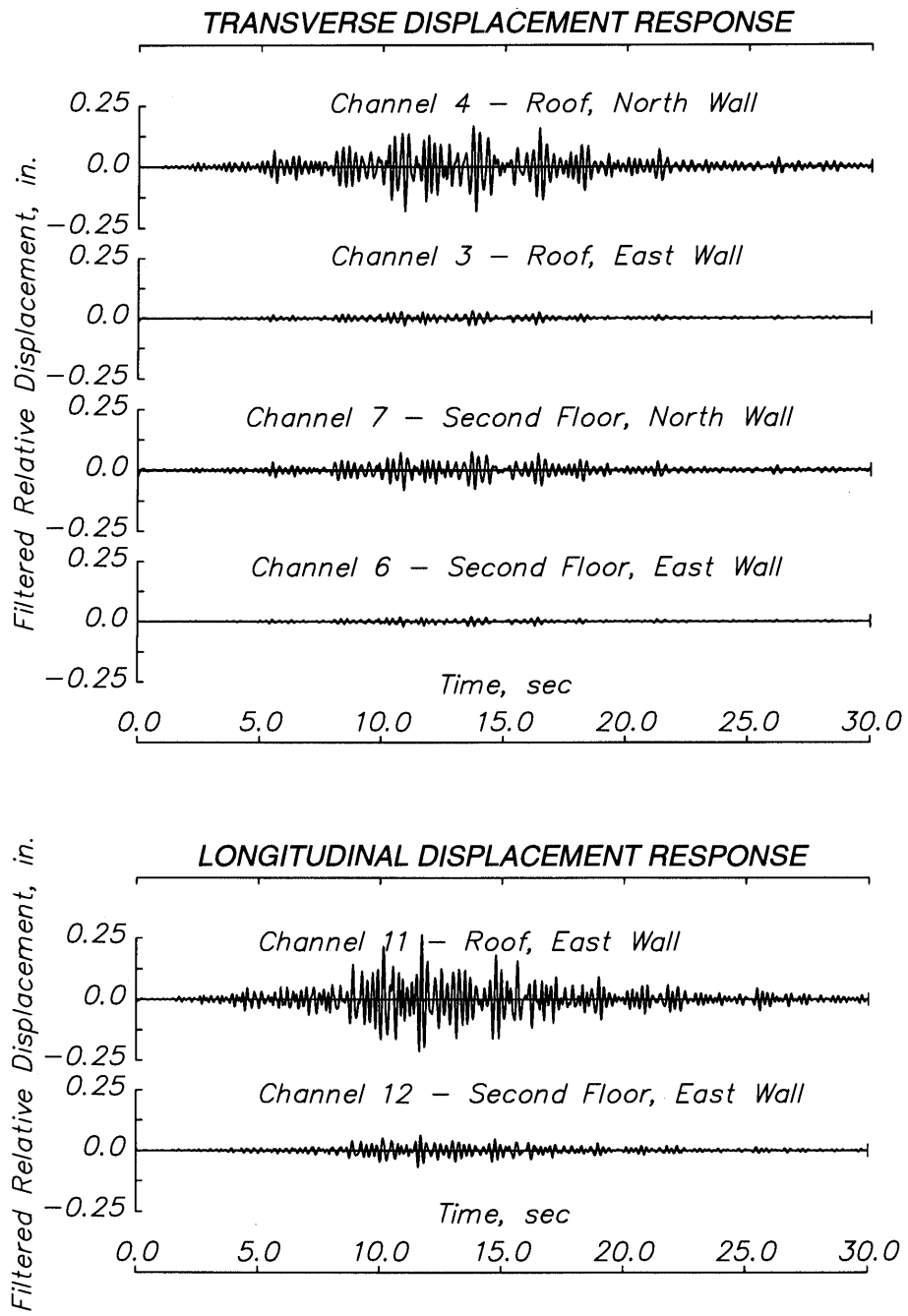


Figure 15.—Relative displacement response of Milpitas industrial building.

THE LOMA PRIETA, CALIFORNIA, EARTHQUAKE OF OCTOBER 17, 1989:
BUILDING STRUCTURES

PERFORMANCE OF THE BUILT ENVIRONMENT

SEISMIC RESPONSE OF A SIX-STORY REINFORCED
CONCRETE BUILDING

By James C. Anderson,
University of Southern California; and
Vitelmo V. Bertero,
University of California, Berkeley

CONTENTS

	Page
Abstract	C91
Introduction	91
Objectives	92
Building details	92
Seismic design criteria	92
UBC (1976) seismic forces	92
UBC (1991) seismic forces	92
Instrumentation and recorded response	94
Mathematical models for elastic response	96
Elastic dynamic response analyses	97
Modal period determination	97
Model verification analyses	98
Strong motion analyses	98
Summary and conclusions	102
Acknowledgments	103
References	104

ABSTRACT

A six-story reinforced concrete building located in San Bruno was instrumented with 13 strong motion accelerometers at the time of the earthquake. Lateral resistance is provided by moment-resisting perimeter frames and one interior moment frame. Spectral analysis procedures were used to evaluate the dynamic properties of the building based on the response recorded during the earthquake.

Linear elastic models of the building were developed for use with commercially available computer programs. Building responses calculated using these models compared well with the recorded response, indicating that the response was predominately linear elastic for this earthquake. Base shears calculated using accelerations recorded at the base of the structure exceed code values by a factor of 3.6 in the longitudinal direction and 2.7 in the transverse direction, indicating that some cracking and limited yielding may have occurred. Base shears developed by other earthquake ground motions recorded in the free field

far exceed code design values and indicate that a nonlinear response analysis will be required to accurately evaluate the building response.

INTRODUCTION

It has been pointed out by Bertero and others (1991) that most human injury and economic loss due to moderate or severe earthquake motions are caused by failures of civil engineering facilities, particularly buildings, many of which were presumably designed and constructed to provide protection against such natural hazards. The two most effective ways to mitigate the destructive effects of earthquakes are the improvement of present methods for designing, constructing, and maintaining new structures and the development of effective methods of seismic upgrading of existing facilities which do not meet current code requirements.

One of the main steps toward the improvement of the design of new facilities and the selection of technically and economically efficient strategies for the seismic upgrading of existing facilities is the ability to predict in a reliable manner the dynamic behavior of the structures when they are subjected to critical seismic excitations that can occur during their expected service life. In order to achieve such improvements, it is necessary to compare the results of analytical calculations with the results of large-scale experiments. The best large-scale experiment is when an earthquake occurs and properly placed instruments record the response of the building to ground motions recorded at the base. This report summarizes the studies conducted on one such structure, a six-story reinforced concrete building.

The Loma Prieta earthquake occurred about 9 miles northeast of Santa Cruz and 60 miles south of San Francisco. Following the earthquake, the U.S. Geological Survey (USGS) (1989) obtained building-response records in approximately eight instrumented structures. At the same

time, the California Strong Motion Instrumentation Program (CSMIP) of the California Division of Mines and Geology (CDMG) (1989) obtained recorded response records from some 30 buildings.

Two reinforced concrete buildings from this group of instrumented structures were selected for detailed study by the authors. The first of these was a 30-story condominium tower which is described in detail by Anderson and others (1991). The second building is a six-story, reinforced concrete office building located in San Bruno, approximately 50 miles from the epicenter.

OBJECTIVES

The main objectives of these studies are the following: (1) to evaluate the reliability of the analytical models presently available for analyzing the dynamic response of buildings; (2) to estimate through static and dynamic analyses the damage that the reference building may have experienced under the recorded ground motion; (3) to estimate the response of the building under critical ground motions to which it may be exposed during its service life; and (4) to assess the implications of the obtained results regarding the reliability of present seismic code regulations for the design of such buildings.

BUILDING DETAILS

The six-story building, which is 78 feet in height and has a rectangular plan of 90 by 200 feet, was built in 1978. Lateral resistance is provided by ductile, moment-resistant concrete frames, four which are located on the perimeter and one which is located on the interior in the transverse direction. Typical beam spans are 16 feet. The exterior concrete columns are cast into precast finish shells which served as forms. Gravity loads are carried to the exterior columns and a center column by prestressed beams having a 42-foot simple span. The foundation under the moment frames consists of heavy grade beams and spread footings. Concrete strength for the moment frames is 5,000 psi with Grade 60 reinforcing steel. Inspection of the structure following the earthquake showed some hairline cracking of the concrete finish shells around the columns. There was no visible damage noted on the interior of the building.

The weight (mass) at the roof level and typical floor level are estimated as follows: (1) roof level; 2,790 kilopounds (kips) ($7.22 \text{ k-s}^2/\text{in}$), (2) typical floor; 3,032 kips ($7.85 \text{ k-s}^2/\text{in}$). Using these values, the total self weight of the structure becomes 17,950 kips.

SEISMIC DESIGN CRITERIA

The structure was built in 1978, and it is assumed that the governing building code was the 1976 Uniform Building Code (UBC76). Lateral seismic design forces specified in this code will be compared to those currently required by the 1991 edition (UBC91).

UBC76 SEISMIC FORCES

Lateral seismic loads specified in the 1976 UBC were expressed in terms of the base shear which was defined as

$$V = C_s W_e,$$

where C_s is the design seismic-resistance coefficient and W_e is the effective seismic dead load. The design seismic resistance coefficient is in turn given by the formula

$$C_s = Z K C I S,$$

where

$$C = 1/(15\sqrt{T}) = 0.086;$$

$$T = 0.1 * N = 0.6 \text{ s};$$

$$K = 0.67;$$

$$Z = S = I = 1.0.$$

Using these values, the design seismic resistance coefficient becomes

$$C_s = 1.0 * 0.67 * 0.086 * 1.0 * 1.0 = 0.058.$$

This states that the total lateral force requirement will be 5.8 percent of the effective seismic dead load, which for most types of building occupancy is equal to the total self weight of the structure. Using the estimated self weight of the building of 17,950 kips, the base shear requirement becomes

$$V = 0.058 * 17950 = 1,041 \text{ kips.}$$

UBC91 SEISMIC FORCES

The 1991 UBC defines the design seismic-resistance coefficient as

$$C_s = (Z I C / R_w),$$

where the period, T , can be estimated as either

$$T = 0.030 * h^{3/4} = 0.030 * (78)^{3/4} = 0.787$$

or

$$T_{(\text{computer})} = 0.885 \text{ s (N-S)}$$

$$T_{(\text{computer})} = 1.032 \text{ s (E-W)}$$

and the site coefficient, C , is specified by the formula

$$C = 1.25 * S / T^{\frac{2}{3}}.$$

The site coefficient based on the empirical formula for the period is the same for both directions and has the value

$$C = 1.25 * 1.0 / (0.787)^{\frac{2}{3}} = 1.47,$$

whereas the values for this parameter obtained using the computed fundamental periods are

$$C_{(\text{N-S})} = 1.356; C_{(\text{E-W})} = 1.224.$$

The code further requires that these values be at least 80 percent of those calculated using the empirical formula. It can be seen that this requirement is satisfied. Using $Z=0.4$; $R_w=12$ and $S=I=1.0$, the design seismic resistance coefficients become

$$C_{s(\text{N-S})} = 0.4 * 1.0 * (1.356) / 12 = 0.045$$

$$C_{s(\text{E-W})} = 0.4 * 1.0 * (1.224) / 12 = 0.041$$

and the corresponding base shears

$$V_{(\text{N-S})} = 0.045 * 17,950 = 807.8 \text{ kips}$$

$$V_{(\text{E-W})} = 0.041 * 17,950 = 736.0 \text{ kips.}$$

It should be noted that these values are 22.4 and 29.3 percent less respectively than the lateral force requirement used to design the building in 1976. The authors do not feel this reduction in lateral force requirement is justified.

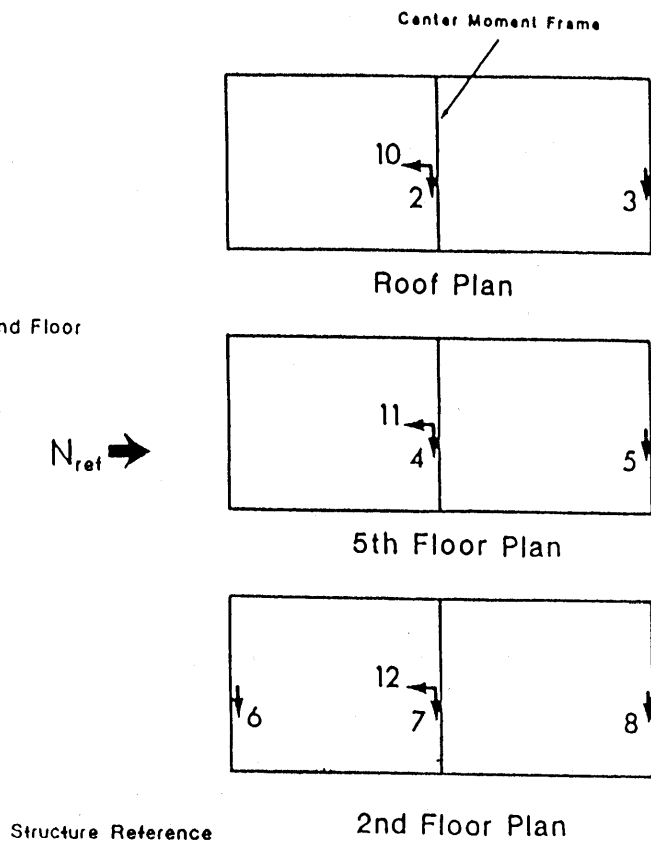
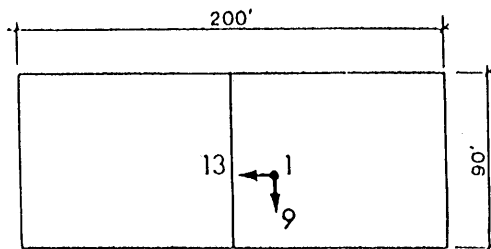
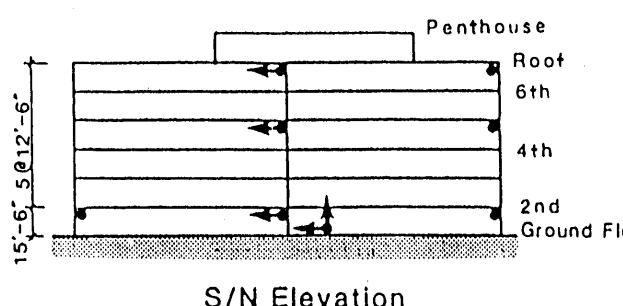


Figure 1.—Location of strong motion instrumentation.

INSTRUMENTATION AND RECORDED RESPONSE

The building was instrumented by the California Strong Motion Instrumentation Program (CSMIP) with 13 strong motion accelerometers at the time of the earthquake. These instruments were distributed throughout the building as shown in figure 1 which is taken from the California Department Mines Geology (California Division of Mines and Geology, 1989). The time histories of the recorded accelerations are shown in figures 2 to 14. The vertical accelerations recorded at ground level near the center of the building are shown in figure 2. Here it can be seen that the vertical acceleration has a peak value of 0.12 g , which is almost equal to the peak horizontal acceleration of 0.14 g recorded in the north-south direction (fig. 14).

The transverse acceleration recorded at the roof, near the center of the building, is shown in figure 3. Here it can be seen that the peak acceleration reaches 0.31 g and

that the duration of strong motion response is approximately 17 s. The transverse accelerations recorded at the roof level near the north end of the building are shown in figure 4. At this location the peak acceleration reaches $45\text{ percent of gravity}$. A comparison of this record with the one just discussed indicates that there is a torsional response of the structure at this level. Similar acceleration data for the fifth story level is shown in figure 5 for the center and in figure 6 for the north end. At the center, the peak acceleration is 0.20 g and at the north end it increases to 0.23 g , which also indicates a torsion response but not as much as the roof level. Transverse acceleration data at the south, center, and north locations at the second-floor level is shown in figures 7 to 9. At these locations the peak recorded accelerations are 0.11 , 0.11 , and 0.14 g , respectively. The recorded base acceleration at the center of the building in the transverse (east-west) direction is shown in figure 10. Here it can be seen that the peak acceleration is 0.11 g and that the duration of strong ground motion is about 7 s.

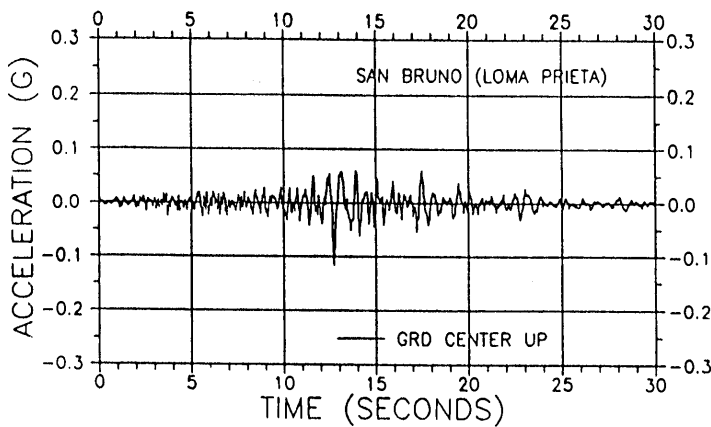


Figure 2.—Recorded acceleration, vertical, base level, center.

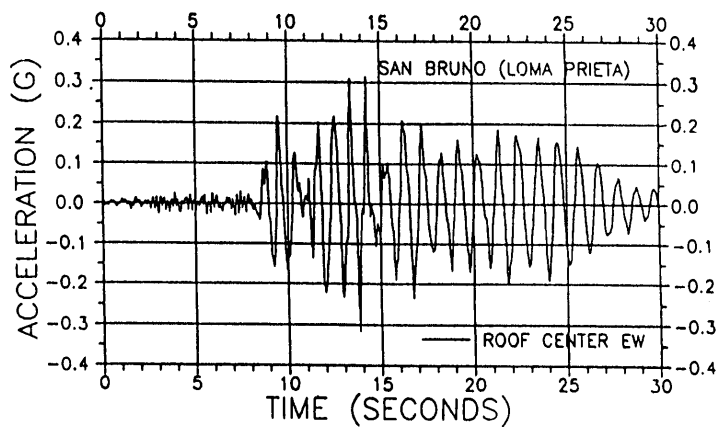


Figure 3.—Recorded acceleration, east-west, roof level, center.

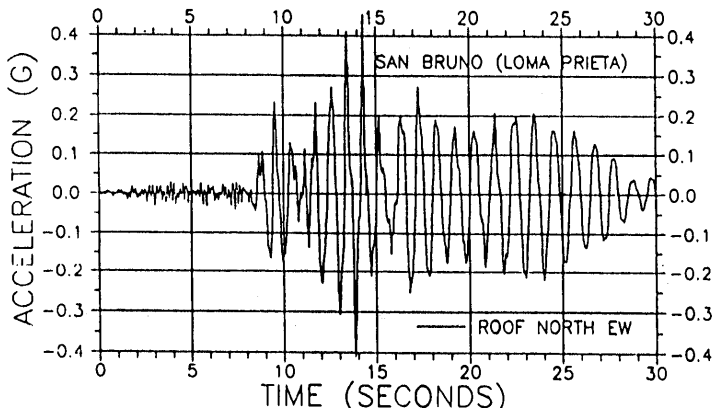


Figure 4.—Recorded acceleration, east-west, roof level, north.

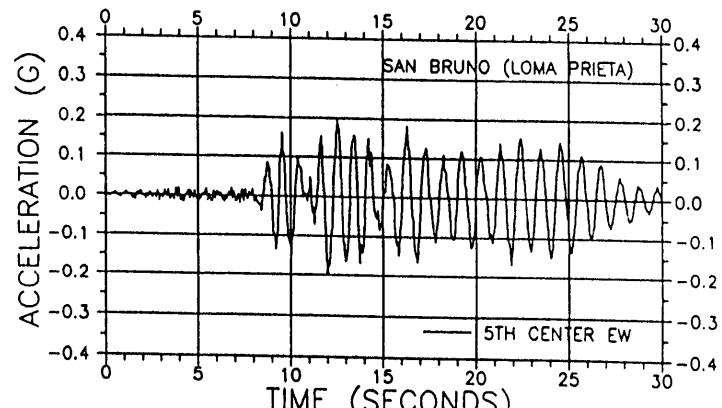


Figure 5.—Recorded acceleration, east-west, fifth level, center.

In the longitudinal (north-south) direction, all recordings were from instruments located near the center of the building. The acceleration recorded at the roof level is shown in figure 11, which indicates a peak acceleration in

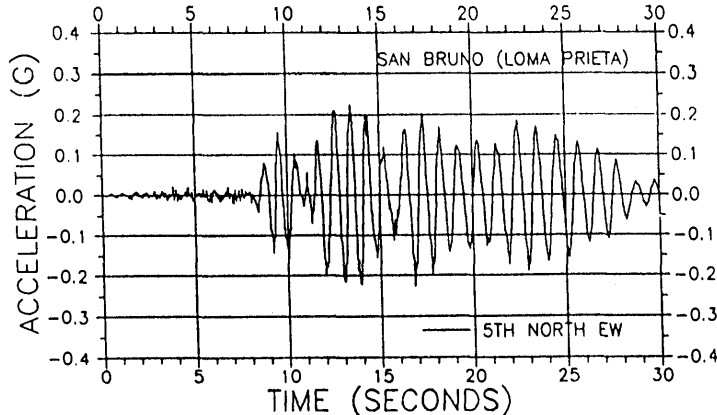


Figure 6.—Recorded acceleration, east-west, fifth level, north.

the longitudinal (north-south) direction of 0.25 g which compares with 0.32 g in the east-west direction. Recall that the direction of fault propagation was approximately north-south. Also, at this location, the duration of strong

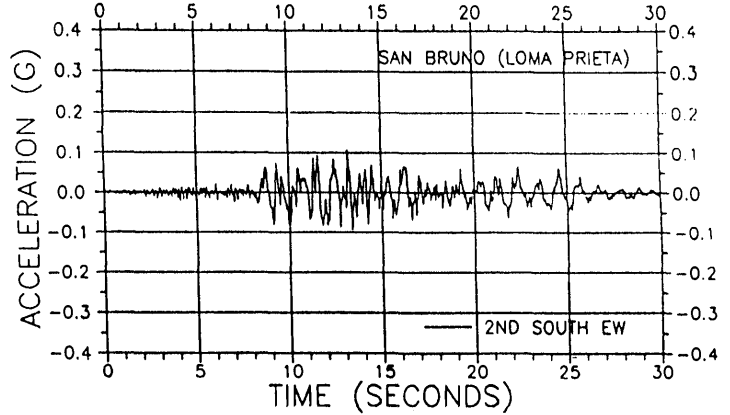


Figure 7.—Recorded acceleration, east-west, second level, south.

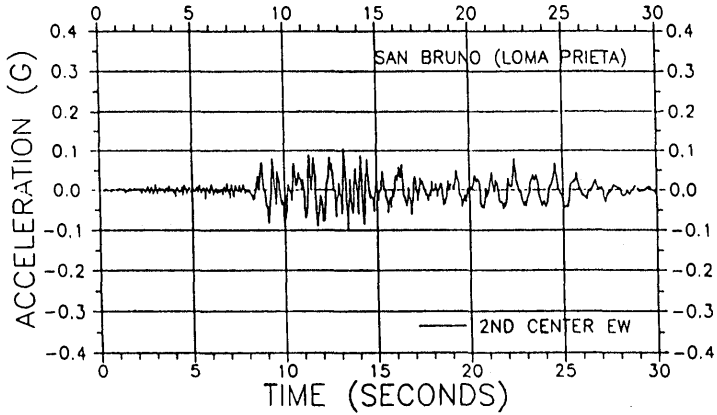


Figure 8.—Recorded acceleration, east-west, second level, center.

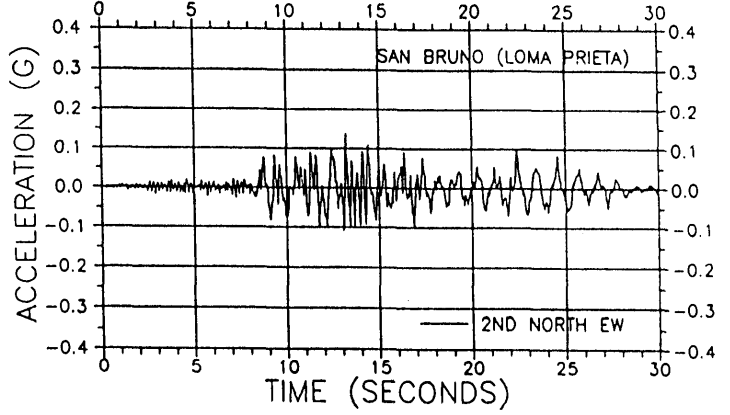


Figure 9.—Recorded acceleration, east-west, second level, north.

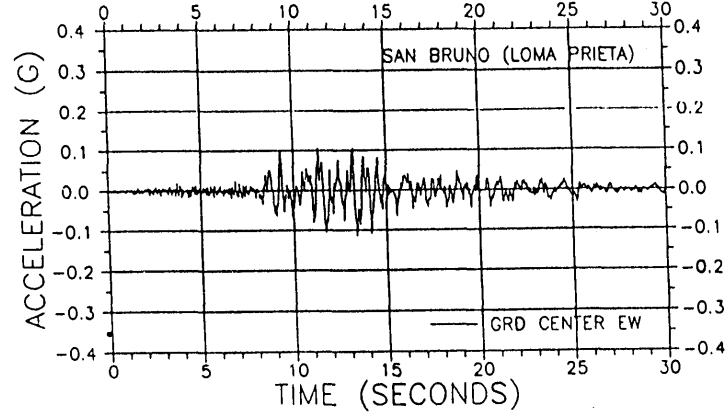


Figure 10.—Recorded acceleration, east-west, base level, center.

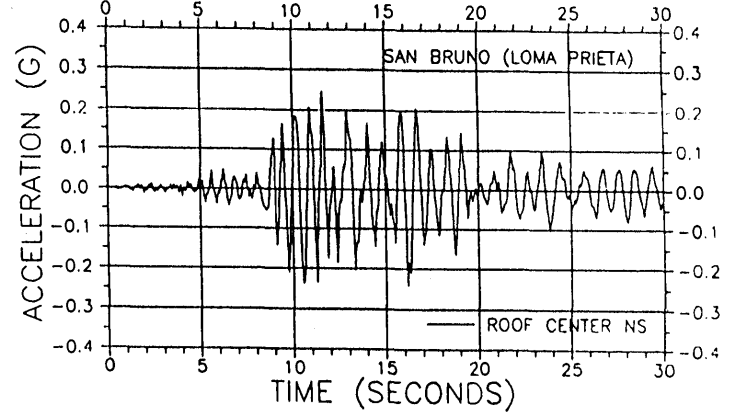


Figure 11.—Recorded acceleration, north-south, roof level, center.

motion response is approximately 10 s compared with 17 s in the transverse direction. Acceleration data at the fifth and second floors is given in figures 12 and 13. The recorded base acceleration is shown in figure 14, where it can be seen that the peak acceleration is 0.14 g compared to 0.11 g transverse.

Linear elastic response spectra (LERS) showing the spectral accelerations for the three components of motion recorded at the base of the building are shown in figure 15 along with the acceleration spectrum of the 1976 UBC.

Based on this review of the recorded acceleration data, the following observations are made:

1. The vertical accelerations recorded at the base have a peak amplitude which is similar to that of the horizontal accelerations at the same location.
2. Peak ground acceleration occurred in the longitudinal (north-south) direction, whereas peak building response occurred in the transverse (east-west) direction.
3. Examination of the acceleration data recorded at the roof level indicates that the fundamental period of vibration in both directions is in the range of 0.9 to 1.0 s.

4. Comparisons between accelerations recorded at the center of the building and those recorded at the ends in the transverse direction indicate that there may be a torsional component in the dynamic response of the upper levels.

MATHEMATICAL MODELS FOR ELASTIC RESPONSE

Three dimensional models were developed for the structure using the SAP90 computer program (Wilson and Habibullah, 1989), and the ETABS computer program (Habibullah, 1989), although it is recognized that several alternative programs could have been used for this phase of the response analysis.

The version of the ETABS program available at the time this phase of the study was conducted did not have the capability to produce time-history response plots and therefore did not permit a comparison of recorded response with calculated response. The current version has this capability and could have been used for all response and design analyses for this structure.

An isometric view of the analytical model used in the SAP90 program to represent the lateral force-resisting system of the building is shown in figure 16. Here it can be seen that there are two moment resistant frames in the longitudinal direction (north-south) and three moment resistant frames in the transverse direction (east-west). The floor is modeled as a rigid diaphragm. Views of the building model used in the ETABS program are shown in figure 17. An isometric view of the ETABS model, shown in figure 17A, includes the gravity framing in addition to the lateral force framing. A plan view indicating the two basic types of frames and the location of the column lines is shown in figure 17B.

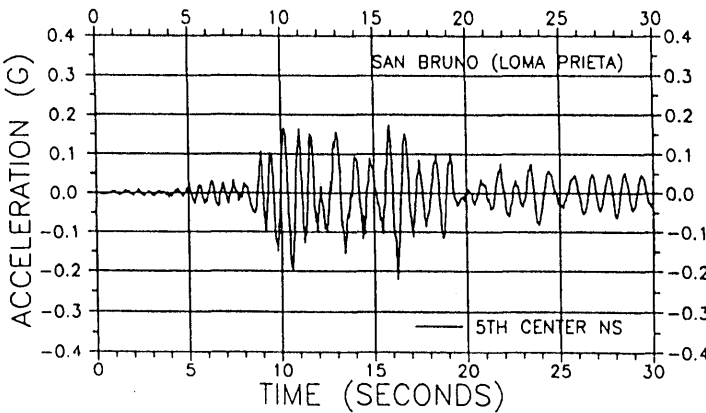


Figure 12.—Recorded acceleration, north-south, fifth level, center.

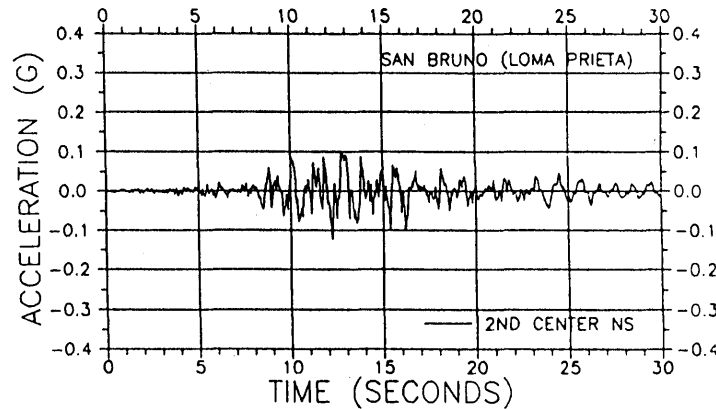


Figure 13.—Recorded acceleration, north-south, second level, center.

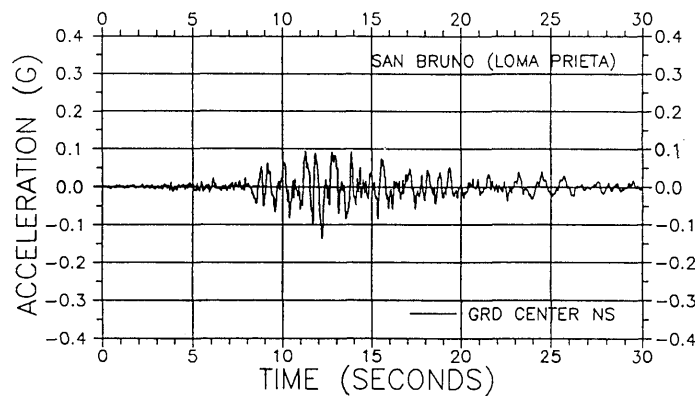


Figure 14.—Recorded acceleration, north-south, base level, center.

The static deflected shape of the building in the longitudinal (north-south) direction obtained using the SAP model with the lateral seismic loads specified in UBC76 is shown in figure 18A. Here it can be seen that the maximum deflection at the roof level is almost 1 inch. A similar plot showing the deflected shape in the transverse (east-west) direction is presented in figure 18B. In this direction the maximum deflection is seen to be 1.3 inches.

The static deflected shapes obtained using the ETABS program and the code lateral loads are shown in figure 19. The deflected shape in the north-south direction is shown in figure 19A and the static deflected shape in the east-west direction is shown in figure 19B. Comparing the results shown in figure 19 with those shown in figure 18 indicates the following: (1) The roof deflection in the longitudinal direction calculated using the SAP90 model

is 0.996 inches and that using the ETABS model is 0.92 inches and (2) the roof deflection in the transverse direction obtained from the SAP90 model is 1.30 inches and that obtained from the ETABS model is 1.23 inches.

ELASTIC DYNAMIC RESPONSE ANALYSES

MODAL PERIOD DETERMINATION

In order to better evaluate the recorded response, spectral analyses were conducted in both the time domain (response spectra) and in the frequency domain (Fourier spectra) in an effort to identify the predominate periods of

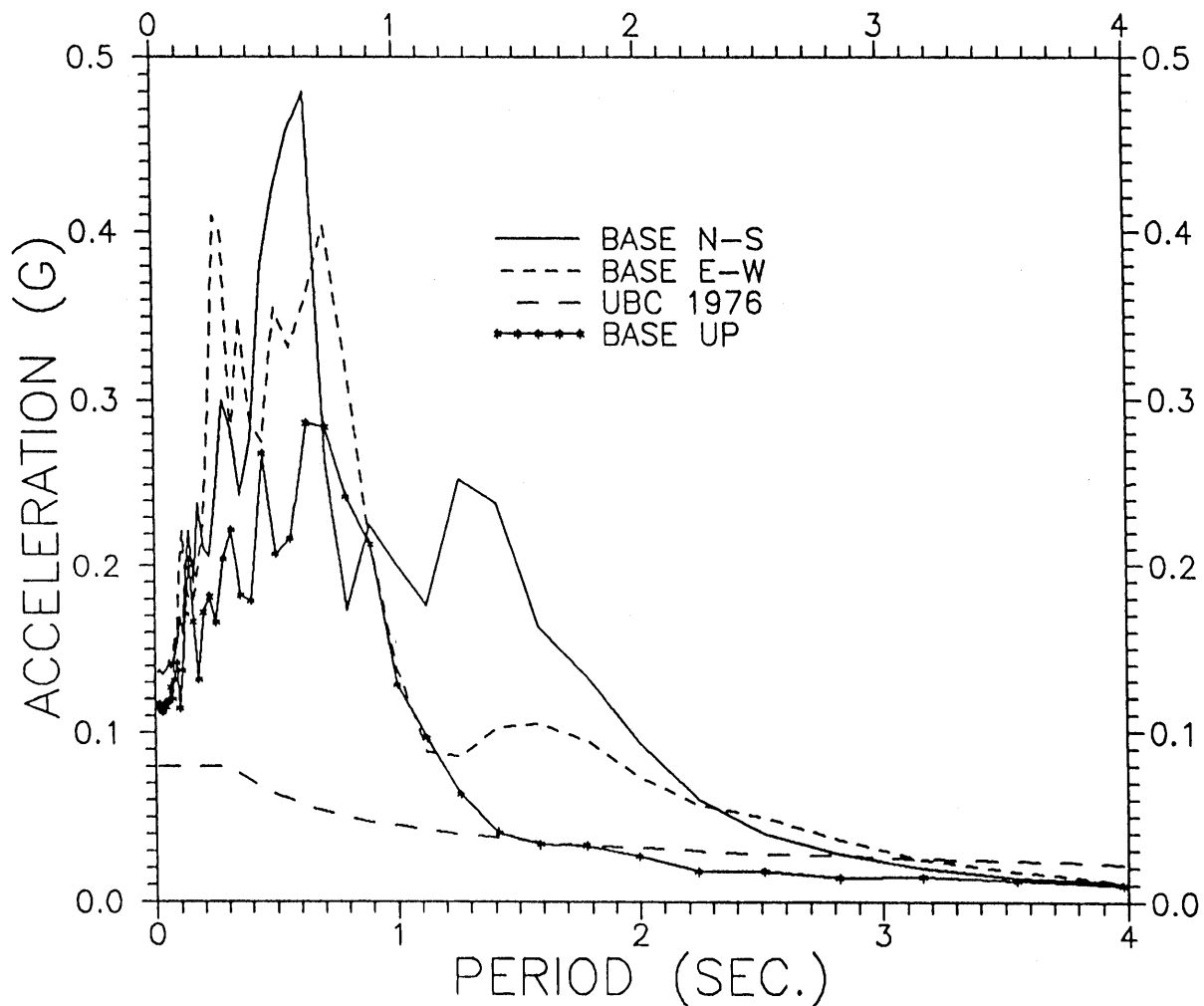


Figure 15.—Spectra of recorded motions vs. code requirement.

vibration. The response spectra are generated by passing the recorded floor accelerations through a single degree of freedom oscillator having 5 percent of critical damping. The Fourier spectra are transfer functions which consider the base input and the floor level output.

Using the three-dimensional analytical models developed for the SAP90 and ETABS programs, the mode shapes and frequencies for the first six modes of vibration were evaluated. Results indicated that these six modes accounted for 95.3 percent of the effective mass in the north-south direction and 94.6 percent in the east-west direction. These analyses indicate that the first mode is a translational mode in the transverse (east-west) direction, the second mode is a translational mode in the longitudinal (north-south) direction and the third mode is a torsional mode. The fourth mode is a second translational mode in the east-west direction, the fifth mode is a second translational mode in the north-south direction, and the sixth mode is the second torsional mode.

The modal periods identified using linear elastic response spectra (LERS) and Fourier transfer functions (FTF) are compared with the modal periods obtained from the mathematical models in table 1. These results show a good correlation between those obtained from the recorded data and those obtained from the analytical models.

MODAL VERIFICATION ANALYSES

In these analyses, the three-dimensional SAP90 model was simultaneously subjected to accelerations recorded in

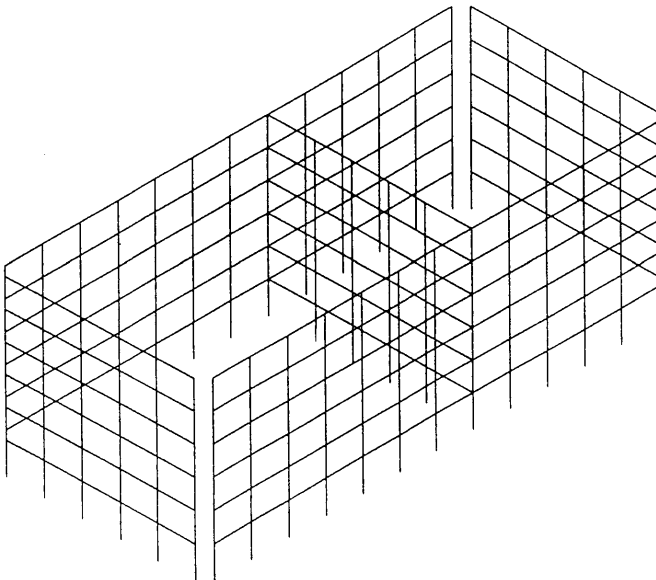


Figure 16.—Lateral force framing system.

the north-south and east-west directions at the base. Time-history comparisons are presented and response spectra are used for a more critical comparison of the recorded and calculated motions. As mentioned previously, the spectra are generated by passing the recorded and calculated accelerations through a single-degree-of-freedom oscillator having 5 percent of critical damping.

The time-history of the accelerations recorded at the roof level in the north-south direction near the center of the building are compared with the calculated values in figure 20A. Here the match with the frequency is quite good; however, the amplitudes of the calculated values tend to exceed the recorded values for a couple of cycles in the 10- to 15-s region of the time-history. The corresponding response spectra are shown in figure 20B. Here it can be seen that the spectra obtained from the calculated accelerations tends to fall above that of the recorded accelerations over much of the period range but the difference is not large.

Similar comparisons in the east-west direction are shown in figure 21. The time histories are shown in figure 21A, where it can be seen that in this direction, the recorded values tend to exceed the calculated values during a couple of cycles in the 10- to 15-s time period. The corresponding spectra are shown in figure 21B where the spectral values for the recorded response tend to fall above the calculated values. A similar pattern to that just described for the roof level is seen in the data for the fifth floor, which is presented in figure 22 (north-south) and figure 23 (east-west), and for the second floor, which is presented in figure 24 (north-south) and figure 25 (east-west).

In general the match between the recorded and calculated values is very good over the complete height of the building. The calculated acceleration amplitudes tend to overestimate the recorded response in the north-south direction and to underestimate the recorded response in the east-west direction. This may be due in part to the fact the exact location of the recording instrument is unknown, and therefore the calculated results may not be at the same location as the recorded results. As noted previously, there appears to be a torsional response in this building, and that may be influencing the comparisons due to the uncertainty of the exact location of the instrument "near the center."

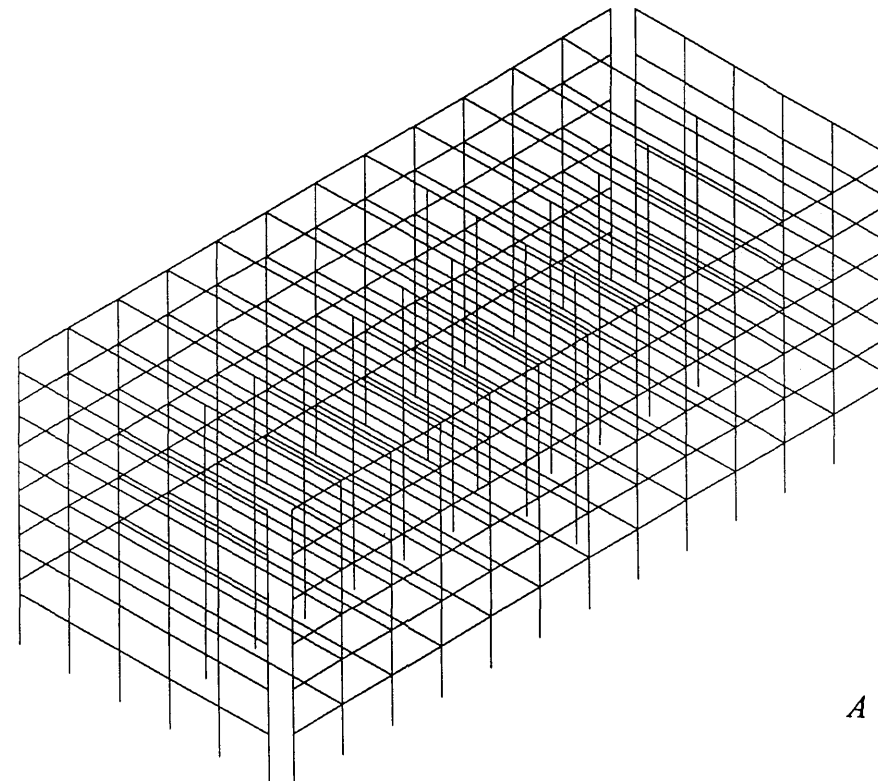
STRONG MOTION ANALYSES

The elastic dynamic behavior of the structure is evaluated by comparing the response to the UBC91 static lateral forces to the time-history demands of the earthquake, which were recorded at the base of the structure, and to the time-history demands of three additional earthquake ground motions. The three ground motions are the following: (1) the north-south component of the ground motion

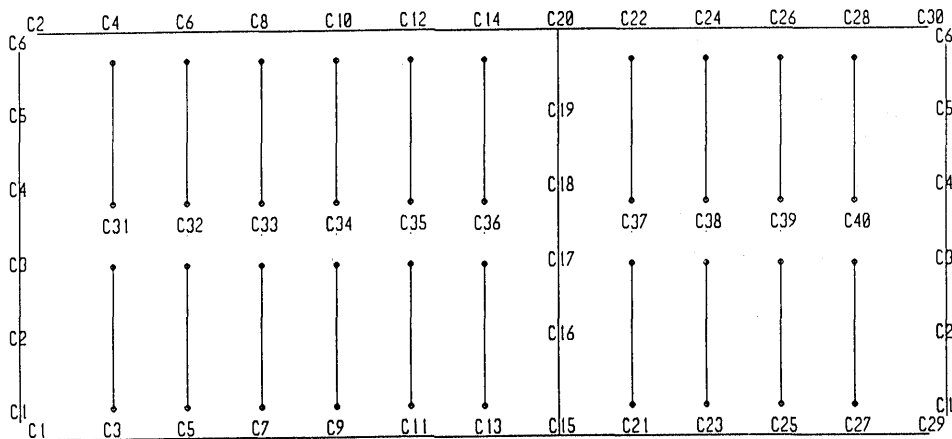
recorded in El Centro (1940), the north-south component of the ground motion recorded at Hollister during the Loma Prieta earthquake (1989) and the S. 45° W. component of the ground motion recorded at James Road during the Imperial Valley earthquake (1979). The acceleration time

histories for these three ground motions are shown in figure 26. Elastic response spectra for these three motions for 5 percent of critical damping are given in figure 27.

Envelopes of maximum response are shown for lateral displacement, interstory drift index, inertia force, and story



A



B

Figure 17.—Gravity and lateral force framing. A, Isometric view; B, plan view.

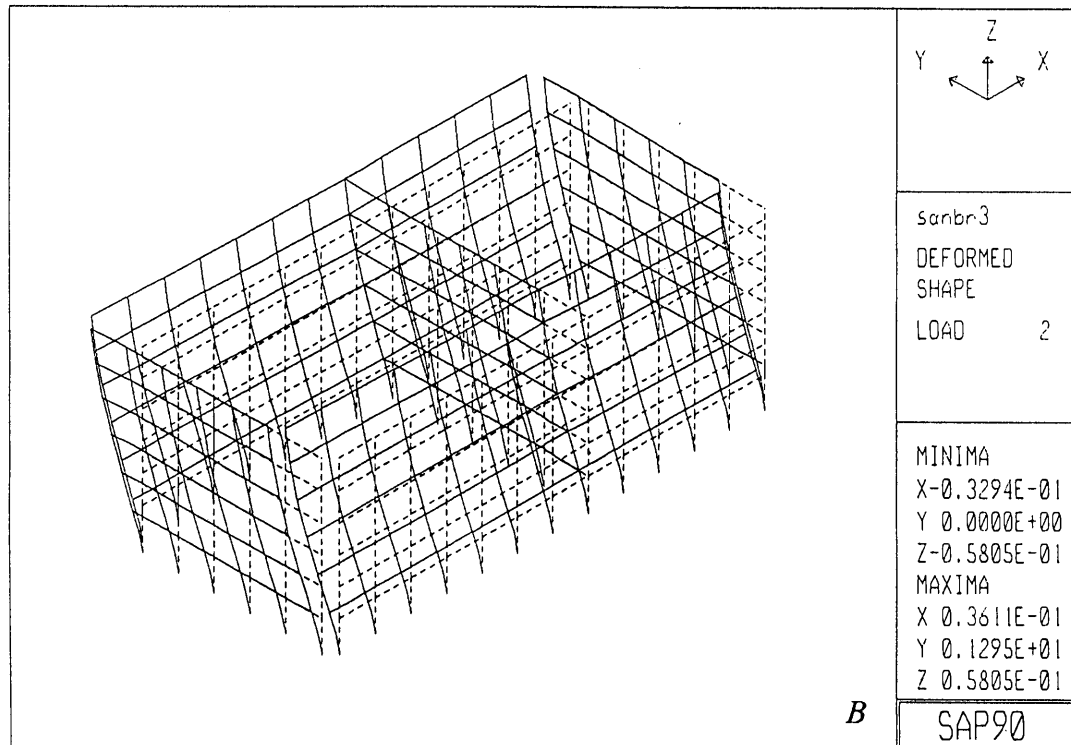
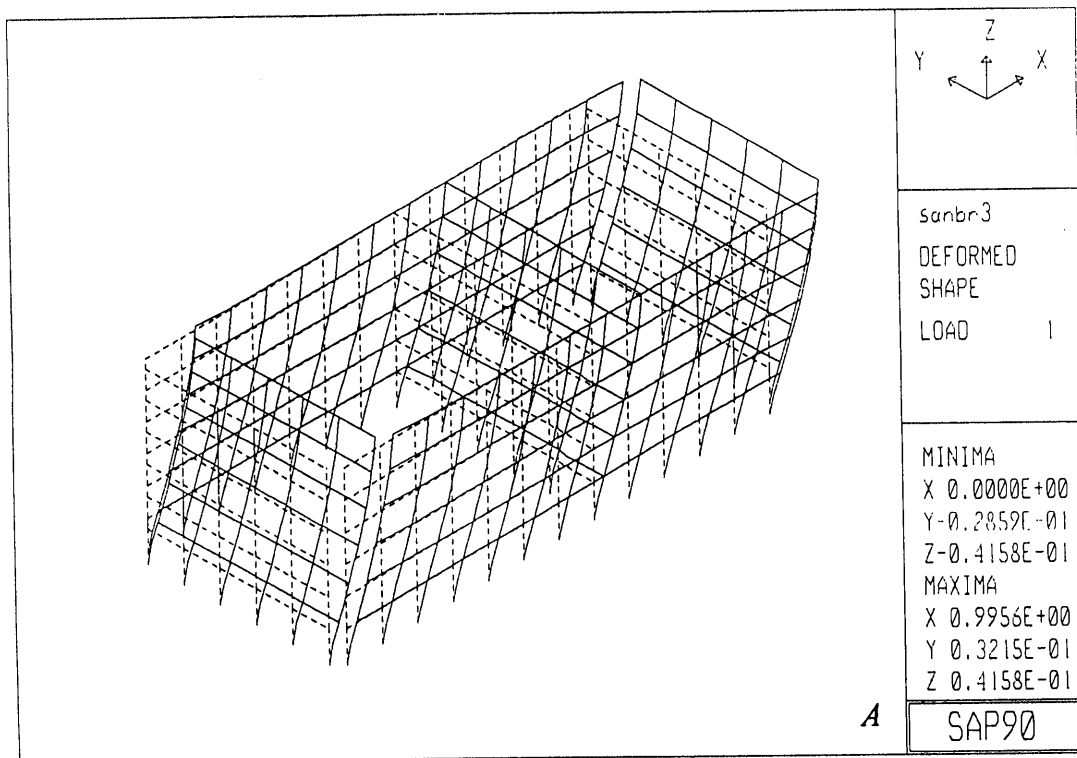


Figure 18.—Static lateral force deflections, SAP90. A, Longitudinal (north-south); B, transverse (east-west).

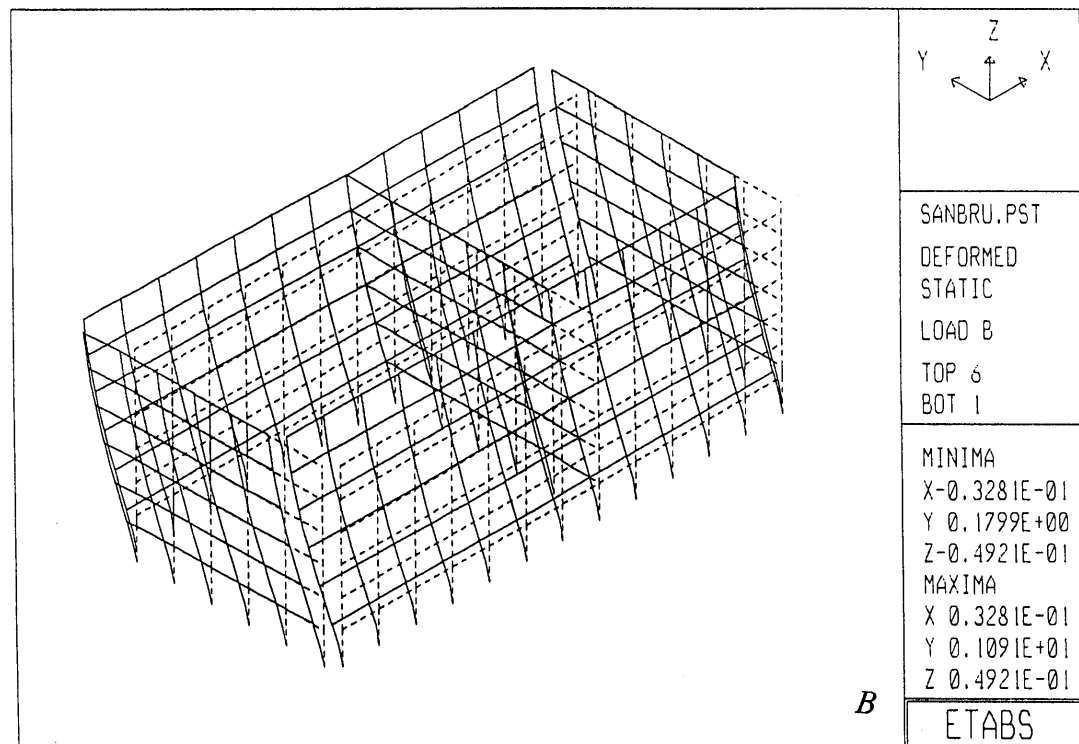
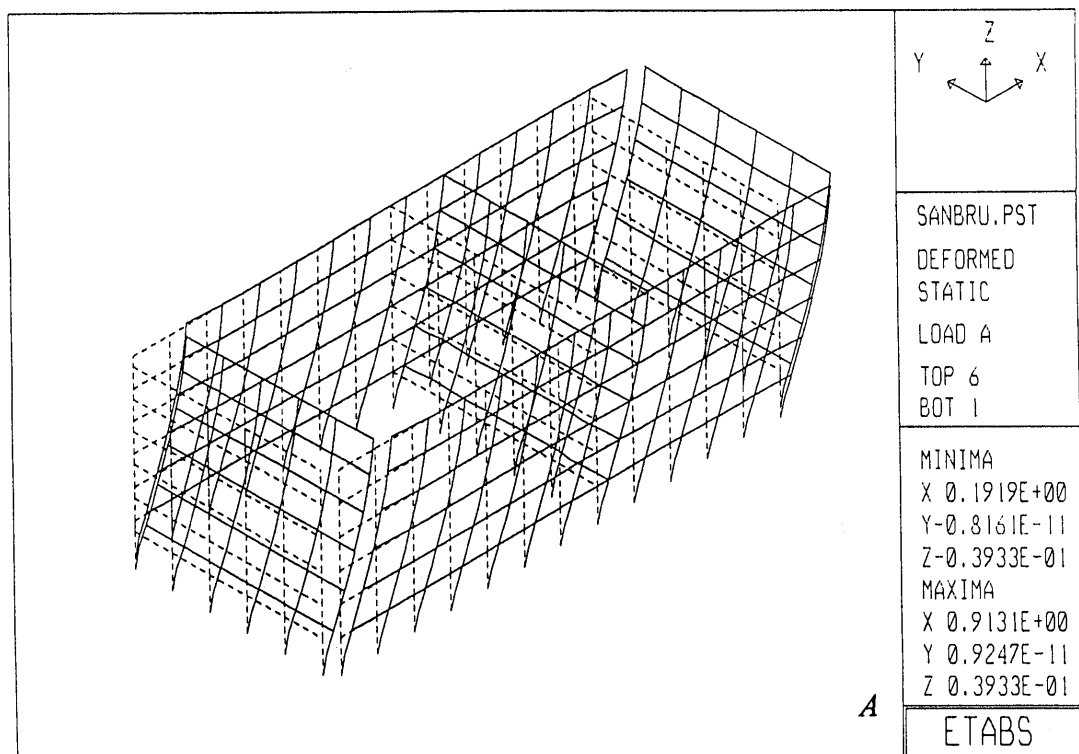


Figure 19.—Static lateral force deflections, ETABS. A, Longitudinal (north-south); B, transverse (east-west).

Table 1.—*Periods of vibrations*

Mode	1	2	3	4	5	6
LERS	1.00	0.90	—	0.30	—	—
FTF	1.05	0.85	0.70	0.34	0.27	—
SAP90	1.06	0.91	0.71	0.34	0.29	0.23
ETABS	1.03	0.89	0.71	0.33	0.29	0.23

shear. Comparisons are made between the static analysis for UBC 1991 lateral forces and the dynamic response analyses for the four earthquake ground motions. The response envelopes in the transverse (east-west) direction are shown in figure 28, and those for the longitudinal (north-south) direction are shown in figure 29.

The envelopes of maximum lateral displacement, shown in figure 28A, indicate that the displacement due to the recorded base motions is 2.35 inches compared to the 0.68 inches due to code loads, a factor of 3.4 larger. The largest displacement is due to the Hollister motion and has a value of 13 inches at the roof. The envelopes of interstory drift index are shown in figure 28B. Under the recorded motion, the maximum drift occurs at the second story level and reaches a value of 0.4 percent; however, a drift of more than 2 percent occurs at the second story level under the Hollister ground motion. This amount of drift would certainly cause damage to both structural and nonstructural components.

The lateral inertia forces specified by the code are compared with those developed during the four time-history analyses in figure 28C. Here it can be seen that the forces developed at the building, based on the recorded base motion, are more than three times larger than those used for the design. In the case of the Hollister ground motion, the forces at the top of the structure are almost 20 times larger than the code values. The envelopes of maximum story shear are shown in figure 28D. Here it can be seen that the story shears developed during the Loma Prieta earthquake are 2.7 times larger than the code values. As in the previous response parameters, the Hollister motion develops a significant increase in the base shear which is 20 times the code values.

The envelopes of maximum lateral displacement in the longitudinal direction are shown in figure 29A. This figure indicates that the displacement under the recorded base motion is approximately three times larger than that produced by the code lateral loads. The largest displacement is due to the Hollister ground motion and has a value of 9 inches at the roof level, 13 times larger than the code

values. Similar data for the interstory drift index is shown in figure 29B. The maximum drift in this direction under the recorded base motion is 0.34 percent at the second story level. Under the Hollister ground motion, this value increases to 1.37 percent.

The envelopes of maximum inertia force are shown in figure 29C. The recorded base motions produce an inertia force at the roof level that is approximately 3.6 times the code value. When the effect of the Hollister ground motion is considered, this value increases to 13 times the code value. The envelopes of maximum story shear, shown in figure 29D, appear very similar to those discussed previously for the transverse direction. However, in this direction, the base shear due to the recorded base motions is 3.7 times the design value.

SUMMARY AND CONCLUSIONS

This study has investigated the dynamic response of a six-story reinforced concrete building which was instrumented with 13 strong motion accelerometers at the time of the Loma Prieta earthquake. The building has a rectangular plan with lateral resistance provided by four moment-resistant frames on the perimeter and one moment-resistant frame on the interior in the transverse direction. Recorded peak accelerations at the base were 0.11 g in the transverse (east-west) direction and 0.13 g in the longitudinal (north-south) direction. Only limited damage was reported as a result of this motion.

Spectral analyses of the recorded acceleration data were used to identify the predominant periods of vibration. Three dimensional, linear elastic models of the building were developed to study the behavior under the recorded base motion and to estimate the effects of stronger ground motions recorded in the free field during previous earthquakes. Comparisons are made between the dynamic responses and the forces and deformations obtained from code prescribed seismic forces.

On the basis of these studies, the following general conclusions are presented:

1. The maximum story shears obtained from the elastic response under the recorded base motions, exceed the code values by 3.7 times in the north-south direction and by 2.7 in the east-west direction. This amount of story shear must have resulted in considerable cracking of the concrete members and may have produced some minor yielding of the main reinforcement.
2. The design resistance coefficient specified by current building codes has been reduced substantially for a building of this type when compared with the value used in the original design in 1977. It is not clear to the investigators how this reduction can be justified.
3. It is clear that the base motions recorded during the earthquake were not strong relative to other recent earth-

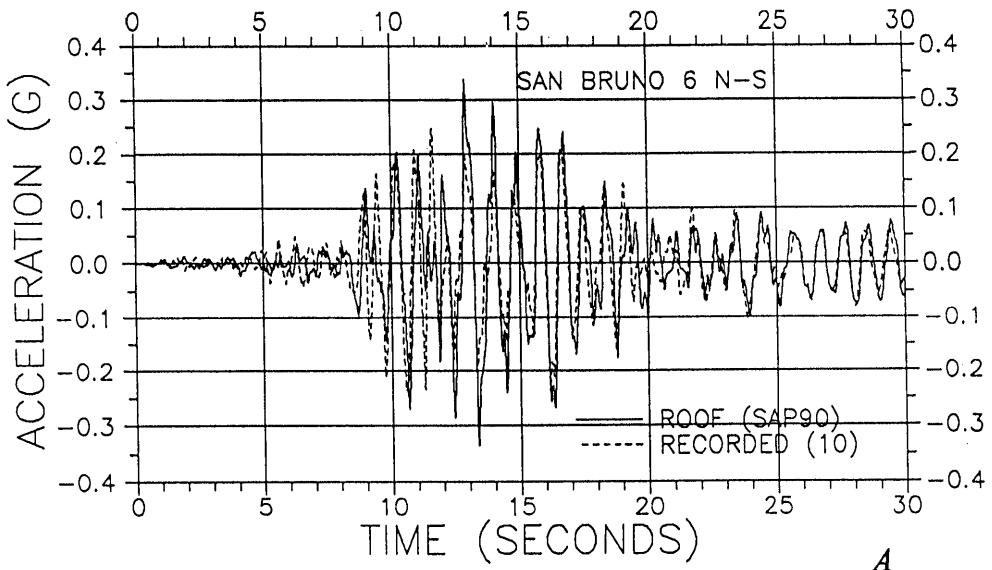
quakes. However, they were still sufficient to drive the structure to the yield level and perhaps a little beyond. Under stronger ground motions, such as those recorded closer to the epicenter at Hollister, the response is much more severe and would have undoubtedly led to severe damage.

4. A static nonlinear analysis needs to be performed on this structure to estimate its lateral force capacity, and nonlinear dynamic analyses need to be done to estimate the ductility and

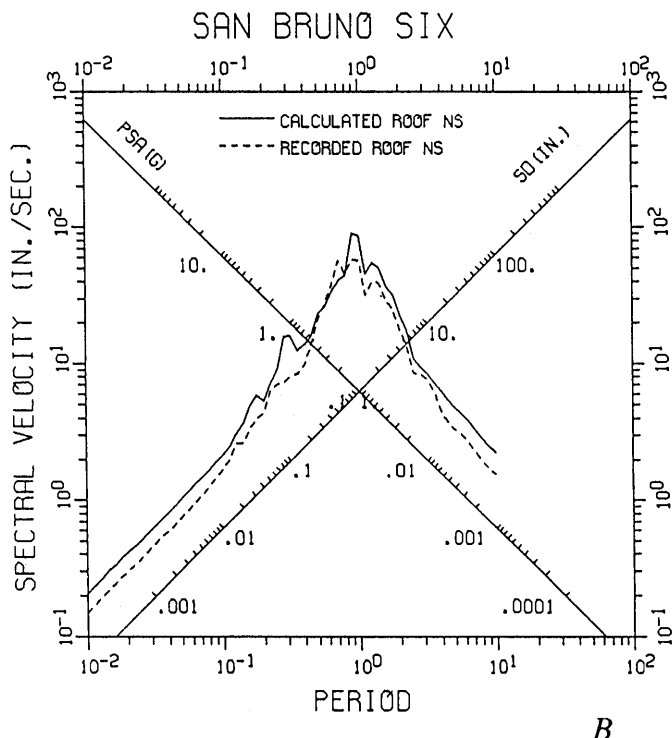
rotation demands of the stronger ground motions. These considerations are discussed in a recent report by the authors (1997).

ACKNOWLEDGMENTS

This report is based on the results of a series of studies that have been conducted by the authors at the



A



B

Figure 20.—Roof response, north-south. *A*, Calculated vs. recorded accelerations; *B*, calculated vs. recorded LERS.

University of California, Berkeley, and the University of Southern California. This study is part of a research project entitled "Implications of Response of Structures to Ground Motions Recorded During the Loma Prieta Earthquake: Evaluation of Structural Response Factors," which was supported by a research grant provided by the National Science Foundation. This support is greatly appreciated.

REFERENCES

- Anderson, J.C., Miranda, E., and Bertero, V.V., 1991, Evaluation of seismic performance of a thirty-story RC building: Report No. UCB/EERC-91/16, Earthquake Engineering Research Center, University of California, Berkeley.
- Anderson, J.C., and Bertero, V.V., 1997, Seismic performance of a six story reinforced concrete building: Report No. UCB/EERC-93/01, Earthquake Engineering Research Center, University of California, Berkeley.

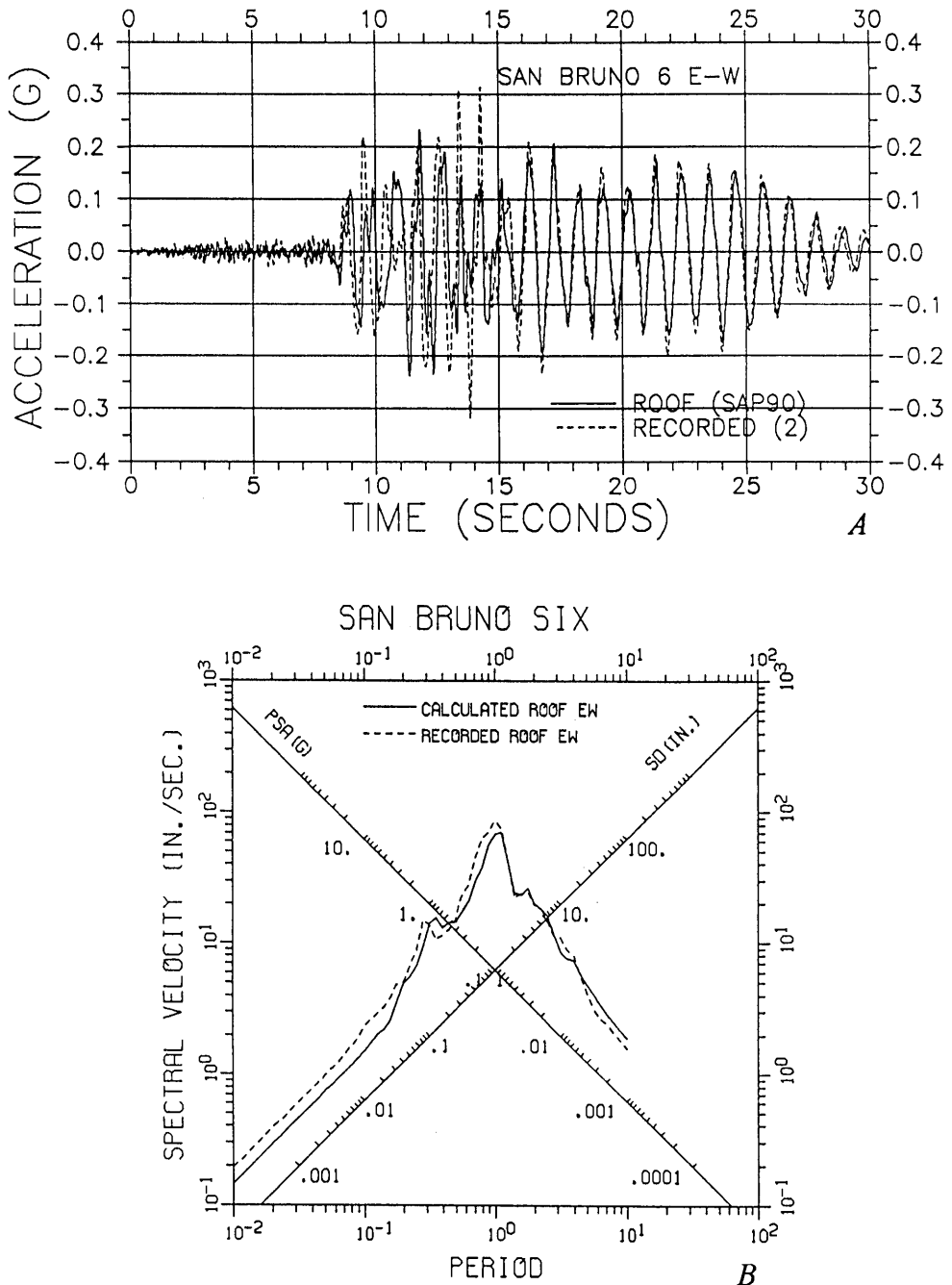


Figure 21.—Roof response, east-west. A, Calculated vs. recorded accelerations; B, Calculated vs. recorded LERS.

- Bertero, V.V., Anderson, J.C., Krawinkler, H., and Miranda, E., 1991, Design guidelines for ductility and drift limits: review of the state-of-the-practice and state-of-the-art on ductility and drift-based earthquake resistant design of buildings: Report No. UCB/EERC 91/15, Earthquake Engineering Research Center, University of California, Berkeley.
- California Division of Mines and Geology, CSMIP strong-motion records from the Santa Cruz Mountains (Loma Prieta) California earthquake of October 17, 1989: Report OSMS 89-06.
- Habibullah, A., 1989, ETABS three dimensional analysis of building systems: User's manual: Computers and Structures, Inc., Berkeley,

- Calif.
- International Conference of Building Officials, 1976, Uniform Building Code [1976 Edition]: Whittier, Calif.
- International Conference of Building Officials, 1991, Uniform Building Code [1991 Edition]: Whittier, Calif.
- U.S. Geological Survey, 1989, Strong motion records from northern California (Loma Prieta) earthquake of October 17, 1989: U.S. Geological Survey Open-File Report 89-568.
- Wilson, E.L., and Habibullah, A., 1989, SAP90, A series of computer programs for the static and dynamic finite element analysis of structures: User's manual: Computers and Structures, Inc., Berkeley, Calif.

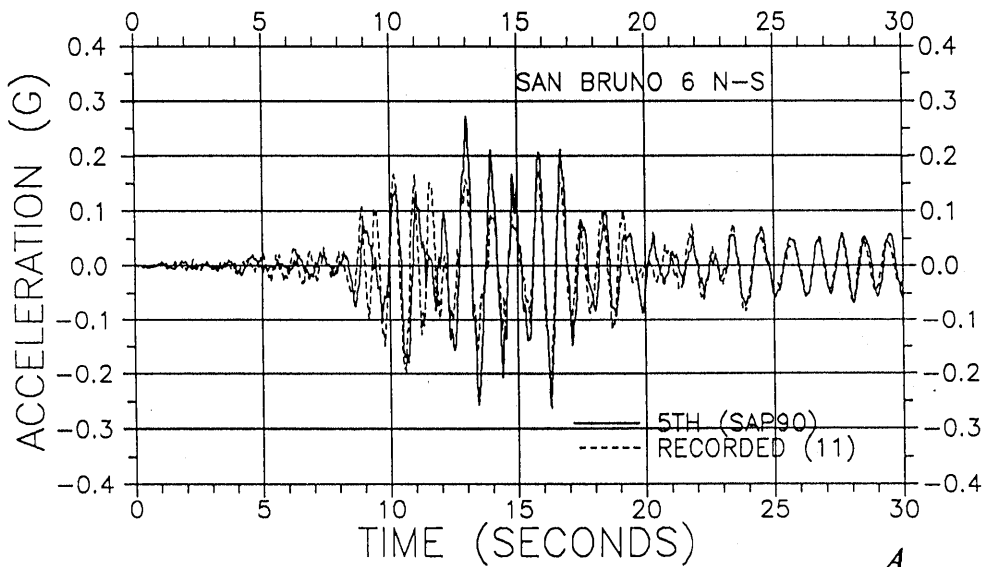
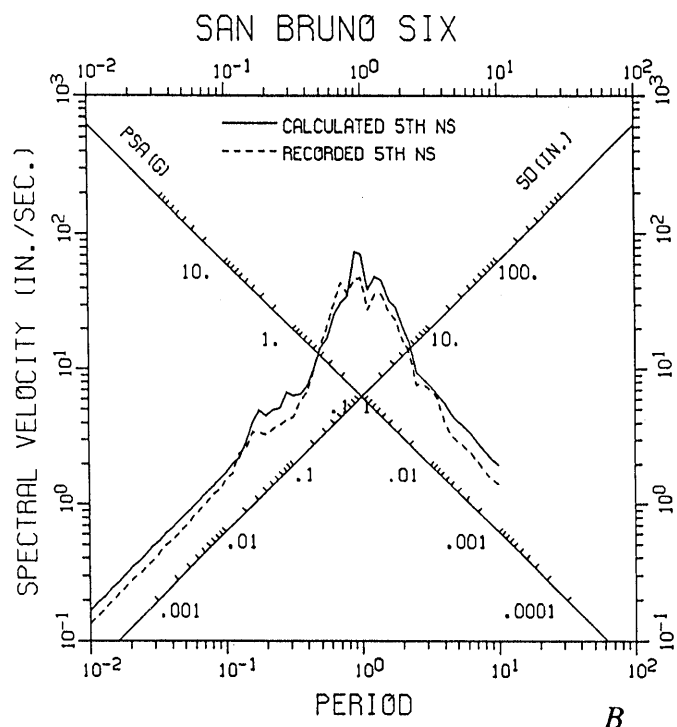
*A**B*

Figure 22.—Fifth floor response, north-south. *A*, Calculated vs. recorded accelerations; *B*, calculated vs. recorded LERS.

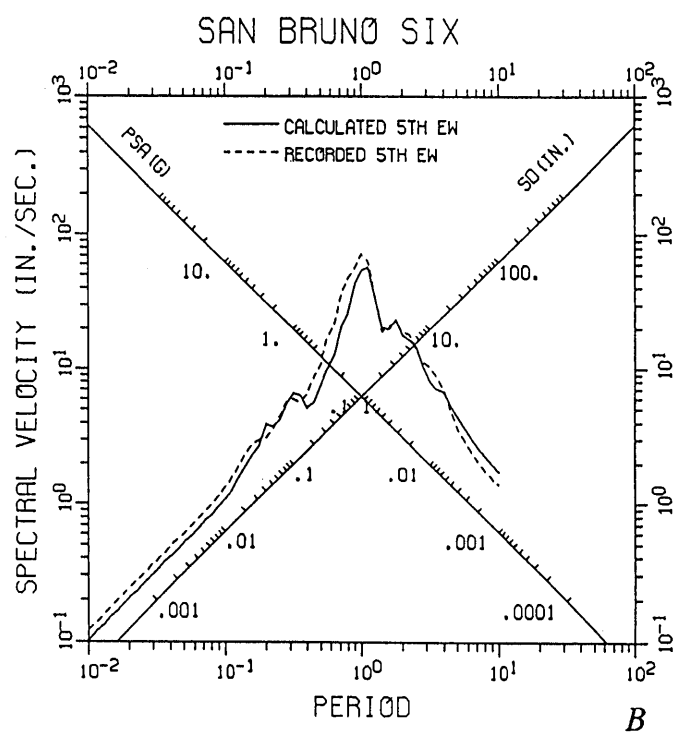
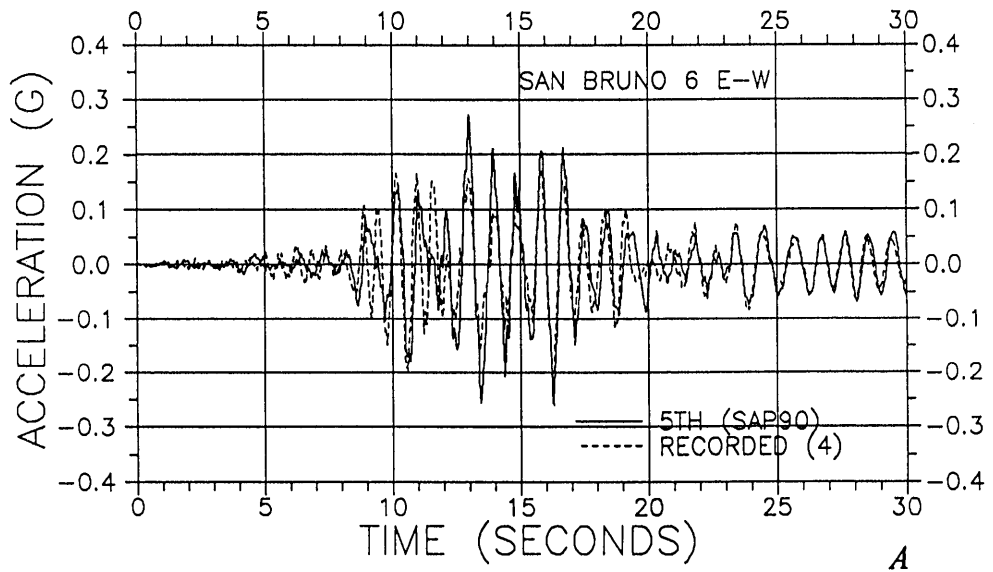


Figure 23.—Fifth floor response, east-west. A, Calculated vs. recorded accelerations; B, calculated vs. recorded LERS.

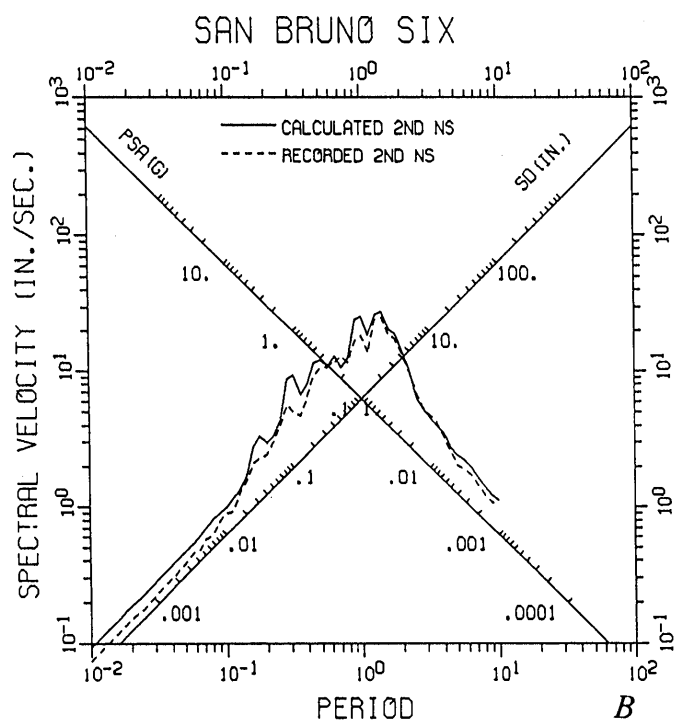
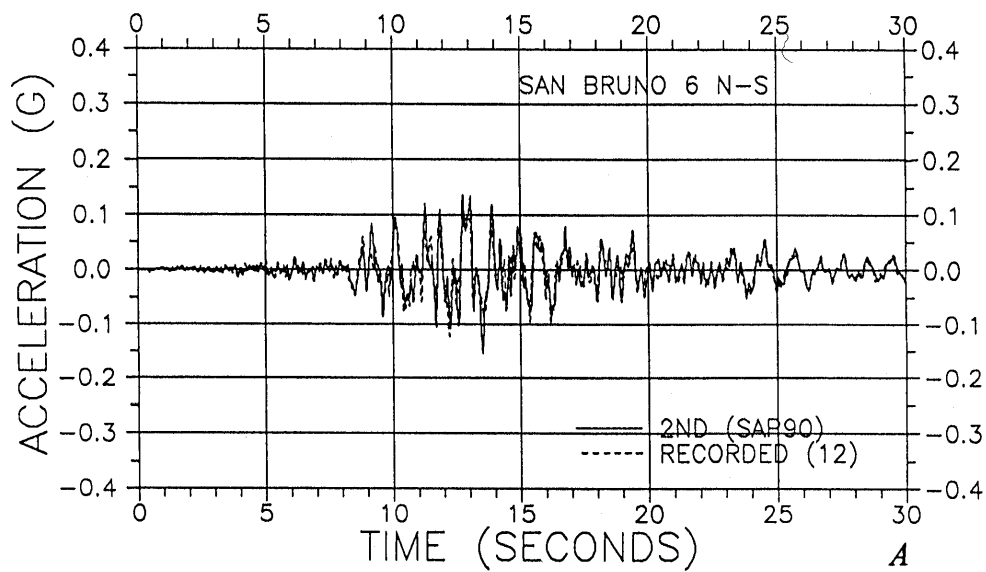


Figure 24.—Second floor response, north-south. A, Calculated vs. recorded accelerations; B, calculated vs. recorded LERS.

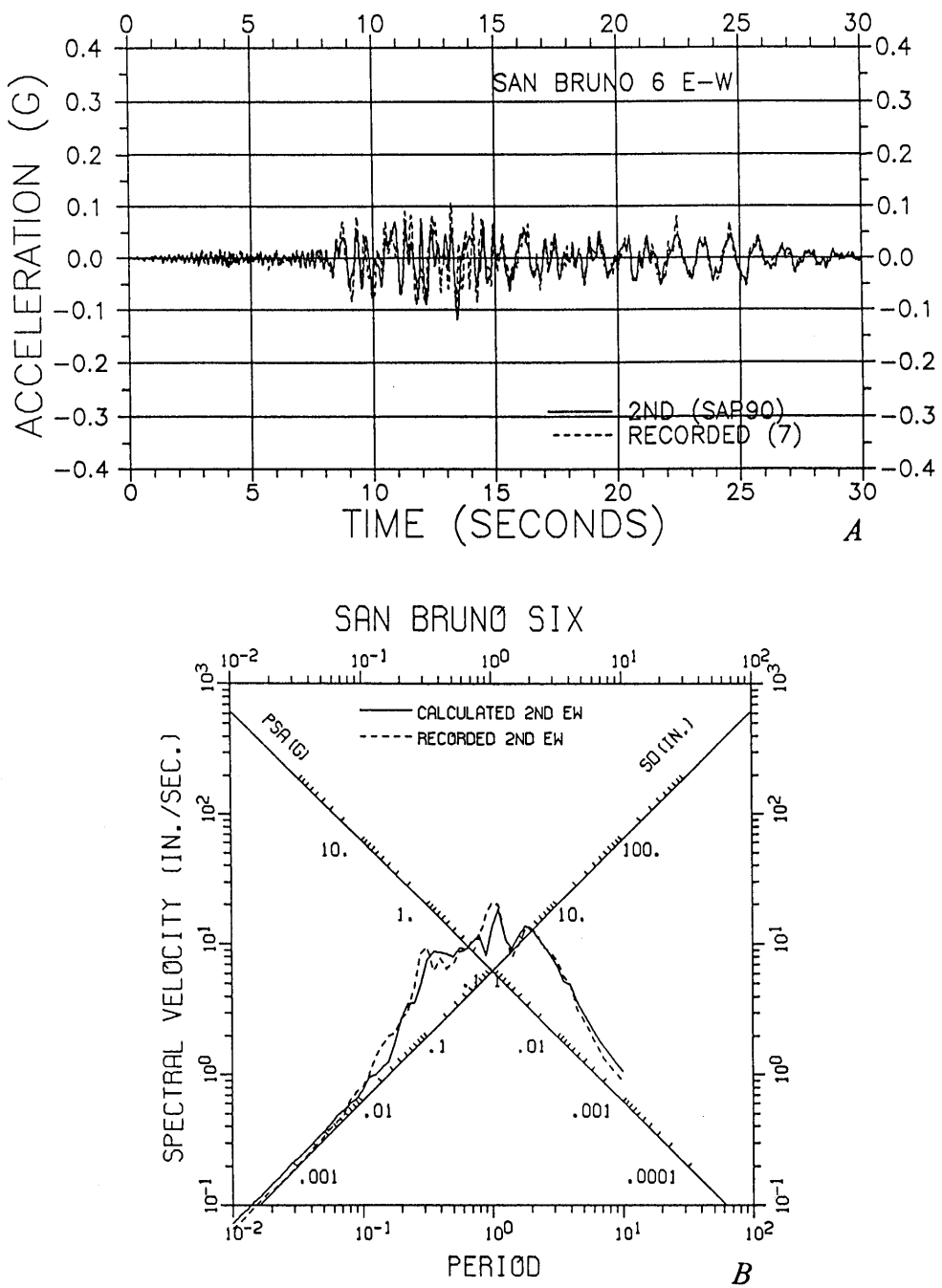


Figure 25.—Second floor response, east-west. A, Calculated vs. recorded accelerations; B, calculated vs. recorded LERS.

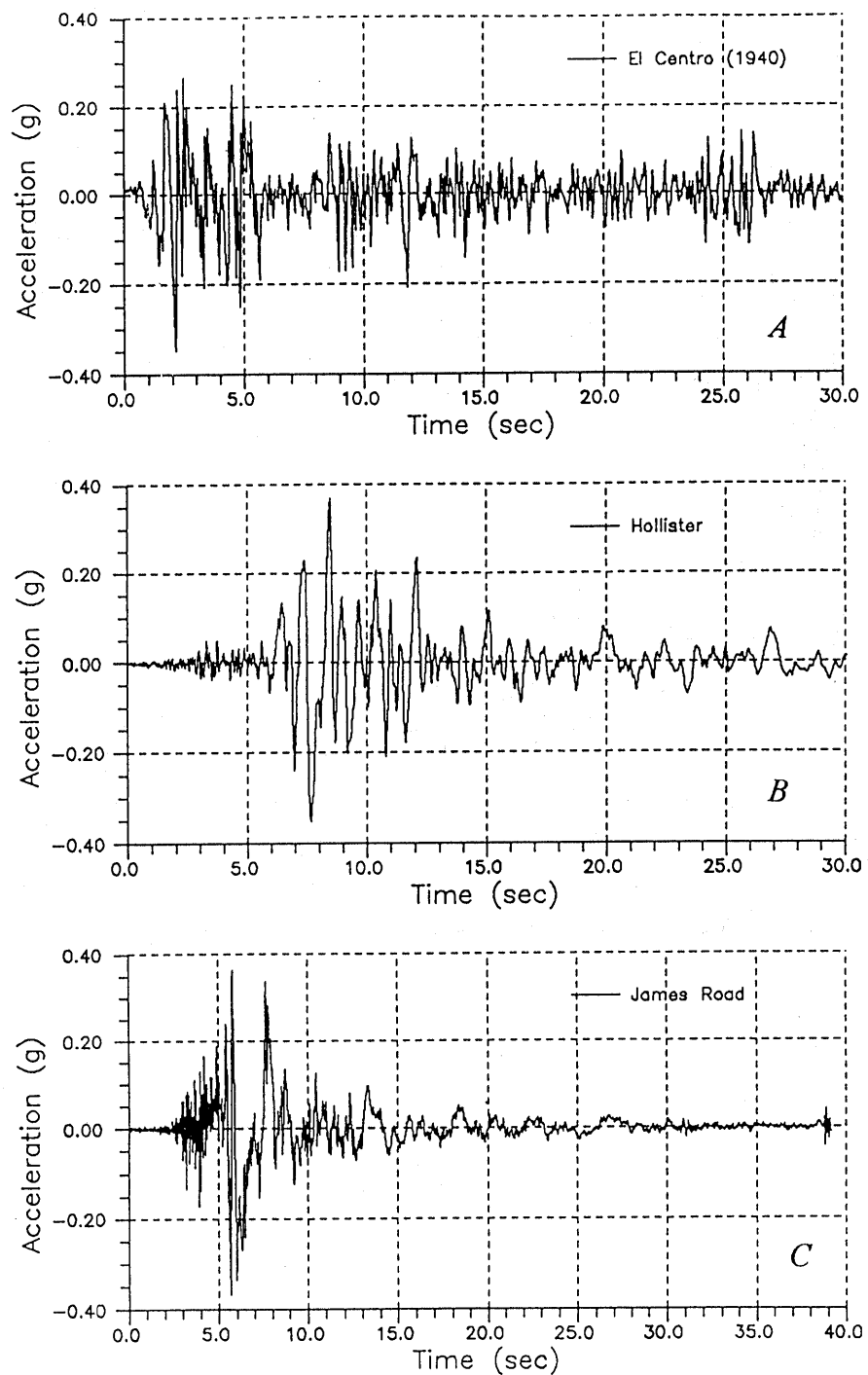


Figure 26.—Recorded free field ground motions. A, *El Centro*, 1940; B, Hollister, 1989; C, James Road, 1979.

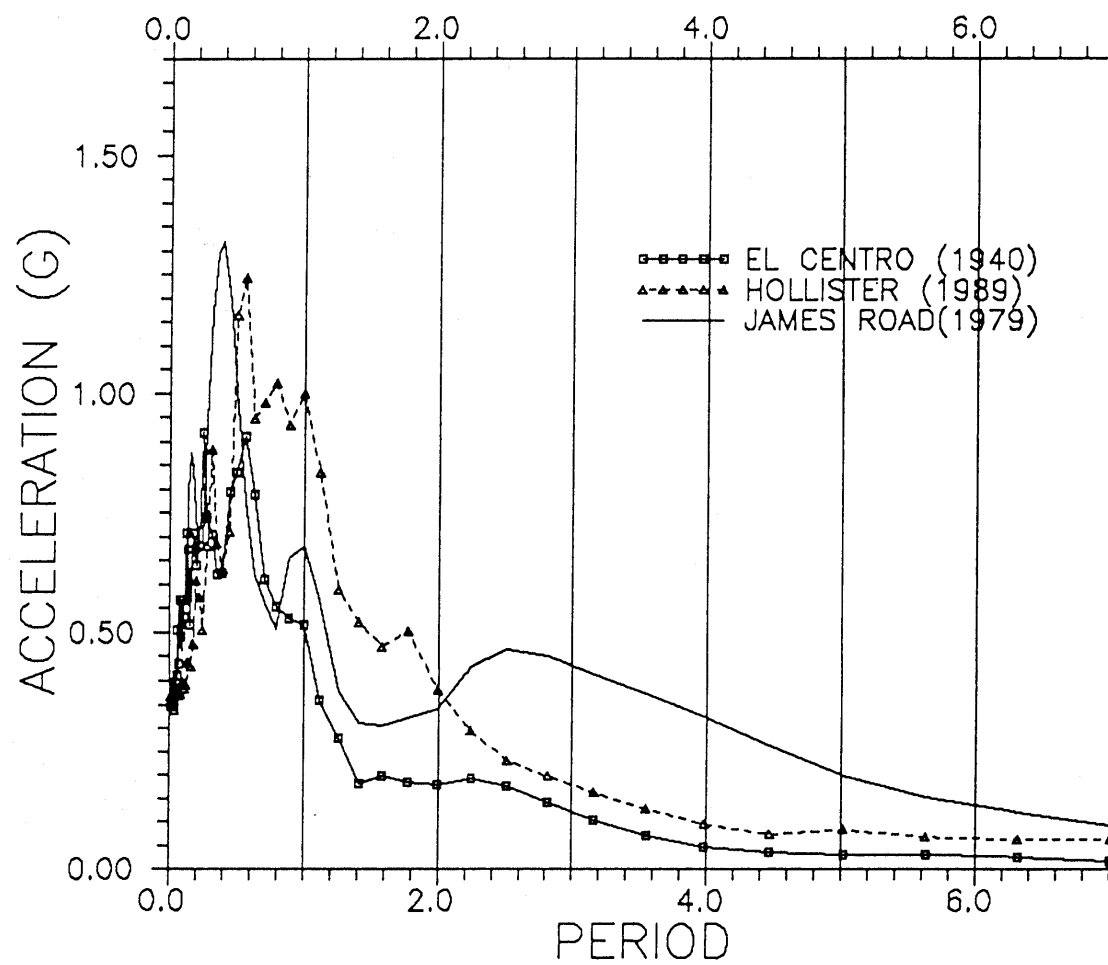


Figure 27.—Spectra of free field motions. A, El Centro, 1940; B, Hollister, 1989; C, James Road, 1979.

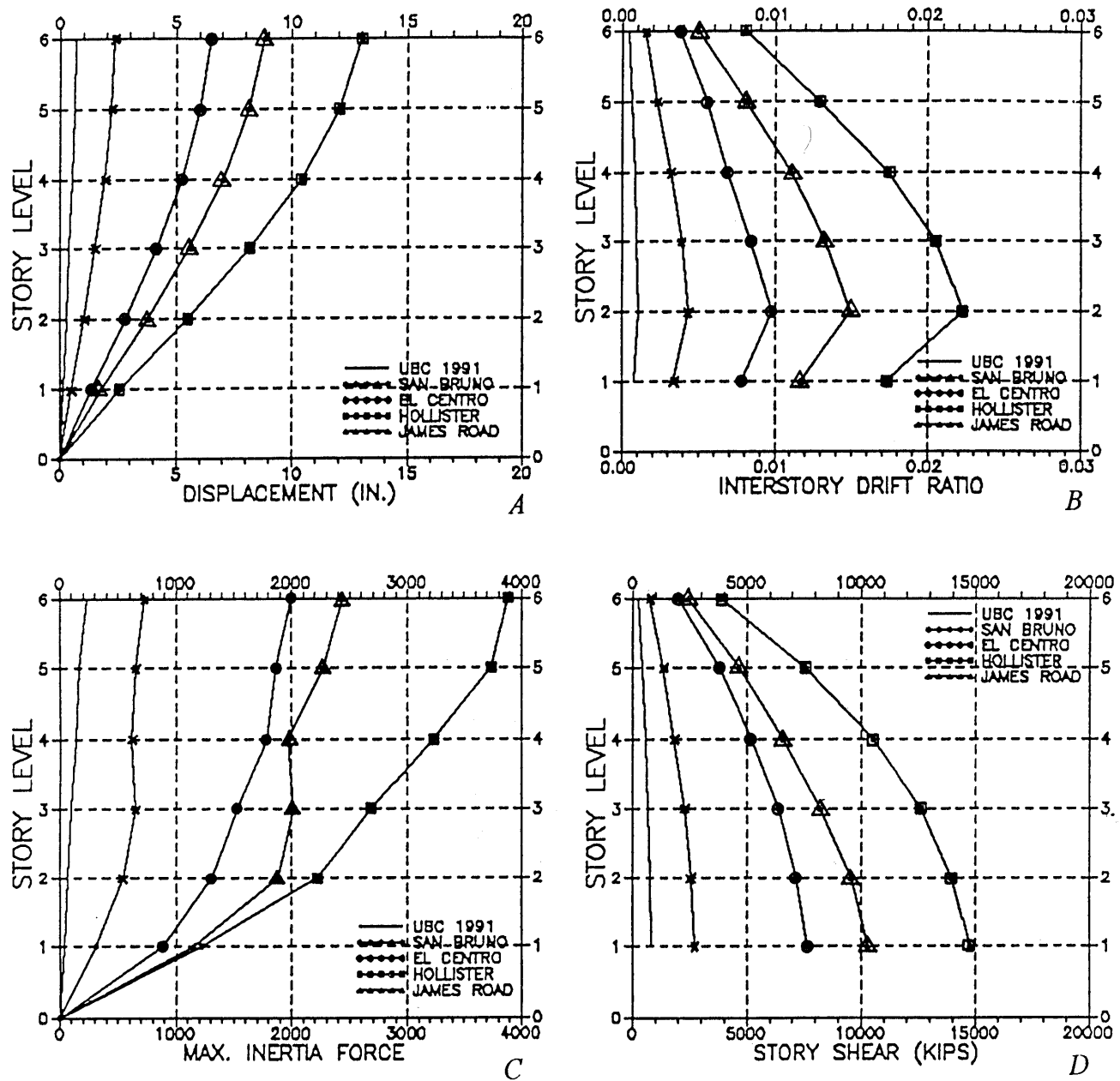


Figure 28.—Maximum response envelopes, transverse. A, Lateral displacement; B, interstory drift index; C, inertia force; D, story shear.

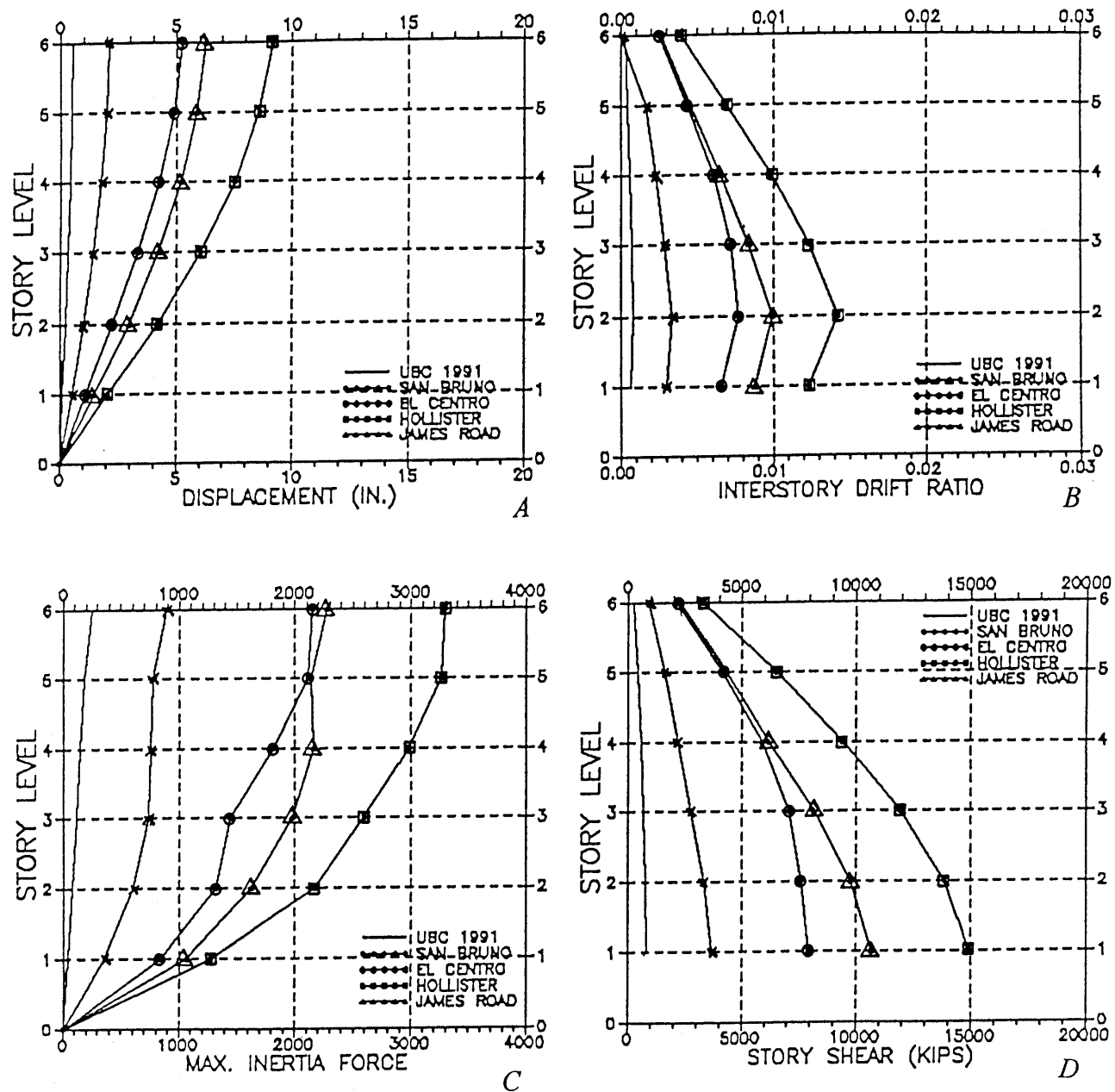


Figure 29.—Maximum response envelopes, longitudinal. A, Lateral displacement; B, interstory drift index; C, inertia force; D, story shear.

**THE LOMA PRIETA, CALIFORNIA, EARTHQUAKE OF OCTOBER 17, 1989:
PERFORMANCE OF THE BUILT ENVIRONMENT**

BUILDING STRUCTURES

SEISMIC RESPONSE OF A 42-STORY STEEL BUILDING

By James C. Anderson,
University of Southern California; and
Vitelmo V. Bertero,
University of California at Berkeley

CONTENTS

	Page
Abstract -----	C113
Introduction -----	113
Objectives -----	114
Building system and instrumentation -----	114
Seismic design criteria -----	115
Mathematical models for elastic response -----	116
Dynamic characteristics -----	118
Analytical model verification -----	118
Input energy -----	124
Modal response contribution -----	125
Stress check -----	126
Elastic response analyses -----	127
Current code design requirements -----	134
Earthquake damage potential -----	136
Conclusions -----	138
Acknowledgments -----	139
References -----	139

ABSTRACT

An instrumented 42-story steel moment resisting space frame located in San Francisco is analyzed in detail. The building was instrumented with 14 strong-motion accelerometers deployed throughout the structure at the time of the earthquake. Inspection of the building following the earthquake did not reveal any damage. Critical comparisons are made between recorded response, calculated response, seismic design criteria, and code lateral force requirements. The response of the building to other more critical ground motions is also investigated.

Results indicate that the response of this building during the earthquake was entirely linear elastic. The building designers opted to use a site-specific design spectrum that was more conservative than the code minimum requirements. However, the study indicated that there may be considerable uncertainty in developing site-specific design spectra for soil sites. It also indicated that for this tall building, the higher vibration modes have a significant effect on the building response. Use of the code design procedure, which requires scaling of the design

spectrum based on the calculated base shear, may lead to unconservative design forces in the upper stories of tall buildings due to the effects of the higher modes on the shear distribution over the height. Use of the minimum code design requirements for the design of this building would have resulted in increased damage potential under service-level earthquakes such as the one experienced by this structure.

INTRODUCTION

It has been noted that most human injury and economic loss due to moderate or severe earthquake ground motions are caused by failures of civil engineering facilities, particularly buildings, many of which were presumably designed and constructed to provide protection against such events. Building codes specify minimum lateral-force requirements, which represent the inertia forces that develop in the structure during ground shaking. Economic considerations usually dictate that these minimum lateral forces, which are predicated on the concept of life safety, become the structural design forces. The relatively high economic loss incurred from the earthquake has created a renewed interest in a two-level design criteria in which damage control under moderate ground shaking is considered along with life safety under strong ground motion.

In order to improve the design criteria used for the design of new construction and the seismic upgrading of existing structures, it is necessary to accurately predict the dynamic behavior of such facilities when they are subjected to seismic excitations that can be expected to occur during their service life. Once this is done, the lateral forces determined from current building codes can be compared with those which develop in the structure during actual earthquakes.

In order to evaluate the accuracy of the seismic provisions of current building codes, it is necessary to compare the results obtained using current analytical methods with the results of large-scale experiments. The best large-scale experiment occurs when instruments located in a structure

reliably measure the building response to the ground motions recorded at the base during an actual earthquake. The Loma Prieta earthquake produced records of strong ground motion in more than 46 well-instrumented buildings. This collection of data included the strong motion recorded in the 42-story steel building which is the subject of this study.

OBJECTIVES

The main objectives of this study are the following: (1) to evaluate the accuracy of current analytical modeling techniques for determining the dynamic response of a tall building; (2) to estimate the damage that the reference building may have experienced under recorded ground motions; (3) to estimate the response of the building under critical ground motions to which it may be exposed during its service life; (4) to evaluate the reliability of the seismic design criteria with respect to recorded response and code requirements; (5) to evaluate the influence of modeling discretizations on the computed response; and (6) to assess the implications of the obtained results regarding the reliability of present seismic code requirements for the design of such buildings.

In order to achieve these objectives, three-dimensional analytical models were developed and linear elastic dynamic analyses were conducted using the recorded base motions for the Loma Prieta earthquake and recorded free-field motions for other strong motion earthquakes. Results are presented in terms of response spectra, time-history-response comparisons and maximum response envelopes, which include lateral displacement, interstory drift index, inertia forces, and story shears.

BUILDING SYSTEM AND INSTRUMENTATION

The 42-story building is a 550-foot-tall office building located in the financial district of San Francisco. The structure has a rectangular plan (79 by 151 ft) with a steel superstructure which can be classified as a special moment-resistant space frame. The building, which was designed in 1972, uses rolled W sections and built-up members of A36 steel for the beams and girders which have typical spans of 27 feet. Welded box sections fabricated from A572 Grade 42 steel in the bottom 33 floors and A36 steel in the upper floors are used for the columns. The box sections vary from 20 by 20 inches to 26 by 26 inches with wall thickness that varies from $1/2$ to $3/8$ inches. Internal stiffeners, equal in thickness to the thickness of the girder flange are used where girders deeper than 30 inches frame into the column. The beams and

girders are connected to the column by full-penetration welds at the top and bottom beam flanges, and the beam web is bolted to the face to the column with a shear plate.

The building is supported on 491 precast concrete piles which are 16 inches square. Pile groups consisting of 13 to 25 piles are located under the 29 column lines. Pile groups are capped by concrete pile caps which are 78 to 84 inches thick. The 29 pile groups are interconnected by concrete tie beams which are typically 24 by 27 inches. An isometric view of the three-dimensional computer model of the building used for the elastic analyses is shown in figure 1.

At the time of the earthquake, the building was instrumented with 14 strong-motion accelerometers located at the base, ground, 25th, 34th, and 42d levels. Each of these levels included a longitudinal and transverse component

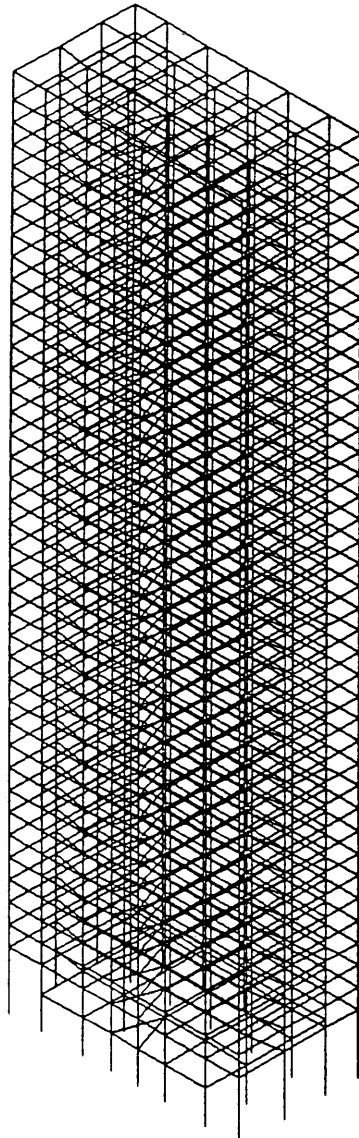


Figure 1.—Schematic plan of 42 story building.

located at the geometric center of the tower. In addition the base included a vertical component, and the 25th, 34th, and 42d floors included a transverse component at the end of the tower. Unfortunately, no vertical-motion accelerometers are located in the building, which would have permitted the effect of vertical ground motion to be evaluated. The location of the instrumentation is summarized in figure 2.

SEISMIC DESIGN CRITERIA

The building was designed in 1972 for the requirements of the building code for the City and County of San Francisco (CCSF). At that time, the code lateral-force requirement for this building was an equivalent static loading

which was defined in terms of the base shear. Lateral forces defined in terms of the base shear have the general form

$$V = C_s W_e$$

where C_s is the design seismic resistance coefficient and W_e is the total seismic dead load, which for an office occupancy is equal to the total dead load, W . At the time the building was designed, the CCSF code required a design base shear given by the expression

$$V = (KC)W$$

where $K = 0.67$, $C = 0.05/(T)^{1/3}$ and $T = 0.1N$ where N is the number of stories. Using N equal to 42 gives an estimate of the period (T) of 4.2 s. Using this estimate, C

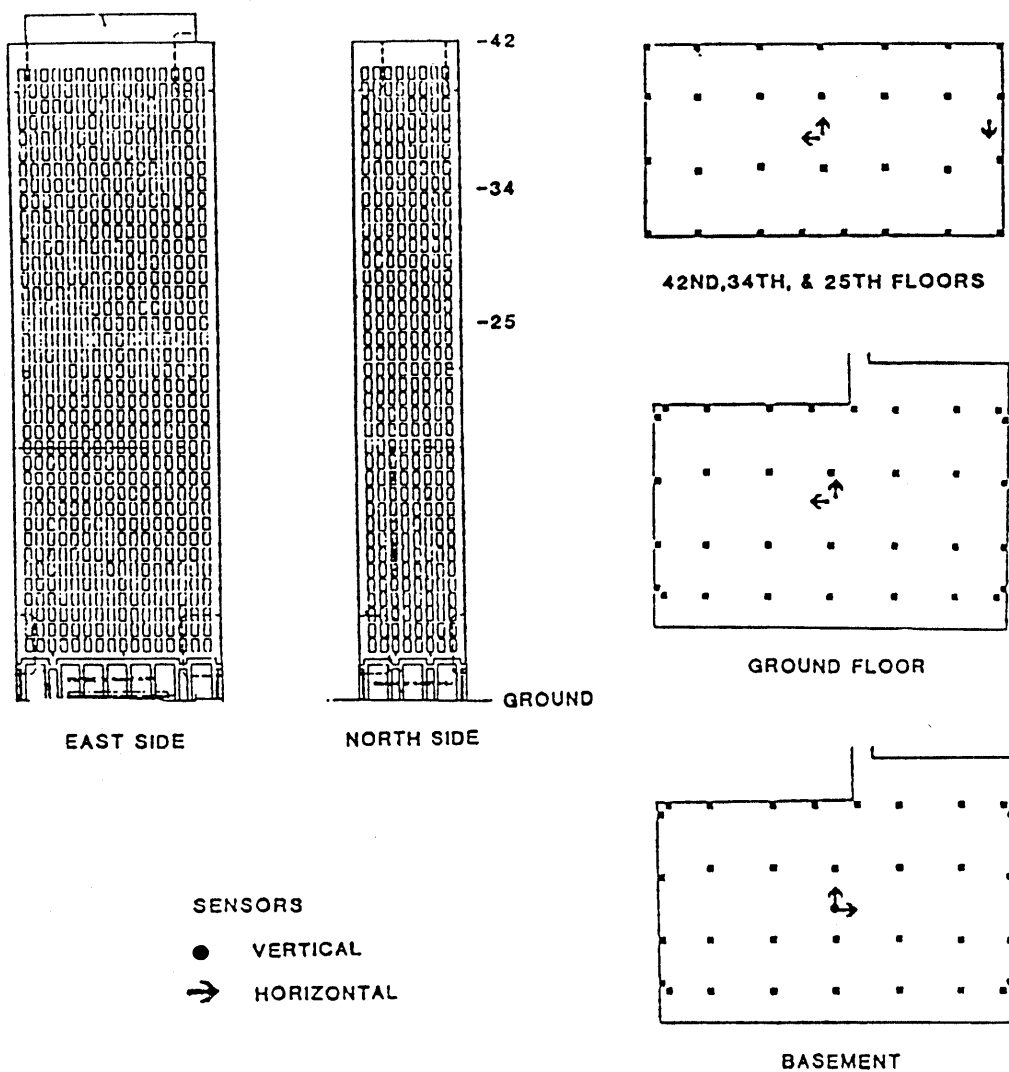


Figure 2.—Instrument locations in building.

becomes 0.031 and results in a design seismic resistance coefficient (C_s) of 0.021, or 2.1 percent of the total dead load. With the total dead load estimated to be 62,473 kilopounds (kips), the base shear required by the 1972 CCSF code would have been 1,312 kips.

In addition, the owner and the structural engineer decided to use a site-specific design spectrum and a dynamic analysis to determine the lateral design forces. The design criteria required that the structural frame should withstand the lateral forces due to the base design spectrum with stresses less than the yield stress. The design earthquake was specified as having an effective peak acceleration on rock of 0.2 g , which was considered representative of an $M=7$ earthquake on either the San Andreas or Hayward fault systems. This design earthquake led to the development of a site-specific spectrum representative of rock motions. The rock spectrum was further modified to reflect the effect of local soil conditions using the methods suggested by Ruiz and Penzien (1969). This led to the development of the base design spectrum (fig. 3) which was used for the design of the structure. The use of this spectrum resulted in design base shears of 3,469 kips longitudinal (north-south) and 3,996 kips transverse (east-west). It must be recognized that the CCSF code

requirements are based on allowable stresses, whereas the design spectrum is based on yield stresses.

MATHEMATICAL MODELS FOR ELASTIC RESPONSE

Detailed three-dimensional finite-element models of the building were developed in order to evaluate the response to the two horizontal components of ground motion recorded at the base. Several computer programs are currently available on a commercial basis for analyzing the elastic dynamic response of three-dimensional structures using a personal computer. The SAP90 program developed by Wilson and Habibullah (1989) was selected for use in the initial phase of this study for the following reasons: (1) An extended memory version, SAP90 Plus, was available which permitted modeling the structure in detail for computation on a personal computer and (2) the program allows the user to plot the time-history response at any node point. This feature was crucial for comparison of the calculated results with the recorded response.

The completed SAP90 model of the structure consisting of 1,260 nodes, 3,116 elements, and 3,690 degrees of

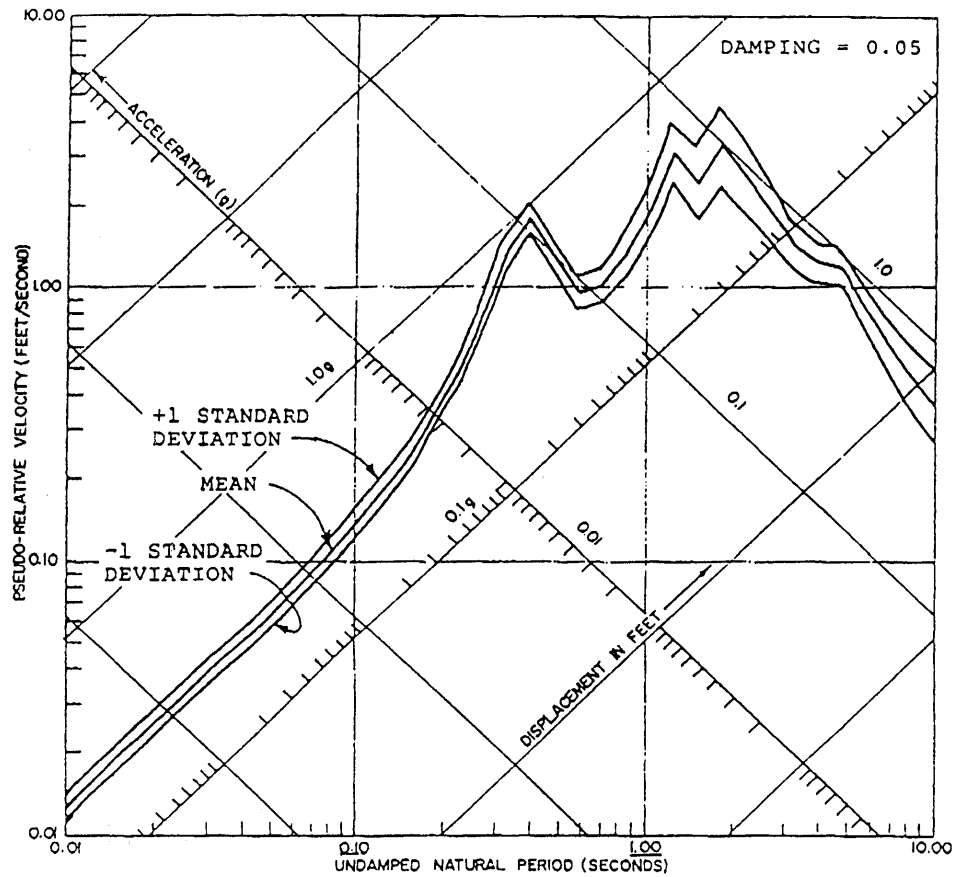


Figure 3.—Site specific design spectra for building.

freedom is shown in figure 4. An overall isometric view is shown in figure 4A and a plan view is shown in figure 4B. This view shows that the structure is symmetrical about the transverse axis but has some nonsymmetry in the stiffness about the longitudinal axis. An elevation view in the transverse (east-west) direction is shown in figure 4C and an elevation view in the longitudinal (north-south) direction is shown in figure 4D.

A second three-dimensional model of the building was developed for use with the ETABS-Plus program, which

is also discussed by Habibullah (1989). This model was used for making comparisons between the earthquake response and the building code requirements in terms of lateral displacement, interstory drift, lateral force, and story shear. It was also used for checking the deflection of the building for wind loading and for performing a stress check of all the main steel members in the building. It should be noted that since this study was completed, a time-history-response capability has been added to this program so that if the study were to be done today, there would be no

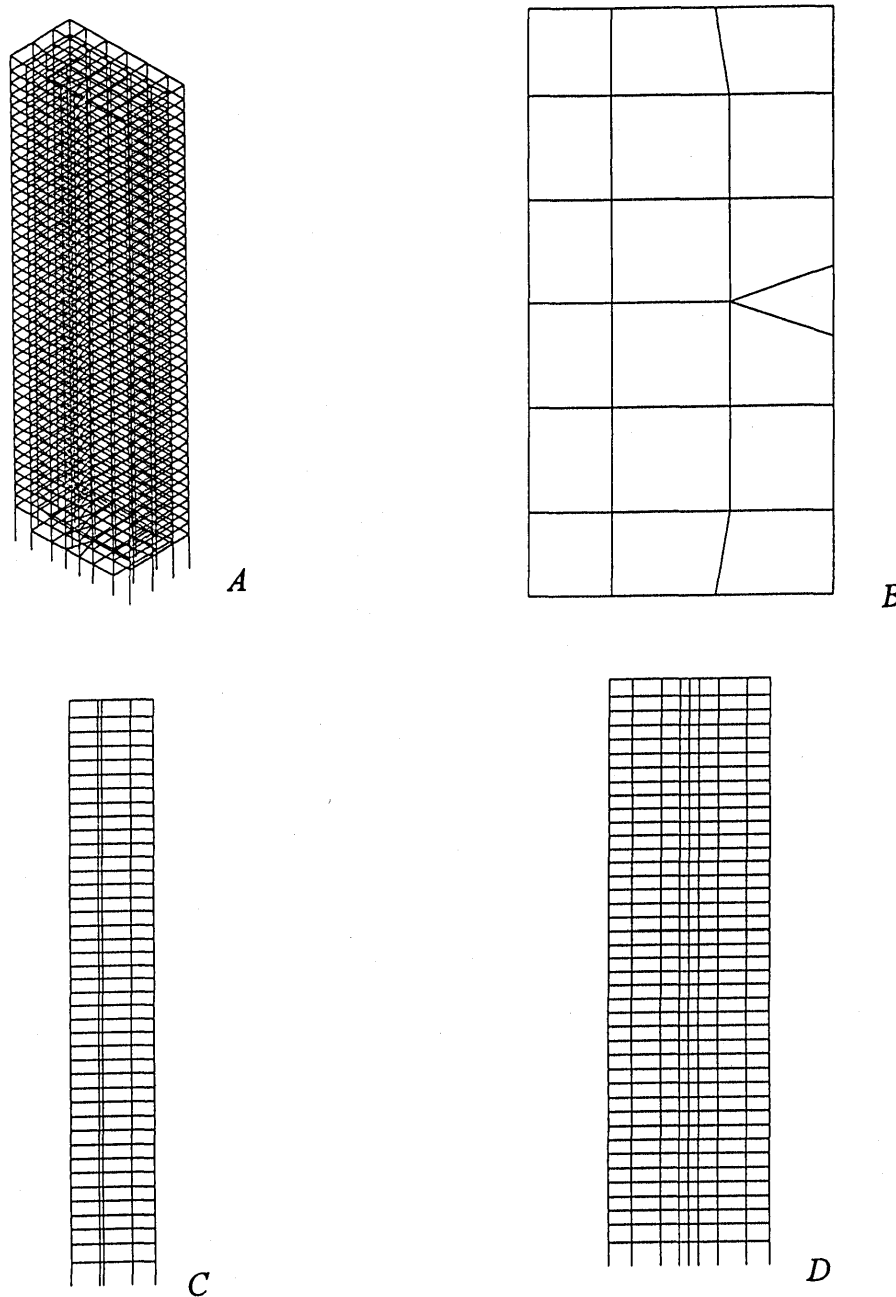


Figure 4.—Building configuration: isometric view (A); plan view (B); transverse elevation (C); longitudinal elevation (D).

need to use the SAP90 program for the analysis of this structure.

An evaluation of the dynamic properties of the building requires that the self weight (mass) of the structure be estimated as accurately as possible. The self weight was estimated as follows:

42d level.—The building has a two story, mechanical penthouse having a 53 by 125 foot plan located above the 42d level. The weight of this structure was added to the weight at the 42d level, resulting in a total weight (mass) of 2,593 kips (6.71 kip-s²/in.).

41st level.—This floor is also a mechanical equipment level, and the general notes on the structural plans indicated an equipment weight of 125 psf. Using this value, the total weight (mass) at this level was estimated to be 2,633 kips (6.81 kip-s²/in.).

25th-40th level.—General notes on the structural plans for these typical floors indicated a partition load of 20 psf. Using this value and estimating the flooring and ceiling weights, the total weight (mass) is estimated to be 1,368 kips (3.54 kip-s²/in.).

3rd-24th level.—Weights of these typical floors are slightly higher than those above due to an increase in the steel weight. The total weight (mass) is estimated to be 1,495 kips (3.87 kip-s²/in.).

2nd level.—The weight of this mezzanine floor was estimated to be higher due to increased loading indicated in the general notes. The total weight (mass) is estimated to be 2,464 kips (6.38 kip-s²/in.).

Summing the weights of all the individual floors results in an estimated building weight (mass) of 62,473 kips (161.7 kip-s²/in.).

DYNAMIC CHARACTERISTICS

In order to determine the periods of vibration from the recorded data, analyses are conducted in both the time and frequency domains. The recorded responses are evaluated in the time domain using a linear elastic-response spectra with 5 percent of critical damping. Analyses in the frequency domain are done using nonparametric time invariant and nonparametric time variant system-identification techniques. The modal periods identified from the recorded data are compared with the calculated values in figure 5. Periods for the transverse direction are compared in figure 5A and periods for the longitudinal direction in figure 5B.

From these analyses of the recorded response of the 42-story building, obtained during the earthquake, the following observations can be made regarding the dynamic response:

1. Translational modes in the two principal directions have the following periods of vibration in seconds for the first

four modes: (a) transverse (east-west)—5.4, 1.8, 1.1, and 0.7; (b) longitudinal (north-south)—5.1, 1.7, 1.0 and 0.7.

2. The second and third modes of vibration of this building make a significant contribution to the response.

3. At the ground level, the peak recorded acceleration was approximately 12 percent of gravity in each direction.

4. Peak accelerations recorded at the 25th level were equal to or larger than those recorded in the upper stories, including the roof.

5. The 34th level has little response from the second mode in either direction, indicating it may be near a modal node.

6. The torsional response of the building was very small and did not make a significant contribution to the total response.

ANALYTICAL MODEL VERIFICATION

Significant advances have been made during the past 20 years in the development of computers and programs which can be used for the seismic response analysis of structures. Along with these developments, it is necessary to evaluate the accuracy of these programs and mathematical modeling techniques in predicting the seismic response of actual buildings. In order to accomplish this, it is necessary to compare the calculated response with that obtained from experiments. The best experiment is obtained when instruments reliably record building response due to motions recorded at the base. The time-history accelerations recorded at the ground-floor level (fig. 6) indicate that the peak values were approximately 0.12 g in both horizontal directions. This recorded acceleration data will serve as input to the dynamic models when calculating the building response to this earthquake.

Using the accelerations recorded on the ground floor as input, the time-history response of the model was evaluated, and the calculated accelerations and displacements were compared to those recorded in the building. In these analyses, accelerations recorded in the east-west (X) and north-south (Y) directions were applied simultaneously to the model, and the dynamic response was calculated using the modal superposition, time-history approach. A total of 21 modes of vibration (seven translational modes in each principal direction and seven torsional modes) were used in the dynamic analyses. These modes represented 97 percent of the reactive mass. It should be noted that only nine modes of vibration would have been required to meet the code requirement that 90 percent of the reactive mass participate in the response.

In order to better evaluate the comparison between the frequency content of the recorded and the calculated floor accelerations, floor response spectra were generated for both motions. This was done by passing the recorded floor accelerations through a single-degree-of-freedom (SDOF) oscillator and generating a response spectrum with 5 percent of critical damping. In a similar manner, the floor

accelerations which were calculated using the 3-D finite-element model were passed through the SDOF oscillator generating another floor response spectrum. These spectra were then plotted on the same tripartite graph for comparison. Initially, the damping in the structure was taken as 6 percent of critical in all modes. Review of the initial comparisons between recorded and calculated response indicated that a lower damping was appropriate, particularly in the higher modes. Therefore, the final damping values were taken as 5 percent of critical for the first three modes and 3 percent of critical in the higher modes.

The data recorded at the 42d level in the east-west (transverse) direction are compared with the calculated results in figure 7. It can be seen in figure 7A that the maximum calculated acceleration (0.21 g) is slightly larger than the recorded value (0.19 g); however, the frequency match is very good. The comparison of displacements (fig. 7B)

shows that the maximum calculated displacement is 5.5 inches versus 5.8 inches recorded. Here the frequency match is good for the first 20 seconds, and beyond that point the period of the recorded values appears to lengthen. Considering the floor spectra (fig. 7C) the comparison is good over the entire period range.

Similar data at the 42d level in the north-south (longitudinal) direction are compared with the calculated results in figure 8. The time-history plots of the acceleration (fig. 8A) indicate that in this direction, the calculated response tends to overestimate the recorded response, although the frequency comparison is reasonably good. A similar result is shown in figure 8B for the displacement response, where the maximum calculated displacement is 5.3 inches compared with 2.8 inches recorded. The floor spectra (fig. 8C) indicate that the calculated response exceeds the recorded response over the entire period range. It should be

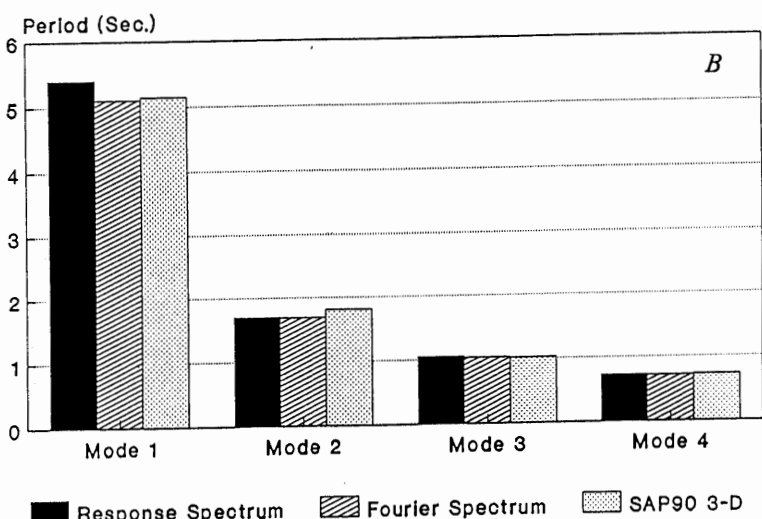
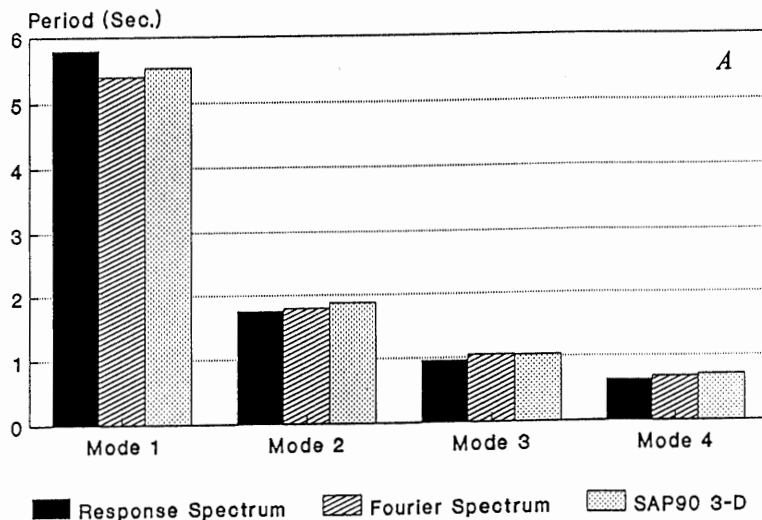


Figure 5.—Identified and calculated periods of vibration: transverse (east-west) direction (A); longitudinal (north-south) direction (B).

noted that this calculated response could be reduced by increasing the damping for the modes in this direction. However, this caused an excessive reduction in the response in this direction in the floors below this level.

The recorded response data at the 34th level in the east-west direction are compared with the calculated results in figure 9. The time-history results are compared in figure 9A. Here it can be seen that the comparison with both amplitude and frequency is very good, with a maximum calculated value of 0.16 g compared to recorded value of

0.148 g. The displacement time history is shown in figure 9B. The maximum calculated displacement is 3.9 inches compared to a maximum recorded value of 3.1 inches. As discussed previously, the period match is good for the first 20 seconds, but beyond this point the period of the recorded data tends to lengthen. The floor spectra (fig. 9C) indicate that the comparison is very good over the complete period range.

Similar comparisons at the 34th level for motions in the north-south direction are shown in figure 10. Considering

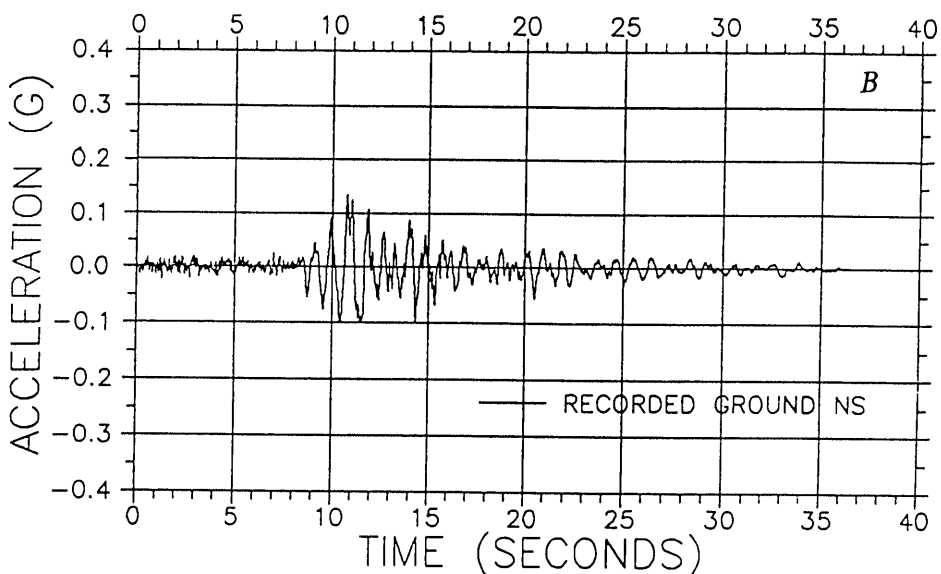
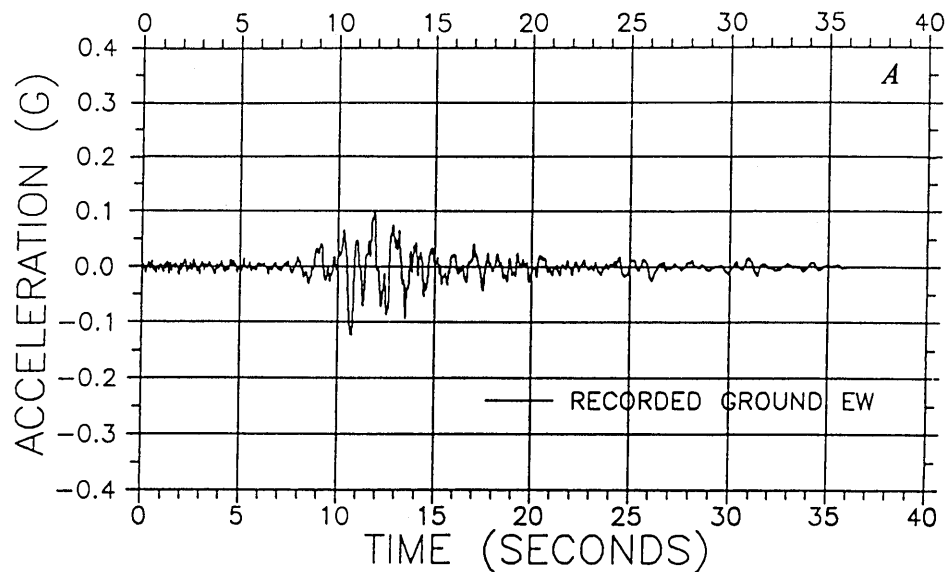


Figure 6.—Recorded base motion (ground level).

the time-history response (fig. 10A) the maximum calculated acceleration is 0.168 g compared with a recorded value of 0.183 g. The displacement response (fig. 10B) indicates a maximum calculated displacement of 3.0 inches compared with a maximum recorded value of 2.5 inches. The floor spectra (fig. 10C) compare favorably over the entire period range.

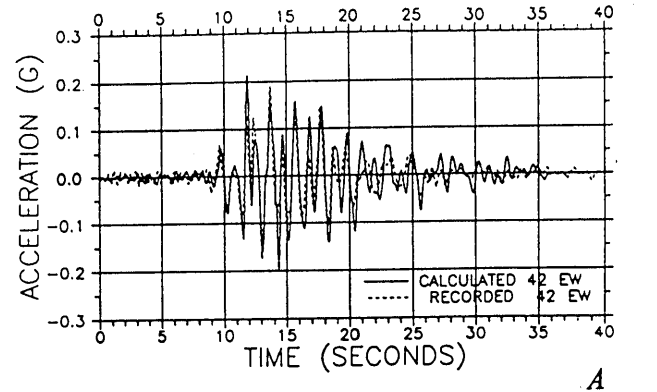
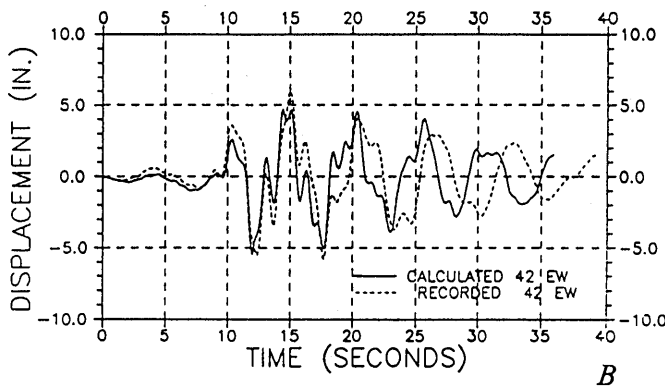
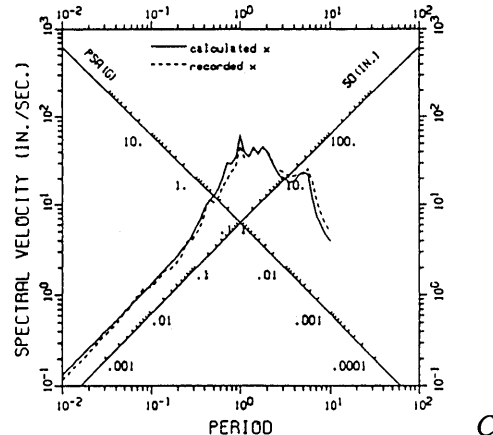
**A****B****C**

Figure 7.—Recorded response vs. calculated, 42d level, east-west.

The recorded response data at the 25th level in the east-west direction is compared with the calculated values in figure 11. The acceleration time-history (fig. 11A) indicates a peak calculated acceleration of 0.18 g compared to a recorded value of 0.22 g. Frequency compari-

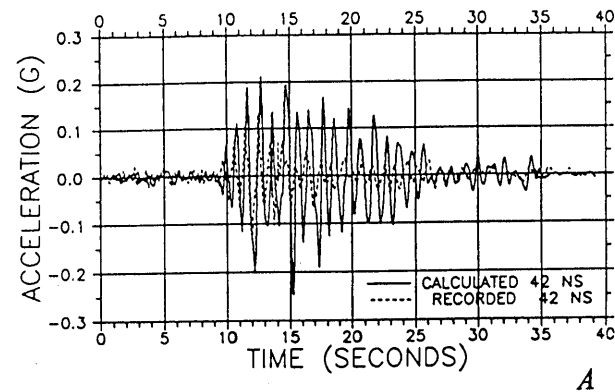
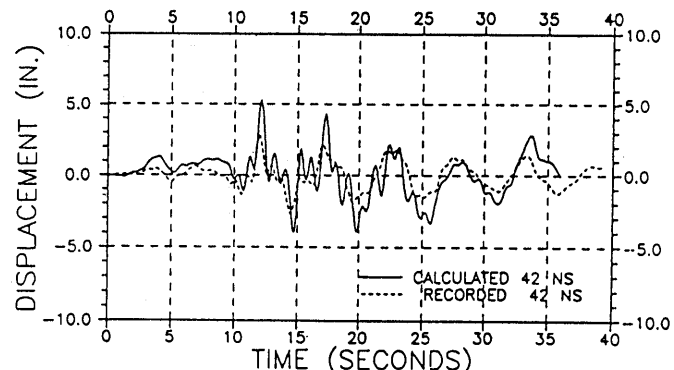
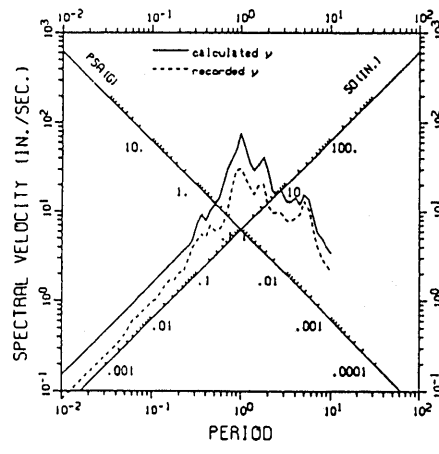
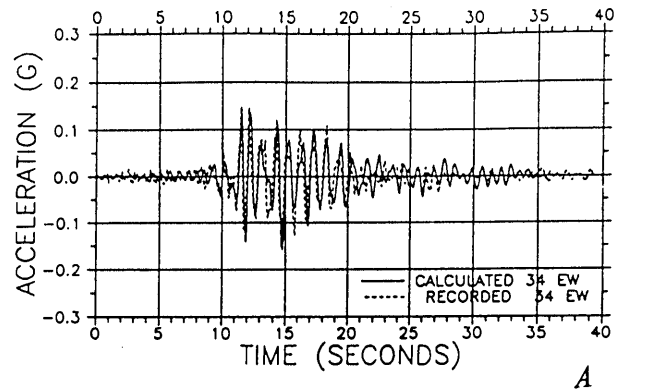
**A****B****C**

Figure 8.—Recorded response vs. calculated, 42d level, north-south.

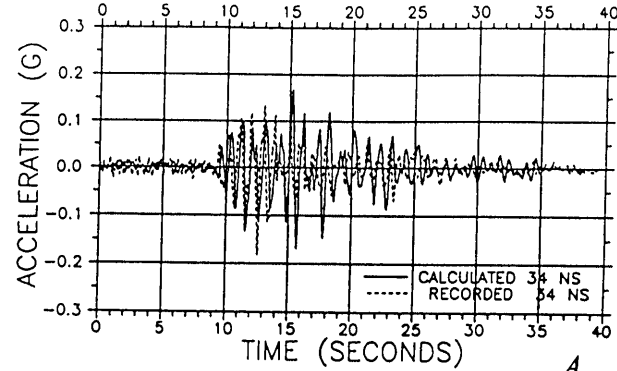
sions are very good, particularly for the first 20 seconds. The time-history of the displacement (fig. 11B) indicates a peak calculated displacement of 3.2 inches compared with a recorded value of 4.6 inches. This underestimation of the response by the calculated results is also reflected

in the floor spectra (fig. 11C). Here it can be seen that the calculated spectrum is below the recorded spectrum over much of the period range.

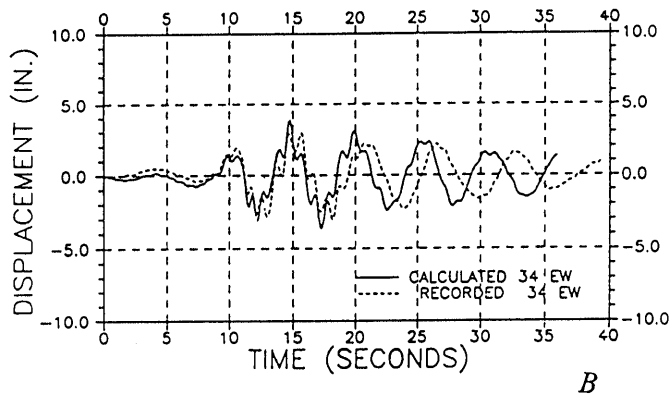
Similar data at the 25th level in the north-south direction are presented in figure 12. The time-history



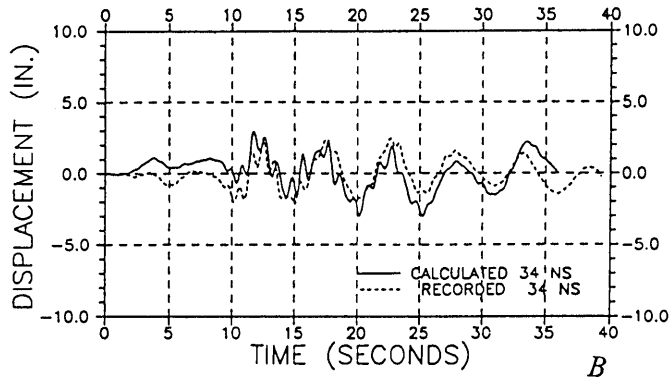
A



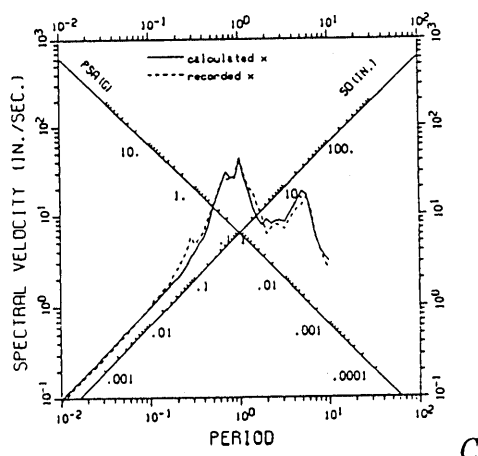
A



B

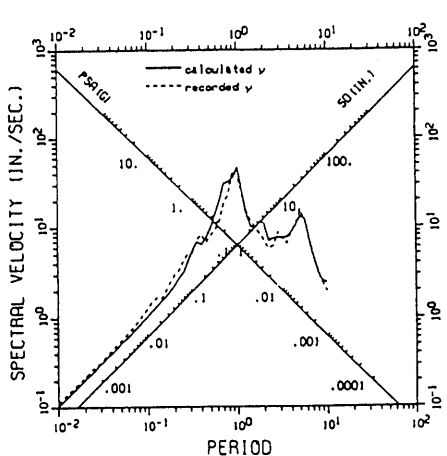


B



C

Figure 9.—Recorded response vs. calculated, 34th level, east-west.

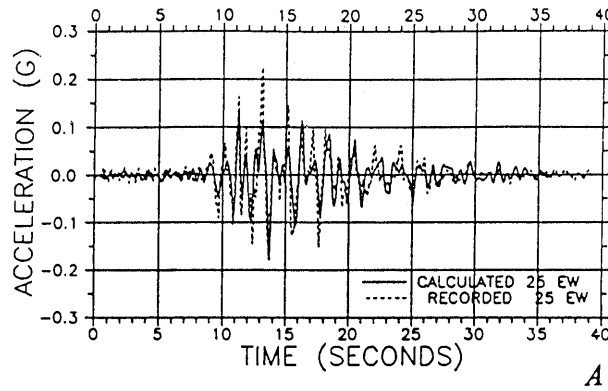


C

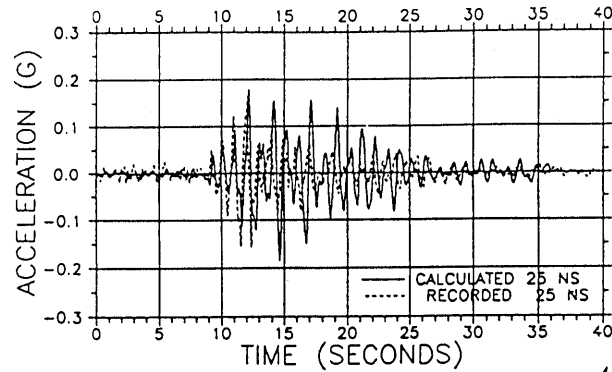
Figure 10.—Recorded response vs. calculated, 34th level, north-south.

data (fig. 12A) indicate a peak calculated acceleration of 0.188 g compared with a recorded value of 0.163 g. The time-history of the displacements is shown in figure 12B. Here it can be seen that the maximum calculated displacement is 2.9 inches compared with a recorded value

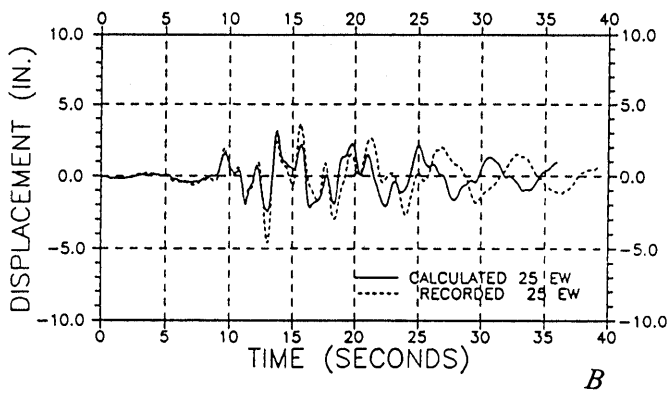
of 2.0 inches. The overestimation of the response by the calculated results is also indicated in the floor spectra (fig. 12C). Here it can be seen that the calculated spectrum falls above the recorded spectrum in most period ranges.



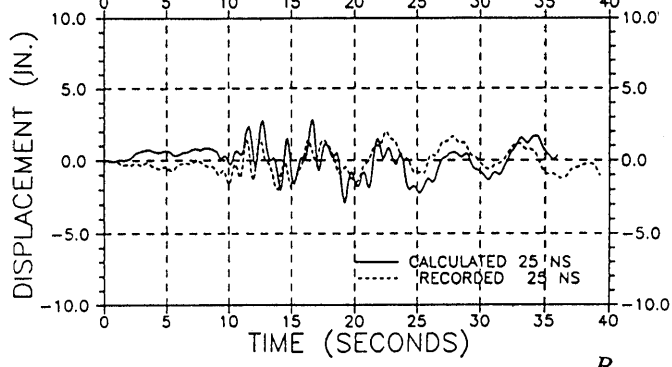
A



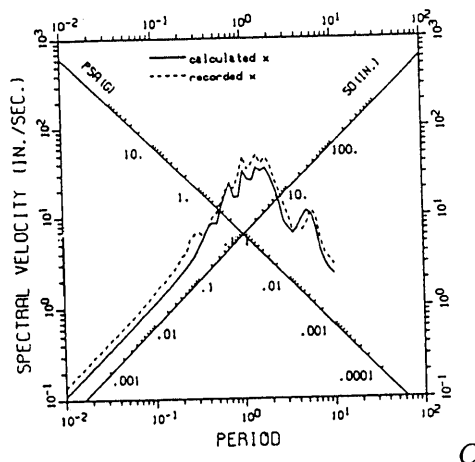
A



B

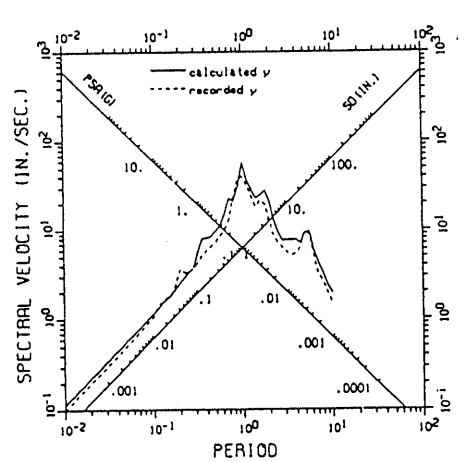


B



C

Figure 11.—Recorded response vs. calculated, 25th level, east-west.



C

Figure 12.—Recorded response vs. calculated, 25th level, north-south.

INPUT ENERGY

In order to evaluate the relative importance of earthquake motions in the north-south and east-west directions, the seismic energy input to the structure in these two directions was evaluated. This was done by considering the product of the recorded base displacement, v_g , and the calculated base shear, V . In incremental form this can be expressed as

$$\text{Input energy} = \sum V \times \delta v_g.$$

The time-history of the base shear in the east-west direction is shown in figure 13A, and the corresponding values for the north-south direction are shown in figure 13B. The figures indicate that the maximum base shears in both directions are almost equal, being 2,000 kips in the east-west direction and 2,200 kips in the north-south direction. A comparison of the elastic input energies (fig. 13C) indicates that there is about 50 percent more input energy in the north-south direction as compared to the east-west direction.

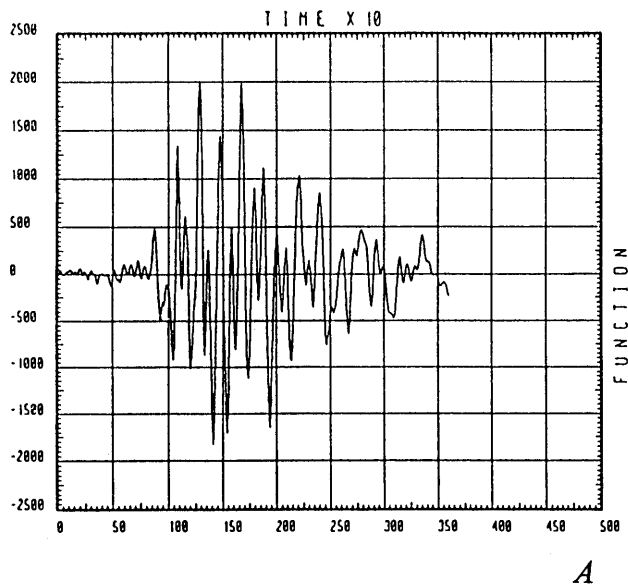
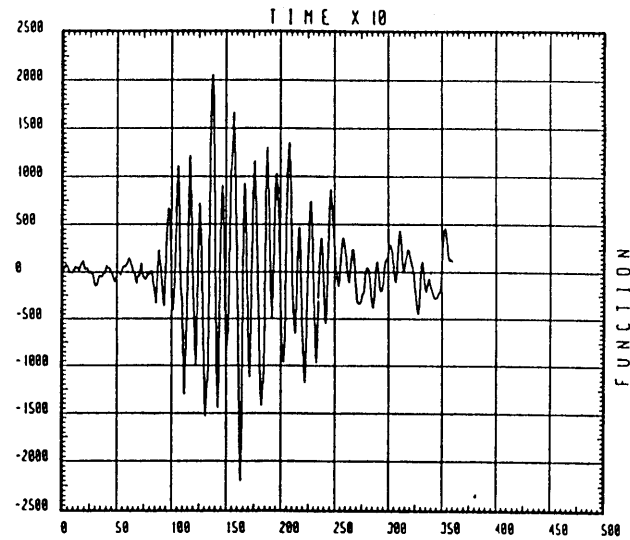
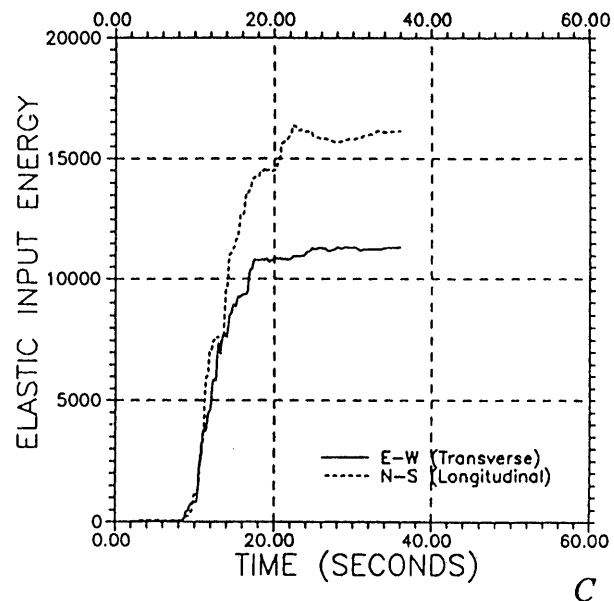
**A****B****C**

Figure 13 Elastic energy input: base shear time history, transverse (A); base shear time history, longitudinal (B); elastic input energy time history (C).

MODAL RESPONSE CONTRIBUTION

The relative contributions of the first four modes of vibration in the east-west (transverse) direction to the absolute acceleration at level 42 are shown in figure 14. The absolute acceleration due to the first mode response (fig. 14a) indicates that the peak acceleration due to this mode is only 0.072 g. Inclusion of the second mode response increases the peak acceleration to 0.17 g (fig. 14b), indicating an increase of more than 100 percent from the second mode. Inclusion of the third mode response (fig. 14c) indicates a peak acceleration of 0.255 g which represents another increase of 50 percent. With the inclusion of the first four modes of vibration (fig. 14d) the peak acceleration increases another 49 percent to a value of 0.38 g. These results indicate that for this tall building, the acceleration response at the top of the building is primarily due to the 2d, 3d, and 4th modes with a minimal contribution from the 1st mode. Note that had the code guideline of considering participation of 90 percent of the reactive mass been followed, the fourth mode would have been neglected,

with a significant truncation of the acceleration at the 42d level.

Displacement data for this level is presented in figure 15. The relative displacement response due to the first mode (fig. 15A) has a maximum value of 4.75 inches. Inclusion of the second mode response (fig. 15B) increases the maximum displacement to 5.5 inches. With three modes, the displacement increases to 5.7 inches (fig. 15C). Considering four modes of vibration, the maximum displacement becomes 6.2 inches (fig. 15D). These results indicate that the displacement response is primarily due to the first mode; however, inclusion of the fourth mode increased the displacement by 9 percent.

The absolute acceleration response at the 25th level is shown in figure 16. The absolute acceleration due to the first mode (fig. 16A) is very small (0.026 g). Inclusion of the second mode response increases the maximum acceleration to 0.10 g (fig. 16B). With the inclusion of the third mode (fig. 16C) the maximum acceleration reaches 0.23 g. Consideration of the first four modes increases the peak acceleration to 0.35 g (fig. 16D). These results indicate

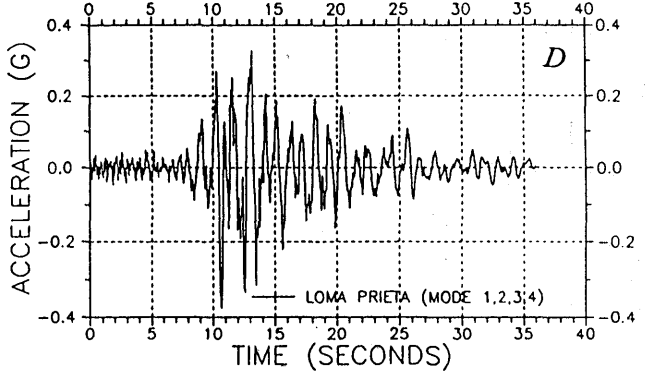
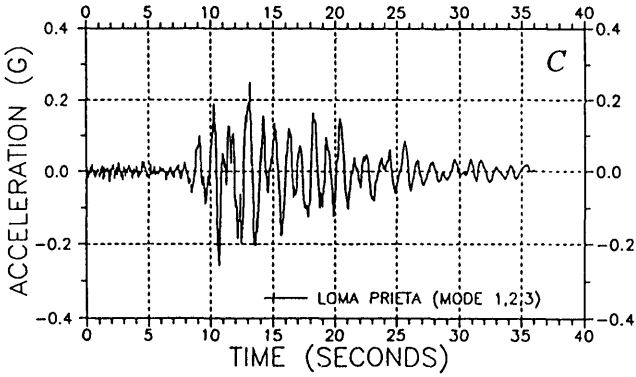
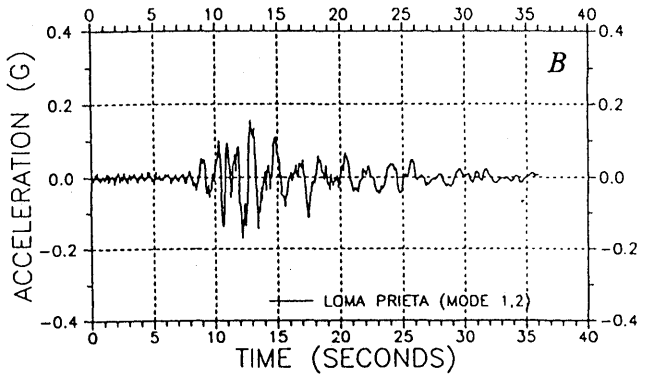
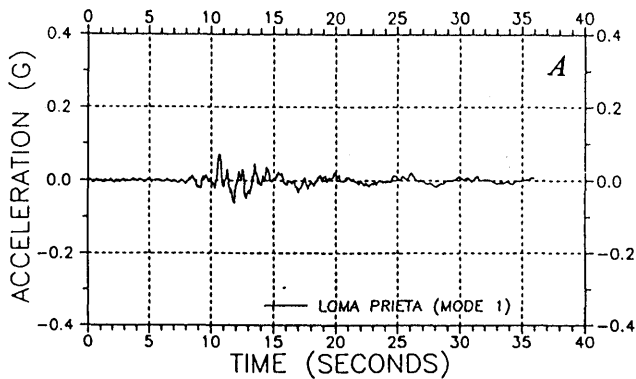


Figure 14.—Modal accelerations, roof level, transverse: first mode (A); first and second modes (B); first, second, and third modes (C) first, second, third, and fourth modes (D).

cate the absolute acceleration at this level is primarily due to the second, third, and fourth mode response with almost no contribution from the first mode.

The relative displacement response at this level is shown in figure 17. The displacement response due to the first mode has a maximum value of 2.5 inches (fig. 17A). Inclusion of the second mode response increases the maximum displacement to 4.2 inches (fig. 17B). Adding the displacement response of the third mode, (fig. 17C) results in no change in the maximum displacement, and inclusion of the fourth mode actually decreases the maximum displacement at this level to 4.05 inches (fig. 17D). These results indicate that the displacement response at this level is primarily due to the first and second modes of vibration in this direction.

These results (figs. 13-17) indicate the importance of the higher modes of vibration in the response of tall buildings. They also indicate that the modal cutoff specified in the current code at participation of 90 percent of the reactive mass may truncate a significant part of the dynamic response for tall buildings such as the one considered in this study. The authors feel that this requirement should be increased to at least 95 percent.

STRESS CHECK

In order to verify the design condition which required that stresses in the members remain below yield under the lateral forces developed by the design spectrum, a stress check was performed using the postprocessing program STEELER, developed by Habibullah (1989). This required that the gravity loading be represented as accurately as possible. Based on the geometry of the framing system, the gravity load was distributed to the members of each floor level as shown in figure 18. Since the design spectra is representative of yield load and not allowable load, use of the stress check program, which is based on allowable stress, requires that the applied load be reduced by a factor of 0.66.

Results of the stress check are summarized in figures 19 and 20. The stress ratios in a typical transverse frame are shown in figure 19, where a ratio of less than unity represents elastic behavior. Stress ratios for levels 41 through 27 (fig. 19A) represent the upper third of the structure. In this region, the maximum value is 1.05 in an exterior column. Values for levels 27 through 13 are shown in figure 19B. In this region, the stress ratios are slightly

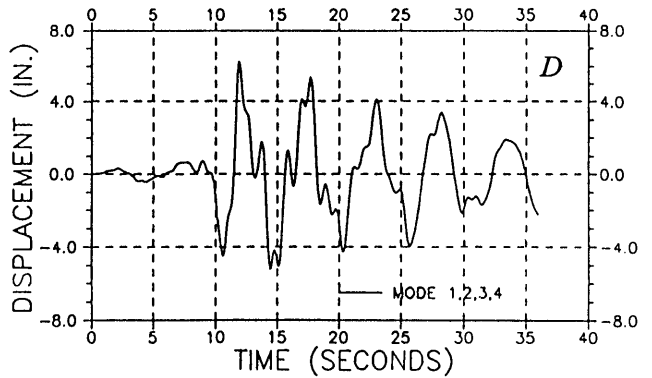
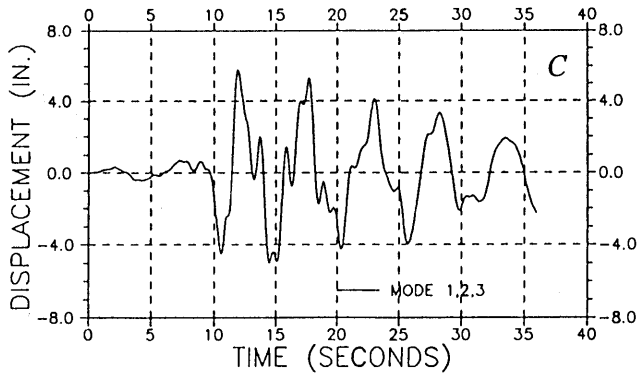
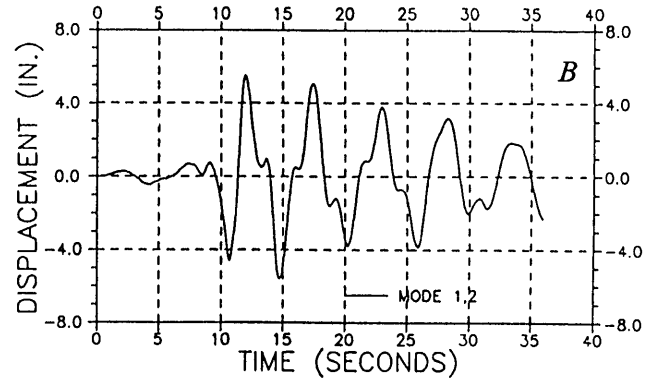
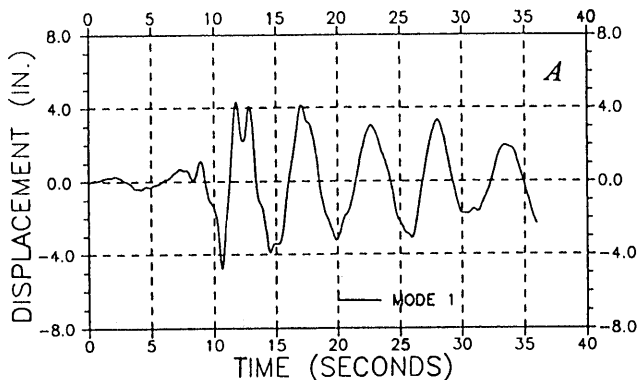


Figure 15.—Modal displacements, roof level, transverse: first mode (A); first and second modes (B); first, second, and third modes (C); first, second, third, and fourth modes (D).

lower, with a maximum value of 0.99 near the 27th level. Stresses in the bottom third of the structure, levels 1 through 13, are shown in figure 19C, where it can be seen that the maximum value of 0.93 occurs in an exterior beam at the third-story level.

The stress ratios in a typical longitudinal frame are shown in figure 20. Stress ratios for levels 41 through 27 are shown in figure 20A. The maximum value in the columns is 0.84, and the maximum value for the girders is 0.87. Values for the middle third of the structure are shown in figure 20B for levels 13 through 27. In this region the stress ratios in both the beams and the columns are lower than those in the upper third of the structure. In the bottom third of the structure, levels 1 through 13, the stresses in the girders increase with the maximum value reaching 0.92 in the exterior girder at the fourth story level (fig. 20C).

The stress check indicates that, with the exception of a few members which are stressed just above nominal yield, the design criteria that required stresses in the members to remain below yield under the site-design spectrum is generally satisfied for these two frames, which are representative of the remaining frames.

ELASTIC RESPONSE ANALYSES

The elastic response of the reference structure is evaluated considering the static lateral force requirements specified by the CCSF code, the dynamic lateral-force requirements of the site-design spectrum, the time-history demands of the Loma Prieta accelerations recorded at ground level, and the time-history demands of the Loma Prieta accelerations recorded at Hollister. The performance is evaluated in terms of the following response envelopes: lateral displacement, interstory drift index (IDI), inertia force, and story shear.

The two horizontal components of the ground accelerations recorded at Hollister are shown in figure 21. Here it can be seen that the north-south component (fig. 21A) of this ground motion is considerably stronger than the east-west component (fig. 21B). These two components are applied simultaneously to the base of the structure and the resulting response is calculated for comparison with the other responses.

The response envelopes for the east-west (transverse) direction are given in figure 22. The envelopes of lateral displacement (fig. 22A) indicate that the displacement due

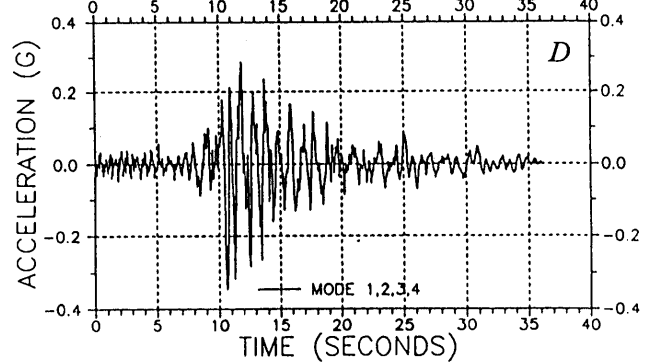
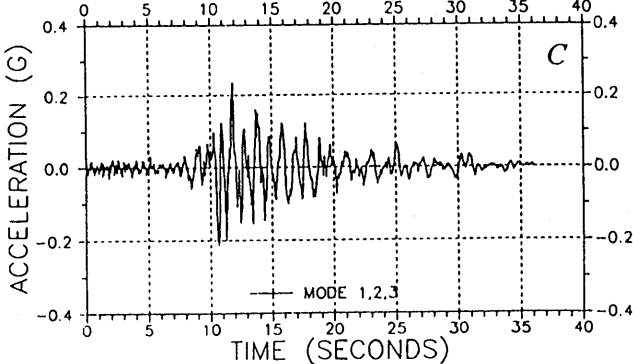
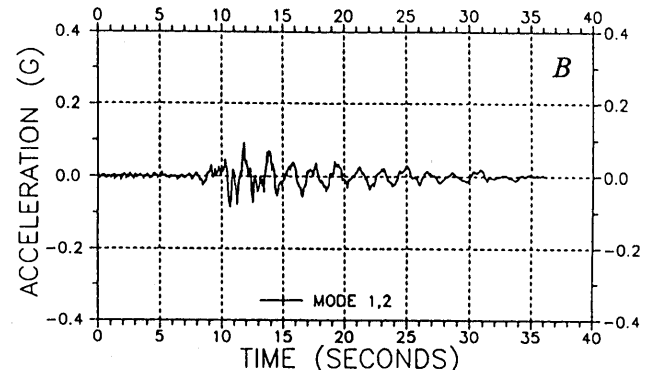
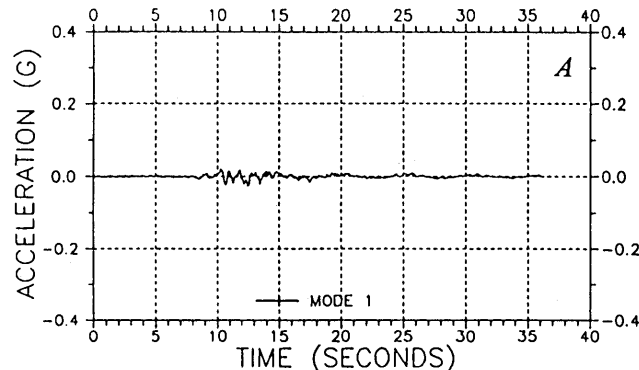


Figure 16.—Modal accelerations, 25th level, transverse: first mode (A); first and second modes (B); first, second, and third modes (C); first, second, third, and fourth modes (D).

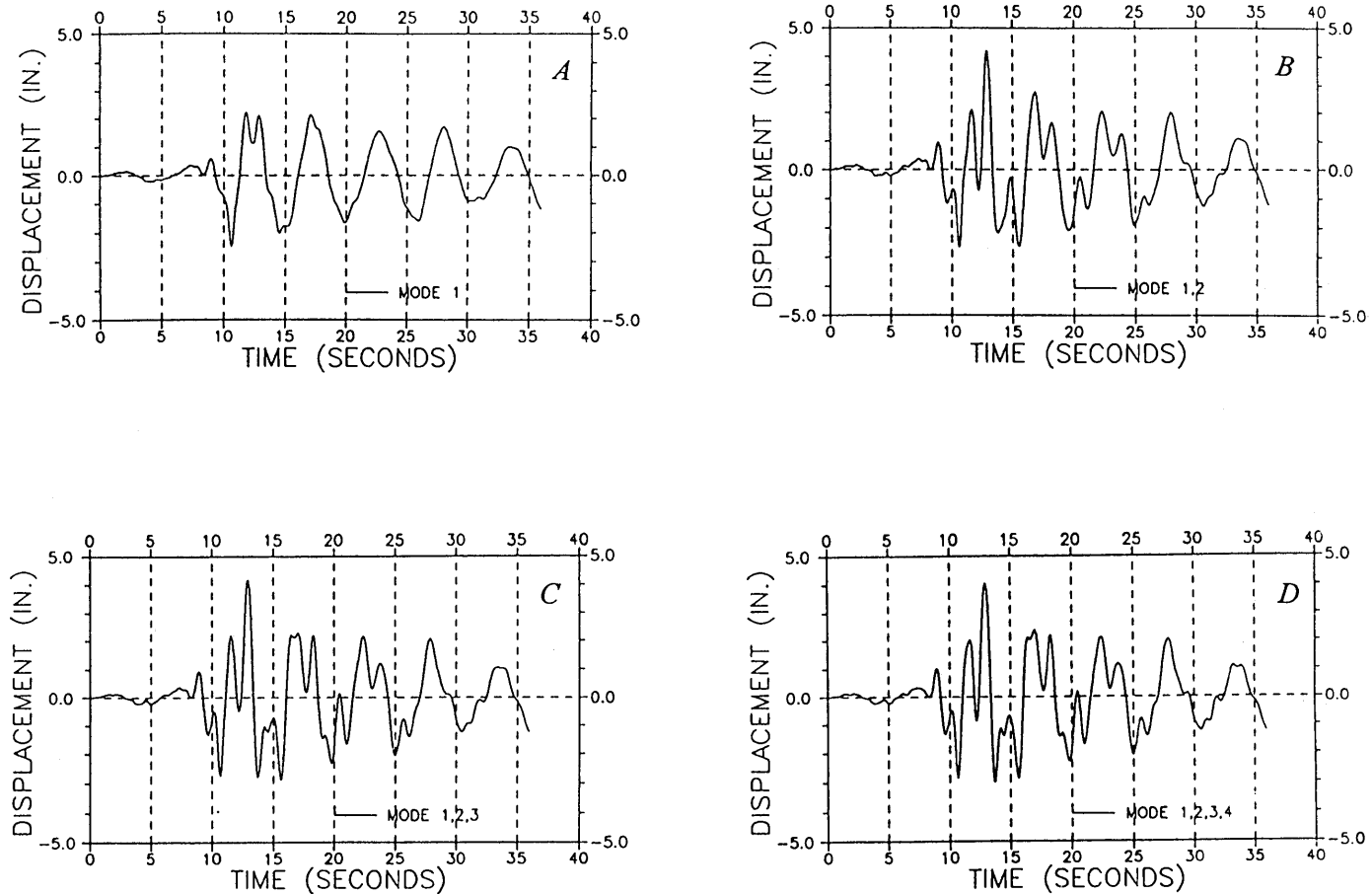


Figure 17.—Modal displacements, 25th level, transverse: first mode (A); first and second modes (B); first, second, and third modes (C); first, second, third, and fourth modes (D).

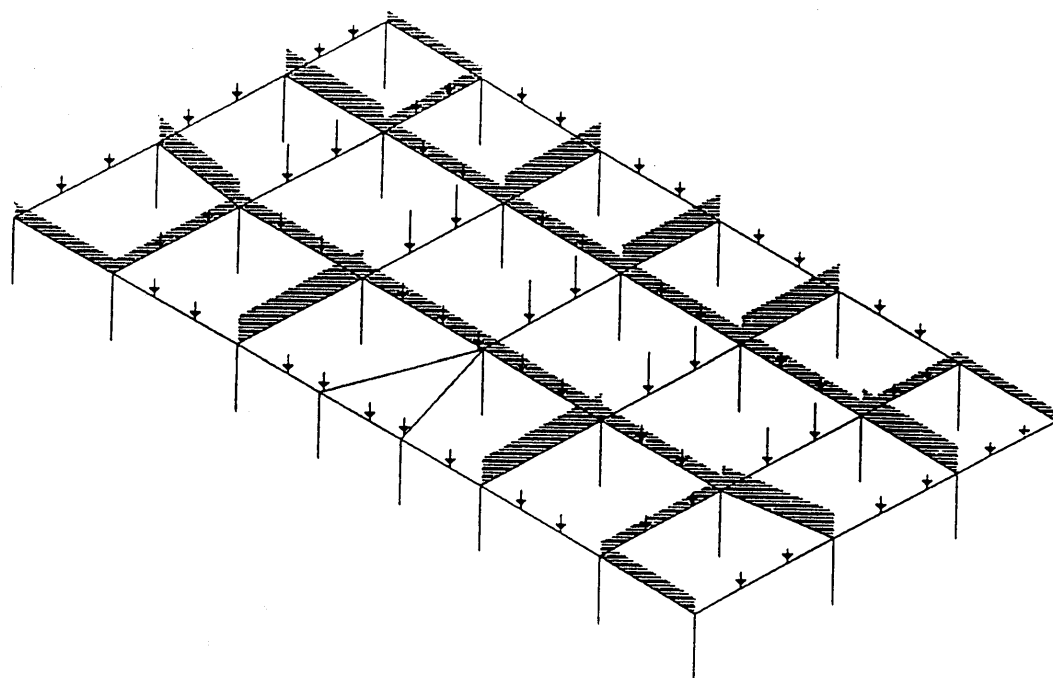


Figure 18.—Gravity load distribution.

	0.31	0.40	0.28
0.49	0.59	0.68	0.39
0.68	0.68	0.68	0.51
0.75	0.78	0.68	0.58
0.81	0.76	0.68	0.66
0.87	0.81	0.75	0.72
0.93	0.83	0.84	0.75
0.97	0.84	0.87	0.77
0.97	0.85	0.78	0.78
0.98	0.67	0.72	0.84
0.88	0.67	0.72	0.84
0.88	0.65	0.72	0.84
0.87	0.64	0.72	0.77
0.86	0.62	0.71	0.71
0.83	0.59	0.69	0.55
0.87	0.77	0.82	0.92
0.84	0.88	0.91	0.97
0.95	0.98	0.97	0.95

A

B

	0.57	0.59
0.57	0.60	0.63
0.57	0.62	0.66
0.58	0.65	0.69
0.59	0.67	0.71
0.60	0.68	0.73
0.61	0.70	0.77
0.62	0.71	0.78
0.63	0.72	0.81
0.64	0.73	0.82
0.65	0.74	0.83
0.66	0.75	0.84
0.67	0.76	0.85
0.68	0.77	0.86
0.69	0.78	0.87
0.70	0.79	0.88
0.71	0.80	0.89
0.72	0.81	0.90
0.73	0.82	0.91
0.74	0.83	0.92
0.75	0.84	0.93
0.76	0.85	0.94
0.77	0.86	0.95
0.78	0.87	0.96
0.79	0.88	0.97
0.80	0.89	0.98
0.81	0.90	0.99
0.82	0.91	1.00
0.83	0.92	1.01
0.84	0.93	1.02
0.85	0.94	1.03
0.86	0.95	1.04
0.87	0.96	1.05
0.88	0.97	1.06
0.89	0.98	1.07
0.90	0.99	1.08
0.91	1.00	1.09
0.92	1.01	1.10
0.93	1.02	1.11
0.94	1.03	1.12
0.95	1.04	1.13
0.96	1.05	1.14
0.97	1.06	1.15
0.98	1.07	1.16
0.99	1.08	1.17
1.00	1.09	1.18

6

Figure 19.—Stress ratios, typical transverse frame: levels 41 through 27 (A); levels 27 through 13 (B); levels 13 through 1 (C).

to the recorded base motion is less than that due to the lateral design forces. It is of interest to note that the displacements due to the CCSF code loads, when factored to represent yield, exceed the lateral displacements due to

the design spectrum in the upper half of the structure. The roof displacements due to the Hollister motion exceed those due to the design spectrum by a factor of 2.4 and recall that the east-west component is the smaller of the

0.84	0.79	0.75	0.84	0.79	0.73	0.68	0.72	0.66	0.71	0.63	0.54	0.45	0.35
0.74	0.74	0.73	0.79	0.75	0.73	0.67	0.72	0.66	0.71	0.63	0.54	0.45	0.35
0.49	0.54	0.46	0.56	0.51	0.51	0.45	0.50	0.50	0.50	0.43	0.39	0.34	0.35
0.46	0.52	0.52	0.54	0.54	0.54	0.45	0.54	0.54	0.54	0.43	0.40	0.40	0.35
0.52	0.61	0.58	0.58	0.58	0.58	0.53	0.54	0.55	0.55	0.58	0.46	0.43	0.35
0.58	0.69	0.74	0.74	0.64	0.64	0.64	0.64	0.65	0.65	0.58	0.52	0.48	0.35
0.62	0.78	0.78	0.78	0.75	0.76	0.76	0.72	0.73	0.73	0.66	0.58	0.52	0.35
0.65	0.82	0.76	0.76	0.75	0.75	0.75	0.74	0.74	0.74	0.75	0.67	0.63	0.35
0.68	0.94	0.89	0.79	0.83	0.83	0.81	0.88	0.88	0.88	0.85	0.68	0.63	0.35
0.69	0.94	0.83	0.84	0.84	0.84	0.84	0.84	0.84	0.84	0.82	0.78	0.71	0.35
0.71	0.75	0.75	0.85	0.85	0.86	0.84	0.71	0.71	0.71	0.66	0.71	0.69	0.35
0.72	0.76	0.76	0.72	0.72	0.69	0.67	0.72	0.72	0.72	0.72	0.72	0.72	0.35
0.73	0.81	0.75	0.85	0.85	0.85	0.85	0.74	0.74	0.74	0.75	0.75	0.75	0.35
0.72	0.71	0.69	0.67	0.67	0.67	0.67	0.69	0.69	0.69	0.70	0.70	0.70	0.35
0.71	0.83	0.82	0.84	0.84	0.84	0.82	0.70	0.70	0.70	0.70	0.70	0.70	0.35
0.70	0.76	0.74	0.71	0.71	0.71	0.72	0.72	0.72	0.72	0.72	0.72	0.72	0.35
0.72	0.71	0.69	0.69	0.69	0.69	0.69	0.70	0.70	0.70	0.70	0.70	0.70	0.35
0.71	0.71	0.70	0.71	0.71	0.71	0.71	0.71	0.71	0.71	0.71	0.71	0.71	0.35
0.70	0.70	0.70	0.70	0.70	0.70	0.70	0.70	0.70	0.70	0.70	0.70	0.70	0.35

A

0.71	0.29	0.83	0.82	0.84	0.82	0.72	0.72	0.75	0.75	0.75	0.75	0.75	0.72
0.66	0.78	0.80	0.79	0.81	0.80	0.72	0.72	0.77	0.78	0.78	0.78	0.78	0.67
0.65	0.72	0.78	0.65	0.77	0.77	0.64	0.64	0.73	0.73	0.73	0.73	0.73	0.70
0.63	0.72	0.76	0.67	0.75	0.76	0.65	0.65	0.73	0.75	0.75	0.75	0.75	0.72
0.62	0.73	0.74	0.68	0.74	0.74	0.66	0.66	0.73	0.73	0.73	0.73	0.73	0.70
0.68	0.67	0.72	0.72	0.72	0.72	0.57	0.57	0.73	0.71	0.71	0.71	0.71	0.68
0.58	0.69	0.69	0.68	0.68	0.68	0.59	0.59	0.78	0.68	0.68	0.68	0.68	0.72
0.51	0.64	0.65	0.67	0.64	0.64	0.61	0.61	0.65	0.63	0.64	0.62	0.62	0.57
0.49	0.63	0.63	0.61	0.61	0.61	0.61	0.61	0.62	0.62	0.62	0.62	0.62	0.58
0.49	0.65	0.62	0.62	0.62	0.62	0.62	0.62	0.62	0.62	0.62	0.62	0.62	0.59
0.49	0.66	0.62	0.62	0.63	0.63	0.63	0.63	0.63	0.63	0.63	0.63	0.63	0.60
0.58	0.62	0.62	0.62	0.62	0.62	0.62	0.62	0.61	0.61	0.61	0.61	0.61	0.51
0.52	0.63	0.63	0.62	0.62	0.62	0.62	0.62	0.62	0.62	0.62	0.62	0.62	0.58
0.54	0.65	0.64	0.64	0.64	0.64	0.62	0.62	0.63	0.63	0.63	0.63	0.63	0.55
0.57	0.62	0.66	0.64	0.64	0.64	0.65	0.65	0.65	0.65	0.65	0.65	0.65	0.66
0.64	0.64	0.64	0.64	0.64	0.64	0.64	0.64	0.64	0.64	0.64	0.64	0.64	0.68

B

0.57	0.66	0.64	0.65	0.64	0.65	0.64	0.64	0.65	0.65	0.65	0.65	0.65	0.58
0.68	0.68	0.64	0.66	0.66	0.66	0.65	0.65	0.66	0.67	0.67	0.67	0.67	0.62
0.64	0.64	0.71	0.73	0.71	0.71	0.69	0.69	0.70	0.70	0.70	0.70	0.70	0.64
0.67	0.64	0.64	0.64	0.64	0.64	0.64	0.64	0.64	0.64	0.64	0.64	0.64	0.64
0.67	0.64	0.64	0.64	0.64	0.64	0.64	0.64	0.64	0.64	0.64	0.64	0.64	0.64
0.75	0.72	0.71	0.71	0.71	0.71	0.71	0.71	0.71	0.71	0.71	0.71	0.71	0.68
0.76	0.76	0.75	0.75	0.75	0.75	0.75	0.75	0.75	0.75	0.75	0.75	0.75	0.72
0.76	0.71	0.72	0.72	0.72	0.72	0.72	0.72	0.72	0.72	0.72	0.72	0.72	0.72
0.77	0.71	0.71	0.71	0.71	0.71	0.71	0.71	0.71	0.71	0.71	0.71	0.71	0.71
0.77	0.71	0.71	0.71	0.71	0.71	0.71	0.71	0.71	0.71	0.71	0.71	0.71	0.71
0.78	0.71	0.71	0.71	0.71	0.71	0.71	0.71	0.71	0.71	0.71	0.71	0.71	0.71
0.78	0.71	0.71	0.71	0.71	0.71	0.71	0.71	0.71	0.71	0.71	0.71	0.71	0.71
0.79	0.71	0.71	0.71	0.71	0.71	0.71	0.71	0.71	0.71	0.71	0.71	0.71	0.71
0.80	0.71	0.71	0.71	0.71	0.71	0.71	0.71	0.71	0.71	0.71	0.71	0.71	0.71
0.81	0.71	0.71	0.71	0.71	0.71	0.71	0.71	0.71	0.71	0.71	0.71	0.71	0.71
0.82	0.71	0.71	0.71	0.71	0.71	0.71	0.71	0.71	0.71	0.71	0.71	0.71	0.71
0.83	0.71	0.71	0.71	0.71	0.71	0.71	0.71	0.71	0.71	0.71	0.71	0.71	0.71
0.84	0.71	0.71	0.71	0.71	0.71	0.71	0.71	0.71	0.71	0.71	0.71	0.71	0.71
0.85	0.71	0.71	0.71	0.71	0.71	0.71	0.71	0.71	0.71	0.71	0.71	0.71	0.71
0.86	0.71	0.71	0.71	0.71	0.71	0.71	0.71	0.71	0.71	0.71	0.71	0.71	0.71
0.87	0.71	0.71	0.71	0.71	0.71	0.71	0.71	0.71	0.71	0.71	0.71	0.71	0.71
0.88	0.71	0.71	0.71	0.71	0.71	0.71	0.71	0.71	0.71	0.71	0.71	0.71	0.71
0.89	0.71	0.71	0.71	0.71	0.71	0.71	0.71	0.71	0.71	0.71	0.71	0.71	0.71
0.90	0.71	0.71	0.71	0.71	0.71	0.71	0.71	0.71	0.71	0.71	0.71	0.71	0.71
0.91	0.71	0.71	0.71	0.71	0.71	0.71	0.71	0.71	0.71	0.71	0.71	0.71	0.71
0.92	0.71	0.71	0.71	0.71	0.71	0.71	0.71	0.71	0.71	0.71	0.71	0.71	0.71
0.93	0.71	0.71	0.71	0.71	0.71	0.71	0.71	0.71	0.71	0.71	0.71	0.71	0.71
0.94	0.71	0.71	0.71	0.71	0.71	0.71	0.71	0.71	0.71	0.71	0.71	0.71	0.71
0.95	0.71	0.71	0.71	0.71	0.71	0.71	0.71	0.71	0.71	0.71	0.71	0.71	0.71
0.96	0.71	0.71	0.71	0.71	0.71	0.71	0.71	0.71	0.71	0.71	0.71	0.71	0.71
0.97	0.71	0.71	0.71	0.71	0.71	0.71	0.71	0.71	0.71	0.71	0.71	0.71	0.71
0.98	0.71	0.71	0.71	0.71	0.71	0.71	0.71	0.71	0.71	0.71	0.71	0.71	0.71
0.99	0.71	0.71	0.71	0.71	0.71	0.71	0.71	0.71	0.71	0.71	0.71	0.71	0.71
0.00	0.71	0.71	0.71	0.71	0.71	0.71	0.71	0.71	0.71	0.71	0.71	0.71	0.71

C

Figure 20.—Stress ratios, typical longitudinal frame levels 41 through 27 (A); levels 27 through 13 (B); levels 13 through 1 (C).

two. Envelopes for the maximum interstory drift index are shown in figure 22B. As before, the IDI due to the recorded base motion is less than that due to the design spectrum. For this parameter, the indices due to the design spectrum exceed those due to the factored CCSF lateral forces over most of the building height with the exception of floor levels 15 to 22. The envelope due to the Hollister ground motion is considerably larger than the others.

The envelopes of maximum inertia force over the building height are shown in figure 22C. It can be seen that the inertia forces due to the design spectrum exceed those due to the recorded ground motion with the exception of three floors near the top of the structure (floors 32-34). It can also be seen that the inertia forces due to the Hollister ground motion exceed those due to the design spectrum at all floor levels except the 39th. The inertia forces speci-

fied in the CCSF code represent the minimum values, which are exceeded by all others.

The envelopes of maximum story shear are shown in figure 22D. This figure indicates that the story shears due to the design spectrum exceed those developed by the recorded base motions at all story levels. This tends to indicate that the behavior of the structure in this direction is linear elastic. However, it is of interest to note that had the minimum lateral-force requirements of the CCSF code been used for design, the story shears due to the recorded base motions would have exceeded the design values in the upper 15 floor levels. The story shears due to the Hollister motions exceed the design values over most of the building and indicate yielding of the structural frames, which will have to be investigated using a nonlinear analysis. It is also of interest to note that the decrease in story shear, indicated by the design spectrum at the 20th story

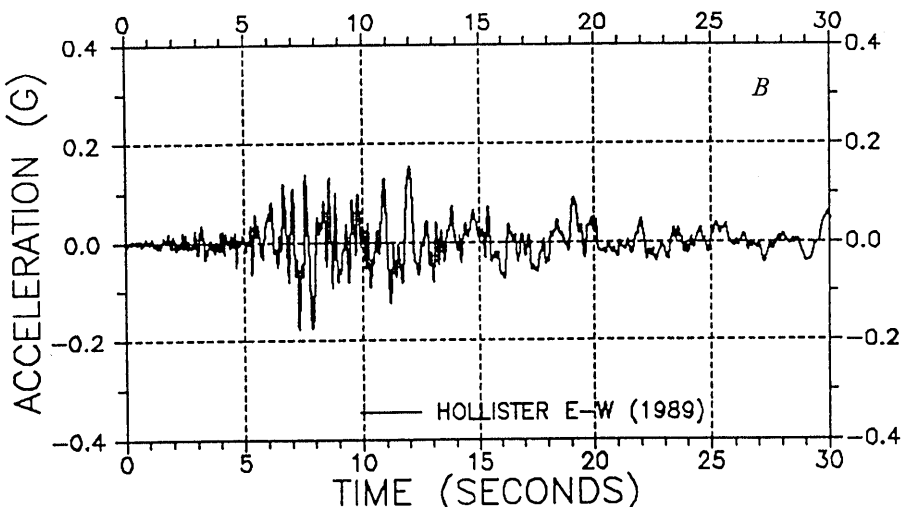
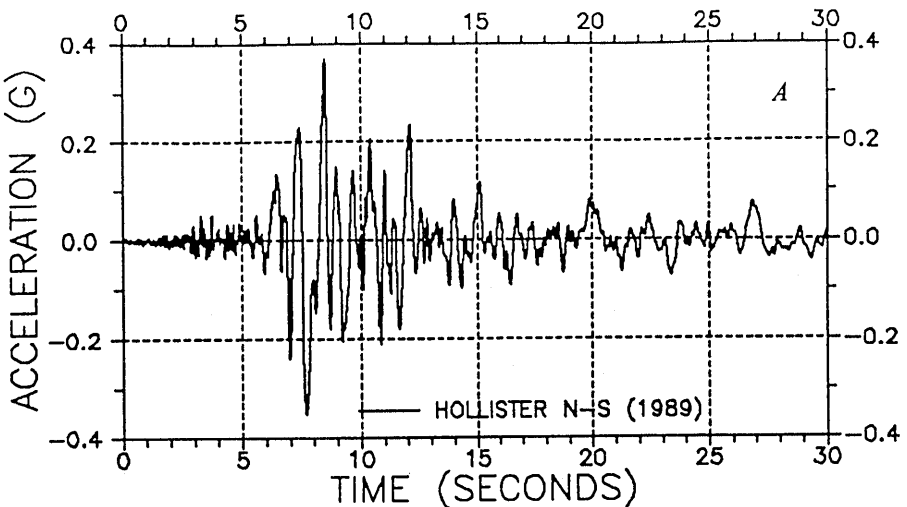


Figure 21.—Ground acceleration recorded at Hollister, Loma Prieta earthquake: north-south component (A); east-west component (B).

level, does not occur in the response envelope of the Hollister motion. Such a decrease, if used to reduce member sizes, could result in a weak section of the structure, although this was not the case for this building.

The response envelopes for the north-south (longitudinal) direction are shown in figure 23. The envelopes of maximum lateral displacement (fig. 23A) are similar to those just discussed for the transverse direction. In this case, the displacements due to the design spectrum ex-

ceed those due to the CCSF code over the height of the structure, and both of these exceed the displacements due to the recorded base motions. The displacement at the roof level due to the Hollister ground motion exceeds that due to the design spectrum by a factor of 1.9, which is slightly less than in the transverse direction. The envelopes of IDI are shown in figure 23B. The values due to the recorded base motions are less than those due to the design spectrum over the height of the structure; how-

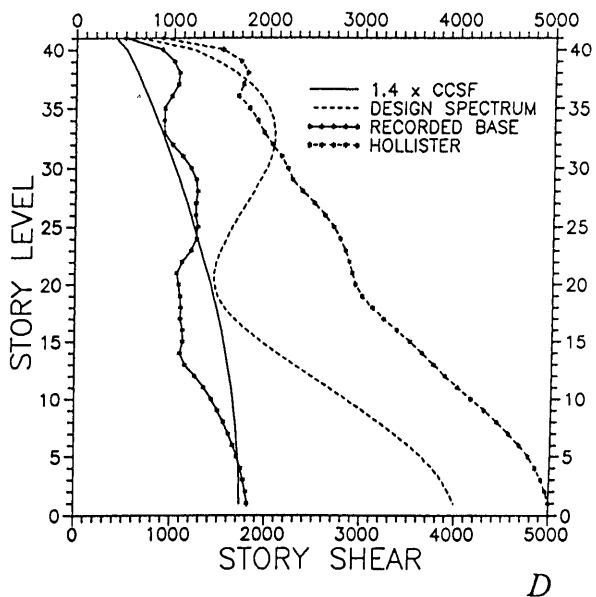
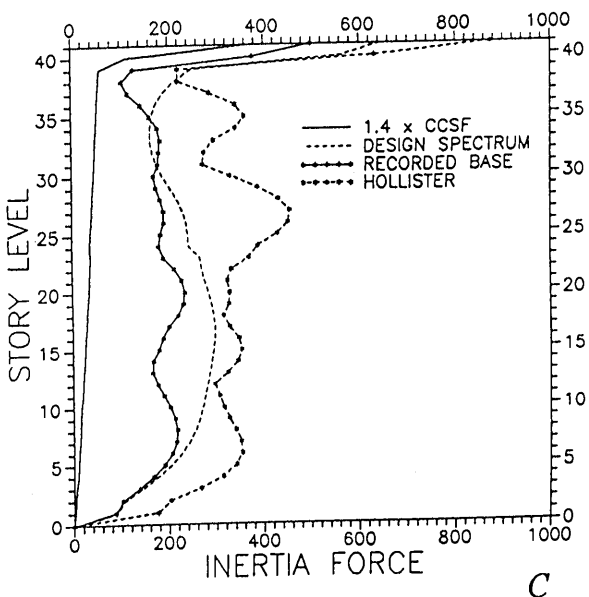
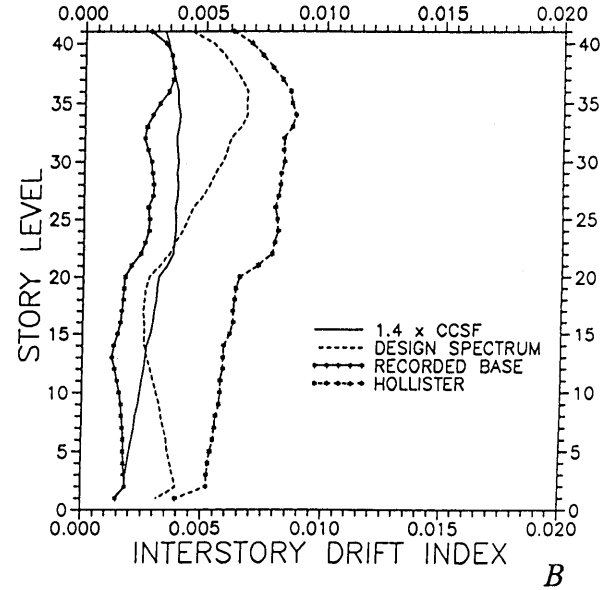
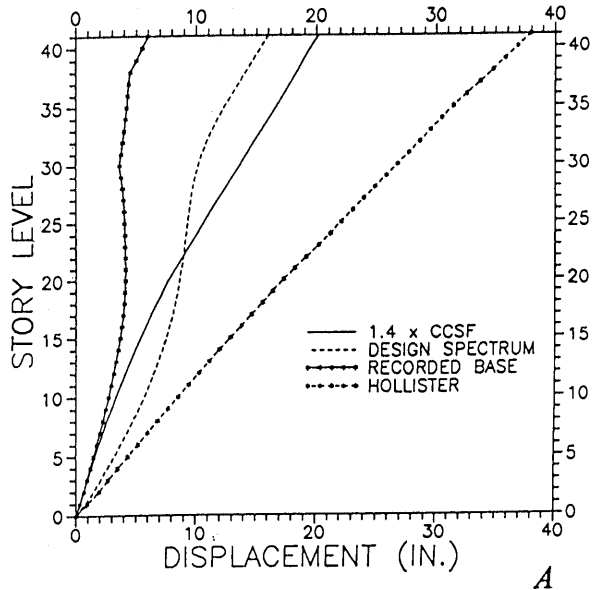


Figure 22.—Transverse response envelopes: lateral displacement (A); interstory drift index (B); inertia force (C); story shear (D).

ever, they do exceed those due to the CCSF code in the upper 10 floors. The IDI due to the Hollister motions is considerably larger than those due to either the design spectrum or the recorded base motions.

The envelopes of maximum inertia force are shown in figure 23C. As before, the forces specified in the CCSF code represent minimum values. It is interesting to note

that the inertia forces due to the recorded base motion exceed those due to the design spectrum between floors levels 26-33. The forces due to the Hollister motions exceed all others by a substantial margin. The envelopes of story shear (fig. 23D) indicate that the shears due to the recorded motions are less than those due to the design spectrum over the total building height. This indicates

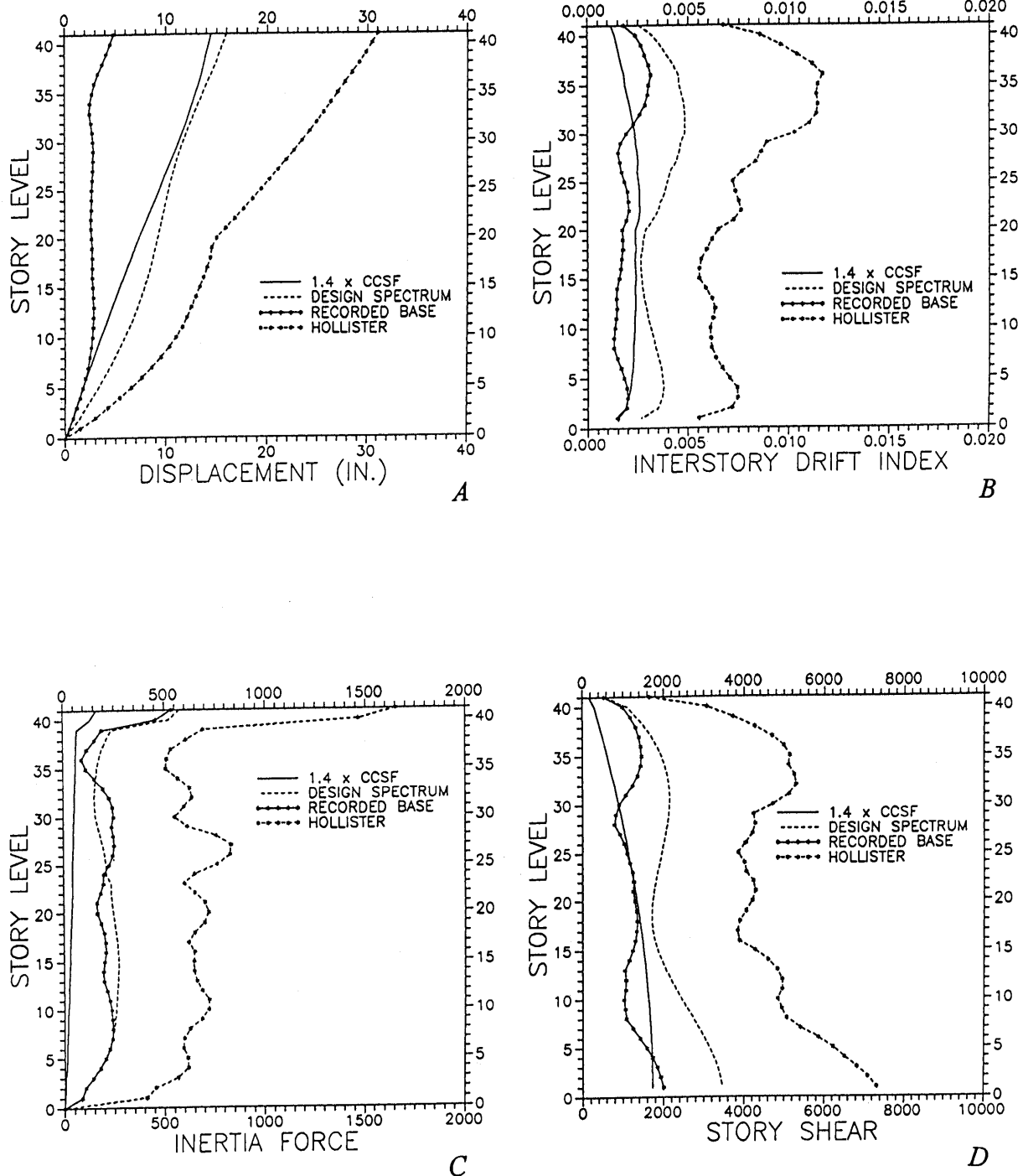


Figure 23.—Longitudinal response envelopes: lateral displacement (A); interstory drift index (B); inertia force (C); story shear (D).

that the behavior of the building in this direction was most likely linear elastic. As in the transverse direction, the shears due to the Hollister motions exceed those due to the design spectrum over the height of the building, indicating inelastic behavior.

CURRENT CODE DESIGN REQUIREMENTS

In the current edition of the Uniform Building Code (1994), the design base shear is given as

$$V = (ZIC/R_w)W,$$

where $C = 1.25S/T^{2/3}$, $I = 1.0$, $R_w = 12$, and $Z = 0.4$.

The fundamental period estimated by code formula is

$$T = C_t h_n^{0.75} = 0.035(549.5)^{0.75} = 3.97 \text{ s},$$

whereas the value calculated using SAP90 is 5.75 s. The code requires that the value of the period not be more than 30 percent greater than the value given by the above formula. Therefore, using 5.16 s for the period and a site

factor of 1.5 (soil type 3), the value of C is calculated as 0.628. Using this value for C , the design seismic resistance seismic coefficient is calculated as

$$C_s = ZIC/R_w = 0.021,$$

which represents 2.1 percent of the dead load and is the same as the CCSF lateral force requirement. However, an additional requirement in the 1994 UBC code requires that

$$C > 0.075R_w = 0.9,$$

which has the effect of placing a lower bound on the base shear for tall buildings. Using this value, the design seismic resistance coefficient becomes

$$C_s = 0.030$$

and results in a base shear of 1,874 kips.

The lateral force requirements in the UBC require a dynamic analysis for a building of this height (550 ft, >240 ft). If a site-specific design spectrum is not provided, the design spectrum provided in the code can be used with the appropriate soil type.

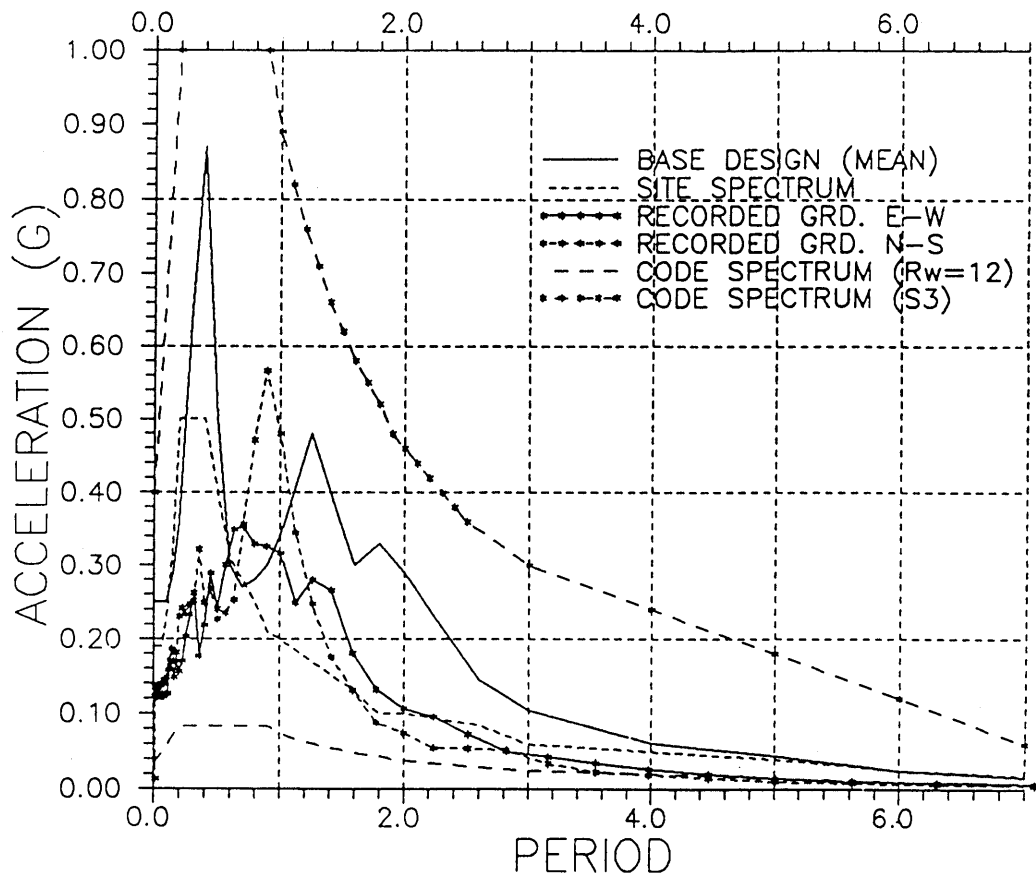


Figure 24.—Design spectra vs. recorded motion.

The code design spectrum and the site-specific design spectrum are compared with the spectra of the recorded ground motions in figure 24. The code spectra with a structural system coefficient ($R_w=1$) results in the highest spectral values, whereas using a system coefficient of $R_w=12$, which is typical for this type of structure, results in the lowest spectral values. Hence the code design spectra envelope the other spectra depending on the value of the structural system coefficient that is used. Based on the results presented, it would appear that the use of a value of 12 is excessive.

The site spectrum has a peak spectral acceleration of 0.5 g in the period range of 0.2 to 0.4 s, which is representative of rock motion at the site. The base design spectrum reflects the influence of local soil conditions on the response. It has a peak spectral acceleration of 0.87 g at a period of 0.4 s and a second peak of 0.48 g at 1.25 s. The spectrum for the recorded ground motion in the east-west direction has a peak spectral acceleration of 0.57 g at a period of 0.9 s. The spectral values of the two components of recorded base motion in the east-west and north-south directions are very similar, with the exception of the period range around 0.9 sec where the spectral acceleration in the north-south direction is truncated and only reaches 0.36 g .

These results emphasize the uncertainty that surrounds the selection of an appropriate structural system factor and the determination of the soil period for site-specific spectra. It is noteworthy that the recorded base accelerations were no greater than 0.12 g , which would certainly be considered a service loading condition.

If the base shear obtained using a dynamic, response-spectrum analysis differs from that obtained using the static lateral force procedure, it may be scaled to the following percentage of the static value: (1) One hundred percent for irregular buildings or (2) ninety percent for regular buildings, except that the base shear shall not be less than 80 percent of that determined using the calculated period. The code further states that "All corresponding response parameters, including deflections, member forces and moments shall be increased proportionately." In the analyses that follow, the base shear has been scaled to 100 percent of the static value. This result is identified as "Scaled UBC" in the figures that follow.

The lateral displacements and forces obtained using the code spectrum for a type 3 soil are compared with the static lateral force requirements and the recorded values in figure 25 for the east-west (transverse) direction. The envelopes of maximum lateral displacement (fig. 25A) indicate that the displacements obtained from the static lateral forces far exceed those obtained from the scaled spectrum. This reflects the influence of the code requirement that places up to 25 percent of the base shear at the top of the structure. The displacement response due to Loma Prieta is less than that obtained using the scaled

spectrum. The envelopes of maximum interstory drift index (IDI) are shown in figure 25B. As before, the IDI for the static lateral loads exceeds the spectral values, with the exception of the bottom four floor levels. The response due to the scaled spectrum is equal to or greater than the recorded response, with the exception of the upper six floors.

The envelopes of the maximum lateral inertia forces are shown in figure 25C, and the corresponding envelopes of maximum story shear are shown in figure 25D. It can be seen in figure 25D that the base shears due to the static forces and the scaled spectrum are equal as a result of the scaling procedure. By coincidence, the base shear due to the recorded ground motion is also approximately equal to the code value. However, it is of particular interest to note that story shears due to the recorded ground motion exceed the scaled code spectrum in the upper half of the structure, with peak differences at the 38th level and the 28th level. This clearly indicates the importance of the response of the higher modes of vibration and their influence on the scaling procedure, which is based on base shear. The higher modes tend to increase the response at the base and in the upper portions of the structure. Scaling upward, based on the base shear, can result in reduced design shear forces over much of the building height.

The lateral displacements and forces obtained using the code spectrum are compared with the static lateral force requirements and the recorded Loma Prieta values in figure 26 for the north-south (longitudinal) direction. The lateral-displacement response shown in (fig. 26A) is very similar to that of the previous case, wherein the displacements of both the static and scaled spectra exceeded the displacements due to the recorded motions over the height of the structure. The envelopes of maximum IDI are shown in figure 26B. It can be seen that the IDI due to the recorded base motion exceeds that of the scaled spectrum for all stories above the 32d floor. It even exceeds that of the equivalent static loading for floor levels 33 to 40.

The envelopes of maximum lateral inertia forces are shown in figure 26c where it can be seen that the forces due to the recorded base motion exceed those of the scaled spectrum over the entire building height. The envelopes of maximum story shear are given in figure 26d. As required by the scaling procedure, the shear due to the static load and that due to the scaled spectrum are equal at the base. This figure indicates that in the upper nine floors the story shears due to the recorded base motion exceed those due to both the static forces and the scaled spectrum. The shears of the scaled spectrum are also exceeded at mid-height, between stories 17 and 25. Toward the base of the structure, both the static and scaled spectrum values are exceeded in the bottom three stories. This indicates that had this structure been designed according to

the current code requirements, the damage due to the relatively low base motions recorded at the site would have been much more substantial. As mentioned previously, the building was designed for a site-specific design spectrum which was substantially higher than current code requirements.

EARTHQUAKE DAMAGE POTENTIAL

In general, the base shear is not a very accurate parameter for estimating the severity and damage potential of earthquake ground motions. A more sensitive parameter is the elastic input energy, which can be calculated as the

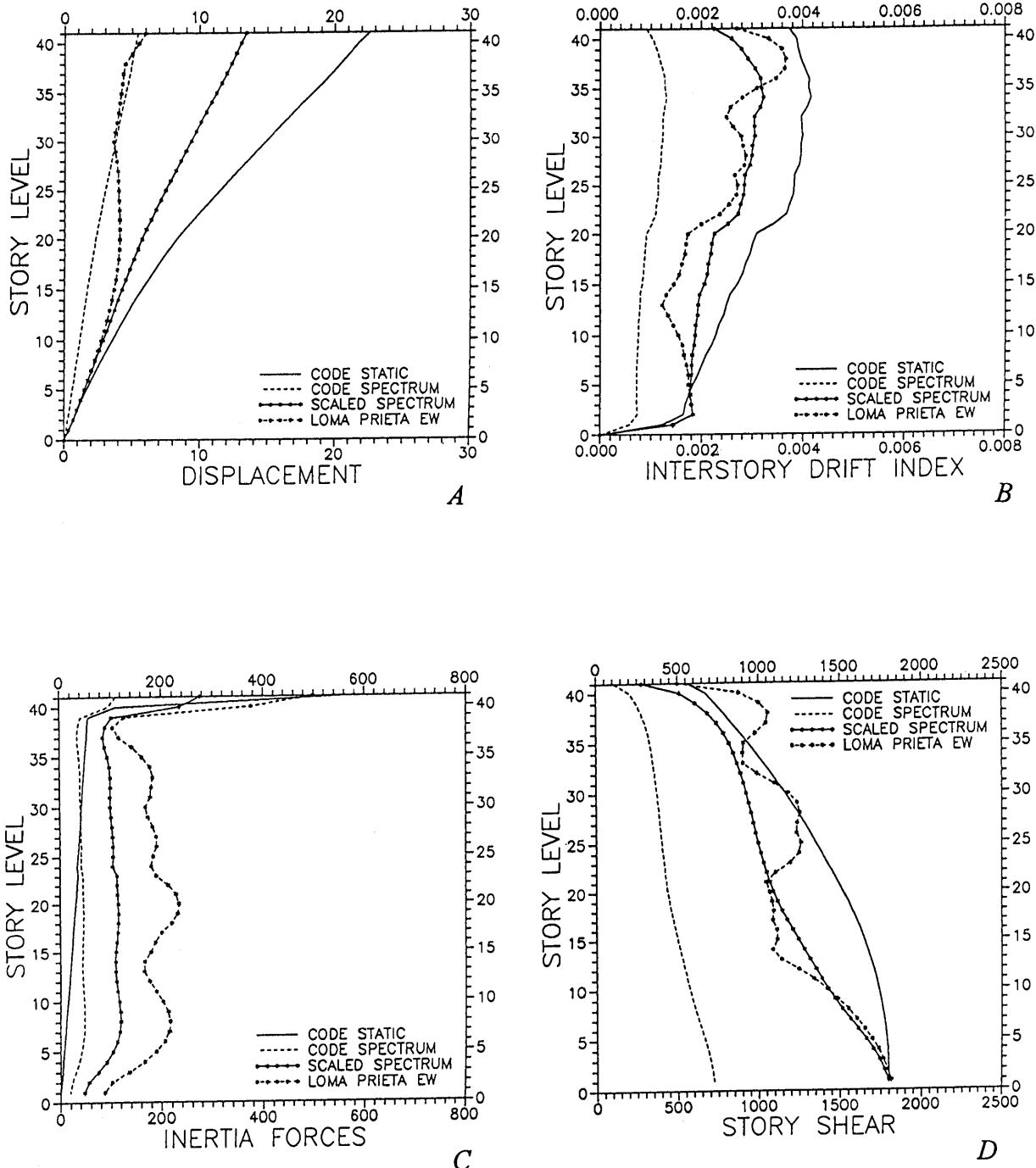


Figure 25.—Code design vs. recorded response, transverse: lateral displacement (A); interstory drift index (B); inertia force (C); story shear (D).

product of the base shear and the base displacement as mentioned previously. The elastic input energy for this structure due to the Loma Prieta base motion is compared with that of three other strong motion earthquakes in figure 27. These include James Road (Imperial Valley, 1979), SCT (Mexico City, 1985) and Hollister (Loma Prieta,

1989). The input energy in the east-west direction is shown in figure 27A, which clearly indicates that the motion from the Loma Prieta earthquake which was recorded at the base of this structure did not input a significant amount of energy to the structural system. It does indicate that the James Road ground motion, discussed previously by

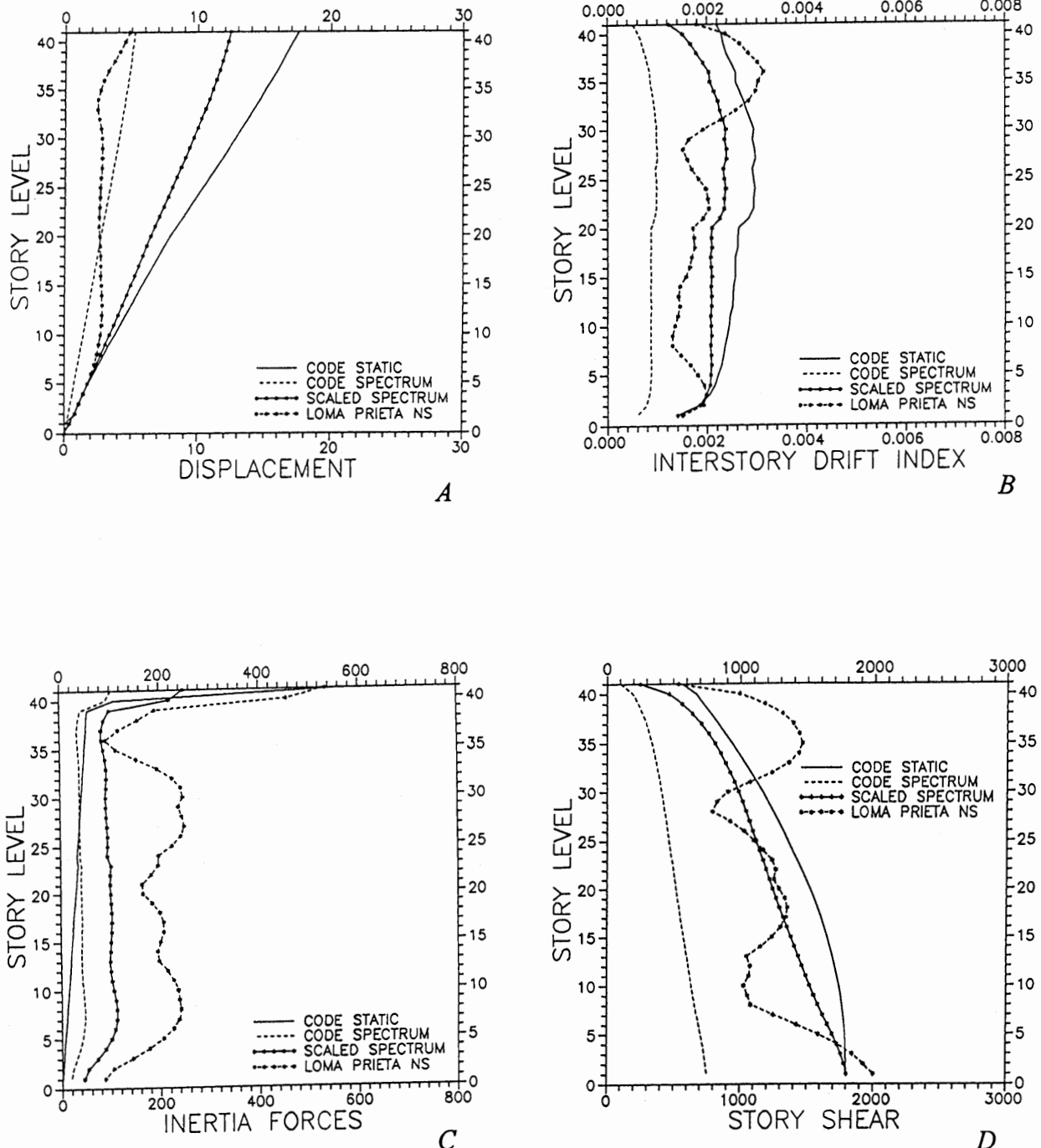


Figure 26.—Code design vs. recorded response, longitudinal: lateral displacement (A); interstory drift index (B); inertia force (C); story shear (D).

Anderson and Bertero (1994), and the Hollister ground motion discussed in this paper are much more severe. It can be seen that the energy input due to James Road occurs with a sudden jump, whereas that due to the SCT ground motion builds up over a long period of time. Recall that the James Road record contains large accelera-

tion pulses and is representative of near-fault motion, whereas the SCT record is almost sinusoidal in character, starts very slowly, and is representative of a large, distant earthquake. Elastic input energy in the north-south direction has similar characteristics and is shown in figure 27B.

CONCLUSIONS

This paper has discussed some of the response studies conducted on an instrumented 42-story steel building. Attention has been focused on the elastic response analysis. More complete details and the results of nonlinear analyses are to appear in a future University of California, Berkeley/Earthquake Engineering Research Center report. The results presented in this paper suggest the following general conclusions:

1. Estimation of the soil periods at a given site is very difficult. This uncertainty should be recognized in the development of a design spectra by using a smoothed spectra with a wide-period band.

2. Few recorded ground motions have a high spectral acceleration at the fundamental period of a tall building such as the one considered in this study (5 s). Therefore the influence of the second and higher lateral modes becomes of increasing importance and must be considered in the design process.

3. This building was designed for a base spectrum which resulted in lateral design forces which were substantially above the minimum values required in the building code. For this reason the response due to the recorded Loma Prieta base motions was linear elastic with no damage. Had the minimum code requirements been used, some inelastic behavior may have occurred in the upper half of the building.

4. The code guideline for considering enough modes of vibration to represent 90 percent of the reactive mass is not adequate for tall buildings. Such a requirement for this building would eliminate the need to consider the fourth translational mode in each direction, and it has been shown that these modes make a significant contribution to the response. Inclusion of the fourth mode can increase the acceleration by as much as 50 percent and the displacement by 10 percent. It is recommended that this requirement be increased to 95 percent for tall buildings.

5. Scaling the dynamic response based on the shear at the bottom story is an oversimplification which can result in reduced design forces over much of the height of a tall building. It would be preferable to use a "correct" design spectrum directly. Currently, a reasonable spectrum is scaled down by the structural system coefficient, R_w , and then scaled up by the ratio of the base shears. In the process, the design forces over much of the building height are reduced to values that are substantially lower than the static design

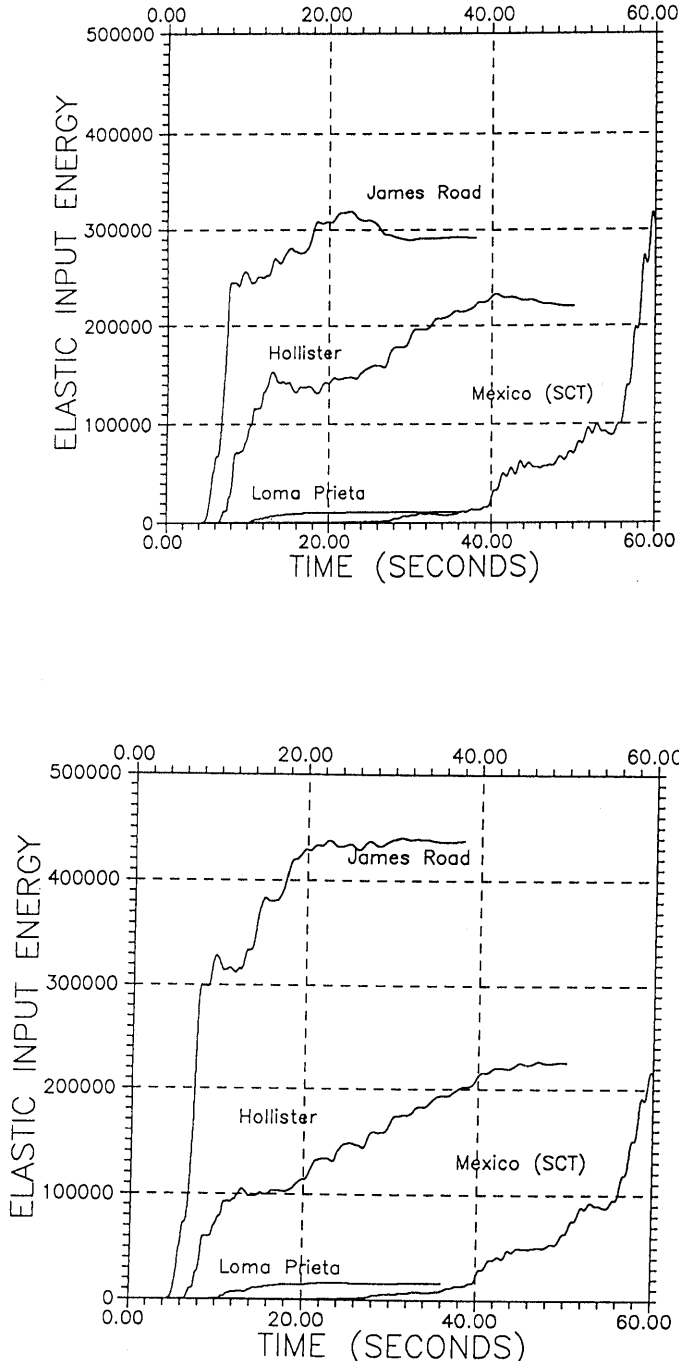


Figure 27.—Elastic input energies, strong earthquakes: transverse (east-west) (A); longitudinal (north-south) (B).

procedure. This reduction does not appear to be reasonable or justifiable and therefore should be eliminated.

ACKNOWLEDGMENTS

This report is based on the results of a series of studies that have been conducted by the authors at the University of California at Berkeley and the University of Southern California. This study is part of a research project entitled "Implications of Response of Structures to Ground Motions Recorded During the Loma Prieta Earthquake: Evaluation of Structural Response Factors," which was supported by a research grant provided by the National Science Foundation.

The authors are grateful to the consulting firm of H.J. Brunnier Associates in San Francisco and particularly to Mr. Edwin Zacher of this firm for providing the drawings and needed information regarding the design of the build-

ing. Records of the recorded motion were provided by the U.S. Geological Survey in Menlo Park. This support is also greatly appreciated.

REFERENCES

- Anderson, J.C., and Bertero, V.V., 1994, Lessons learned from an instrumented high rise building, in Proceedings, Fifth National Conference on Earthquake Engineering, 2: Chicago, Ill., Earthquake Engineering Research Institute,
- Habibullah, A., 1989, ETABS, three dimensional analysis of building systems: Berkeley, Calif., Computers & Structures, Inc.,
- Habibullah, A., 1989, STEELER, stress check of steel frames: Berkeley, Calif., Computers & Structures, Inc.
- Ruiz, R., and Penzien, J., 1969, Probabilistic study of the behavior of structures during earthquakes: Earthquake Engineering Research Center, University of California, Berkeley, Calif., UCB/EERC-69/03
- Wilson, E.L., and Habibullah, A., 1989, SAP90, a series of computer programs for the static and dynamic finite element analysis of structures: Berkeley, Calif., Computers and Structures, Inc.

THE LOMA PRIETA, CALIFORNIA, EARTHQUAKE OF OCTOBER 17, 1989:
PERFORMANCE OF THE BUILT ENVIRONMENT

BUILDING STRUCTURES

A SUMMARY OF UNREINFORCED MASONRY BUILDING DAMAGE
PATTERNS—IMPLICATIONS FOR IMPROVEMENTS IN
LOSS ESTIMATION METHODOLOGIES

By Bret Lizundia, Rutherford & Chekene Consulting Engineers, San Francisco, Calif.;
Weimin Dong, Risk Management Solutions, Menlo Park, Calif.;
William T. Holmes, Rutherford & Chekene Consulting Engineers, San Francisco, Calif.; and
Robert Reitherman, The Reitherman Company, Half Moon Bay, Calif.

CONTENTS

	Page
Abstract -----	C141
Introduction -----	141
Data collected -----	141
Comparison with previous U.S. earthquakes -----	142
Correlation of damage with ground motion and site soils -----	142
Proposed methodology for property loss estimation -----	148
References -----	157

ABSTRACT

This paper summarizes the results of a study of the performance of unstrengthened, unreinforced masonry bearing wall buildings damaged in the earthquake. The collected data, for over 4,800 buildings, are compared with similar damage data obtained from past earthquakes elsewhere in the United States. Observed damage patterns are correlated with modified Mercalli intensity in these past events. In the Loma Prieta event, a number of other, more quantitative measures of ground motion have been developed from strong motion instrument recordings and are correlated with observed damage patterns. The results are used to help develop a new methodology for loss estimation.

INTRODUCTION

In an earthquake, unreinforced masonry (URM) bearing wall buildings are generally considered to be one of the most dangerous building types. They have been responsible for significant property damage and loss of life in previous earthquakes, both in the United States and around the world. In the Loma Prieta earthquake, many

URM bearing wall buildings were seriously damaged and were the cause of nine deaths.

Due to the interest and foresight of the City of San Francisco, a large amount of damage data was collected on URM bearing wall buildings in San Francisco in conjunction with postearthquake emergency building evaluations, using a form created by Rutherford & Chekene, a San Francisco engineering firm. The earthquake affected not only San Francisco but many other cities and communities as well. Funding was obtained from the National Science Foundation and the California Seismic Safety Commission after the earthquake to further investigate URM damage. Substantial data were collected from numerous communities. The results of that work were summarized in Lizundia and others (1991). Lizundia and others (1993) involves more detailed analysis of the damage data and correlation to various ground motion parameters as well as application of the data to and discussion of improvements in loss estimation methodologies. Collected data were organized into computer files that are available to interested researchers.

In this paper, we have organized a presentation of the results of that study into four sections: (1) a discussion of the data collected, (2) comparison of the data with that from previous U.S. earthquakes, (3) correlation of the damage data with various quantitative measures of ground motion, and (4) development of a new proposed methodology for property loss estimation.

DATA COLLECTED

Lizundia and others (1991, 1993) discussed in detail the methodology and sources used to collect the data. Telephone calls, letters, building department records, field surveys by other engineers, and our own field surveys

were used to collect data. In general, the more damage that the buildings in a community suffered, the more time we devoted to obtaining damage data.

The collected data have been categorized into three levels of quality. The lowest level, Level 1, has data from 113 communities in the nine-county Bay Area—a region which easily encompasses the modified Mercalli intensity (MMI)=VI-VII contour line on the USGS intensity map (U.S. Geological Survey, 1989). These communities are shown in figure 1. Level 1 data have the greatest number of building records, but the information is restricted to "general damage status"—the number of damaged, vacated, and demolished buildings in each community. In these nine counties, there were at least 4,824 unstrengthened URM bearing wall buildings, of which at least 758 were damaged. Of those damaged, at least 384 were vacated, and of those vacated, at least 54 were demolished. Using data from the 78 communities with four or more URM buildings, we have generated geographic contour maps showing the percentage of damaged and vacated buildings (figs. 2, 3).

Level 2 data cover a subset of nine cities and 2,356 buildings, but have ATC-13 (Applied Technology Council, 1985) "damage states" as well as other information on building characteristics and damage patterns. The cities included are Campbell, Gilroy, Hollister, Los Gatos, Oakland, Salinas, San Francisco, Santa Cruz, and Watsonville. Table 1 organizes the Level 2 data in the ATC-13 format; table 2 organizes the data by general damage status versus MMI. Table 3 compares damage states with general damage status.

Table 1 also includes the sample mean, standard deviation (biased), and coefficient of variation (COV) for the damage ratio at each MMI. As expected, the mean damage ratio increases as the MMI increases. Another important finding is that the COV is quite large, indicating that there is significant scatter in the collected data. The COV is, in fact, larger than unity for each MMI. As the table shows, the data are not symmetric about the mean; particularly for MMI's of VI, VII, and VIII, there are a large number of very small damage ratios (those equal to zero or 0.005) and a smaller number of higher damage ratios (those equal to 0.055, 0.2, 0.45, 0.8, and 1.0). The result of this distribution is that the mean is close to the low values, but the scatter or variance caused by the higher values being farther from the mean leads to a relatively large standard deviation. Although probabilistic models have not been developed in this paper to represent the data, it is clear that a normal distribution would be an inappropriate representation of the damage ratio. A beta distribution would appear to be a likely candidate; the beta distribution was used to develop the damage probability matrices in ATC-13.

The best set of data, Level 3, covers only the 896 buildings in San Francisco; it includes cracking patterns, other

damage information, ATC-13 and ATC-20 (Applied Technology Council, 1989) ratings and building characteristics. Note that over 1,000 buildings which have been addressed by the city's parapet strengthening program have not been included in this study because they are not truly "unstrengthened." Statistical t-testing has been done in an attempt to correlate ATC-13 levels of damage in these buildings with site soils and building attributes. We found that soil conditions and mean story height had a statistically significant influence on the average damage ratio (defined as the ATC-13 assumed repair cost divided by replacement value). Table 4 provides a comparative summary of results. For additional details, see Lizundia and others (1993).

COMPARISON WITH PREVIOUS U.S. EARTHQUAKES

To place the Loma Prieta event in a larger context, we compare our collected damage data with that obtained from past U.S. events. Foreign damage data was deliberately excluded because of concerns about comparability of building construction details. The resulting compilation of earthquake data is believed to be one of the most comprehensive ever. A rigorous attempt has been made to use a consistent format for data presentation so that damage at different MMI levels can be compared with current prediction tools such as the ATC-13 damage probability matrices (DPM's). Table 5 summarizes the results. We are aware that table 5 contains significant simplifications of the concepts in ATC-13. The information in the literature is not specific enough to allow separating ATC-13 damage states 1 and 2, or 3 and 4, or MMI=VIII and IX. Table 5 includes data sets from the following earthquakes: 1886 Charleston (South Carolina), 1906 San Francisco, 1933 Long Beach, 1952 Bakersfield, 1971 San Fernando, 1983 Coalinga, 1983 Mackay (Idaho), 1984 Morgan Hill, and 1989 Loma Prieta (Level 2 data only). Data from the 1987 Whittier and 1994 Northridge earthquakes are not included.

CORRELATION OF DAMAGE WITH GROUND MOTION AND SITE SOILS

Because of the absence of strong motion instruments in most past earthquakes, correlation of damage with ground motion has typically been done using intensity. For the Loma Prieta earthquake, more than 20 quantitative measures of ground motion developed from 90 California Strong Motion Instrumentation Program and U.S.

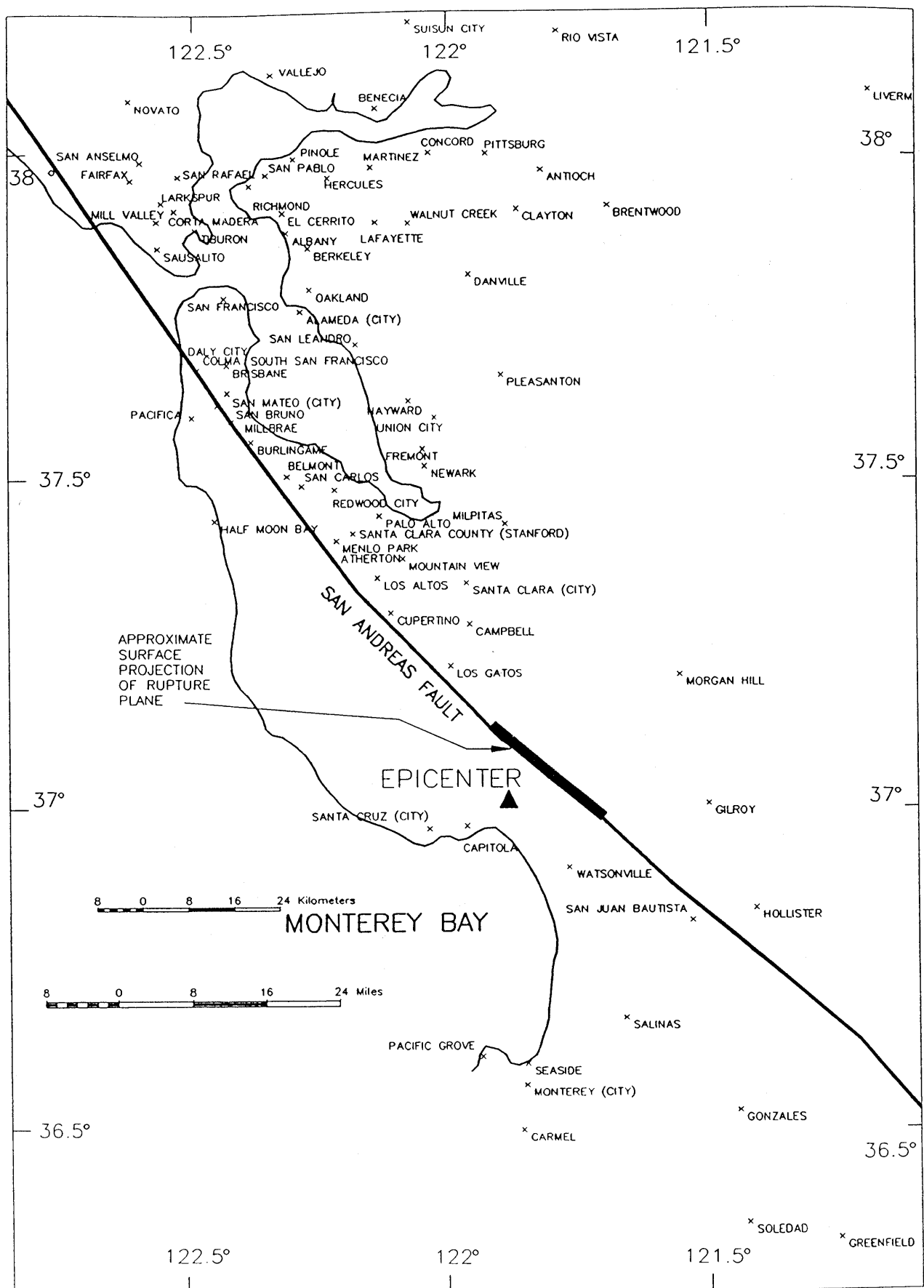


Figure 1.— Cities with URM buildings and with known numbers of damaged and vacated buildings

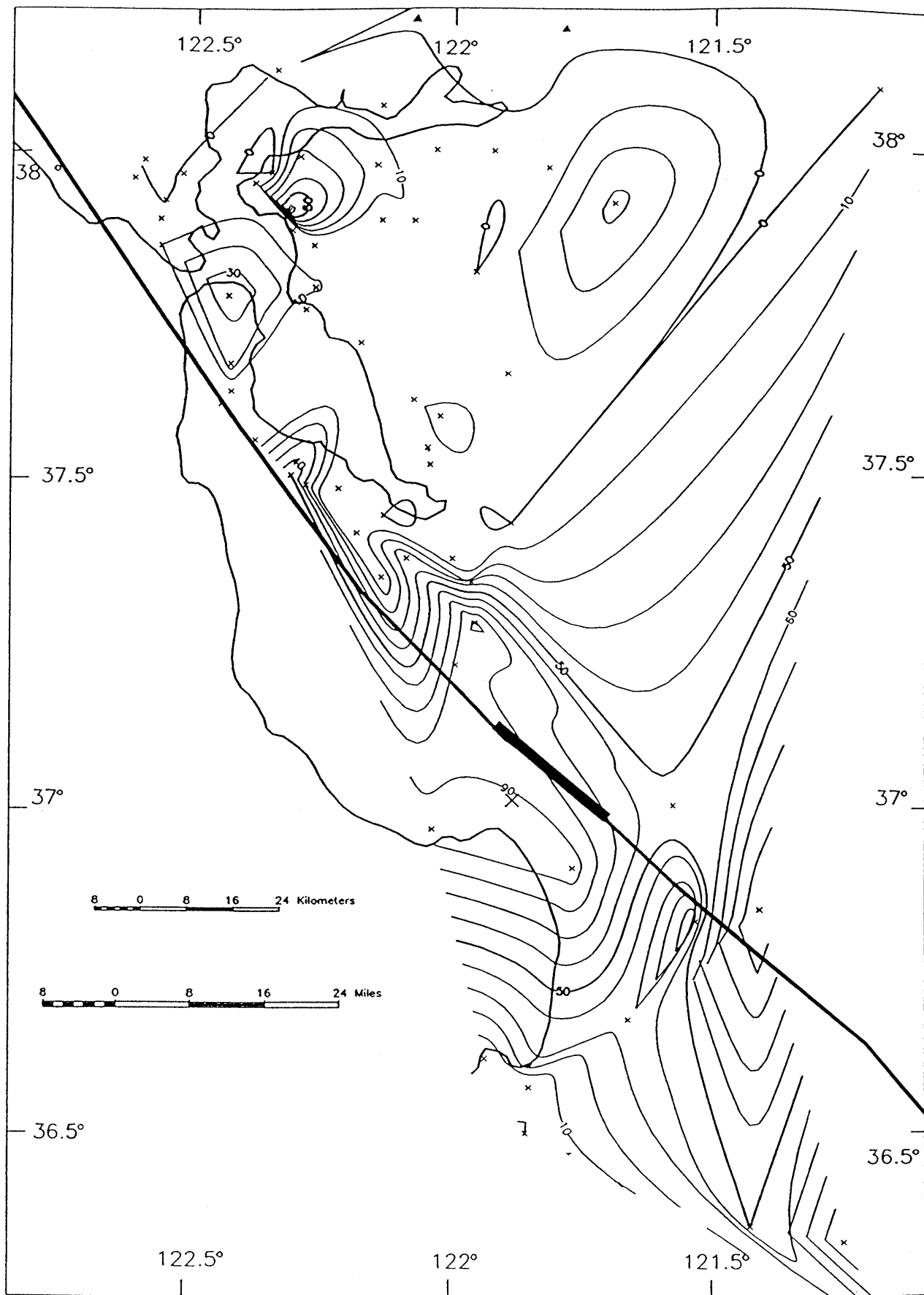


Figure 2.— Contour percentages of total URM buildings which were damaged (cities with four or more total buildings)

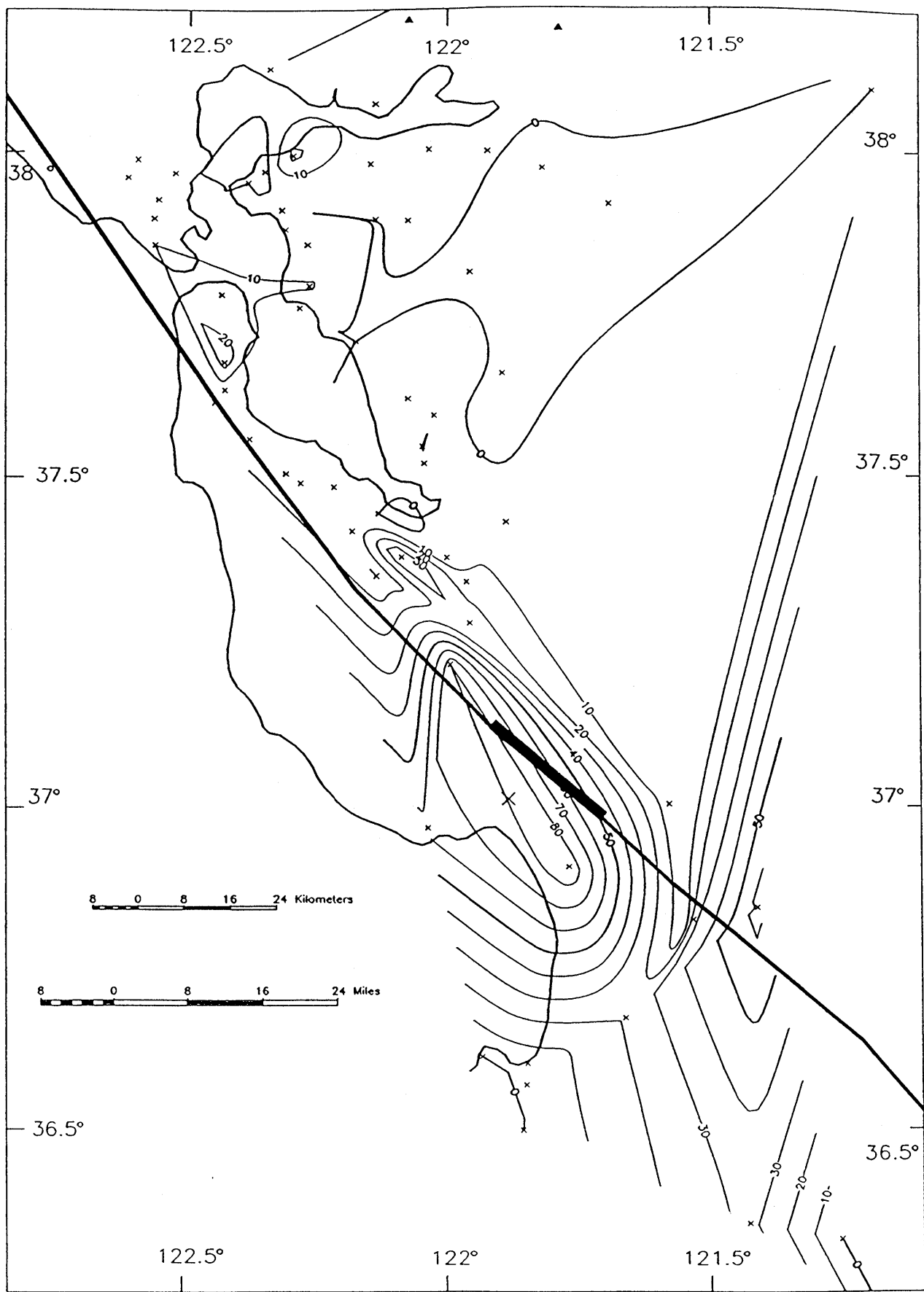


Figure 3.— Contour percentages of total URM buildings which were vacated (cities with four or more total buildings)

Table 1.—*Level 2 damage state data*

Damage state	Damage state description	Assumed central damage ratio	MMI							
			VI		VII		VIII		IX	
			#	%	#	%	#	%	#	%
1	None	0	409	69.08	1199	78.21	82	45.81	0	0
2	Slight	0.005	98	16.59	141	9.20	20	11.17	6	22.22
3	Light	0.055	53	8.98	111	7.24	29	16.20	14	51.85
4	Moderate	0.20	24	4.06	34	2.22	12	6.70	3	11.11
5	Heavy	0.45	5	0.85	40	2.61	33	18.43	3	11.11
6	Major	0.80	3	0.51	8	0.52	2	1.12	1	3.70
7	Destroyed	1.00	0	0	0	0	1	0.56	0	0
Total with known damage state			592	100	1533	100	179	100	27	100
Total with unknown damage state				4		21		0		0
Mean damage ratio				2.17%		2.48%		12.04%		13.15%
Standard deviation				7.99%		9.55%		19.69%		18.69%
Coefficient of variation				3.68		3.85		1.64		1.42

Table 2.—*General damage status for Level 2 data vs. MMI*

General damage status	MMI							
	VI		VII		VIII		IX	
	#	%	#	%	#	%	#	%
Damaged (but not vacated or demolished)	115	68.86	128	41.56	5	5.38	1	3.85
Vacated (but not demolished)	49	29.34	165	53.57	56	60.22	25	96.15
Demolished	3	1.80	15	4.87	32	34.41	0	0
Total with known damage status	167	100	308	100	93	100	26	100
Unknown damage status	58		74		10		1	

Table 3.—*Comparison of damage states and general damage status in Level 2 data*

Damage states		General damage status							
Damage state	Damage state description	Damaged (but not vacated or demolished)		Vacated (but not demolished)		Demolished		Unknown	
		#	%	#	%	#	%	#	%
1	None	0	0	10	3.39	0	0	61	50.83
2	Slight	175	70.28	63	21.36	3	6.25	24	20.00
3	Light	64	25.70	119	40.34	2	4.17	22	18.33
4	Moderate	10	4.02	50	16.95	1	2.08	12	10.00
5	Heavy	0	0	43	14.58	37	77.08	1	0.83
6	Major	0	0	10	3.39	4	8.33	0	0
7	Destroyed	0	0	0	0	1	2.08	0	0
Total		249	100	295	100	48	100	120	100

Table 4.—*Influence of site soil type and mean story height on damage*

	Variable	Mean damage ratio (%)	Number of buildings with known damage ratios	Number of buildings with unknown damage ratios
1991 UBC site soil classification	1	0.49	45	0
	2	4.78	660	12
	3 or 4	6.68	171	8
Mean story height	≤ 4.9 m (16 ft)	3.95	637	16
	> 4.9 m (16 ft)	7.90	239	4

Table 5.—Comparison of historical data with ATC-13

[Source: The Reitherman Company, Half Moon Bay, Calif.]

Damage state	Assigned central damage ratio	MMI					
		VII		VIII-IX		#	%
		Historical	ATC-13 ¹	Historical	ATC-13 ^{1,2}		
1 and 2	0.005	1,352	87	1	712	16	0
3	0.05	116	7	56	1,047	24	6
4	0.20	43	3	43	1,608	37	43
5 and 6	0.65	48	3	1	738	17	50
7	1.00	0	0	0	267	6	0
Totals		1,559	100	100	4,372	100	100
Mean damage factor ³		---	3	12	---	25	40

¹From facility class = 75, low rise (1-3 stories).
²Mean of the MMI=VIII-IX values.
³Mean damage factor here is the sum of the assigned central damage ratio times the percentage in the damage state.

Geological Survey free-field strong motion recordings have been correlated with observed damage patterns. These measures include the maxima and mean of horizontal and vertical components of acceleration, velocity, pseudospectral acceleration and pseudospectral velocity, "frequency" (defined as the number of zero crossings in the acceleration record), bracketed duration, Arias Intensity, the "destructiveness potential factor" of Araya and Saragoni (1985), and the number of horizontal acceleration peaks over 0.10 g and the sum of those excursions. Selected strong motion stations are shown in figure 4. Several different correlation techniques were used. The first technique was a visual comparison of the building damage contour maps (figs. 2, 3) with similar maps of the various ground motion parameters. Pseudospectral acceleration (SPA) and pseudospectral velocity (SPV) maps at a 0.5-s period were found to provide potentially the best match with the damage maps. They are shown in figures 5 and 6. Figure 7 shows the maxima of the two horizontal acceleration records (AHMAX) plot when all soil types are included. Strong motion stations were, in fact, assigned to three different site soil types. Soil Types 1 and 2 correspond to 1991 UBC categories. Soil Type 3 is a combination of UBC categories 3 and 4 since there are so few records for these soft soil sites. Comparison of plots of ground motion instruments from one soil type with another clearly shows the impact of surficial soils in influencing the recorded ground motion. See figures 8, 9, and 10 for the influence on AHMAX.

Other correlation techniques were used to quantitatively compare damage and ground motion. Before this could

occur, however, it was necessary to interpolate the ground motion at each building site since the strong motion locations do not correspond to the building locations. A rigorous process was used to take into account the proximity of the instrument to a building, the attenuation of the ground motion, and the site soil characteristics. Details are contained in Lizundia and others (1993). Following the interpolation process, one alternative correlation technique involved sorting the Level 2 damage data by groups within the ground motion parameters. The characterization of damage states uses the ATC-13 classifications and provides similar DPM's. Table 6 provides an example for horizontal acceleration. Note that the mean damage ratio does not consistently increase as the acceleration increases, and, like table 1, the standard deviations are quite large.

The last and the most rigorous correlation procedure involved the use of multivariate regression analysis and discriminant analysis discussed in Miller (1962). Using this procedure, we found pseudospectral velocity and, to a lesser extent, frequency to be statistically significant predictors of the average damage ratio. For details on this process, see Lizundia and others (1993).

PROPOSED METHODOLOGY FOR PROPERTY LOSS ESTIMATION

Popular loss estimation methodologies currently in use, such as ATC-13, directly equate a damage state with a

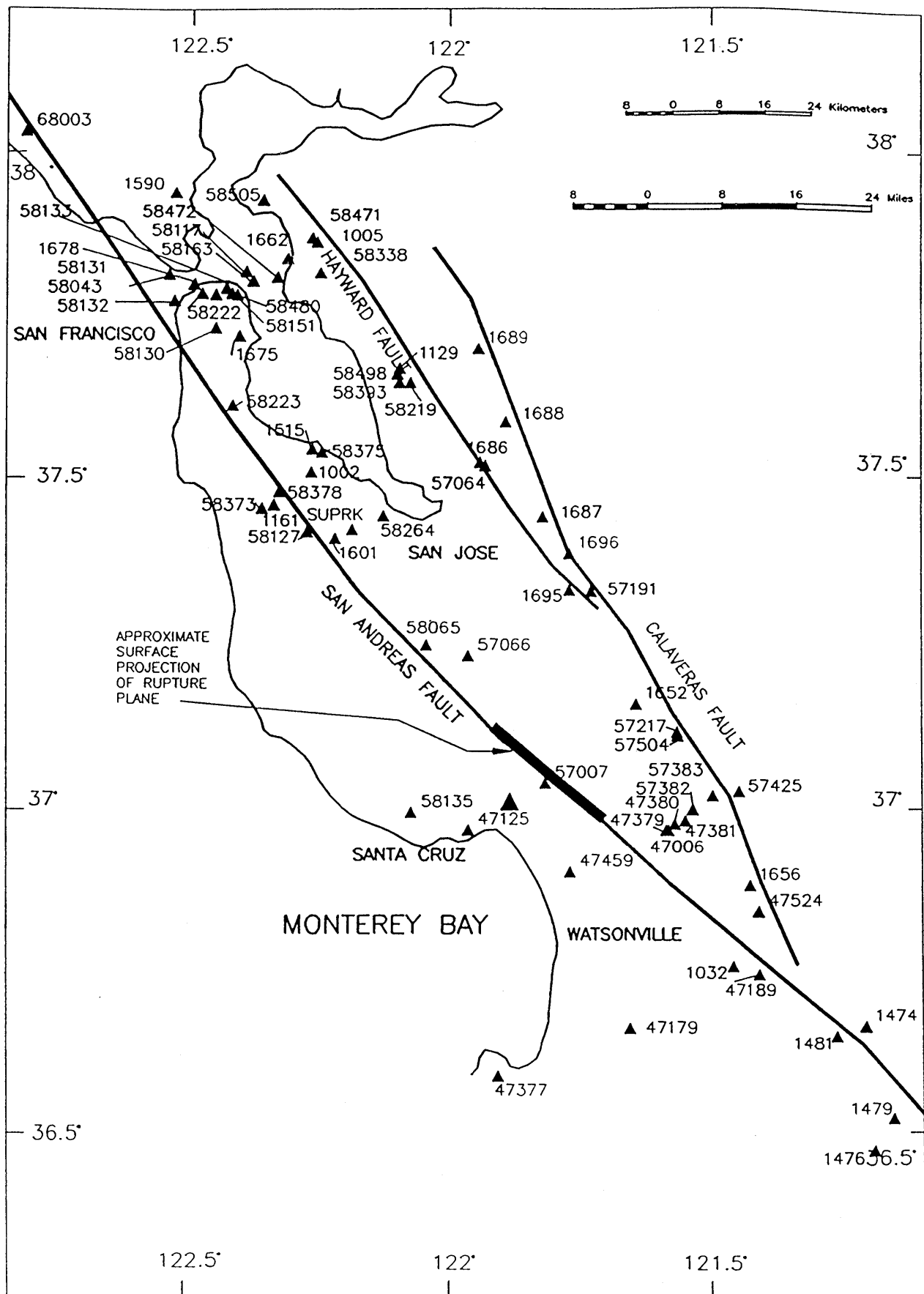
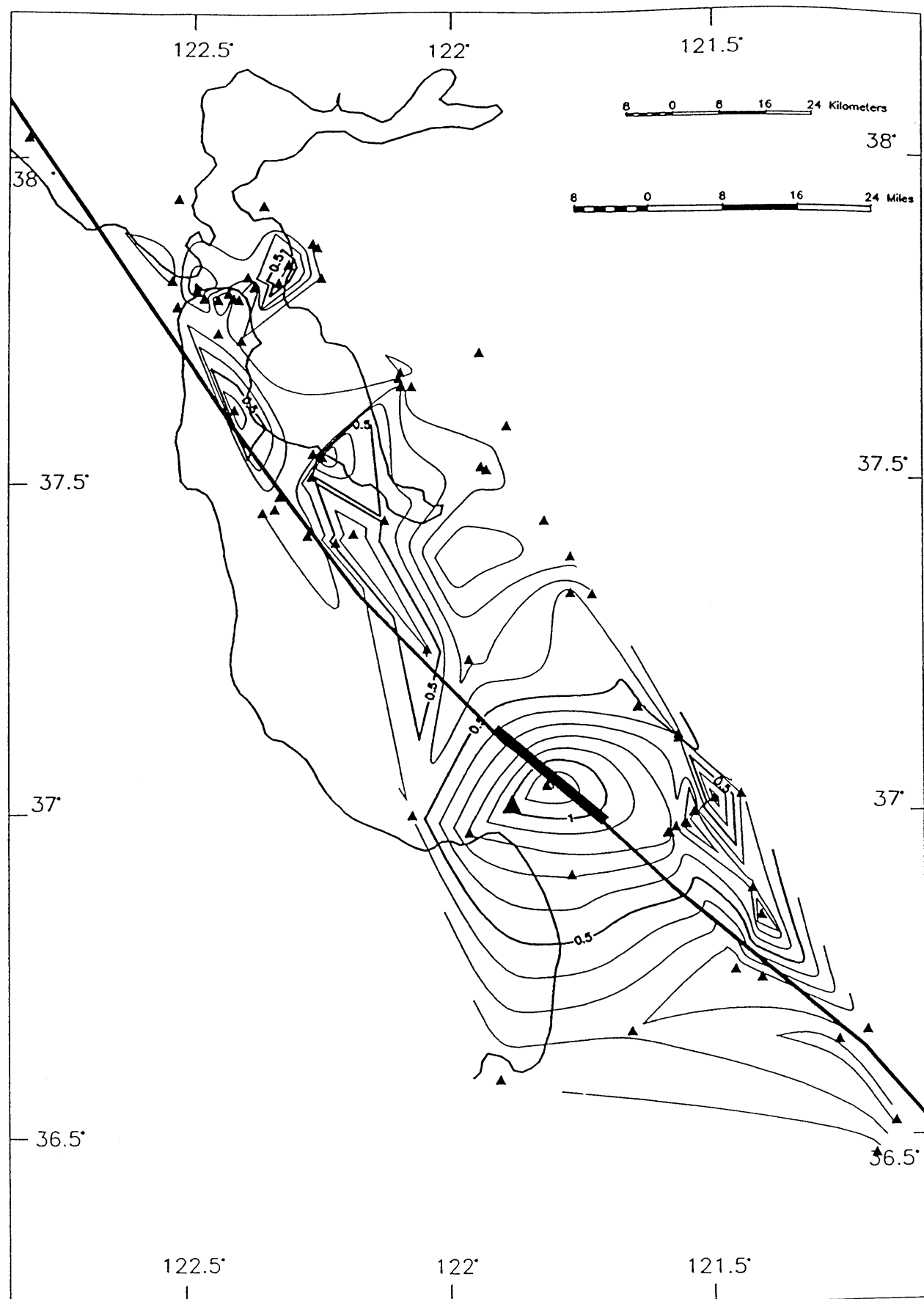
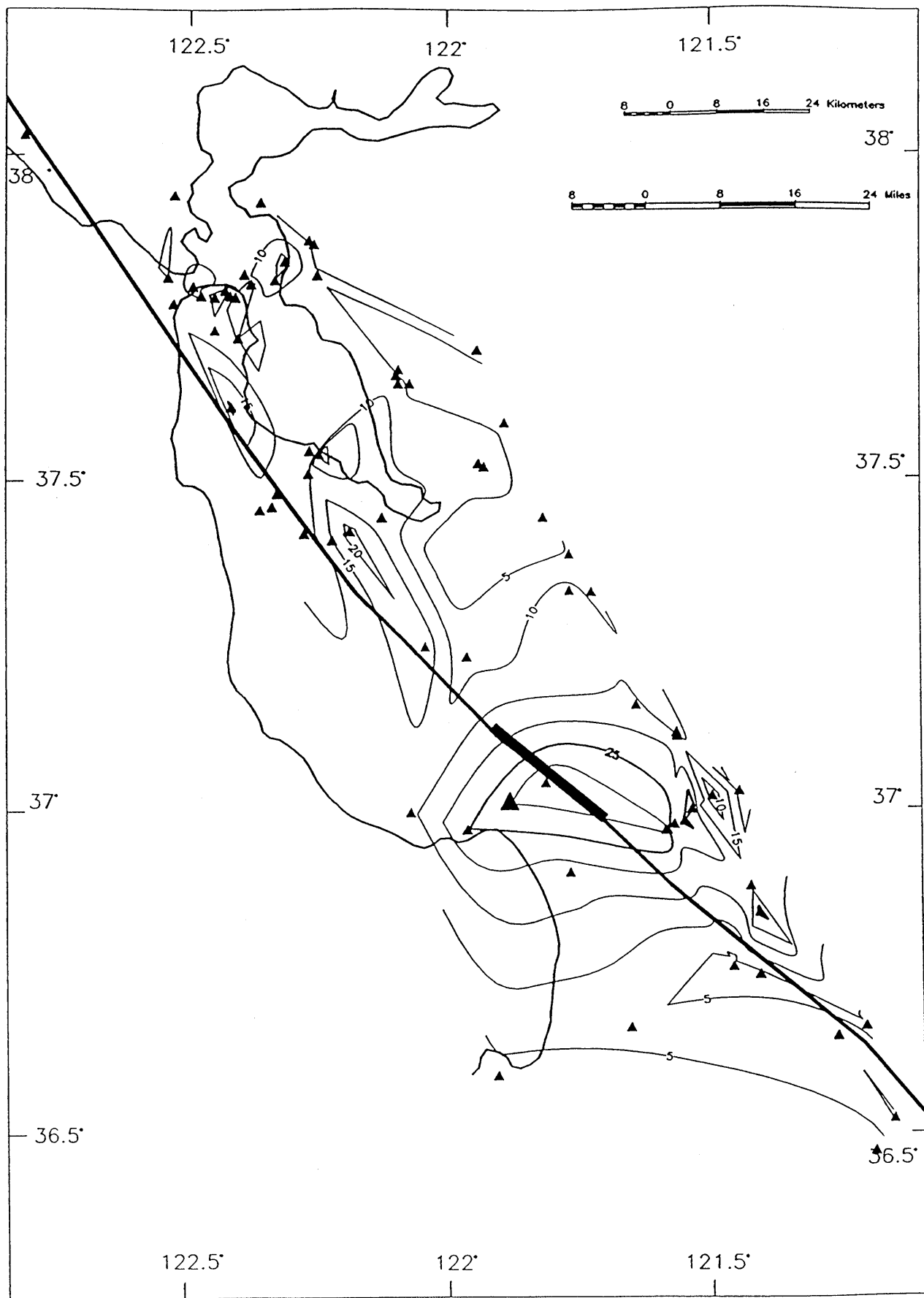


Figure 4.— Location of all stations selected

Figure 5.—Pseudospectral acceleration ($T=0.5$ s)—all soil types

Figure 6.—Pseudospectral velocity ($T=0.5$ s)—all soil types

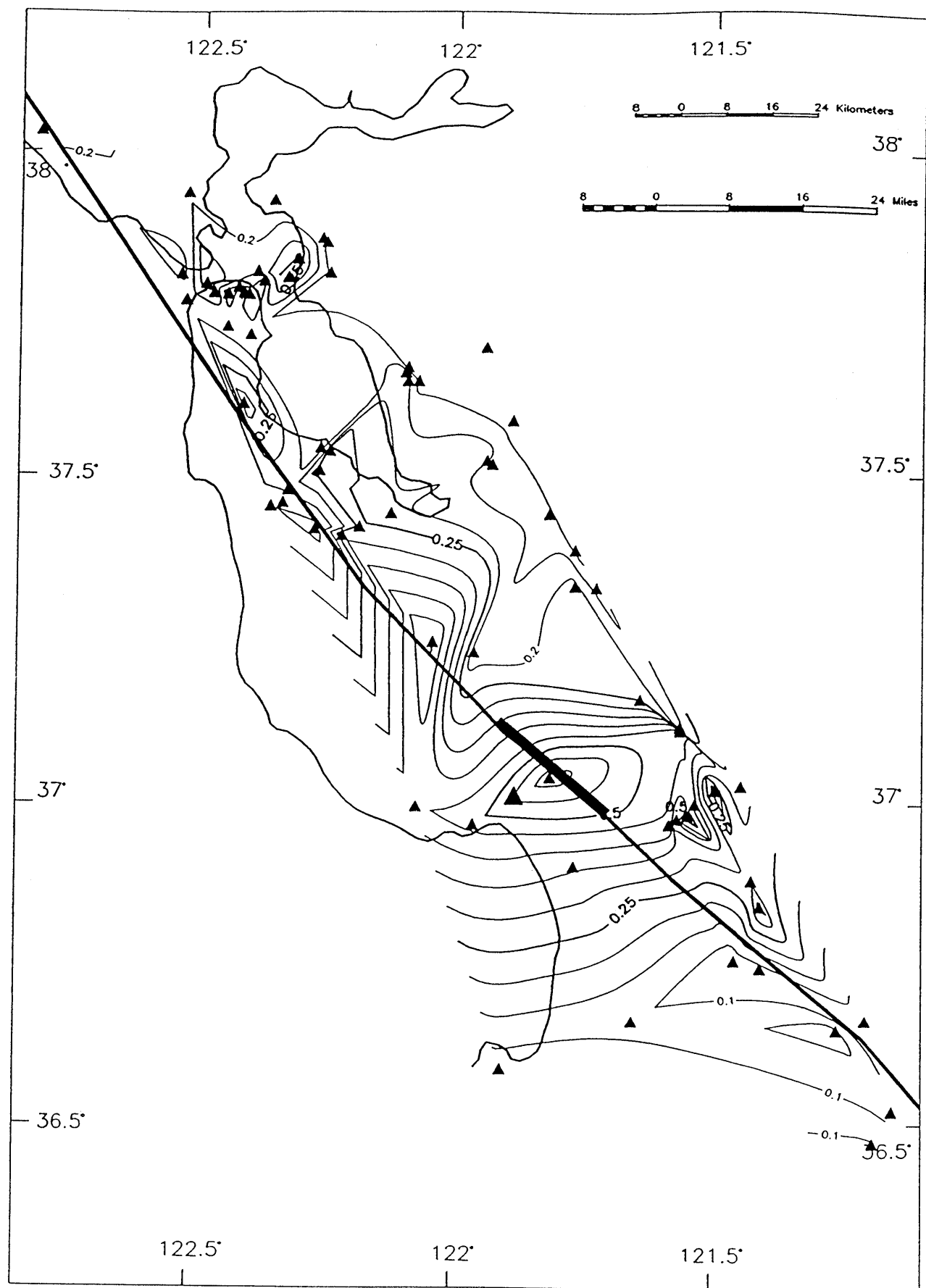


Figure 7.—Maximum horizontal acceleration—all soil types

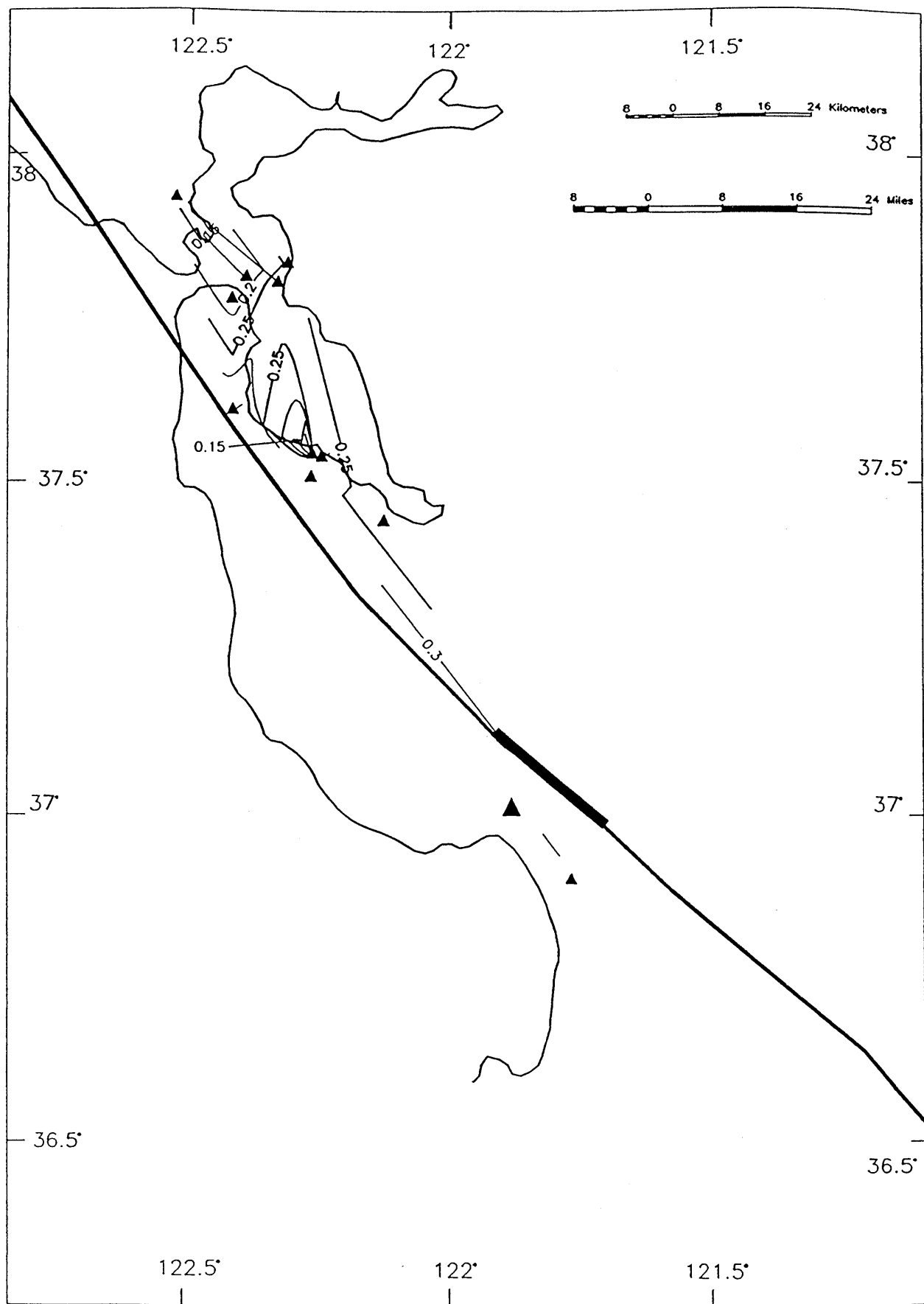


Figure 8.—Maximum horizontal acceleration—Soil Type 1

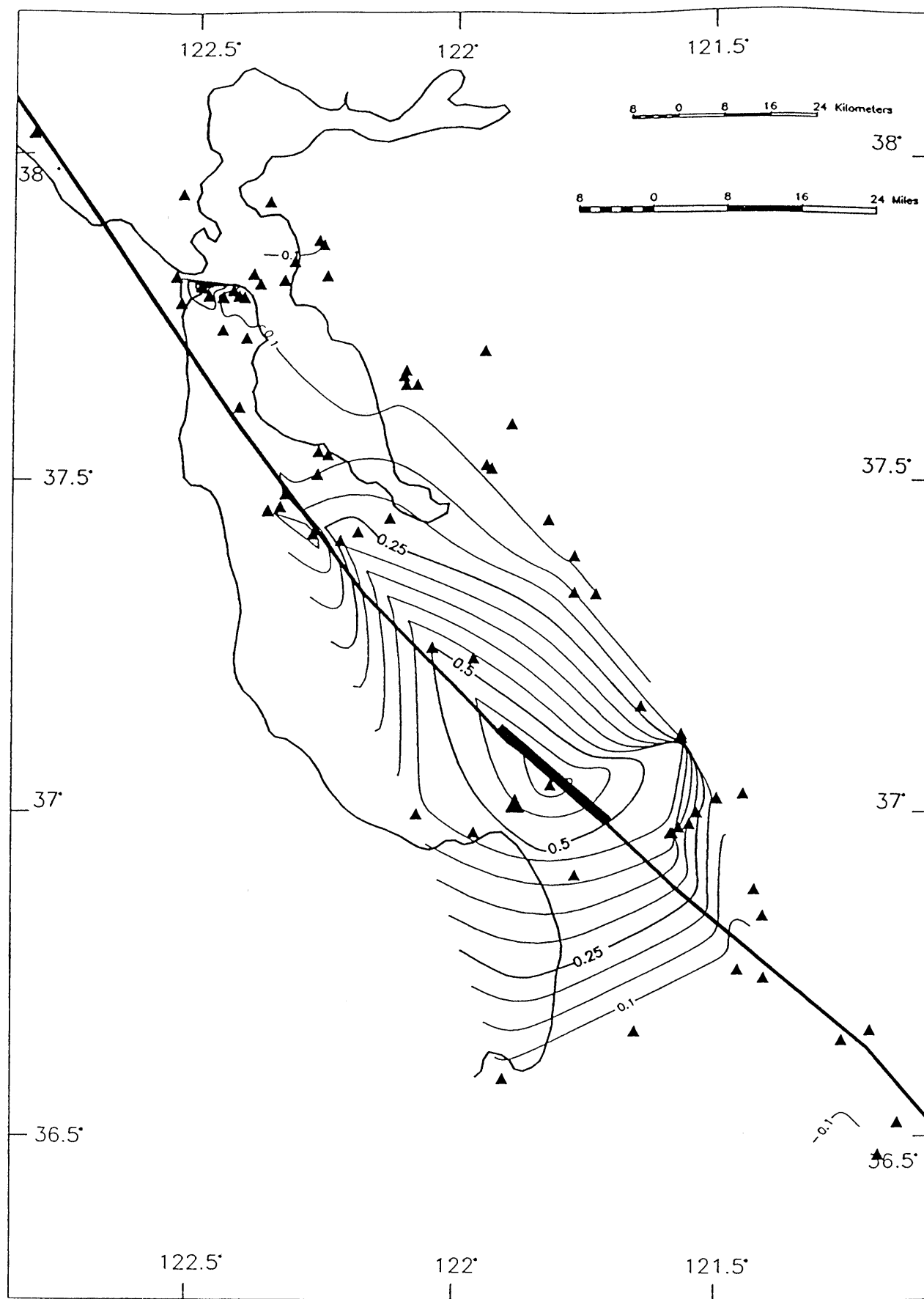


Figure 9.—Maximum horizontal acceleration—Soil Type 2

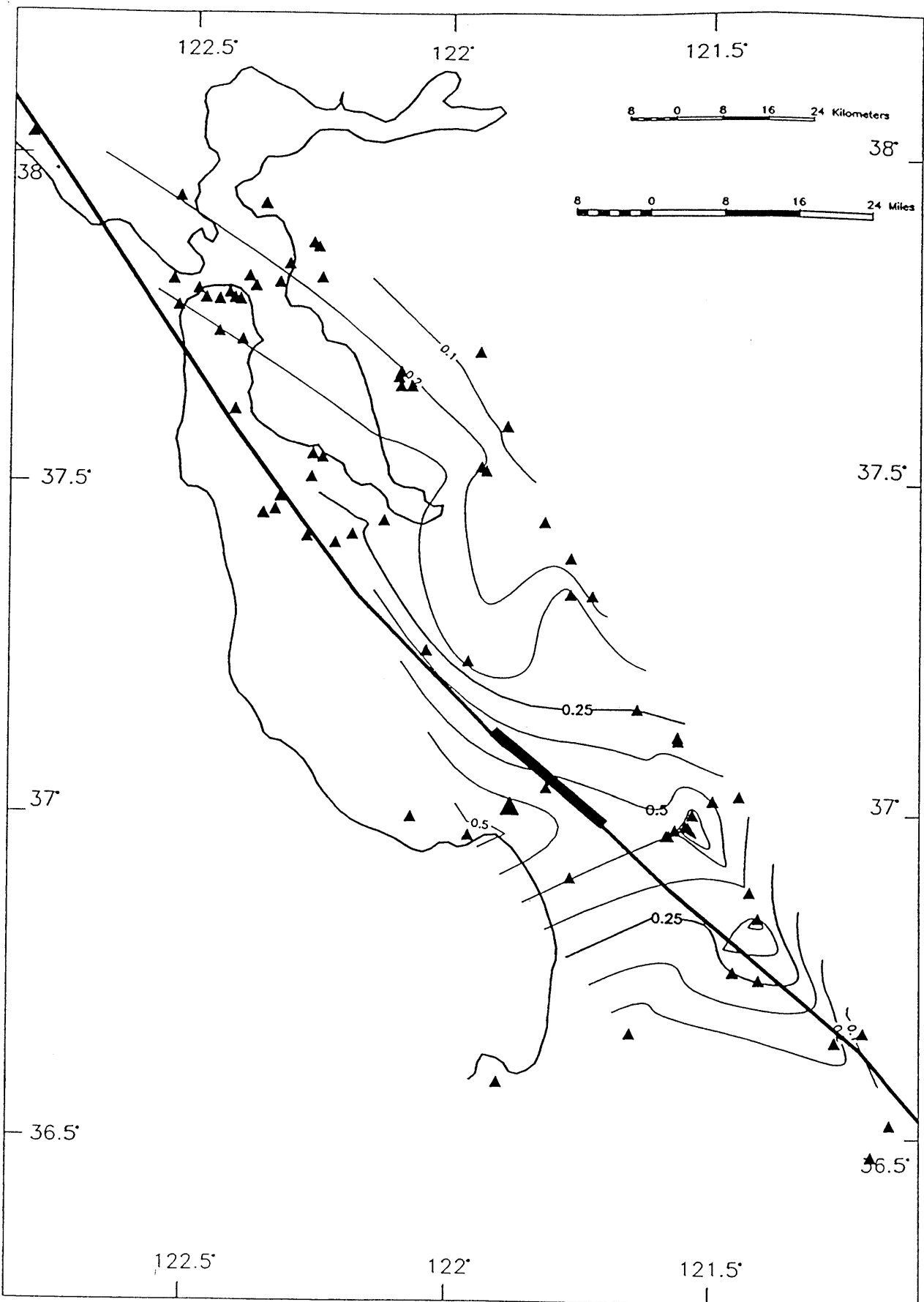


Figure 10.—Maximum horizontal acceleration—Soil Type 3

Table 6.—Correlation of Level 2 damage data with AHMAX

Damage state	Assumed central damage ratio %	AHMAX									
		<0.1g		0.1-0.2g		0.2-0.3g		0.3-0.4g		>0.4g	
		#	%	#	%	#	%	#	%	#	%
1	0	34	97.14	1154	71.32	479	85.38	0	0.00	23	22.77
2	0.5	0	0.00	202	12.48	29	5.17	2	12.50	32	31.68
3	5	0	0.00	153	9.46	41	7.31	5	31.25	8	7.92
4	20	1	2.86	55	3.40	1	0.18	4	25.00	12	11.88
5	45	0	0.00	43	2.66	11	1.96	4	25.00	23	22.77
6	80	0	0.00	11	0.68	0	0.00	1	6.25	2	1.98
7	100	0	0.00	0	0.00	0	0.00	0	0.00	1	0.99
Totals		35	100	1618	100	561	100	16	100	101	100
Mean damage ratio		0.57%		3.00%		1.35%		23.03%		15.79%	
Standard deviation		3.33%		10.24%		6.39%		22.03%		22.08%	

damage ratio. This is reasonable if dollar losses in regional loss estimates are intended to measure out-of-pocket expenditures directly resulting from *only* repair of damage. Based on our observations of activity following the Loma Prieta earthquake, however, we believe that attempting to translate the state of observed damage to a dollar-loss value presents the most significant problem in establishing dollar losses, primarily because of the ambiguity and variability of acceptable criteria to define what work is actually required as a result of the earthquake-caused damage. This work may not merely be associated with "repair." To address this issue, we propose a new model, as shown in figure 11.

Step 1 involves the traditional approach of correlating ground motion with a damage state. Many methods can be used: fragility curves, Markov models, or DPM's. An example of a Markov model approach is Thiel and Zsutty (1987). We use DPM's here.

Once a baseline DPM is established in Step 1, if information is available on building characteristics such as story heights, height-to-thickness wall ratios, adjacency conditions, mortar quality, etc., then Step 2 is where the baseline DPM is separated into final DPM's associated with subpopulations of the total group of buildings under study. Rutherford & Chekene (1990) provides an example of this process for San Francisco.

We believe the damage ratio depends significantly on the course of action taken by an owner following an earthquake. There are many ways that linkage between damage

state and course of action can occur. In Step 3 we use a "Course-of-action probability matrix," which covers common postearthquake actions the owner could take (table 7).

In using a matrix like table 7, it is expected that the loss estimator will make appropriate modifications using local standards of practice or existing local regulations. Significantly different results would be anticipated, for example, in a community like Oakland which has enacted an ordinance requiring strengthening of damaged URM bearing wall buildings when the lateral capacity has been reduced by more than 10 percent.

There is, of course, no direct correlation between the percentage loss of lateral capacity and the seven damage states. Determination of these percentage-loss-of-capacity figures in Oakland has been quite controversial. Nonetheless, we can make an attempt to qualitatively show how such an ordinance would alter table 7. Table 8 is the result.

In table 8, we assume that the 10 percent loss-of-strength trigger lies in the vicinity of damage states 3 and 4. Any buildings in these damage states with more than 10 percent damage will require repair as well as strengthening. It is expected that all of the damage state 5 and 6 buildings would be over the 10 percent trigger. As table 8 shows, the result of an ordinance like Oakland's is to increase the damage ratio and thus the losses in an earthquake. Of course, in the next earthquake, losses would presumably be much lower because of the presence of strengthened buildings.

Once the course of action is chosen, then the damage ratio can be established. Traditional methodologies, such as ATC-13, generally focus only on the repair costs of the "evaluation and repair" course of action. Table 9, by contrast, shows the great variety of property loss costs which can actually be triggered by postearthquake rehabilitation activity. Table 9 includes only structural and nonstructural property losses; not included are contents losses; the many kinds of economic losses; and tax, housing, and social losses.

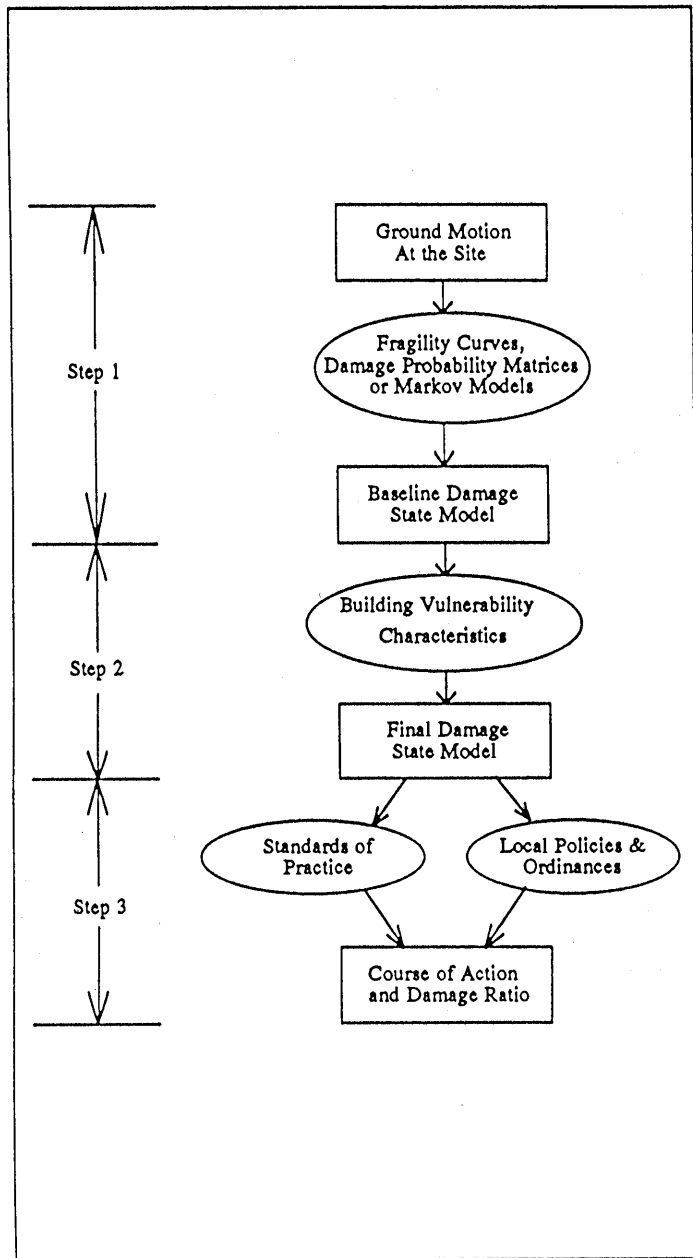


Figure 11.—Proposed loss estimation model

One of the key concepts shown in tables 7 and 8 and observed following the Loma Prieta earthquake is that when the cost of strengthening a damaged building rises to a certain level—what we call here the economic critical loss ratio (ECLR)—then an owner will choose not to repair and strengthen the building. The building may lie vacant for a long period of time, or it may be demolished and replaced. Little effort has been applied to determining the ECLR, but Rutherford & Chekene (1990) used 40 percent. Regardless of the exact value, it will certainly be much less than 100 percent. Using the ECLR concept, we can represent the resulting probability mass and density functions (PMF and PDF) for a selected damage state. Figure 12 is a PMF representation where each course of action in tables 7 and 8 is given a discrete damage ratio. Figure 13 smooths out the nonzero portion of the damage ratios into a PDF to provide a range of damage ratios for each course of action. Note the gap between the ECLR and 100 percent. A similar gap between 0 percent and the "Evaluation Only" line occurs because even the most minimal evaluation by a consulting engineer has a nonzero cost. Figures 12 and 13 apply only to a single building and are expected in an actual loss estimate to be aggregated across the total population of buildings, resulting in a smoothed, nonzero PDF measuring "average" damage for the population.

REFERENCES

- Applied Technology Council, 1985, Earthquake damage evaluation data for California: Redwood City, Calif., Applied Technology Council Report ATC-13, 492 p.
- Applied Technology Council, 1989, Procedures for postearthquake safety evaluation of buildings: Redwood City, Calif., Applied Technology Council Report ATC-20, 152 p.
- Araya, R., and Saragoni, G.R., 1985, Earthquake accelerogram destructiveness potential factor, in Proceedings of the Eighth World Conference on Earthquake Engineering: San Francisco, Earthquake Engineering Research Institute, p. 835-842.
- Lizundia, Bret, and others, 1991, Damage to unreinforced masonry buildings in the October 17, 1989 Loma Prieta earthquake, Technical report to the National Science Foundation and the California Seismic Safety Commission, 65 p.
- Lizundia, Bret, Dong, W., Holmes, W.T., and Reitherman, R.K., 1993, Analysis of unreinforced masonry building damage patterns in the Loma Prieta earthquake and improvement of loss estimation methodologies: Technical report to the U.S. Geological Survey, 239 p.
- Miller, R.G., 1962, Statistical prediction by discriminant analysis: Meteorological Monograph 4, no. 25.
- Rutherford & Chekene, 1990, Seismic retrofitting alternatives for San Francisco's unreinforced masonry buildings: Estimates of construction cost and seismic damage, San Francisco Department of City Planning, 351 p.
- Thiel, Charles, and Zsutty, T., 1987, Earthquake parameters and damage statistics: Technical report, San Francisco, Calif., Forell/Elsesser Engineers, 264 p.
- U.S. Geological Survey, 1989, Lessons learned from the Loma Prieta, California earthquake of October 17, 1989: U.S. Geological Survey Circular 1045.

Table 7.—*Sample course-of-action probability matrix*

Damage state	Damage state description	No action taken	Evaluation only	Evaluation and repair	Evaluation repair and strengthening	Demolition
1	None	80	20	0	0	0
2	Slight	20	60	20	0	0
3	Light	10	20	60	10	0
4	Moderate	3	5	45	45	2
5	Heavy	0	0	10	60	30
6	Major	0	0	10	50	40
7	Destroyed	5	0	0	0	95

Table 8.—*Course-of-action probability matrix for a community with a loss of strength trigger of 10 percent*

Damage state	Damage state description	No action taken	Evaluation only	Evaluation and repair	Evaluation repair and strengthening	Demolition
1	None	80	20	0	0	0
2	Slight	20	60	20	0	0
3	Light	10	20	50	20	0
4	Moderate	3	5	10	80	2
5	Heavy	0	0	0	70	30
6	Major	0	0	0	60	40
7	Destroyed	5	0	0	0	95

Table 9.—*Costs of addressing earthquake-caused damage organized by the course of action taken*

Type of property loss costs	Course of action				
	Evaluation only	Evaluation and repair	Evaluation, repair and strengthening	Evaluation and demolition for economic reasons	Evaluation and demolition for imminent life-safety reasons
Engineering assessment	Very likely	Very likely	Very likely	Likely	Very likely
Engineering study	Less likely	Likely	Very likely	Likely	Unlikely
Architectural study	Less likely	Possible	Likely	Possible	Very unlikely
Construction documents	No	Fairly simple	Extensive	Possible	No
Structural costs of repair work	No	Yes	Yes	No	No
Architectural refinishing costs of repair work	No	Yes	Yes	No	No
Structural costs of strengthening work	No	No	Varies widely	No	No
Architectural refinishing costs of strengthening work	No	No	Varies widely	No	No
Building permits and testing costs	No	Low	Higher	No	No
Owner project management costs	Small	Moderate	Higher	Moderate	Small
Asbestos and Soil contamination costs	No	Very unlikely	Possible	No	Possible
Accessibility requirements	No	Unlikely to be triggered	Possibly triggered	No	No
Fire upgrade requirements	No	Unlikely to be triggered	Possibly triggered	No	No
Additional costs for working in occupied building	Minimal	Can add a premium	Adds a bigger premium	No	No
Additional costs for working in historical building	Minimal	Can add a premium	Adds a bigger premium	Can add premium	No
Legal fees	Unlikely	Unlikely	Possible	Possible	Unlikely
Financing costs (interest and fees)	No	Less likely	More likely	Less likely	Unlikely
Repair of existing conditions (e.g., Dry rot and termites)	No	Less likely	More likely	No	No
Concurrent renovation work (can include mechanical and electrical)	No	Unlikely	Possible	No	No
Demolition permit	No	No	No	Yes	Yes
Demolition costs	No	No	No	Yes	Yes
Building replacement	No	No	No	Probable	Probable

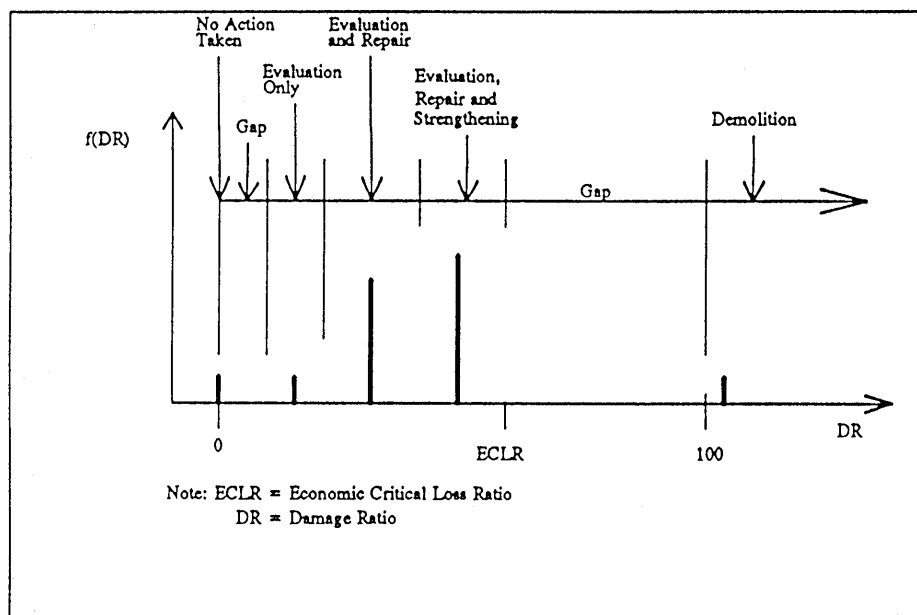


Figure 12.—Probability mass function for a given damage state

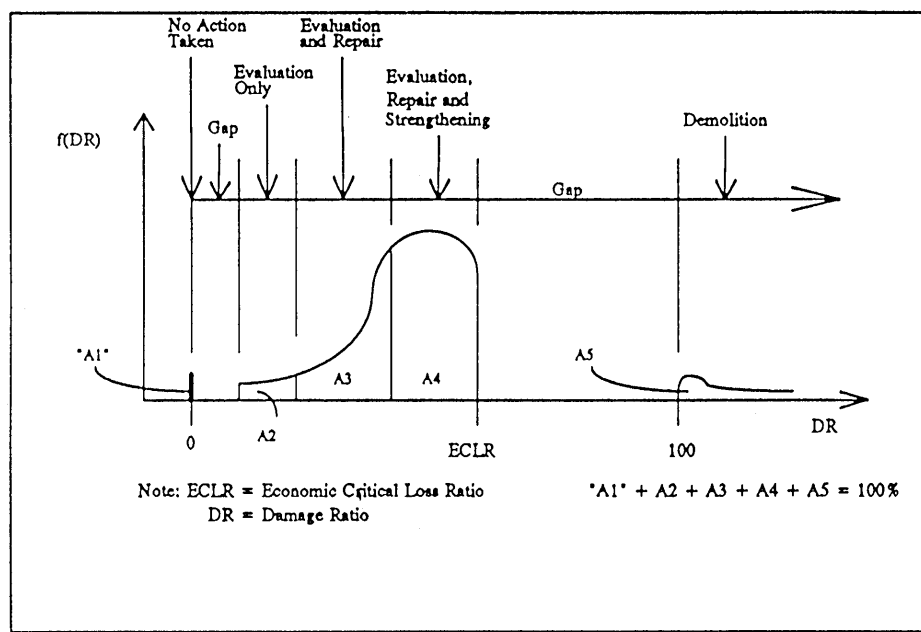


Figure 13.—Probability density function (with discrete component at DR=0%) for a given damage state

**THE LOMA PRIETA, CALIFORNIA, EARTHQUAKE OF OCTOBER 17, 1989:
BUILDING STRUCTURES**

PERFORMANCE OF THE BUILT ENVIRONMENT

HOUSING REPAIR AND RECONSTRUCTION AFTER THE EARTHQUAKE

By Mary C. Comerio, University of California, Berkeley

CONTENTS

	Page
Abstract -----	C161
Housing losses -----	161
Emergency sheltering -----	162
Repair of single-family houses -----	163
Repair of multifamily structures -----	164
One-time solutions -----	164
Economics of housing recovery -----	165
Lessons -----	166
Postearthquake recovery -----	166
Existing recovery programs -----	166
Housing recovery -----	167
Acknowledgments -----	167
References -----	167

ABSTRACT

This paper describes the housing losses that occurred and the attempt to provide emergency, temporary, and housing recovery services. The first section briefly describes the losses in four key areas, San Francisco, Oakland, Santa Cruz, and Watsonville. The second section describes the differences between single-family and multifamily housing needs as well as the services provided by relief agencies and the patchwork of one-time extra-agency housing-relief solutions. The final section reviews the cost and effectiveness of the overall assistance provided in the aftermath of the earthquake and discusses the lessons which can be learned to improve housing recovery in future disasters.

HOUSING LOSSES

Data from a variety of sources (De Monte, 1990; U.S. Government, 1991; U.S. Department of Housing and Urban Development, 1991) contribute to an estimate of approximately 12,000 housing units lost or severely damaged and another 30-35,000 moderately damaged in the nine-county San Francisco Bay area. Of the 12,000 lost or severely damaged, approximately 7,000 (60 percent) were rental units and 4,500 (40 percent) were low-cost units (tables 1, 2).

Media coverage of the earthquake focused on the dramatic collapse of apartments in San Francisco's Marina district, but this was not the whole story. There was extensive damage to older residential buildings throughout San Francisco. A total of 25,000 housing units incurred some damage; of these, 1,450 were officially declared uninhabitable (red-tagged), and almost 5,000 units were in need of substantial repair. Only 25 percent of those units lost or substantially damaged were located in the Marina district. Of the remaining 75 percent, half were in downtown neighborhoods—South of Market, Tenderloin, Bush Street corridor, and Chinatown—and half were distributed around the city, with concentrations in the Richmond and Sunset districts (City of San Francisco, 1989). The damaged buildings typically were three- and four-story wood-frame structures with soft first stories, except in the downtown area. There the damaged buildings were older, four- to six-story unreinforced-masonry (URM) construction.

The 1,300 units destroyed or significantly damaged in Oakland were in 10 unreinforced-masonry downtown single-room-occupancy (SRO) hotels. Here again, these hotels served as the last affordable housing resource for many minority and elderly residents in an urban community high property values, high rents, and few options for those at the bottom of the income ladder. The city estimates that the earthquake added 2,500 people to the roster of homeless in the city. By comparison, the 2,000 units which sustained moderate damage were primarily wood-frame single-family houses with cracked chimneys, foundations, porches, and stairs. By and large, the inhabitants of the latter group did not need temporary or alternative housing. They were able to live with the damages and repair them over time (City of Oakland, 1993).

The greatest concentrated loss of commercial and residential buildings was in the Pacific Garden Mall area of the City of Santa Cruz, a seaside community and university town of 48,000. In addition to the loss of approximately 25 commercial structures, four residential hotels with approximately 400 units were lost. Three of these housed low-income elderly tenants, and only one of the smaller hotels had a more transient population. Numerous single-family residences and small apartments were rendered unoccupiable, and throughout the county, something

Table 1.—*Damages to housing units*

County	Destroyed or significantly damaged	Estimate of in need of some repair	Total
San Francisco	6,300	18,500	24,800
Alameda	1,300	2,000	3,300
Santa Cruz	3,000	10,000	13,000
Santa Clara	400	600	1,000
Others	500	500	1,000
Total	11,500	31,600	43,100

Table 2.—*Estimated rental and low income units destroyed or significantly damaged*

	Destroyed or significantly damaged	Rental Units (pct)	Affordable Units (pct)
San Francisco	6,300	75%	66%
Alameda	1,00	100%	100%
Santa Cruz	3,000	33%	10%
Santa Clara	400	0%	10%
Others	500	0%	0%
Total	11,500	60%	40%

on the order of 10,000 housing units incurred moderate damage (Santa Cruz County, 1989).

Watsonville sustained the greatest single-family housing loss. Some 850 housing units (10 percent of the city's housing stock) was severely damaged or destroyed. These were small wood-frame houses and apartment buildings literally knocked off their foundations: 40 percent were owner occupied; more than 75 percent were low-cost housing units. Largely occupied by farm worker and cannery worker extended families, these houses typically had one permanent owner/tenant as well as informal subtenants who were relatives or friends, some legal, some illegal, some permanent, and some migrant workers. There were reports of 30-40 people living in one house, and individuals and families living in converted garages and chicken coops. In inspecting the damage, city officials found as many as 300 "illegal" dwellings (Phillips, 1991; Comerio, 1992).

One year after the earthquake, the damaged wood-frame single-family stock had largely been repaired or replaced, except in cases near the epicenter where geotechnical studies and land-use issues forced delays. The picture for masonry and wood-frame multifamily housing is quite different. Less than half of the units severely damaged or lost have been repaired or replaced. The reason is two-fold. First, the existing programs designed to assist housing recovery are geared toward the single-family homeowner, and as such there is very little funding available that can be used for multifamily buildings. Second, the assumption built in to the existing programs is that the

private market will adjust and provide alternative housing resources in the postdisaster period. The concentrated losses of inner-city affordable housing resulting from the earthquake proved this assumption false and forced a re-evaluation of existing housing recovery and reconstruction programs.

EMERGENCY SHELTERING

Although the State of California and the local chapters of the American Red Cross (ARC) consistently receive high praise for their planning and execution of emergency services in the first 24 to 48 hours after a disaster, the emergency response to the earthquake left many victims with the perception that services were financially and racially biased. According to plan the ARC set up mass-care shelters in schools and public buildings. Tents were also used in Watsonville and Santa Cruz. Although the procedures were routine, the levels of service and the attitudes of volunteers varied considerably. It was widely believed that volunteers gave "better" service to white middle-class owners and renters and lacked sensitivity to low-income, ethnic, minority, and transient disaster victims. In part, the problem is institutional in that the rental assistance for temporary housing provided by both the ARC and FEMA requires "permanent" resident status; that is, documentation of ownership or lease agreements for a period of longer than 30 days. As such, mass-care shelter operators sometimes applied the criteria to those seeking

shelter instead of following the "humanitarian care first, questions later" motto of senior ARC staff.

The insensitivity problem is also a function of the pool of volunteers (locally and nationally) who are predominantly white and middle class and who have no training in working with people from culturally diverse backgrounds. In Watsonville, the ARC was unwilling to recognize the informal tent camps in town parks as official shelters for several days. There were few Spanish speaking volunteers and little tolerance for the victims' fear of returning to any structure, despite the documented problems in the milder Whittier earthquake of 1985, when many Hispanic victims camped in their cars and on street curbs for almost a month before returning to their homes and apartments.

ARC and FEMA provide "temporary" shelter by providing up to 18 months of rental assistance for homeowners until they could package their loans, and/or insurance settlement, and rebuild their homes, and providing two months' rental assistance for renters. Unfortunately, a disproportionate number of the victims were living in low-income rental accommodations without any security of tenure. For these victims, access to FEMA or Red Cross temporary rental assistance was blocked by their inability to produce a lease or other documentation of residency at the same time that the number of affordable units in their community had been seriously reduced. Although in some areas and in some cases, FEMA and the Red Cross accepted vouchers from clergy and other nontraditional proof of residency, the majority of people living in downtown San Francisco and Oakland hotels with 28-day rental limits, the elderly living in Santa Cruz hotels, the roommates, extended family members, and informal subtenants in Watsonville and Santa Cruz county houses did not qualify for any housing service other than emergency shelter. Most agency personnel now believe that the 30-day rule needs to be changed so that all victims can receive some temporary rental assistance, for the obvious reason that it is better, safer, and healthier to accommodate victims in traditional housing units rather than to keep large numbers of unrelated individuals and families in mass-care shelters in public buildings.

REPAIR OF SINGLE-FAMILY HOUSES

Individual homeowners with repairable damage found a variety of resources in Federal and state housing-recovery programs. The majority of the single-family housing reconstruction funding came through the Small Business Administration (SBA) loan program. Other programs included: a \$5,000 minimum home repair (MHR) grant from FEMA for limited repairs to primary dwellings, and Individual Family Grants (IFG) combining FEMA and state

funds (maximum \$21,500) for real and personal property replacement. Mortgage assistance and Additional Living Expenses (ALE) were also available if needed through a FEMA program. Finally, if homeowners' needs were not met through these programs, they could apply for a loan from the California Disaster Assistance Program (CALDAP), administered by the state office of Housing and Community Development (HCD). The CALDAP program was initially set up in two tracks: CALDAP-O for owner occupiers and CALDAP-R for rental housing owners; it was initially funded with \$23 million in each track for loans and grants. Four years after the event, CALDAP-O has provided \$43 million in loans to homeowners, and there are still some loans applications pending (California Natural Disasters Assistance Rental Program, 1992).

All in all, the resources available for homeowners to repair or rebuild single-family residences seem entirely adequate for a moderate disaster the scale of Loma Prieta. The major criticism of this aspect of the housing recovery program is that it is a bureaucratic nightmare. Each loan program has its own application forms and approval procedures, and each sends its own inspector to review and assess the damage. Further, an individual must be rejected from one program before they can apply for the next, saddling disaster victims with lengthy time delays and mountains of paperwork.

Ironically, in the town of Watsonville, where more than 800 single-family homes were destroyed or significantly damaged, very few victims applied for or received Federal and state assistance. Yet, one year after the earthquake, 75 percent of the houses were repaired or replaced. How? The city received over \$1 million in donations from individuals, corporations, foundations, and their sister city in Japan. The Red Cross supplemented this fund with \$2.5 million for affordable housing assistance. Watsonville officials recognized that the majority of their population would not qualify for SBA loans and probably would not attempt the complex process of applying for FEMA and state assistance. The city quickly decided to use the donations for small grants of \$20,000 to \$40,000 to any residents in need of construction funds.

Further, numerous volunteer organizations and religious groups (for example, the Mennonites, the Christian World Relief Committee, Habitat for Humanity, and others) donated time and funds in the rebuilding effort. Many weekends were marked by volunteer construction workers involved in "barn raising" new residences. The close-knit Latino community also contributed to the self-help atmosphere. In addition, the wood-frame small-scale buildings made it easy for unskilled labor to assist in the construction efforts, and the city decided to be "easy on permits and tough on inspections," allowing people to get on with the work without delays.

REPAIR OF MULTIFAMILY STRUCTURES

A simplistic view of any postearthquake rebuilding phase, as suggested by the name itself, assumes rebuilding the destroyed housing units as they were before, or replacing them with similar structures that will provide the same features, service, and value that the destroyed buildings provided. That is, however, not what happens, nor is it, in fact, what is needed. Virtually all the FEMA and SBA housing-assistance programs are designed for a prototypical, or ideal, victim, who owns or rents a housing unit which is adequate, conventional, and replaceable. Unfortunately, a significant portion of the individuals and families who lost housing in the Loma Prieta earthquake lived in old, poorly maintained, overcrowded, structurally unsound buildings because they could not afford better quality accommodations.

The earthquake exposed the lack of specific programs targeted for the repair and reconstruction of multifamily and low-cost housing. The SBA is the only Federal agency making loans to apartment owners, and these are managed through the business (not the housing) loan program; moreover, loans will not be made if rents cannot cover the additional debt. The state created CALDAP to fill the gap of unmet housing needs. The program was based in the Department of Housing and Community Development (HCD) and staffed by individuals from other low-income housing programs.

Unfortunately, the CALDAP rental program could not meet the needs of most private or nonprofit entities attempting the reconstruction of low-income housing. Several factors contribute to the problems CALDAP encountered. The program was new, with no set procedures or guidelines, and the rules changed each time the agency had to return to the legislature for additional funds. As a relief program, it was modeled after other relief programs which provide funds to assist in restoring residential units to preearthquake conditions. For run-down, old buildings, the requirement to return buildings to preearthquake conditions was unreasonable and illogical.

For example, a 160-unit residential hotel in San Francisco was demolished. After a long process involving foreclosure and purchase by the Redevelopment Agency, the site was made available to a nonprofit housing agency. Zoning regulations limited the height to eight stories to protect a nearby park from shadow. Given the site size, the nonprofit could only build 140 of the smallest possible units within the zoning envelope. This discrepancy, along with the limitation on quality upgrades and the limited support for development costs, rent requirements, and tenant-relocation requirements imposed by CALDAP, led to innumerable delays and an ultimate resolution that CALDAP funding would only be used for 40 percent of the total project.

Despite the fact that the CALDAP program became a source of frustration to all people trying to utilize it, it was the only source of financing for the replacement of low-income housing in all areas affected by the earthquake. Overall, the CALDAP rental program loaned \$44 million and provided 142 rental-property owners, a total of about 2,800 units, with loans averaging \$15,000 per unit.

ONE-TIME SOLUTIONS

The frustration experienced by local governments and affordable-housing advocates over the lack of resources for low-income victims took form in a frontal attack on FEMA by San Francisco Mayor Art Agnos and enormous pressure on the Red Cross to redirect all contributions directly to the Bay Area instead of reserving some portion of the funds raised for future disasters. The critical media blitz captured national attention and led to a number of special assistance programs that were unique to Loma Prieta. These special sources of funding for low-income housing renovation and reconstruction have become the primary mechanisms for aiding low-income victims, but unfortunately, each is perceived as a one-time solution by relief agencies.

The Legal Aid Society of Alameda County sued FEMA to contest FEMA's interpretation of the relief regulations requiring 30-day residency for financial assistance, which disqualified many SRO dwellers, the lack of due process in the appeal procedure, and the incomplete information provided by FEMA regarding the assistance to which the disaster victims were entitled. While the strictly legal recourse to the grievance would have been to ask FEMA to provide rental assistance to the people concerned, Legal Aid recognized that the temporary rental assistance would not have solved the problem when no comparable units were available on the market. Therefore, Legal Aid decided to ask for money to replace the units lost in the earthquake. After agreeing to that solution, FEMA appeared to renege on the settlement, and it took another year of legal and media battles to create a second settlement, which provided \$23 million to fund 2,200 SRO units. The settlement sum was arrived at by multiplying the number of SRO units lost by a unit cost of about \$10,500. The money was divided among the various counties based on their proportional number of SRO units lost. The flexibility of the final settlement was ideal from the point of view of the local agencies, because the funds were provided in a block-grant fashion to the counties and as such allowed them the freedom to decide how to put the money to best use, with very few restrictions. Overall, 1,200 to 1,500 units were actually rebuilt using lawsuit funds.

Alameda County received the largest share, \$11.8 million, of the settlement funds. Although \$2 million was used for emergency sheltering costs, the remainder went to Oakland, where 1,300 of the lost SRO housing units were located. The city pledged \$1 million to a multiservice homeless shelter and used the remainder to rehabilitate damaged buildings. Due to FEMA restrictions, the funds could not be used to assist private owners. Thus, the city assisted in arranging the sale of these buildings to nonprofits and committed city and community development block-grant funds to complete the projects. The transactions slowed the recovery process so that one year later, only one hotel with 84 units was completed. Four years after the event, two additional hotels and the multiservice center were completed for a total of 300 units restored to service. Six other hotels with approximately 600 units are in varying stages of construction, still leaving a deficit of 400 units.

The American Red Cross responded to political pressure to use some of the \$52 million generated in the highly successful fund-raising drive after the earthquake for housing-recovery purposes. ARC set aside a special fund for various human service projects to earthquake victims, and about \$13.15 million for housing-recovery projects. Of that, \$900,000 was given as grants to low-income homeowners, \$10 million was set aside for various multifamily projects, as part of the financing needed to rebuild, and \$2.25 million was allocated as predevelopment loans to nonprofits to enable them to start the development process (American Red Cross, 1992).

Many of the nonprofit agencies who purchased damaged buildings with the intent of renovating them with funds from CALDAP and/or the FEMA lawsuit settlement were quite skilled in financing low-income housing rehabilitation. These organizations leveraged ARC, CALDAP, or FEMA settlement funds to obtain additional financing from Redevelopment Agencies, tax credits, other state (HCD) housing funds, and private lenders. Because the disaster-recovery funding covered only 20 to 50 percent of the rebuilding costs, the funds provided by traditional low-income-housing lenders were not available for their original function, to increase the affordable housing stock.

Further, the Federal programs at HUD were not made available for disaster recovery. Despite a memorandum from the Region IX office to Secretary Kemp in Washington, dated February 1990, describing the crisis and recommending additional allocations of section 8 vouchers and rental rehabilitation program funds to the affected cities, HUD was unwilling to assume the responsibility of assisting in the rebuilding of housing for low-income populations. Its only action was the allocation of 500 rental assistance vouchers and 664 moderate-rehabilitation vouchers to the area. This did not represent any extra allocation, only an attempt to speed up existing allocations, which

because of bureaucratic delays, did not materialize until the summer of 1990.

ECONOMICS OF HOUSING RECOVERY

The reason housing is not rebuilt after natural disasters is not solely a function of recovery program design or implementation, it is tied with the economics of the marketplace. Someone, usually the building owner or potential lender, compares the cost of rebuilding with the potential for recovering those costs in the marketplace and decides the two just do not add up.

Different types of housing are valued according to different attributes. Single-family homes are bought, sold, built—and following a disaster, rebuilt—on the basis of three attributes: the shelter provided (the space, the lot, the design features), the location (neighborhood, schools, proximity to work, etc.), and the wealth potential (appreciation, tax shelter, cash flow). Because the long-term value of an owner-occupied house is linked to its condition, homeowners have a powerful incentive to maintain their properties and to rebuild them after a disaster. Even at moderate appreciation rates of 2-4 percent, homeowners can absorb significant postdisaster rebuilding costs up to 20 percent of the initial home value and still make a reasonable profit (Comerio and others, 1994).

By contrast, renters rent housing for two reasons, shelter and location, but not for reasons of profit enhancement. Investors in rental housing (including developers, landlords, and partners) have a different set of concerns. Investors care about shelter and location only as much as they impact a particular property's profit potential. Unlike homeowners, investors have an incentive to maintain their properties only to the extent that the maintenance directly enhances cash flows. Following this logic, postdisaster rebuilding expenses are unlikely to be undertaken if they cannot be quickly recovered out of rents.

Put simply, the likelihood of a single-family homeowner rebuilding a damaged or destroyed unit depends jointly on personal and financial concerns. The likelihood of a multifamily investor rebuilding a damaged building depends primarily on their ability to raise rents without losing tenants. Except in very tight housing markets, landlords have little ability to unilaterally raise rents, because if they do, the tenants will move elsewhere. Thus, when a building owner is faced with additional debt to cover damages for 20 percent of the initial building value, the owner would have to raise rents 8-10 percent in order to maintain predisaster levels of operating capital. The implication is clear: There is little if any economic incentive to rebuild multifamily housing, even with relatively favorable financing terms. The greater the repair cost, the more highly the owner is leveraged, the higher the market va-

cancy rate, or the poorer the tenant base, the greater the incentives for property abandonment. This basic economic reality was clearly demonstrated after Loma Prieta. Of the 12,000 units lost, 9,000 were in multifamily buildings. Of these, nearly 90 percent were still out of service one year after the earthquake, and 4 years later, about 50 percent of these remain unrepairs or unreplaced (Comerio and others, 1994).

LESSONS

Major disasters change the physical and social fabric of cities in unalterable ways. Agencies as well as individuals use the disaster as an opportunity to change the status quo, to their advantage. An individual rebuilding his house may want to make some changes that he was contemplating even before the disaster struck. A city may use funds available from earthquake reconstruction to finance homeless shelters and multiservice centers (as was the case in Oakland and San Francisco). A region may seize the opportunity of major destruction in the roads and infrastructure to transform and renew the infrastructure of the area. It is within this context that the design of assistance programs has to take place. The stress in the rebuilding phase is the rebuilding of the individual and community lives, not on the rebuilding of the particular artifacts that sustain it.

The Loma Prieta earthquake deepened an already-existing housing crisis in the Bay Area. Many homeowners and multifamily building owners were probably carrying as much debt as the property could carry, and could not afford to take further loans to rebuild or rehabilitate the property. It was apparent that the normal single-family housing-oriented recovery programs would not be sufficient to enable real housing recovery. Furthermore, because the earthquake hit hardest in areas of concentrated multifamily low-income housing, the market was not able to provide alternative or replacement housing at affordable rents, without some assistance from the public. Overall, only 40 percent of the housing losses were served through the normal disaster-assistance process, and 60 percent can be described as a residue of unmet needs. Of these, half found some assistance through the one-time solutions, but these are not models for future disaster relief and recovery programs.

Table 3 summarizes the expenditures made by various public agencies toward housing assistance and recovery in the Bay Area after the earthquake. The expenditures by government agencies and private insurance show that out of an estimated \$1,130,000 spent on earthquake recovery, 66 percent (\$750 million) was spent on assistance for owner occupiers, although only 40 percent of the stock of damaged units was in single-family dwellings. Eliminat-

ing funds paid by insurance, and looking only at the public assistance money, homeowners still received proportionally more funding than renters, 62 percent of the funds compared to 40 percent of the damaged units. Furthermore, the aid that is given to rental housing is not direct aid that goes to the renter, but aid given to owners of rental housing. Some of it goes into predevelopment expenses and organizational overhead, not only into construction and repair. Therefore, the net sums used to restore the rental units is probably at least another 20 percent less.

In summary, it seems that state and Federal governments should step in to aid local and county governments and individuals in the housing recovery process. Existing programs are biased toward homeowners. A more equitable approach would be to insure that the funds are distributed evenly across housing types. A proactive approach would insist that the earthquake presents an opportunity to redress some of the housing inequities and direct more funds on the basis of need, not on the basis of the losses incurred. The housing-recovery experience after Loma Prieta leads to three lessons to improve postdisaster housing recovery:

1. *Postearthquake housing recovery requires preearthquake planning.*—Although California is rightfully proud of its planning and readiness for emergency response in the event of a disaster, Loma Prieta taught a valuable lesson in exposing the gaps in housing recovery and provides a roadmap for thinking about recovery planning. There is a need to promote hazards mitigation in all structures but particularly in vulnerable multifamily structures. Mitigation is the single most cost-effective method of reducing damage and limiting the human and financial costs after disasters. There is a need to create recovery funding programs for multifamily low-income housing. This requires rethinking the current Federal and state programs and their relation to ongoing housing strategies, and it requires standardized reporting of damage and realistic budgeting.

The entire structure of postdisaster housing-recovery needs to be rethought in terms of the method for estimating housing losses and recovery needs and in terms of the delivery system for assistance. A careful damage assessment based on common methods of data collection for each locale could be used to prepare a Federal housing recovery budget for the state, which could in turn develop its own assistance budget. These funds could be distributed through an agreed-upon delivery system which is already providing affordable housing assistance. The concept is one of state and Federal block grants administered through existing agencies in which state and local governments, which are familiar with the rules and regulations of the administering agencies, are notified as to how much they have to work with.

2. *Existing recovery programs should be streamlined to expedite services.*—The single most important thing govern-

Table 3.—*Summary of expenditures on building repair by client group*

Agency	Owner/ Occupier (\$ millions)	Mean per unit (\$)	Rental (\$ millions)	Mean per unit (\$)	Total (\$ millions)
Insurance	373.98	20,215	~152.00	N/A	~525.98
ARC	0.90	13,000	12.25	11,400	13.15
FEMA			23.00	N/A	23.00
IFG	~23.03	N/A	~23.03	N/A	46.06
SBA	309.14	26,900	~126.50	N/A	435.64
CALDAP	43.31	13,000	43.63	15,865	86.94
Total public assistance	376.38	15,055	228.41	10,380	604.79
Total	750.36		380.41		1,130.77

ment and relief agencies can do for disaster victims is to expedite the process of getting back to normal. The Disaster Application Centers (DAC's) are established to provide information and assistance in the recovery process to disaster victims, and each individual or family is assigned a case number when they come in. FEMA has created a single intake form which allows them the ability to computerize information on the victims which is shared through an electronic network with all the recovery funding agencies. There could be one similar application form for housing-recovery assistance which could be devised to cover all the information needed by each of the possible funding agencies. One agency could take the lead in assessing the actual damage through a single inspection by a qualified knowledgeable contractor and then have a loan officer analyze which combination of loans, grants, and temporary assistance should be provided.

3. *Housing recovery programs will be most effective if they are administered at the local level.*—Housing recovery involves the development and redevelopment of land and buildings, a process which requires localized construction expertise, the involvement of local private lenders, and local government approvals (as well as interactions among owners and tenants). This is not a process which can be managed by state and Federal agencies alone.

A well-planned process for distribution of housing-recovery funds could avoid the mistakes and delays that occurred after Loma Prieta. The excursions taken by FEMA, and particularly ARC, into housing finance because of the political pressure to provide affordable housing assistance were taxing both for the organizations and for the clients. The agencies were afraid to make mistakes because of their lack of expertise in the field of housing, and as a result, officials tended to make stricter interpretations of regulations than what might have been necessary. Further, their tendency to distrust local housing officials created an atmosphere in which unusual and/or creative local solutions were perceived as fraudulent. The piecemeal housing aid and the process through which it was achieved is not a model for future disasters. The best and most expedient method for low-income housing

recovery is to allow local governments the ability to make decisions on how best to serve the affected populations in their community and to provide funding through existing channels.

ACKNOWLEDGMENTS

The data for this paper were developed in a research project for the California Governor's Office of Emergency Services, conducted by the author with John Landis and Yodan Rofe. The final report, "Post-Disaster Residential Rebuilding," is published as Working Paper #608 by the Institute of Urban and Regional Development (IURD), University of California at Berkeley, February 1993.

REFERENCES

- American Red Cross, 1992, Special disaster relief fund: Quarterly Report on Project Status (December 31), 21 p.
- California Natural Disasters Assistance Rental Program (CALDAP-R), 1992, Activity summary and production report: Department of Housing and Community Development (June 30), 7 p.
- City of Oakland, 1993, Loma Prieta damaged properties list: Office of Planning and Building (March 18), 52 p.
- City of San Francisco, 1989, Earthquake impact on low and moderate income housing Rept. 4: Mayor's Office of Housing (November 20), 4 p.
- Comerio, Mary, 1992, Hazards mitigation and housing recovery, in Disasters and the Small Dwelling: London: James and James, p. 127-135.
- Comerio, Mary, John Landis, and Yodan Rofe, 1994, Post-disaster residential rebuilding: University of California, Berkeley, Institute of Urban and Regional Development, 85p.
- De Monte, Robert, 1990, Memorandum on proposed earthquake response by region IX: U.S. Department of Housing and Urban Development (Feb.), in Proceedings of the symposium on policy issues in the provision of postearthquake shelter and housing, January 26-28, 1992: National Center for Earthquake Engineering and Bay Area Regional Earthquake Preparedness Project, 15 p.
- Housing and Urban Development, 1991, Status of recovery from the earthquake in San Francisco, Oakland, Santa Cruz and surrounding

- areas: U.S. Department of Housing and Urban Development Region IX Report (Sept.), *in* Proceedings of the symposium on policy issues in the provision of postearthquake shelter and housing, January 26-28, 1992, National Center for Earthquake Engineering and Bay Area Regional Earthquake Preparedness Project, 11 p.
- Phillips, B.D., 1991, Post-disaster shelter and housing of Hispanics, the elderly, and the homeless: Southern Methodist University (Report to the National Science Foundation), 75 p.
- Santa Cruz County, 1989, Summary damage report: County Information Services (December 8), 1 p.
- U.S. Government, 1990, Housing needs in earthquake disaster areas: Washington D.C., U.S. Government Printing Office Serial 101-115 (field hearings before the Subcommittee on Housing and Community Development, House of Representatives), 1,217 p.

**THE LOMA PRIETA, CALIFORNIA, EARTHQUAKE OF OCTOBER 17, 1989:
PERFORMANCE OF THE BUILT ENVIRONMENT**

BUILDING STRUCTURES

**IMPACT OF THE EARTHQUAKE ON HABITABILITY OF
HOUSING UNITS**

By Jeanne B. Perkins and Ben Chuaqui,
Association of Bay Area Governments, Oakland, Calif.

CONTENTS

	Page
Abstract -----	C169
Background -----	169
Type of structures -----	170
Structure -----	170
Configuration -----	170
Age of construction -----	171
Overall classification -----	171
Postearthquake habitability data collection -----	172
Loma Prieta -----	172
Northridge -----	172
Overall residential building stock data -----	178
Calculating vulnerability by construction type and intensity -----	181
Sample application—assessing impacts and possible damage patterns in future earthquakes -----	182
Conclusions -----	183
Acknowledgments -----	185
References -----	186

ABSTRACT

The Loma Prieta earthquake produced over 16,000 uninhabitable housing units throughout the Monterey and San Francisco Bay areas, including almost 13,000 in the Bay Area. Although this number is only about a third as high as the more than 48,000 units made uninhabitable in the 1994 Northridge earthquake, the impact on housing stock was significant.

Data on habitability of housing structures were collected through a combination of telephone and in-person interviews with city and county building departments following the earthquake. Subsequent efforts were made to improve the quality of data regarding age, type of construction, and number of units associated with those structures. Similar data were collected following the 1994 Northridge earthquake. The data collection effort focused on obtaining data for several categories of wood-frame construction, while minimizing the number of nonwood categories.

These data were collected as part of a larger project and tied to ground-shaking modeling in order to predict

the impacts of 11 future likely earthquakes on the housing stock of the San Francisco Bay region.

These two damaging earthquakes emphasize the importance of creating housing-loss estimates for emergency-response planning in metropolitan areas subject to strong ground shaking. They also point out the impact of non-life-threatening damage on people's lives. Design standards need further evaluation to better ensure functionality to these structures, most of which are nonengineered.

BACKGROUND

This data-collection effort on the impact of the Loma Prieta earthquake on habitability of housing units is part of a much larger program at the Association of Bay Area Governments (ABAG). The goal of the larger program is to develop estimates of the number of uninhabitable dwellings from future earthquakes affecting the San Francisco Bay area. This program began in 1991 with funding from the American Red Cross, the California Office of Emergency Services, and ABAG itself (Perkins, 1992). George Washington University (GWU) used these estimates to develop projections of shelter populations in future earthquakes in the San Francisco Bay area. More recently, funding from the National Science Foundation has supported our research using the data on housing impacts collected following the Loma Prieta and Northridge earthquakes, together with more sophisticated ground-shaking intensity models, to greatly improve the estimates of housing impacts following future earthquakes. These estimates also incorporate better data on all the existing residential housing stock, including location (see Perkins and others, 1996).

Data were collected on housing units designated as non-functional, or uninhabitable. "Uninhabitable" is defined as unable to be occupied due to structural problems. It is equivalent of the Applied Technology Council (ATC) red-tagging definition for unsafe buildings where entry is prohibited for single-family homes. For multifamily units, the structure can be either red tagged (unsafe) or yellow

tagged (entry restricted) (see Applied Technology Council, 1991). Building departments in California uniformly use the ATC definitions in their postearthquake tagging. Uninhabitable dwellings are not necessarily destroyed; most are repairable.

The Loma Prieta earthquake provided extremely valuable information on the performance of several categories of housing when exposed to various levels of shaking. The residential structures tagged by local government building officials following the earthquake have been carefully examined and analyzed.

Data on housing performance from a single earthquake are not nearly as useful as data from multiple events. Thus, ABAG staff collected similar information on habitability following the Northridge earthquake in the Los Angeles area. The ratios between green-, yellow-, and red-tagged housing units for different types of housing construction in the Los Angeles area obtained following the Northridge earthquake were combined with the Loma Prieta data and additional data from earlier earthquakes (from Dunne and Sonnenfeld, 1991) before being incorporated into the ABAG model which predicts housing impacts following future Bay Area earthquakes.

Our goal has been to provide information that can improve mitigation, disaster response, and residential rebuilding efforts in future earthquakes. The overall program should serve to motivate retrofitting of homes and apartments, planning for responding to future earthquakes, and rebuilding faster after those earthquakes.

TYPE OF STRUCTURES

For the purposes of collecting data on the extensive Bay Area housing stock both habitable and uninhabitable following this earthquake, residential buildings have been broadly classified in table 1 according to three basic characteristics: (1) the building's structure, (2) the configuration or shape of the building, and (3) the age of the building.

STRUCTURE

Because of the large variation in housing stock in the nine Bay Area counties, implementing a detailed classification scheme that would account for both horizontal and vertical elements of the structure, as well as the methods by which they are connected, was not practical. Rather, this paper categorizes residential structures according to the material of their principal vertical elements. This "material/structure" classification follows established groupings from the building industry:

1. *Wood frame*.—Includes buildings which consist of a concrete podium with a wood frame of several stories above;
2. *Masonry*.—Includes brick and concrete block (reinforced or unreinforced);
3. *Steel frame*.—Includes braced frames and moment-resisting frames, with and without concrete or masonry infill walls; and
4. *Concrete*.—Includes cast-in-place and precast or a combination of the two.

Since wood-frame buildings are by far the largest component of the housing stock in the Bay Area (up to 93.4 percent), the structural types have been further regrouped into wood and nonwood classifications. Because the combined structural types of concrete, masonry, and steel frame represent only 1.5 percent of the Bay Area's total housing stock, they have been consolidated into a single structural type—nonwood. At the same time, since unreinforced masonry buildings have been identified by local building officials and they present specific seismic hazards, they have been isolated as a category in and of themselves.

Two classifications used in the paper which do not follow the above rules are the categories of "mobile homes" and "other." Since mobile homes are accounted for in the U.S. Census and are a clearly distinguishable building type with particular seismic concerns, they have been classified into a category of their own. The category defined as "other" is used in accord with the U.S. Census Bureau Definitions (U.S. Bureau of the Census, 1991) and includes shelters such as boats, tents, caves, and railcars.

The five categories used in this paper to classify the type of structure of the Bay Area's housing stock are therefore:

1. *Mobile homes*.—Represent 2.8 percent of the total;
2. *Unreinforced masonry*.—Represents 1.0 percent of the total;
3. *Wood*.—Represents 93.4 percent of the total;
4. *Nonwood*.—Includes concrete, reinforced masonry, and steel frame, and represents 1.5 percent; and
5. *Other*.—Represents 1.3 percent of the total.

CONFIGURATION

While the structure of a building plays an important role in the mitigation of seismic forces, its configuration will likewise influence its earthquake resistance. Configuration deals with issues such as building height, building shape, and general width-to-height proportions. It might also include the location and arrangement of the major structural elements within the building. Due to the size of the Bay Area's housing stock, and due to the fact that height is perhaps the most important element in a building's

configuration, this paper categorizes a building's configuration only by its height. Accordingly, for the purposes of this paper, the height of a building determines whether it is classified as:

1. *Low*.—Three stories and under;
2. *Medium*.—Between four and seven stories; and
3. *High*.—Eight stories and over.

When classifying a building according to its height, parking levels have consistently been included. Whether the parking level is below grade, half a level below grade, or above grade, it has been included in the story count of a building.

Note that eight-story buildings are often considered high-rise structures by the Uniform Fire Code for they exceed 75 feet. In addition, the U.S. Bureau of the Census used these height classifications for data through 1980. (The question on number of stories was dropped from the 1990 census.)

AGE OF CONSTRUCTION

The age of construction plays an important role in the seismic performance of buildings. Over time, building technologies have improved, and code requirements have increased. The age of a building can give clues as to how buildings were detailed and put together. The age of a building can also suggest information about the quality of the materials used and the quality of craftsmanship during construction. Since significant changes in construction practices over time typically have been triggered by earthquakes, the age of a building determines whether construction occurred before or after a code change or before or after the use of a particular building technology. Age, therefore, can serve as an indicator of how well a building will resist earthquakes in the future.

The Uniform Building Code was first published and organized in 1927. The extensive use of plywood and other modern building materials, together with the wider existence and implementation of the building code, occurred with the large-scale developments following World War II (WW II). It was not until suburbanization and the increase in demand for housing occurred that there were significant changes in construction practices (Gideon, 1948; Kostof, 1985; Hayden, 1986). Note that the 1940 cut-off date is extremely important. For example, foundation bolting of single-family wood-frame dwellings was more common after 1940. In the San Francisco Bay area almost 80 percent of the region's housing stock was built after 1940; this preponderance is slightly greater than the almost three-quarters value nationwide.

One of the most noticeable differences between pre- and post-1940 buildings is the degree of parking both

within multifamily and single-family buildings. It is common for most multifamily buildings built after WW II to have all or most of the ground floor dedicated to parking. (Residential buildings with tucked-under parking or first-floor parking are more vulnerable to damage than those buildings without such parking.)

Although 1940 is identified as the key cut-off point in this study, the actual decade of construction has been catalogued in our database. In addition, when the information was available and a precise record of construction existed, it was catalogued. Typically, the decade of construction was identified through field visits or from data obtained from building departments. Hence, a building built in 1936 has been identified as a 1930's building; a building built in 1967 as a 60's building, a building built in 1940 as a 40's building, and so on.

The significance of WW II as the cut-off point in the classification of building age is corroborated by preliminary statistics from the Northridge earthquake. Insurance company statistics on percentage losses to single-family homes by decade of construction show that there was no significant difference in performance by year of construction other than pre- and post-WW II buildings. These companies speculate that, to some degree, improvements in the codes and construction practices have been offset by the extensive use of complex configurations, large amounts of glass, and cathedral ceilings in newer construction (Robert Downen, oral commun., 1994).

While the age of buildings has been identified by decade or by year in the database, the statistics in this study classify building age on the basis of pre- or post-WW II (1940's) vintage. Thus, this study classifies the age of buildings according to two periods:

1. *Pre-1940*; and
2. *1940 to present*.

OVERALL CLASSIFICATION

For the purposes of this study, the housing stock has broadly been classified according to the three sets of criteria: the material, the height or number of stories of the building, and the age of the building. These three categories enable classification of the Bay Area's housing stock into the 13 building types listed in table 1. Note that six of the 13 types are subdivisions of wood-frame construction. This classification system is extremely valuable for residential buildings in the Bay Area, where 93.4 percent of the housing stock is wood-frame construction, but unusual for earthquake studies. In the more typical Applied Technology Council study of earthquake damage (Applied Technology Council, 1985), only one of the 40 categories was wood-frame construction.

Table 1.—Summary of characteristics of building types used in this paper

Building type	Structure	Configuration	Age	Single vs. multifamily
Type 1	Mobile Homes	1-3 stories	Post 1940	Single Family
Type 2	Unreinforced Masonry	Varies	Pre 1940	Multi-family
Type 3	Non-Wood	4-7 stories	Pre 1940	Multi-family
Type 4	Non-Wood	4-7 stories	Post 1940	Multi-family
Type 5	Non-Wood	8 and up	Pre 1940	Multi-family
Type 6	Non-Wood	8 and up	Post 1940	Multi-family
Type 7	Wood	4-7 stories	Pre 1940	Multi-family
Type 8	Wood	4-7 stories	Post 1940	Multi-family
Type 9	Wood	1-3 stories	Pre 1940	Multi-family
Type 10	Wood	1-3 stories	Post 1940	Multi-family
Type 11	Wood	1-3 stories	Pre 1940	Single Family
Type 12	Wood	1-3 stories	Post 1940	Single Family
Type 13	Other	Varies	Varies	Varies

POSTEARTHQUAKE HABITABILITY DATA COLLECTION

LOMA PRIETA DATA

A telephone survey of all jurisdictions affected by the Loma Prieta earthquake was conducted in 1991 in order to determine the extent of residential damage (other than mobile homes) and the displacement of residents. Unclear or incomplete data was rechecked with follow-up surveys in 1993 and 1994. Information was obtained from city and county building departments. These building departments were the agencies that immediately inspected and assessed the structural damage within their jurisdictions. Buildings were tagged with red (unsafe for occupancy), yellow (limited access), and green (safe). Survey respondents were asked to identify the residential red- and yellow-tagged buildings within their jurisdictions, as well as structure type and street address.

One problem with the information was that some cities kept incomplete or no records of their tagging. Not all departments with red-tagged buildings could provide addresses. Some cities had extensive records, but these were disorganized to the point of being unusable. Other jurisdictions summarized their inspections very early on; therefore their summary of total red-tagged units may be low relative to the actual number (such as may have been the case in Gilroy and San Jose). Many building departments discovered new quake damage long after the earthquake as homeowners applied for repair permits.

Local city and county building departments have no authority over mobile homes because they are not classi-

fied as buildings. However, data on uninhabitable mobile homes were centrally compiled by the State of California Department of Housing and Community Development (H&CD) (1991).

Table 2 contains the results of the survey of cities, counties, and H&CD. It summarizes the total number of red-tagged housing units, as well as the yellow-tagged multifamily units, by jurisdiction for the nine-county San Francisco Bay area, as well as the three-county Monterey Bay area.¹ Tables 3 and 4 contain the results of the building type classification used in table 1 by tagging type and by intensity level. The distribution of the red-tagged residential buildings is shown in figure 1.

NORTHRIDGE DATA

ABAG duplicated the process of collecting data on red- and yellow-tagged residential buildings following the Loma Prieta earthquake in the Bay Area for the Northridge earthquake in the Los Angeles and Ventura County areas. As in the Loma Prieta survey, ABAG project staff conducted a telephone survey of the affected city and county building departments. This interview effort was supplemented by approximately 20 person-days in the impacted area to check data supplied by the building departments to ensure

¹For those interested in the actual street address information, a PC-formatted diskette of all red-tagged units in the nine-county Bay Area, as well as all multifamily yellow-tagged units, is available from ABAG as Publication P960001EQK.

Table 2.—Results of ABAG survey conducted in 1994 of cities and counties related to unreinforced masonry buildings and housing damage from the Loma Prieta earthquake

County	City	No. of URM ^s	No. of historic URM ^s ¹	No. of residential URM ^s	No. of residential URM ^s within residential URM ^s	No. of yellow-tagged residential units	No. of yellow-tagged residential buildings	No. of red-tagged residential units	No. of red-tagged residential buildings
Alameda County	Alameda	82	7	9	64	0	0	0	0
Alameda County	Albany	58	0	1	46	0	0	0	0
Alameda County	Berkeley	444	0	41	897	150	150	45	3
Alameda County	Dublin	0	0	0	0	0	0	0	0
Alameda County	Emeryville	101	1	41	100	35	35	2	1
Alameda County	Fremont	32	5	5	14	50	50	0	0
Alameda County	Hayward	49	49	1	40	10	10	0	0
Alameda County	Livermore	48	3	1	1	0	0	0	0
Alameda County	Newark	0	0	0	0	0	0	0	0
Alameda County	Oakland	1,666	120	153	3,264	2,008	199	1,349	87
Alameda County	Piedmont	0	0	0	0	0	0	0	0
Alameda County	Pleasanton	36	0	0	0	0	0	0	0
Alameda County	San Leandro	59	0	1	24	1	1	0	0
Alameda County	Union City	7	0	0	0	0	0	0	0
Alameda County	Unincorporated	18	0	0	0	0	0	0	0
Contra Costa Co	Antioch	64	0	8	21	0	0	0	0
Contra Costa Co	Brentwood	7	0	0	0	0	0	0	0
Contra Costa Co	Clayton	0	0	0	0	0	0	0	0
Contra Costa Co	Concord	9	2	0	0	18	18	0	0
Contra Costa Co	Danville	5	4	0	0	16	16	0	0
Contra Costa Co	El Cerrito	32	0	0	0	0	0	0	0
Contra Costa Co	Hercules	3	2	0	0	0	0	0	0
Contra Costa Co	Lafayette	0	0	0	0	0	0	0	0
Contra Costa Co	Martinez	58	0	0	0	0	0	0	0
Contra Costa Co	Moraga	0	0	0	0	0	0	0	0
Contra Costa Co	Orinda	0	0	0	0	0	0	0	0
Contra Costa Co	Pinole	10	2	0	0	0	0	0	0
Contra Costa Co	Pittsburg	24	16	0	0	0	0	0	0
Contra Costa Co	Pleasant Hill	0	0	0	0	0	0	0	0
Contra Costa Co	Richmond	70	5	14	104	0	0	0	0
Contra Costa Co	San Pablo	0	0	0	0	0	0	0	0
Contra Costa Co	San Ramon	0	0	0	0	0	0	0	0
Contra Costa Co	Walnut Creek	12	0	1	4	0	0	0	0
Contra Costa Co	Unincorporated	66	0	19	42	12	12	0	0
Marin County	Belvedere	0	0	0	0	0	0	0	0
Marin County	Corte Madera	4	0	0	0	0	0	0	0
Marin County	Fairfax	4	0	3	15	0	0	0	0
Marin County	Larkspur	8	0	1	1	1	1	0	0
Marin County	Mill Valley	18	0	0	0	0	0	0	0
Marin County	Novato	2	0	0	0	0	0	0	0
Marin County	Ross	1	0	0	0	0	0	0	0
Marin County	San Anselmo	22	1	4	6	0	0	0	0
Marin County	San Rafael	50	0	17	109	1	1	0	0
Marin County	Sausalito	10	7	5	16	0	0	0	0
Marin County	Tiburon	1	0	0	0	0	0	0	0
Marin County	Unincorporated	1	0	0	0	0	0	2	2

Table 2.—Continued.

County	City	No. of URM ^s	No. of historic URM ^s ¹	No. of residential URM ^s	No. of residential URM ^s	No. of yellow-tagged residential units	No. of yellow-tagged residential buildings	No. of red-tagged residential units	No. of red-tagged residential buildings
Napa County	American Canyon	0	0	0	0	0	0	0	0
Napa County	Calistoga	30	0	0	0	0	0	0	0
Napa County	Napa	45	12	0	0	0	0	0	0
Napa County	Saint Helena	27	27	1	1	0	0	0	0
Napa County	Yountville	9	3	0	0	0	0	0	0
Napa County	Unincorporated	7	5	0	0	0	0	0	0
San Francisco	San Francisco	2,080	1,400	628	18,921	7,318	759	2,078	215
San Mateo Co	Atherton	1	1	0	0	0	0	0	0
San Mateo Co	Belmont	4	0	1	4	0	0	0	0
San Mateo Co	Brisbane	4	0	0	0	0	0	0	0
San Mateo Co	Burlingame	63	0	4	13	0	0	0	0
San Mateo Co	Colma	4	0	0	0	0	0	0	0
San Mateo Co	Daly City	1	0	1	3	20	20	0	0
San Mateo Co	East Palo Alto	0	0	0	0	0	0	0	0
San Mateo Co	Foster City	0	0	0	0	0	0	0	0
San Mateo Co	Half Moon Bay	2	1	0	0	26	26	0	0
San Mateo Co	Hillsborough	0	0	0	0	0	0	0	0
San Mateo Co	Menlo Park	2	0	0	0	0	0	0	0
San Mateo Co	Millbrae	2	0	0	0	150	150	0	0
San Mateo Co	Pacifica	0	0	0	0	3	3	0	0
San Mateo Co	Portola Valley	0	0	0	0	0	0	0	0
San Mateo Co	Redwood City	33	4	1	53	0	0	53	1
San Mateo Co	San Bruno	5	0	0	0	0	0	1	1
San Mateo Co	San Carlos	10	2	3	4	25	25	1	1
San Mateo Co	San Mateo	28	0	3	71	300	300	1	1
San Mateo Co	So. San Francisco	23	3	4	4	42	42	12	2
San Mateo Co	Woodside	0	0	0	0	0	0	0	0
San Mateo Co	Unincorporated	7	4	0	0	32	32	8	8
Santa Clara Co	Campbell	11	4	0	0	36	36	1	1
Santa Clara Co	Cupertino	1	0	0	0	50	50	0	0
Santa Clara Co	Gilroy	35	0	2	2	350	350	52	52
Santa Clara Co	Los Altos	1	0	0	0	1	1	1	1
Santa Clara Co	Los Altos Hills	0	0	0	0	65	65	10	10
Santa Clara Co	Los Gatos	21	6	2	21	500	500	25	24
Santa Clara Co	Milpitas	1	0	1	1	5	5	0	0
Santa Clara Co	Monte Sereno	0	0	0	0	0	0	1	1
Santa Clara Co	Morgan Hill	7	2	0	0	1	1	43	43
Santa Clara Co	Mountain View	25	7	2	24	0	0	46	11
Santa Clara Co	Palo Alto	49	0	1	26	0	0	2	1
Santa Clara Co	San Jose	196	0	0	0	18	18	8	8
Santa Clara Co	Santa Clara	24	0	0	0	0	0	0	0
Santa Clara Co	Saratoga	0	0	0	0	0	0	6	6
Santa Clara Co	Sunnyvale	86	30	0	0	10	10	3	3
Santa Clara Co	Unincorporated	14	0	0	0	303	303	210	208

IMPACT OF THE EARTHQUAKE ON HABITABILITY OF HOUSING UNITS

C175

Table 2.—Continued.

County	City	No. of URM ^s	No. of historic URM ^s ¹	No. of residential URM ^s	No. of residential URM ^s within residential URM ^s	No. of yellow-tagged residential units	No. of yellow-tagged residential buildings	No. of red-tagged residential units	No. of red-tagged residential buildings
Solano County	Benicia	39	18	0	0	0	0	0	0
Solano County	Dixon	12	0	0	0	0	0	0	0
Solano County	Fairfield	4	0	0	0	0	0	0	0
Solano County	Rio Vista	10	0	0	0	0	0	0	0
Solano County	Suisun City	24	0	0	0	0	0	0	0
Solano County	Vacaville	20	7	0	0	0	0	0	0
Solano County	Vallejo	64	8	6	56	2	2	0	0
Solano County	Unincorporated	2	0	0	0	0	0	0	0
Sonoma County	Cloverdale	18	2	0	0	0	0	0	0
Sonoma County	Cotati	0	0	0	0	0	0	0	0
Sonoma County	Healdsburg	18	0	2	5	0	0	0	0
Sonoma County	Petaluma	90	32	1	1	0	0	0	0
Sonoma County	Rohnert Park	0	0	0	0	0	0	0	0
Sonoma County	Santa Rosa	68	0	2	4	5	5	0	0
Sonoma County	Sebastopol	30	0	2	6	0	0	0	0
Sonoma County	Sonoma	51	29	3	19	0	0	0	0
Sonoma County	Windsor	0	0	0	0	0	0	0	0
Sonoma County	Unincorporated	174	16	7	28	0	0	0	0
Monterey	Carmel	22	0	0	0	0	0	0	0
Monterey	Del Rey Oaks	0	0	0	0	0	0	0	0
Monterey	Gonzales	3	1	0	0	1	1	0	0
Monterey	Greenfield	7	0	1	4	0	0	0	0
Monterey	King City	7	0	0	0	0	0	0	0
Monterey	Marina	0	0	0	0	0	0	0	0
Monterey	Monterey	60	0	6	30	0	0	0	0
Monterey	Pacific Grove	9	6	0	0	0	0	0	0
Monterey	Salinas	70	0	0	0	200	200	12	12
Monterey	Sand City	0	0	0	0	0	0	0	0
Monterey	Seaside	13	1	0	0	0	0	2	2
Monterey	Soledad	4	0	0	0	0	0	1	1
Monterey	Unincorporated	0	0	0	0	20	20	10	10
San Benito	Hollister	3	0	0	0	48	48	63	63
San Benito	San Juan Bautista	28	0	20	0	0	0	0	0
San Benito	Unincorporated	0	0	0	0	80	80	12	12
Santa Cruz	Santa Cruz	46	24	1	1	372	372	72	72
Santa Cruz	Capitola	1	0	0	0	0	0	6	6
Santa Cruz	Scotts Valley	0	0	0	0	160	160	11	11
Santa Cruz	Watsonville	72	1	0	0	200	200	275	275
Santa Cruz	Unincorporated	11	0	0	0	3,717	3,717	2,619	2,619
TOTALS		6,919	1,880	1,030	24,070	16,362	7,994	7,043	3,774

¹ As defined by each individual city and county. At a minimum, these numbers include structures with state and national designations.

Table 3.—*Dwelling units red tagged due to the Loma Prieta earthquake in the San Francisco Bay area*

TYPE	MODIFIED MERCALLI INTENSITY					
	V	VI	VII	VIII	IX	X+
Mobile homes	0	0	94	7	0	0
Unreinforced masonry	0	2	553	32	0	0
Nonwood, 4-7 stories, <1940	0	0	720	0	0	0
Nonwood, 4-7 stories, >1939	0	0	0	0	0	0
Nonwood, 7+ stories, <1940	0	0	403	0	0	0
Nonwood, 7+ stories, >1939	0	0	0	0	0	0
Wood frame, 4-7 stories, <1940, multifamily	0	68	456	291	0	0
Wood frame, 4-7 Stories, >1939, multifamily	0	0	22	0	0	0
Wood frame, 1-3 Stories, <1940, multifamily	0	30	420	424	3	0
Wood frame, 1-3 Stories, >1939, multifamily	0	18	27	14	0	0
Wood frame, 1-3 Stories, <1940, single family	3	33	74	38	76	77
Wood frame, 1-3 Stories, >1939, single family	0	8	47	13	2	5
"Other" (tents, caves, boats, etc.)	0	0	0	0	0	0

consistency, add missing data (particularly number of units and age for multifamily housing), and improve accuracy.

Minimal effort was made to field check and supplement data supplied by the City of Los Angeles because most of these data seemed to be remarkably accurate. The one problem with Los Angeles's data was the inconsistency in the labeling of number of stories. Based on a two-day field survey of residential multifamily buildings in the San Fernando Valley, ABAG staff estimated that approximately half of the units described as being in three-story structures were actually in three-story structures over a one-story parking garage (which, for purposes of this effort, should have been labeled as four-story structures). Rather than arbitrarily re-categorizing half of these structures as four-story buildings, we used available data on year built, number of units, construction type and square footage to assign the specific structures most likely to be four-story buildings to the four-story category. Approximately half of the total units in three-story buildings were

reassigned to four-story buildings. Because we carefully documented the specific buildings involved, we will be able to field check these buildings as part of future data-collection efforts. In addition, a few obvious inconsistencies in the data were corrected (such as a 26-story wood-frame building with less than six units) that were probably data-entry errors by the city. Again, these changes were documented.

This time-consuming data collection and field-checking process was not part of the original plan for the research. It had been anticipated that data on tagging would be readily available from the California Governor's Office of Emergency Services (OES) in Pasadena. However, in spite of the extensive data-collection effort conducted by the staff of this group, they were unable to release the data in a form that we could use due to restrictions placed on data release by some cities and counties, as well as by the management of OES. The data OES staff were able to release were aggregated by census tract and stripped of

Table 4.—*Dwelling units yellow tagged due to the Loma Prieta earthquake in the San Francisco Bay area by construction type and intensity*
 [Single-family units and mobile homes not rendered uninhabitable]

TYPE	MODIFIED MERCALLI INTENSITY					
	V	VI	VII	VIII	IX	X+
Mobile homes	0	0	0	0	0	0
Unreinforced masonry	0	127	1,180	42	0	0
Nonwood, 4-7 stories, <1940	0	102	1,159	0	0	0
Nonwood, 4-7 stories, >1939	0	0	0	0	0	0
Nonwood, 7+ stories, <1940	0	113	488	226	0	0
Nonwood, 7+ stories, >1939	0	0	664	0	0	0
Wood frame, 4-7 stories, <1940, multifamily	0	81	1,763	1,124	0	0
Wood frame, 4-7 Stories, >1939, multifamily	0	12	621	12	0	0
Wood frame, 1-3 Stories, <1940, multifamily	0	84	748	309	0	0
Wood frame, 1-3 Stories, >1939, multifamily	10	28	81	38	0	0
Wood frame, 1-3 Stories, <1940, single family	0	0	0	0	0	0
Wood frame, 1-3 Stories, >1939, single family	0	0	0	0	0	0
"Other" (tents, caves, boats, etc.)	0	0	0	0	0	0

¹ Single family homes remain habitable if yellow tagged. Formal tagging does not occur with mobile homes, so a distinction between "red" and "yellow" has not been applied.

the actual dwelling-unit count information essential to estimating displaced persons and peak shelter populations. OES staff was also unable to provide us with addresses so that we could collect the dwelling-unit data needed and add it to their databases. This extensive data-collection duplication effort could have been avoided if release of data to Federally-funded researchers was required as a condition of funding city and county, as well as state, emergency-response efforts. This data "security" issue was not present during our data collection efforts following the Loma Prieta earthquake.

Table 5 shows ABAG data collected for housing impact analysis. It compares data collected by ABAG to two sources of data supplied by the OES Pasadena group—the first was a FAX dated 2-7-95; the second was a report (EQE International and Office of Emergency Ser-

vices, 1995) dated in April. Although the total numbers are within 15 percent of each other among the three sources, the data discrepancies for some individual jurisdictions are huge. We believe that the ABAG data are more accurate than the OES and EQE/OES data for several reasons. First, we collected the data later than OES, and therefore the cities and counties had a better understanding of the impact on their housing stock. In addition, the people collecting the data at ABAG had experience in collecting similar data after Loma Prieta, and therefore they knew the questions to ask and the types of people to talk to. Because ABAG knew the importance of collecting accurate data, a great deal of effort was made to ensure that all affected jurisdictions were contacted. Finally, to improve quality control and to ensure that data on housing units and construction type were as accurate as pos-

sible given the time and money constraints, ABAG staff visited the impacted areas and checked samples of impacted buildings within the City of Los Angeles and checked *all* buildings with incomplete records in the remaining jurisdictions. If cities, counties, and the state cooperate in sharing these types of data following future earthquakes, more effort could be directed toward data-quality assurance.

OVERALL RESIDENTIAL BUILDING STOCK DATA

During 1994, ABAG staff developed an extensive inventory of existing residential buildings in the San Francisco Bay area. The work was conducted using the base date of April 1990 to make it consistent with the 1990 census. This inventory groups buildings by numbers of dwelling units (not numbers of buildings) according to four sets of categories: material, number of stories (1-3, 4-7, and 7+), age (by decade), and multifamily vs. single

family. Material categories include: Wd (wood frame), MH (mobile home), LM (light metal), RM (reinforced masonry), UM (unreinforced masonry), SF (steel frame), RC (reinforced concrete, including ductile and nonductile frame), and CS (concrete or steel frame, unknown). These inventory data were created for each 1990 census tract-city map unit.

The data on total number of dwelling units in 1990 were obtained directly from the 1990 census. That census data were also used to obtain a count of mobile homes, as well as a breakdown of housing units by decade of construction and by single-family versus multifamily types. (See U.S. Bureau of the Census, 1991 and 1992.)

The data on unreinforced-masonry residential buildings are based on actual inventory data collected by local governments and provided to ABAG during a telephone survey. Follow-up building surveys cleaned up the local data. For example, several jurisdictions did not collect data on type of use (i.e. residential vs. commercial) and even more did not obtain data on the number of residential dwelling units.

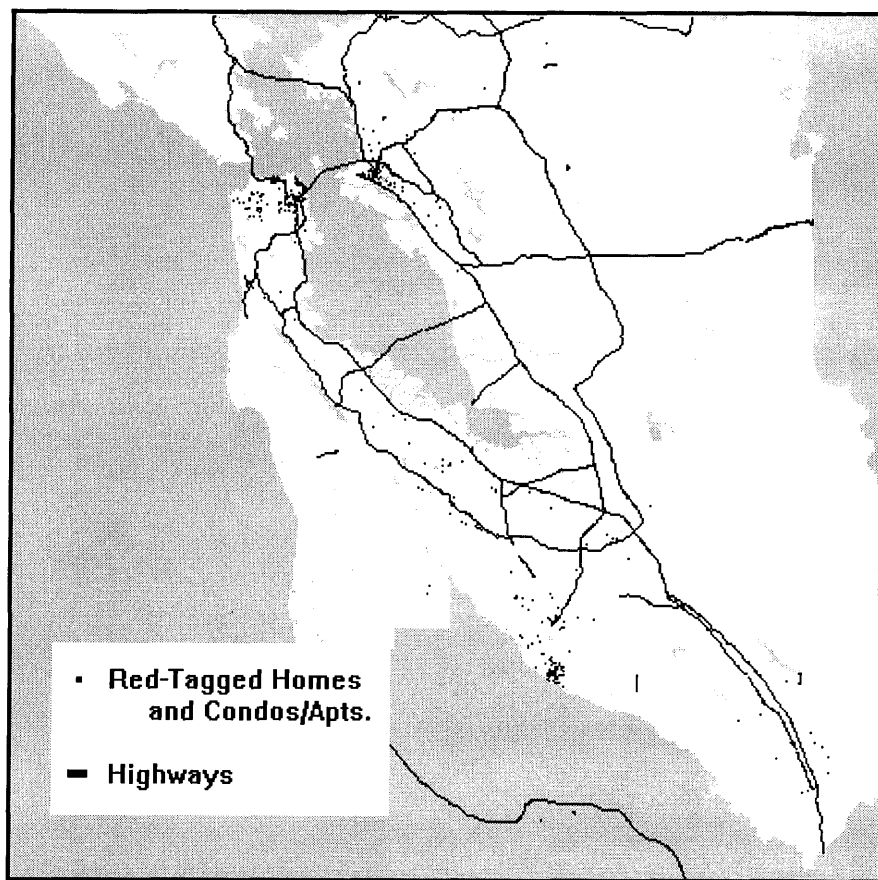


Figure 1.—The Loma Prieta earthquake resulted in 13,000 uninhabitable Bay Area housing units, including 3,960 units in the 691 red-tagged residential buildings shown here. (From Perkins and others, 1996.)

Table 5.—*Northridge earthquake residential tagging data*

[Data from ABAG survey compared with OES FAX (2-7-95) and OES report (EQE and OES, April 1995)]

City	Red-Tagged Residential						OES (FAX)	EQE/OES (Report)		
	ABAG			Total Units in Buildings	Mobile Homes	Total Residential Units				
	Residential Buildings	Single Family	Multi-Family							
		Buildings	Units							
Beverly Hills	18	12	6	130	142	0	142	22	21	
Burbank	12	8	4	47	55	0	55	30	3	
Calabasas	10	5	5	44	49	0	49	0	0	
Culver City	20	19	1	2	21	0	21	14	15	
Glendale	6	4	2	64	68	0	68	10	17	
Los Angeles	1,300	781	519	11,358	12,139	2,083	14,222	1,519	1,604	
Manhattan Beach	2	2	0	0	2	0	2	3	0	
Pasadena	1	0	1	12	12	0	12	4	5	
San Fernando	99	52	47	170	222	105	327	82	27	
Santa Clarita	80	64	16	184	248	1606	1854	60	83	
Santa Monica	27	12	15	301	313	0	313	60	67	
West Hollywood	3	0	3	13	13	0	13	3	4	
Unincorporated	46	44	2	7	51	193	244	0	28	
Fillmore	120	117	3	12	129	86	215	0	144	
Moorpark	1	1	0	0	1	3	4	0	2	
Simi Valley	13	9	4	22	31	519	550	0	25	
Thousand Oaks	53	47	6	18	65	0	65	0	55	
Unincorporated	14	14	0	0	14	0	14	0	14	
TOTALS	1,825	1,191	634	12,384	13,575	4,595	18,170	1,807	2,114	

Yellow-Tagged Residential

City	ABAG						OES (FAX)	EQE/OES (Report)	
	Residential Buildings	Single Family	Multi-Family		Total Units in Buildings	Mobile Homes	Total Residential Units		
			Buildings	Units					
Beverly Hills	84	68	16	95	163	0	163	80	53
Burbank	31	24	7	80	104	0	104	71	7
Calabasas	233	222	11	59	281	0	281	220	0
Culver City	46	43	3	6	49	0	49	10	12
Glendale	2	1	1	167	168	0	168	11	9
Los Angeles	7,214	5,359	1,855	27,856	33,215	1,033	34,248	7,340	7,715
Manhattan Beach	272	268	4	8	276	0	276	242	0
Pasadena	15	2	13	179	181	0	181	13	13
San Fernando	137	93	44	195	288	64	352	113	117
Santa Clarita	188	163	25	226	389	0	389	150	184
Santa Monica	91	28	63	890	918	0	918	212	239
West Hollywood	1	1	0	0	1	0	1	5	8
Unincorporated	201	159	42	639	798	15	813	0	85
Fillmore	263	254	9	27	281	0	281	0	228
Moorpark	59	59	0	0	59	0	59	0	22
Simi Valley	203	171	32	96	267	50	317	0	299
Thousand Oaks	213	205	8	29	234	0	226	0	121
Unincorporated	37	36	1	3	39	0	39	0	47
TOTALS	9,290	7,156	2,134	30,555	37,711	1162	38,873	8,467	9,159

Table 6.—*Existing (1990) dwelling units by construction type in the San Francisco Bay area*

[Data for buildings over three stories that are not unreinforced masonry are estimated for San Francisco and Oakland]

Construction Type	Alameda	Contra Costa	Marin	Napa	San Francisco	San Mateo	Santa Clara	Solano	Sonoma	TOTAL
Mobile homes	6,904	7,412	8,880	3,878	113	3,512	20,926	4,646	11,797	68,068 (2.8 %)
Unreinforced masonry	4,408	171	147	1	18,921	152	74	56	63	23,993 (1.0 %)
Nonwood, 4-7 stories, <1940	730	0	0	0	3,194	60	204	136	0	4,324 (0.2 %)
Nonwood, 4-7 stories, >1939	599	107	0	0	2,496	1,064	999	0	77	5,342 (0.2 %)
Nonwood, 7+ stories, <1940	436	0	0	0	3,309	0	64	0	0	3,809 (0.1 %)
Nonwood, 7+ stories, >1939	4,435	292	281	0	17,289	1,355	1,246	155	412	25,465 (1.0 %)
Wood frame, 4-7 stories, <1940, multifamily	748	0	27	0	22,718	155	6	0	0	23,654 (1.0 %)
Wood frame, 4-7 Stories, >1939, multifamily	18,590	3,509	1,640	0	12,462	13,490	8,143	0	0	57,834 (2.3 %)
Wood frame, 1-3 Stories, <1940, multifamily	48,008	4,773	6,648	1,291	85,123	7,461	10,204	2,907	2,799	169,214 (6.9 %)
Wood frame, 1-3 Stories, >1939, multifamily	115,057	68,342	35,924	6,801	51,757	56,451	141,277	24,283	24,772	524,664 (21.3 %)
Wood frame, 1-3 Stories, <1940, single family	58,929	12,960	20,058	4,077	48,943	17,264	20,190	6,009	14,687	203,117 (8.3 %)
Wood frame, 1-3 Stories, >1939, single family	240,701	215,812	114,805	27,654	56,173	147,437	330,682	80,418	104,452	1,318,134 (53.6 %)
"Other" (tents, caves, boats, etc.)	5,771	2,767	3,225	493	6,350	3,381	6,216	923	1,998	31,124 (1.3 %)
TOTAL	505,316	316,145	191,635	44,195	328,848	251,782	540,231	119,533	161,057	2,458,742
	20.6 %	12.8 %	7.8 %	1.8 %	13.4 %	10.2 %	22.0 %	4.9 %	6.5 %	

The location of tall (over three story) residential buildings was collected by ABAG staff to the extent possible given time and budget constraints. The inventory includes information on location by street address, building construction type and approximate age, and number of dwell-

ing units. The most incomplete areas are the City of Oakland and the City of San Francisco, where only some buildings are identified by street address.

The results of this process, aggregated to the county level, are provided in table 6.

Table 7.—*Composite percent of dwelling units red tagged by construction type and intensity*

TYPE	MODIFIED MERCALLI INTENSITY					
	V	VI	VII	VIII	IX	X+
Mobile homes	0	0	0.87	40	90	100
Unreinforced masonry	0	0.05	2.9	45	70	80
Nonwood, 4-7 stories, <1940	0	0.30	8.0	45	70	80
Nonwood, 4-7 stories, >1939	0	0	0	16	54	70
Nonwood, 7+ stories, <1940	0	0.30	8.0	45	70	80
Nonwood, 7+ stories, >1939	0	0	0	16	54	70
Wood frame, 4-7 stories, <1940, multifamily	0	1.4	2.5	45	70	80
Wood frame, 4-7 Stories, >1939, multifamily	0	0	0.09	10	15	25
Wood frame, 1-3 Stories, <1940, multifamily	0	0.05	0.53	11	44	64
Wood frame, 1-3 Stories, >1939, multifamily	0	0.01	0.04	6.5	15	25
Wood frame, 1-3 Stories, <1940, single family	0.01	0.04	0.12	1.8	8.4	12
Wood frame, 1-3 Stories, >1939, single family	0	0	0.02	0.18	0.69	1.8
"Other" (tents, caves, boats, etc.)	0	0	0	0	0	0

Similar data were compiled for the area impacted by the Northridge earthquake in 1994 and early 1995. The data on tall (over three story) buildings are very incomplete. The information on these tall buildings is much more complete in the heavily impacted areas; we assumed that any residential building over three stories would have been inspected (and at least green tagged) in this area. Thus, we did not rely on the data for these less-common tall structures in the outlying less-impacted areas.

CALCULATING VULNERABILITY BY CONSTRUCTION TYPE AND INTENSITY

The purpose of collecting the data on uninhabitable units and total exposed housing stock for these two earthquakes was as data input for the analysis which ultimately produced the composite tables relating modified Mercalli intensity and building construction to percent of dwelling units made uninhabitable, as shown in tables 7 and 8 for

red-tagged units and yellow-tagged multifamily units (Perkins and others, 1996).

Data on modified Mercalli intensity for the Loma Prieta earthquake are from the intensity models developed, in part, using these same data (Perkins and Boatwright, 1995). Data on intensity exposures for the core impacted areas of the Northridge earthquake are based on tagging of post-1940 single-family homes and extrapolating the data to other building types. (See J. Boatwright's research summarized in U.S. Geological Survey, 1996, p. 54-55, as well as Perkins and others, 1996.)

Prior to ABAG's work on housing habitability, the only published matrix for relating these variables was developed by Dunne and Sonnenfeld (1991). The matrices developed for red-tagged and yellow-tagged units by Perkins and others (1996) have been modified from this earlier Dunne and Sonnenfeld (1991) matrix based on actual data from the Loma Prieta and Northridge earthquakes. Additional information on the analysis process is provided in Perkins and others (1996). The percentages are provided in tables 7 and 8 using two significant digits, with the

Table 8.—Percent of dwelling units yellow tagged by construction type and intensity

[Single-family units are not rendered uninhabitable¹]

TYPE	MODIFIED MERCALLI INTENSITY					
	V	VI	VII	VIII	IX	X+
Mobile homes	0	0	0	0	0	0
Unreinforced masonry	0	3.3	6.2	8.5	30	20
Nonwood, 4-7 stories, <1940	0.30	7.7	37	25	30	20
Nonwood, 4-7 stories, >1939	0	0	0	38	16	16
Nonwood, 7+ stories, <1940	0.30	7.7	37	25	30	20
Nonwood, 7+ stories, >1939	0	0	4	38	16	16
Wood frame, 4-7 stories, <1940, multifamily	0	1.7	9.7	25	10	10
Wood frame, 4-7 Stories, >1939, multifamily	0	0.05	2.6	17	25	25
Wood frame, 1-3 Stories, <1940, multifamily	0	0.15	0.94	6.6	20	20
Wood frame, 1-3 Stories, >1939, multifamily	0.01	0.02	0.10	12	13	22
Wood frame, 1-3 Stories, <1940, single family	0	0	0	0	0	0
Wood frame, 1-3 Stories, >1939, single family	0	0	0	0	0	0
"Other" (tents, caves, boats, etc.)	0	0	0	0	0	0

¹ Single-family homes remain habitable if yellow tagged. Formal tagging does not occur with mobile homes, so a distinction between "red" and "yellow" has not been applied.

smallest value equal to 0.01 percent. These percentages are depicted graphically in figure 2.

Note that the "0" values in these tables are actually greater than zero, but quite small. Although occasional dwellings are "tagged" in these categories, there are also large numbers of dwellings exposed to these relatively low levels of shaking.

SAMPLE APPLICATION—ASSESSING IMPACTS AND POSSIBLE DAMAGE PATTERNS IN FUTURE EARTHQUAKES

Given the percentages in tables 7 and 8, and estimates of modified Mercalli intensity levels in future earthquakes

from Perkins and Boatwright (1995), ABAG produced estimates of uninhabitable housing units in future Bay Area earthquakes (Perkins and others, 1996). Small changes to these percentages have a significant impact on estimates of uninhabitable units. In particular, damage to wood-frame dwellings is an extremely significant component of the dwelling losses. The intensity maps used were based on the most recent version of ABAG's ground-shaking models (Perkins and Boatwright, 1995). These data were combined with the location of existing residential building stock (Perkins, 1994). A more complete description of this modeling process is contained in the full report for the research project (Perkins and others, 1996). The results of this modeling effort, by county, are shown in table 9. This table shows the models for the Loma Prieta

earthquake, as well as the actual data from that earthquake, for comparison, along with the results for models of future expected Bay Area earthquakes.

Another way of expressing the model results is in terms of construction type, rather than by county area. These numbers emphasize ways in which building retrofits can be targeted to reduce the number of uninhabitable dwelling units predicted. The results of the models for the Loma Prieta earthquake, as well as actual data from that earthquake, again along with model results of future expected Bay Area earthquakes, are provided in table 10.

CONCLUSIONS

This data-collection and analysis effort emphasizes the impact of both the Loma Prieta and Northridge earthquakes on nonengineered housing stock. Although single-family wood-frame homes are less susceptible to becoming uninhabitable than multifamily units, their predominance (over 60 percent of the existing building stock in the Bay Area) makes the impact significant (almost 1,200 in Northridge and 376 in Loma Prieta). For high shaking intensities, pre-1940 single-family homes are roughly 10

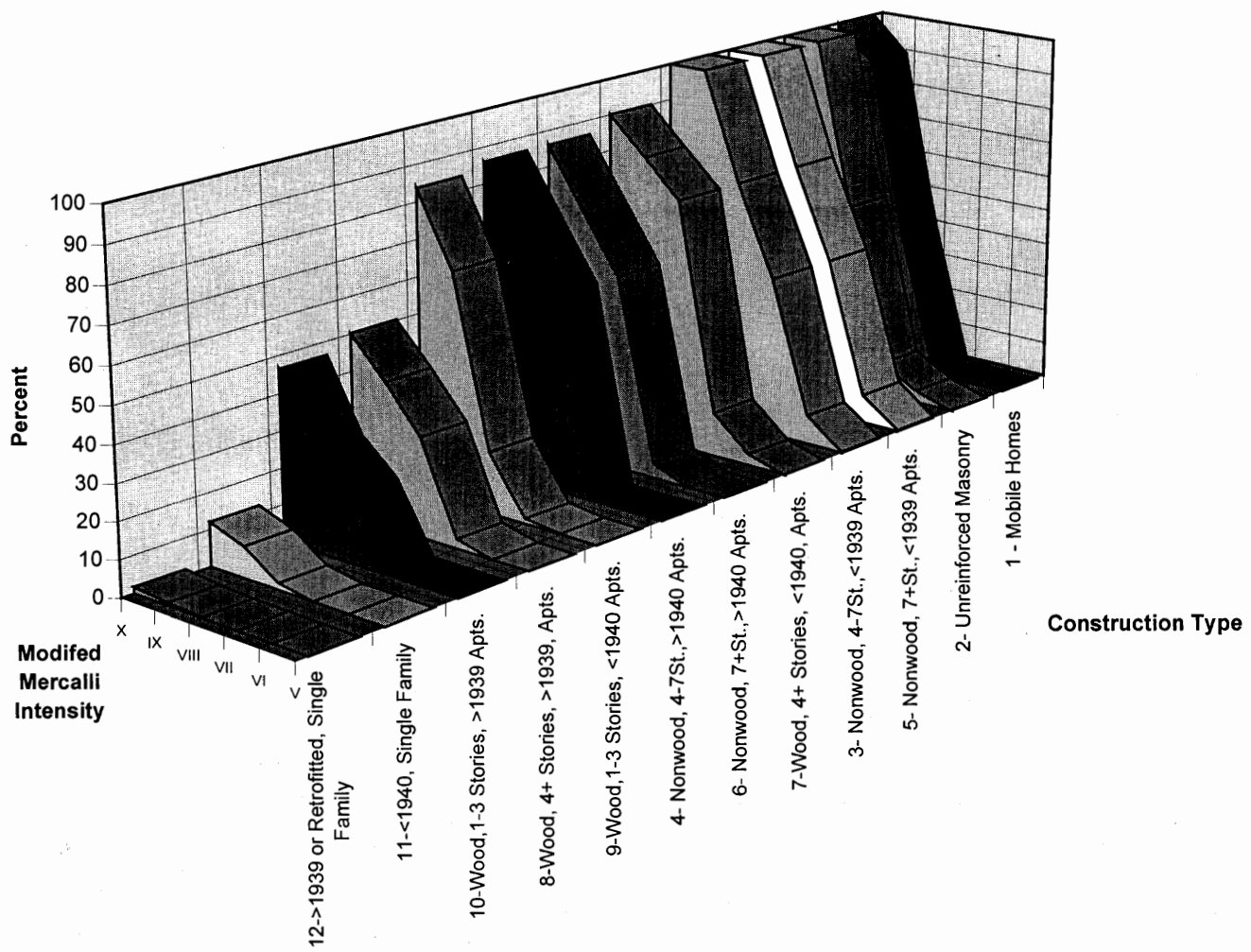


Figure 2.—Result of analysis and comparison of percentages of units rendered uninhabitable, by construction type, obtained by summing the percents in tables 7 and 8.

Table 9.—*Uninhabitable units in Bay Area counties for selected earthquake scenarios*

County data for earthquake scenarios ¹	Alameda	Contra Costa	Marin	Napa	San Francisco	San Mateo	Santa Clara	Solano	Sonoma	TOTAL
Loma Prieta, actual M = 6.9	3,284	0	2	0	9,202	76	408	0	0	12,972
Loma Prieta, modeled M = 6.9	1,968	159	297	1	11,781	223	1,239	2	3	15,673
Hayward combined M = 7.3	82,563	9,623	2,128	34	38,739	1638	13,443	1,028	892	150,087
Southern Hayward M = 7.0	52,200	1,070	1,040	7	11,630	241	9,963	127	30	76,309
Northern Hayward M = 7.1	61,901	7,552	2,007	22	15,264	237	360	333	156	87,831
Healdsburg Rodgers Creek M = 7.1	3,256	618	1,222	46	11,101	71	70	139	13,669	30,192
Maacama M = 6.8	325	17	27	22	1986	11	11	15	798	3,212
Peninsula segment of San Andreas M = 7.1	3,139	46	800	2	19,233	13,166	9,336	10	4	45,735
San Gregorio M = 7.1	1,976	28	808	2	11,650	1,317	324	10	6	16,119
Northern Calaveras M = 6.9	6,231	4,114	27	15	2,354	58	2,490	134	5	15,428
Concord- Green Valley M = 7.1	3,546	12,195	28	1,173	3,191	74	324	2,865	35	23,431
Greenville M = 7.1	2,413	1,734	27	14	576	16	120	324	5	5,230
West Napa M = 6.7	1,382	284	27	4,129	2,011	15	29	1,650	126	9,652

¹ Expected moment magnitude provided based on length of fault segment.

times more likely to become uninhabitable than post-1940 homes.

The results of this effort also point out the problems with mobile homes, which were responsible for almost 4,600 of the 48,000 uninhabitable units from the Northridge earthquake. Because local city and county building departments have no jurisdiction over these units, preearthquake planning and retrofitting for this housing type are more difficult.

Multifamily soft-story wood-frame housing units (that is, with tucked under or first-floor parking) were surprisingly vulnerable to becoming uninhabitable. They were responsible for 7,000 of the 16,000 housing units made

uninhabitable by the Loma Prieta earthquake, and over 11,000 of the 48,000 housing units made uninhabitable by the Northridge earthquake.

Our efforts in using these data to predict the impact of future Bay Area earthquakes emphasize the need to collect data on the number of units in multifamily structures. Red Cross and other shelter providers require information on people displaced, not buildings impacted. The most practical means of collecting this information is to collect data on the number of housing units within the impacted buildings.

Because of the relative scarcity of nonwood housing structures, it is extremely difficult to gather enough data

Table 10.—*Uninhabitable units by residential construction type for selected earthquake scenarios*

Construction type data for earthquake scenarios ¹	Mobile homes	Unreinforced masonry	Non-wood, 4-7 stories, <1940	Non-wood, 4-7 stories, >1939	Non-wood, 7+ stories, <1940	Non-wood, 7+ stories, >1939	Wood, 4-7 stories, <1940	Wood, 4-7 stories, >1939	Wood, 1-3 stories, <1940, multi-family	Wood, 1-3 stories, >1939, multi-family	Wood, 1-3 stories, <1940, single family	Wood, 1-3 stories, >1939, single family
Loma Prieta, actual M = 6.9	101	1,936	1,981	0	1,230	664	3,783	667	2,018	216	301	75
Loma Prieta, modeled M = 6.9	232	2,159	1,778	158	1,491	1,822	2,819	1,108	2,278	1,583	161	84
Hayward combined M = 7.3	10,892	13,135	3,053	1,810	2,580	8,194	9,419	9,569	34,234	49,782	5,273	2,147
Southern Hayward M = 7.0	7,793	3,852	2,009	368	1,633	3,783	3,096	4,962	12,920	32,405	2,070	1,417
Northern Hayward M = 7.1	3,615	7,187	2,171	707	1,740	4,741	3,838	7,398	26,274	24,735	4,443	983
Healdsburg Rodgers Creek M = 7.1	6697	2204	1,739	216	1,462	1,994	2,672	1,172	3,232	7937	465	404
Maacama M = 6.8	475	703	311	0	262	103	630	83	301	245	74	27
Peninsula segment of San Andreas M = 7.1	1,659	2,490	1,901	1,549	1,494	3,220	5,283	4,905	6,303	15,909	605	416
San Gregorio M = 7.1	328	2,107	1,791	152	1,465	1,658	2,817	1,270	2,230	2,061	168	75
Northern Calaveras M = 6.9	1,688	1,159	608	12	454	445	743	1,228	1,108	7,296	166	521
Concord-Green Valley M = 7.1	3,660	1,220	735	9	448	709	1,157	1,590	1,952	11,060	322	569
Greenville M = 7.1	974	351	330	0	191	105	426	207	571	1,871	98	107
West Napa M = 6.7	2,315	929	604	0	403	206	683	180	1,313	2,577	256	188

¹ Expected moment magnitude provided based on length of fault segment.

on these units for a pure statistical approach to estimate habitability. The matrices (tables 7 and 8) are least reliable for these types of structures. (See Perkins and others, 1996, for a more complete description of this analysis effort.)

Rigorous data-collection efforts in future earthquakes should continue to improve our knowledge of the functionality of our housing stock. These efforts should minimize duplication of data-collection efforts and maximize data sharing and quality control.

ACKNOWLEDGMENTS

We would like to thank the following individuals for their thoughtful comments on this paper: Linda Seekins and Paul Thenhaus, U.S. Geological Survey, and Edward Wyatt, ABAG. Additional comments were received on research which forms the basis for this work: Thelma Rubin, Councilmember, City of Albany (committee chair); Chris Arnold, Building Systems Development (BSD), Inc.; Roger Borcherdt, U.S. Geological

Survey; Laurence Kornfield, City and County of San Francisco; Frank McClure, Consulting Structural Engineer; Patrick McClellan, formerly with City of San Leandro; Gregg O'Ryon, American Red Cross, Bay Area; Paula Schulz, California Office of Emergency Services; Roy Schweyer, City of Oakland Office of Community Development; Martha Blair Tyler, Spangle and Associates; and Frannie Winslow, City of San Jose Office of Emergency Services.

In addition, the analysis described in this paper would not have been possible without the support in data collection provided by Dan Friess and Edward Wyatt, ABAG, as well as the programming assistance of Paul Wilson of Mapframe Corp., and Fred Parkinson.

The research which forms the basis of this paper was financed in part with National Science Foundation (NSF) Grants No. BCS-9302612 and CMS-9416181. Any opinions, findings, conclusions, or recommendations expressed in this material are those of the authors and do not necessarily reflect the views of any Federal agency, including NSF.

REFERENCES

- Applied Technology Council, 1985, ATC-13—Earthquake damage evaluation data for California: Redwood City, Calif., Applied Technology Council, p. 51-52.
- 1991, Procedures for postearthquake safety evaluation of buildings (ATC-20): Sacramento, Calif., State of California Governor's Office of Emergency Services, 144 p.
- Dunne, R.G., and Sonnenfeld, P., 1991, Estimation of homeless caseload for disaster assistance due to an earthquake: Pasadena, Calif., Southern California Earthquake Preparedness Project, 189 p. [from a 1980 draft document originally prepared for FEMA]
- EQE International and Governor's Office of Emergency Services (Geographic Information Systems Group), 1995, The Northridge earthquake of January 17, 1994—Preliminary report of data collection and analysis; Part A, Damage and inventory data: Sacramento, Calif., State of California Governor's Office of Emergency Services, 316 p.
- Gideon, Siegfried, 1948, Mechanization takes command: New York, Oxford University Press, 743 p.
- Hayden, Dolores, 1986, Redesigning the American dream: The Future of housing, work, and family life: New York, W.W. Norton & Co., 270 p.
- Kostof, Spiro, 1985, A history of architecture: New York, Oxford University Press, 788 p.
- Perkins, J.B., 1992, Estimates of uninhabitable dwelling units in future earthquakes affecting the San Francisco Bay region: Oakland, Calif., Association of Bay Area Governments, 89 p.
- 1994, Existing land use in 1990: Data for Bay Area cities and counties: Oakland, Calif., Association of Bay Area Governments, 308 p.
- Perkins, J.B., and Boatwright, J., 1995, The San Francisco Bay area—On shaky ground: Oakland, Calif., Association of Bay Area Governments, 56 p.
- Perkins, J.B., Chuquai, B., Harrald, J., and Jeong, D., 1996, Shaken Awake! Estimates of uninhabitable dwelling units and peak shelter populations in future earthquakes affecting the San Francisco Bay area: Oakland, Calif., Association of Bay Area Governments, 143 p.
- State of California Department of Housing and Community Development, 1991, Evaluation of manufactured housing support system performance in the Loma Prieta earthquake: Sacramento, Calif., State of California Department of Housing and Community Development, 14 p.
- U.S. Bureau of the Census, May 1991, Standard Tape File 1 (STF-1A): Washington, D.C., U.S. Bureau of the Census [computer file].
- U.S. Bureau of the Census, May 1992, Standard Tape File 3 (STF-3): Washington, D.C., U.S. Bureau of the Census [computer file].
- U.S. Geological Survey, 1996, USGS response to an urban earthquake—Northridge '94: Reston, Virginia, U.S. Geological Survey Open-File Report 96-263, p. 54-55.